DRUG RE-PURPOSING FOR THE TREATMENT OF BACTERIAL AND VIRAL INFECTIONS

EDITED BY: Maria Tomas, Thomas Keith Wood and Rodolfo García-Contreras
PUBLISHED IN: Frontiers in Cellular and Infection Microbiology

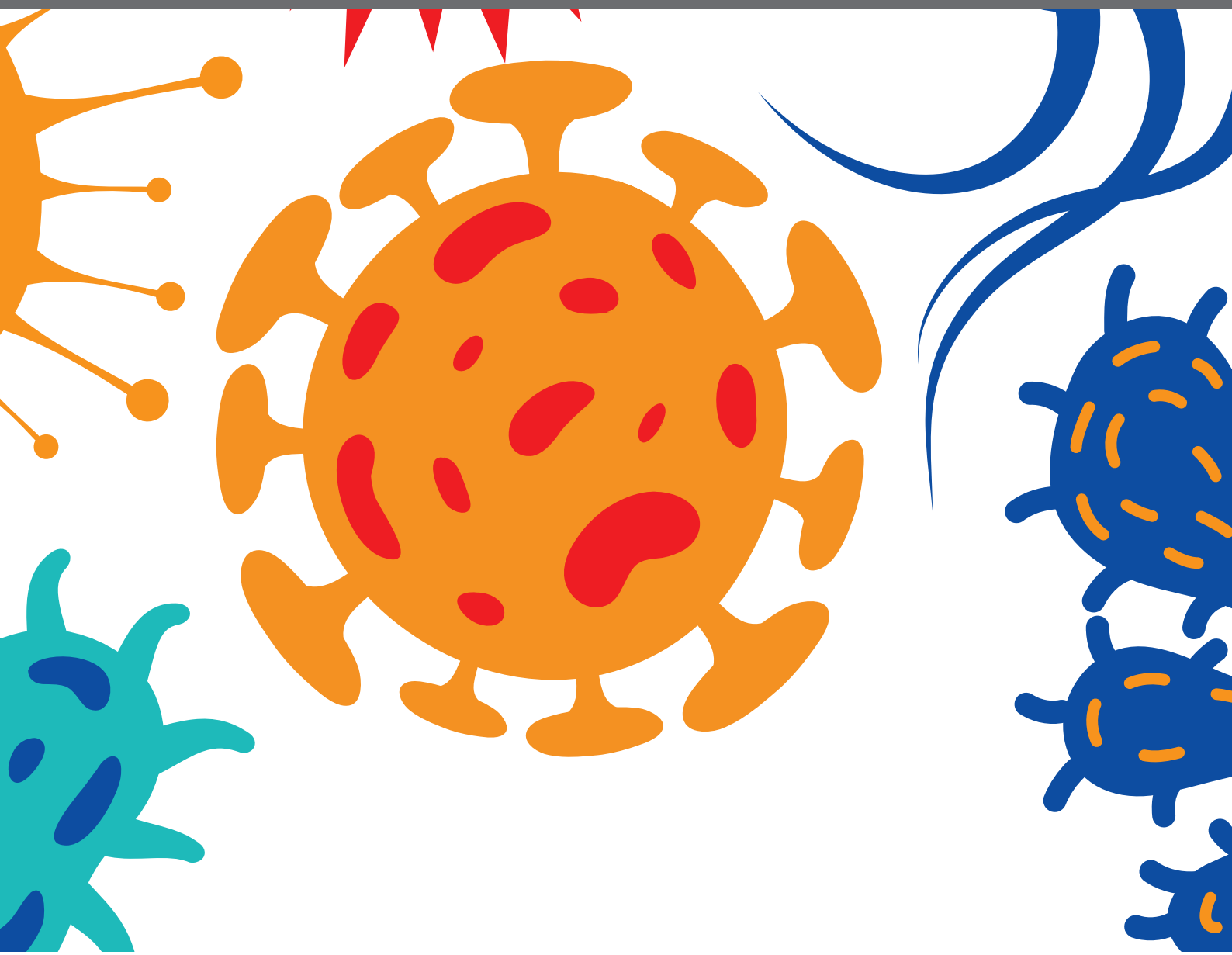

frontiers Research Topics

ISSN 1664-8714
ISBN 978-2-88963-246-6
DOI 10.3389/978-2-88963-246-6

About Frontiers

Frontiers is more than just an open-access publisher of scholarly articles: it is a pioneering approach to the world of academia, radically improving the way scholarly research is managed. The grand vision of Frontiers is a world where all people have an equal opportunity to seek, share and generate knowledge. Frontiers provides immediate and permanent online open access to all its publications, but this alone is not enough to realize our grand goals.

Frontiers Journal Series

The Frontiers Journal Series is a multi-tier and interdisciplinary set of open-access, online journals, promising a paradigm shift from the current review, selection and dissemination processes in academic publishing. All Frontiers journals are driven by researchers for researchers; therefore, they constitute a service to the scholarly community. At the same time, the Frontiers Journal Series operates on a revolutionary invention, the tiered publishing system, initially addressing specific communities of scholars, and gradually climbing up to broader public understanding, thus serving the interests of the lay society, too.

Dedication to Quality

Each Frontiers article is a landmark of the highest quality, thanks to genuinely collaborative interactions between authors and review editors, who include some of the world's best academicians. Research must be certified by peers before entering a stream of knowledge that may eventually reach the public - and shape society; therefore, Frontiers only applies the most rigorous and unbiased reviews.
Frontiers revolutionizes research publishing by freely delivering the most outstanding research, evaluated with no bias from both the academic and social point of view. By applying the most advanced information technologies, Frontiers is catapulting scholarly publishing into a new generation.

What are Frontiers Research Topics?

Frontiers Research Topics are very popular trademarks of the Frontiers Journals Series: they are collections of at least ten articles, all centered on a particular subject. With their unique mix of varied contributions from Original Research to Review Articles, Frontiers Research Topics unify the most influential researchers, the latest key findings and historical advances in a hot research area! Find out more on how to host your own Frontiers Research Topic or contribute to one as an author by contacting the Frontiers Editorial Office: researchtopics@frontiersin.org

DRUG RE-PURPOSING FOR THE TREATMENT OF BACTERIAL AND VIRAL INFECTIONS

Topic Editors:
Maria Tomas, Complexo Hospitalario Universitario A Coruña (INIBIC-CHUAC)
Thomas Keith Wood, Pennsylvania State University (PSU), United States
Rodolfo García-Contreras, National Autonomous University of Mexico, Mexico

Citation: Tomas, M., Wood, T. K., García-Contreras, R., eds. (2019). Drug Re-Purposing for the Treatment of Bacterial and Viral Infections. Lausanne: Frontiers Media SA. doi: 10.3389/978-2-88963-246-6

Table of Contents

frontiers in Cellular and Infection Microbiology

EDITORIAL
published: 13 November 2019
doi: 10.3389/fcimb.2019.00387

Editorial: Drug Re-purposing for the Treatment of Bacterial and Viral Infections

Rodolfo García-Contreras[1]*, *Thomas K. Wood*[2]* and *Maria Tomás*[3]*

[1] Department of Microbiology and Parasitology, Faculty of Medicine, National Autonomous University of Mexico, Mexico City, Mexico, [2] Department of Chemical Engineering, Pennsylvania State University, University Park, PA, United States, [3] Department of Microbiology, Instituto de Investigación Biomédica, Complejo Universitario a Coruña, Universidad de a Coruña, A Coruña, Spain

Keywords: antimicrobial peptides, phages, anti-tumoral, anti-virulence, drug libraries, antiprotozoal, anthelmintic

Editorial on the Research Topic

Drug Re-purposing for the Treatment of Bacterial and Viral Infections

OPEN ACCESS

Edited and reviewed by:
Nahed Ismail,
University of Illinois at Chicago, United States

***Correspondence:**
Rodolfo García-Contreras
rgarc@bq.unam.mx
Thomas K. Wood
tuw14@psu.edu
Maria Tomás
ma.del.mar.tomas.carmona@sergas.es

Specialty section:
This article was submitted to Clinical Microbiology, a section of the journal Frontiers in Cellular and Infection Microbiology

Received: *25 September 2019*
Accepted: *29 October 2019*
Published: *13 November 2019*

Citation:
García-Contreras R, Wood TK and Tomás M (2019) Editorial: Drug Re-purposing for the Treatment of Bacterial and Viral Infections. Front. Cell. Infect. Microbiol. 9:387. doi: 10.3389/fcimb.2019.00387

In this Research Topic, about the repurposing for the treatment of bacterial and viral infections, 13 works were published on the use of peptides; on channel-inhibitors and both PBox and LOPAC 1280 molecule libraries; on drugs using infectology, oncology, central nervous system, and metabolism, as well as on phage therapy and natural compounds.

In reference to the use of peptides, Baker et al. performed screening using synthetic peptidomimetics in combination with the antibiotics rifampicin and azithromycin (mainly active for Gram positive bacteria) against multidrug resistant *Escherichia coli* and *Klebsiella pneumoniae* in order to identify those combinations that could enhance the antibiotic's activity, finding that two subclasses of α-peptide/β-peptoid hybrids were suitable. Moreover, some of the combinations also potentiated ticarcillin/clavulanate and erythromycin against *E. coli*, and clindamycin against *K. pneumoniae* and increased the sensitivity of *Pseudomonas aeruginosa* ATCC 27853 as well (Baker et al.).

In addition, two drugs were analyzed with antimicrobial agents in this Research Topic from the infectiology field. The first one, pentamidine, which is an antiprotozooal and antifungal compound, was analyzed alone and in combination with antimicrobials (aminoglycosides, rifampicin, tigecycline, and doripenem) in strains of carbapenemase-producing and/or colistin-resistant *Enterobacteriaceae* (*Klebsiella pneumoniae*, *Escherichia coli,* and *Enterobacter cloacae*) (Cebrero-Cangueiro et al.). Pentamidine plus rifampicin was the combination that showed synergism in the strains analyzed, making it a new alternative for the treatment of infections caused by carbapenemase-producing and/or colistin-resistant *Enterobacteriaceae*. For the second drug, niclosamide, an anthelmintic drug increased the effects of colistin against colistin sensitive and resistant strains of *A. baumannii* and *K. pneumoniae,* the authors showed that this potentiation is due an increase in the negative bacterial surface charge which favors electrostatic interactions with cationic colistin (Ayerbe-Algaba et al.).

Compounds from two libraries of the molecules were also studied in this Research Topic, the PBox library and LOPAC 1280 library. The Open Access Pathogen Box (PBox) presents a platform to identify new treatments against antibiotic-resistant bacteria through repurposing (Bhandari et al.). Bhandari et al. analyzed the PBox library, which is composed of ∼400 compounds, finding

13 compounds with potent antibacterial activity against planktonic and biofilm of isolates of *S. aureus*, ATCC 29213 (methicillin sensitive) and ATCC 700699 (methicillin resistant). These compounds were not cytotoxic for the mouse macrophage cell line, RAW264.7. Of the 13 compounds, two of them (MMV687251 and MMV676477) have structural similarity to vancomycin when comparing their fingerprints of atomic pairs using the Tanimoto coefficient method (Bhandari et al.). Using the LOPAC 1280 and NPC libraries, Cheng et al. found that seven approved drugs with non-antimicrobial indications were effective against *Acinetobacter baumannii* strain AB5075, a highly virulent and MDR strain (resistant to 25 first-line antibiotics for Gram-negatives). Moreover, of the seven candidates, three of them (5-fluorouracil, fluspirilene, and Bay 11-7082) restored the sensitivity of the strain against azithromycin and colistin (Cheng et al.).

For phage therapy, three reviews have been published in this Research Topic. In the first one, Fernández et al. analyzed the current applications of phages and phage-derived lytic proteins in veterinary medicine (prevention and treatment of animal infectious diseases), agriculture (control of bacterial plant diseases), food safety (control of zoonotic bacteria in primary production, sanitizing, and disinfection as well as food biopreservation), and finally, environmental protection (wastewater treatment). In this work, several products from phage therapy were analyzed against pathogens such as *Salmonella*, *Clostridium perfringens*, *Escherichia coli* O157:H7, and *Listeria monocytogenes* (Fernández et al.). In the second review, Furfaro et al. studied the clinical trials and regulatory hurdles for bacteriophages therapy (including lysins and magistral phages) for *A. baumannii*, *P. aeruginosa* and *Enterobacteriaceae*. Moreover, the authors provided a current summary of human phage therapy trials and the range of target sites/infections obtained in the www.clinicaltrials.gov website: Chronic otitis, diarrhea and gastrointestinal disorders, diabetic foot and venous leg ulcers, infected burn wounds, life-threatening as well as urinary tract infections (Furfaro et al.). In the last work, Tagliaferri et al. performed a deep overview about studies using phage-antibiotic combinations (ß-lactams, aminoglycosides, fluorquinolones, polymyxins, tetracyclines, and others) against pathogenic bacteria separated *in vitro* (plaque, planktonic, and biofilm) and *in vivo* (human, mouse/rat, broiler, and *Galleria mellonella*) as well as studies for Gram negative strains such as *P. aeruginosa*, *Escherichia coli*, *Klebsiella pneumoniae*, *Burkholderia cepacia,* and Gram positive isolates, such as *Staphylococcus aureus* and *Enterococcus faecalis* (Tagliaferri et al.).

In a theoretical work, Mujawar et al. explored the potential of 19 anti-typhoid- drugs, two phenalenone-furanone derivatives and other 15 drugs with phenalenone or furanone moieties mostly used against Gram positive bacteria to bind and inhibit a set of seven important chaperones or members of two component signal transduction systems (including DnaK, SicA, and EnvZ), finding that XR770, one of the two phenaleno-furanone moiety-based derivatives included, had the best binding interactions and stability suggesting it is the best candidate for a new anti-*Salmonella* drug. Nevertheless, experimental work is needed in order to validate this finding.

For combat-related infections, to prevent them is pivotal, and in this regard, Liu et al. focused on the design of a novel antimicrobial coating for intravascular catheters, which are the main source of nosocomial bacteremia and caused mainly by Gram positive bacteria. Interestingly, the active component of this coating is the antirheumatic drug auranofin which also has antibacterial antifungal and anti-biofilm activities due the inhibition of thioredoxin reductase causing a Redox imbalance. This novel coating that also includes polyurethane as a drug carrier was able to inhibit the growth of MRSA and its biofilm formation *in vitro*, and was also biocompatible with both erythrocyte and liver cells (Liu et al.).

Gallium nitrate is commonly used to treat hypercalcemia malignancy, and previously it was shown that it had remarkable antibacterial properties against *P. aeruginosa* and *A. baumannii*, interfering with iron transport and metabolism, hence making it a suitable drug for repurposing. In their work, Hijazi et al. performed the first comparison of the effects of gallium nitrate and another two gallium formulations gallium maltolate and Ga(III)-protoporphyrin IX (GaPPIX) in strains of all the ESKAPE bacteria in different culture media including RPMI supplemented with human serum with low free iron concentrations and which mimic the *in vivo* environment. Interestingly, gallium maltolate and gallium nitrate had similar activities in this medium but GaPPIX lost its activity due its complexation with albumin. Moreover, this work allowed the identification of the *hemO* gene cluster as the main route for the intake of GaPPIX in *A. baumanii* (Hijazi et al.).

According to the discovery of suitable drug candidates for its repurposing as antibacterial compounds, Radosevic et al. performed a virtual sequential screening of 2,627 approved small compounds as inhibitors of the M2 channel protein of the Influenza A virus that were able to inhibit the wild-type channel as well as a channel with the S31N mutation that rendered resistant to adamantanes (the canonical blockers of the M2 channel), finding five potential candidates. One of the best candidates, guanethidine, successfully decreased viral titers of H1N1 infected cells (Radosevic et al.).

Finally, in this Research Topic, a review was presented about drug repurposing from infectology (antiretroviral, anthelminthic, antiprotozoal, and antifungal), oncology (antineoplastic and selective estrogen receptor modulator), the central nervous system (antidepressant and antipsychotic), metabolism (anti-inflammatory and diuretic), and natural compounds (stilbene, anticancer, antioxidant, and essential oil) to fight colistin and carbapenem-resistant belonging ESKAPE-group bacteria (*Enteroccocus faecium, S. aureus, K. pneumoniae, A. baumannii, P. aeruginosa, Enterobacter* species) (Peyclit et al.).

In conclusion, "re-purposing" (defined as investigating new uses for existing approved drugs) has gained renewed interest, as reflected in the works published in this this special issue of Frontiers in Cellular and Infection Microbiology which may help to speed up the drug development process and save years of expensive research invested in antimicrobial drug development.

AUTHOR CONTRIBUTIONS

RG-C and MT wrote the manuscript using papers revised as editors in this Research Topic. TW participated in the supervision of the writing of the manuscript.

FUNDING

This study was funded by grant PI16/01163 awarded to MT within the State Plan for R + D + I 2013–2016 (National Plan for Scientific Research, Technological Development and Innovation 2008–2011) and co-financed by the ISCIII-Deputy General Directorate for Evaluation and Promotion of Research—European Regional Development Fund A way of Making Europe and Instituto de Salud Carlos III FEDER, Spanish Network for the Research in Infectious Diseases (REIPI, RD16/0016/0006) and by the Study Group on Mechanisms of Action and Resistance to Antimicrobials, GEMARA (SEIMC, http://www.seimc.org/).

Conflict of Interest: The authors declare that the research was conducted in the absence of any commercial or financial relationships that could be construed as a potential conflict of interest.

frontiers in Cellular and Infection Microbiology

OPINION
published: 22 August 2018
doi: 10.3389/fcimb.2018.00296

Application of Bacteriophages in the Agro-Food Sector: A Long Way Toward Approval

*Lucía Fernández, Diana Gutiérrez, Ana Rodríguez and Pilar García**

Departamento de Tecnología y Biotecnología de Productos Lácteos, Instituto de Productos Lácteos de Asturias (IPLA-CSIC), Villaviciosa, Spain

Keywords: bacteriophage, phage lytic proteins, phage therapy, food industry, disinfection

The rapid increase in multi-drug resistant (MDR) pathogens has put notable pressure on Health Authorities, who foresee an uncertain future for global human health. In June 2017, the European Commission adopted the "EU One Health action plan against antimicrobial resistance," thereby providing a framework for reducing the emergence and spread of antimicrobial resistance as well as boosting the development of new effective antimicrobials. Nowadays, nobody doubts that the use of antibiotics in agro-food production should be properly controlled, as it represents a major source of bacterial resistance acquisition that further reaches clinical settings. Therefore, bacteria control measures other than antibiotics are presently being assessed in order to both reduce food-borne outbreaks and stop the spread of MDR zoonotic bacteria. Among the many antimicrobials suggested to replace or complement traditional antibiotics, bacteriophages and phage-derived proteins (collectively known as phage therapy) are strong candidates for the treatment of human bacterial infections, rescuing the idea from previous work made in Eastern Europe (Sulakvelidze and Morris, 2001). However, after their resurgence almost 20 years ago, it is rather puzzling that we do not have more commercial phage-based products to fight against MDR bacteria. To understand why phage therapy strategies are taking so long to reach the market, we need to examine in detail the nature and properties of these antimicrobials, as well as the existing legal framework.

While bacteriophages can be rightfully considered the natural enemies of bacteria, these viruses also maintain an important relationship with their hosts through modulating microbial populations and promoting their evolution by horizontal gene transfer (Clokie et al., 2011). Indeed, as the most abundant organisms in the biosphere, the role of phages in different ecosystems, such as the oceans (Breitbart, 2012) or the human gut, is generating a huge interest (Manrique et al., 2017). As antimicrobials, phages offer some compelling advantages over more conventional agents, including specificity, safety, effectiveness against MDR bacteria, and easy genetic manipulation. Moreover, phage lytic enzymes (endolysins and virion-associated peptidoglycan hydrolases) are considered as a new class of antibiotics, named enzybiotics, and also exhibit many desirable properties. Thus, in addition to high lytic ability, specificity and modular structure, it is worth noting that bacteria resistant to enzybiotics have not been detected so far (Fischetti, 2010; Rodríguez-Rubio et al., 2013).

Following publication of the early successful results of phage therapy, the idea was quickly translated to other fields such as agriculture, veterinary medicine, food safety, and wastewater treatment, where this approach was well received (García et al., 2010; Jassim et al., 2016; Carvalho et al., 2017; **Figure 1**). In the agro-food context, both types of antimicrobials (phages and phage lytic proteins) can be used to ensure food safety along the whole food chain (from farm to fork) (García et al., 2008). One potential target sector for the application of bacteriophages is primary production, where they can replace or complement antibiotics and pesticides. As a result, phages could help to limit the rise in antibiotic resistance associated with agricultural and livestock farming practices. Indeed, bacteriophages have already given successful results against bacterial crop diseases, and three different phage-based products (Agriphage in the US, Erwiphage in Hungary, and Biolyse in the UK) are currently on the market despite limitations due to the sensitivity of phages to UV

OPEN ACCESS

Edited by:
Maria Tomas, Complexo Hospitalario Universitario A Coruña, Spain

Reviewed by:
Adelaide Almeida, University of Aveiro, Portugal
Jorge Reinheimer, National University of the Littoral, Argentina

****Correspondence:***
Pilar García
pgarcía@ipla.csic.es

Received: *31 May 2018*
Accepted: *03 August 2018*
Published: *22 August 2018*

Citation:
Fernández L, Gutiérrez D, Rodríguez A and García P (2018) Application of Bacteriophages in the Agro-Food Sector: A Long Way Toward Approval. Front. Cell. Infect. Microbiol. 8:296. doi: 10.3389/fcimb.2018.00296

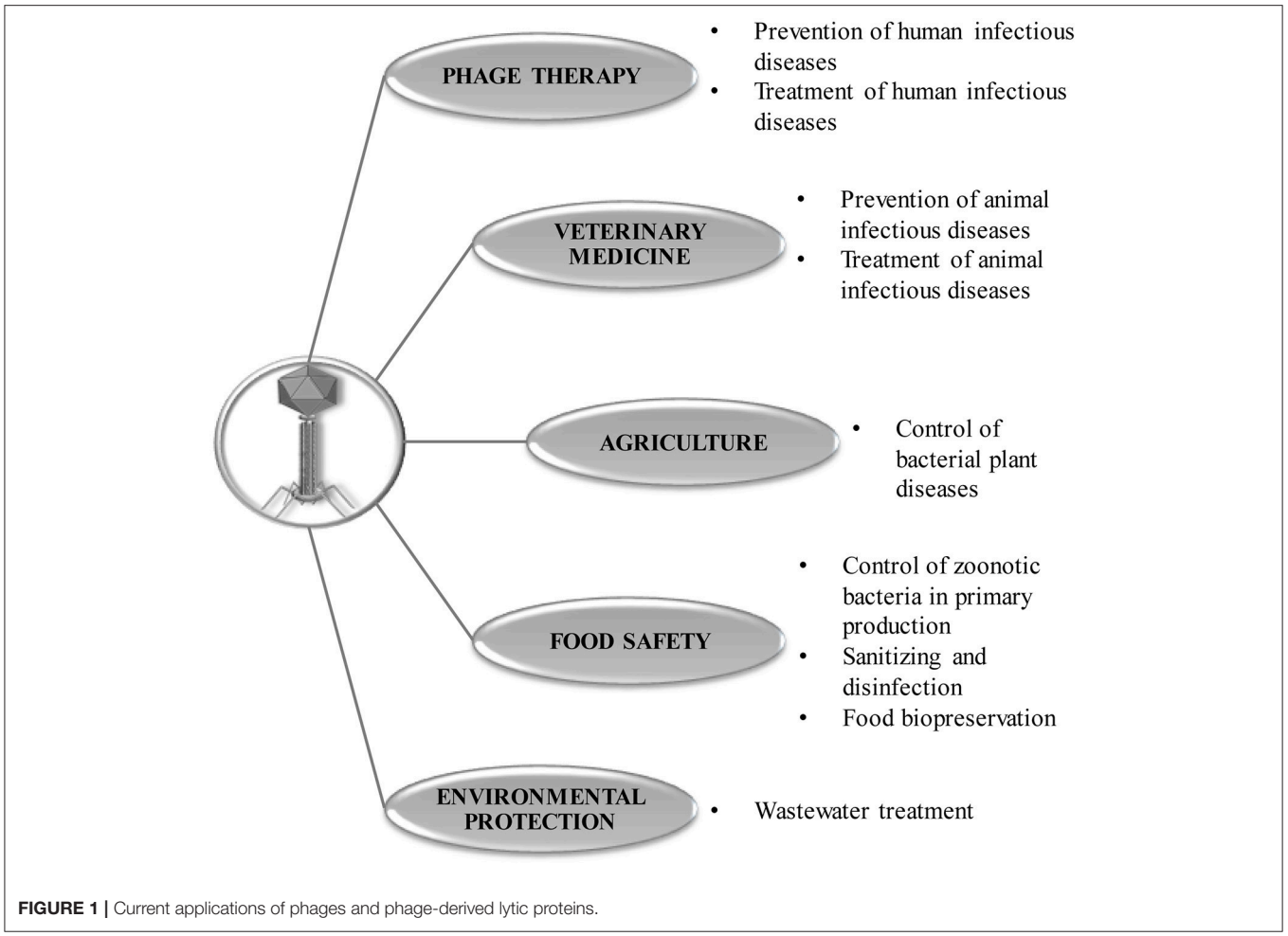

FIGURE 1 | Current applications of phages and phage-derived lytic proteins.

light or certain soil conditions (Buttimer et al., 2017). The other large sector in primary production includes livestock farming and aquaculture, where the need for antibiotics is expected to continue increasing dramatically to meet the growing demand for meat and fish (Van Boeckel et al., 2015). The use of bacteriophages to reduce zoonotic bacteria in animals is promising (Atterbury, 2009), with the main drawbacks being inactivation of phages in the gut and removal of phages from the circulatory system following oral and parenteral administration, respectively. However, there are several studies demonstrating the efficacy and potential of phage therapy in animals for the control of infectious diseases (Richards, 2014; Carvalho et al., 2017; Doss et al., 2017; Wernicki et al., 2017). Furthermore, a US company has developed and licensed bacteriophage-based animal healthcare products effective against *Salmonella* (PLSV-1^{TM}) and *Clostridium perfringens* (INT-401^{TM}) in poultry, aimed at both prophylaxis and treatment.

Although more indirectly, surface sanitizing in livestock facilities and food industries also constitutes a source of antimicrobial resistance emergence due to the existence of cross-resistance between biocides and antibiotics (Hernández et al., 2011). In this regard, phages can also provide an attractive alternative to traditional disinfectants and some products have already been approved for this purpose. For example, two US companies commercialize products for the disinfection of surfaces against *Salmonella* (BacWash^{TM}) and *E. coli* O157:H7 (Finalyse^{TM}). Besides surface decontamination, phages can also be applied as food biopreservatives. Although this application appears even more complicated from a regulatory perspective, several phage products intended as food additives are currently marketed in the US. Thus, phage preparations against *Listeria monocytogenes* (Listshield^{TM}), *Salmonella enterica* (SalmoFresh^{TM}), and *Escherichia coli* (Ecoshield^{TM}) have received GRAS designation by the FDA for direct application to food and are commercially available. In the EU, on the other hand, the use of bacteriophages in food from animal origin was evaluated by the European Food Safety Authority (EFSA) in 2009. More recently, the use of PhageGuard Listex for removing *L. monocytogenes* from raw fish was assessed in 2012. In both studies, EFSA concluded that bacteriophages are harmless for consumers but it is not clear whether they can protect against food re-contamination. Finally, bacteriophages have been approved as processing-aids in food processing and handling in several countries. Indeed, two such products against *L. monocytogenes* (PhageGuard Listex) and *Salmonella* (PhageGuard S) are currently available.

Both products can also be used for decontamination of surfaces.

Overall, the main hurdles for the extensive use of bacteriophages in the agro-food industry can be summarized in technical and legal inconveniences. From a legal perspective, regulatory frameworks for antimicrobials are very restrictive in most countries, seriously limiting the introduction of new compounds in the agro-food sector.

Regarding technical shortcomings, some of the problems encountered affect phage stability, bacterial resistance or gene transfer, many of which can potentially be solved in a relatively easy way with the current engineering techniques e.g., CRISPR-Cas (Bari et al., 2017). However, further work is still necessary to adapt lab-scale results to large-scale bacteriophage production and purification by companies according to good manufacturing practices (GMP). Another important drawback regarding the commercialization of phage-based products is the need to design phage mixtures effective against the highest possible number of strains belonging to the target bacterium. Additionally, these mixtures often have to be regularly adapted to avoid the emergence of phage-resistant strains in the place of application. Moreover, this disadvantage is frequently aggravated by the existence of restrictive regulations. For instance, in the EU, changes in the phage mixture composition of a plant protection product may require a new registration (1107/2009 EC).

In addition to the setbacks indicated above, there are other unsolved concerns such as the consequences of introducing high concentrations of phages in the environment. In that sense, it is worth analysing carefully the previous mistakes made with antibiotics. For example, the scientific community is now aware that the possibility of selecting multi-phage resistant bacteria, the evolution of the target bacteria or how phages may affect microbial communities in nature should be evaluated during the development of novel antimicrobial strategies. The frequency of phage resistance development can vary depending on the specific phage between 10^{-4} and 10^{-7} (Gutiérrez et al., 2015; Silva et al., 2016; Valério et al., 2017). However, it must be mentioned that this frequency can be 10- or even 100-fold lower than that of antibiotic resistance development (Carlton, 1999; Valério et al., 2017). Moreover, there are some interesting characteristics of phage resistance that make it different from antibiotic resistance and are, as a result, also worth mentioning here (Oechslin, 2018). Most importantly, phage resistance would only arise in cells of the target species and it is generally the result of mutations and, consequently, non-transmissible. Moreover, these mutations frequently affect phage receptor proteins which often play essential roles for the bacterium, thereby leading to fitness and/or virulence loss. Finally, unlike other antimicrobials, bacteriophages can themselves evolve to adapt to the appearance of bacterial resistance as part of a co-evolutionary arms race. Several studies have shown that phage resistant mutants do indeed appear during the course of phage therapy in farm animal and clinical trials; however, there has been success in overcoming this problem by using different phage cocktails until complete eradication of the infection (Oechslin, 2018). In addition to phage resistance development, phage-mediated horizontal gene transfer should be avoided to prevent the spread of antibiotic resistance and virulence determinants. Taking into account all these potential problems, it appears that bacteriophages, despite being a "green solution," should be inactivated before their release outside industrial settings and farms. Of note, phages are frequently susceptible to sanitizers commonly used in the industry (Agún et al., 2018), as well as some environmental factors like pH, temperature, etc. (Jonczyk et al., 2011; Ly-Chatain, 2014), although they tend to be overall more resistant to environmental challenges than bacteria are. Nonetheless, phage inactivation can prove to be challenging following certain applications, such as crop treatment (Jones et al., 2012) or infection control in aquaculture (Richards, 2014). However, it must be noted that phage persistence in some environments is severely limited by UV-light inactivation, as is the case of the phyllosphere (Jones et al., 2012) or in aquaculture settings (Duarte et al., 2018). To overcome this limitation, some authors have recommended the application of bacteriophages at the end of the day or at night (Duarte et al., 2018). Overall, additional research is still required to examine not only the effectiveness of phages as antimicrobials, but also their persistence in the environment and the emergence of bacterial resistance in field trials.

As it can be gathered from all the above information, our knowledge about bacteriophages and their prospective use is still fairly limited. This leads funding agencies, companies and consumers to feel distrust of these new strategies, although they would be considered eco-friendly. Even for large companies, which are more suitable candidates to invest in this research, the limitations in intellectual property protection of bacteriophages (since they are isolated from nature) is a serious drawback and the implementation of the Nagoya Protocol could further complicate the matter. While a huge effort is being made from scientific institutions by requesting a change in the current path toward approval of phage products for human therapy applications (Verbeken et al., 2014; Kutter et al., 2015), there is no EU regulation allowing the use of phages as disinfectants or as prophylactic/treatment of infectious diseases in animals and plants. In the US, however, the USDA allows the application of phages to livestock animals prior to slaughtering as long as they meet the FSIS Directive 7120.1. Similarly, other countries such as Israel, Canada, Switzerland, Australia and New Zealand have adopted similar regulations.

With "a priori" fewer problems to reach the market, phage lytic proteins are taking a strong impulse in recent years. In fact, there is a significant body of work on endolysins against both Gram-positive and Gram-negative bacteria, and several proteins against *S. aureus* are now being assayed in human clinical trials (Gerstmans et al., 2017; Gutiérrez et al., 2018). These and other proteins in preclinical studies are expected to be commercialized in the next few years, and might be used in veterinary applications. In fact, the effectiveness of endolysins to treat, for instance, staphylococcal cow mastitis was revealed in a recent study carried out by Fan et al. (2016). Similarly, endolysins have been proven to be effective against the main farm animal pathogens such as *C. perfringens* (Swift et al., 2015), *Salmonella* (Rodríguez-Rubio et al., 2016) and *Streptococcus suis* (Wang et al., 2009) and even the bee

pathogen *Paenibacillus larvae* (Oliveira et al., 2015). Phage lytic proteins are also promising adjuvants for classical disinfectants for surface decontamination (Gutiérrez et al., 2016). However, there are three main challenges that should be addressed before the implementation of endolysins in the veterinary sector. For instance, the immunogenicity of phage-derived proteins might result in decreased efficacy as well as in an undesirable immune response (Jun et al., 2014). Nevertheless, this issue can be solved by protein modification (Filatova et al., 2016). Another difficulty is the cost associated to endolysin production. Remarkably, new cost-effective and sustainable strategies to scale up endolysin production have been developed. For instance, recent work published by Stoffels et al. (2017) shows the suitability of a unicellular alga, *Chlamydomonas reinhardtii*, to express phage lytic proteins. Finally, the current regulatory pathways need to be adapted for these new substances. Nevertheless, approval should be more straightforward for endolysins than for phages, as multitude of therapeutic proteins are currently on the market (Dimitrov, 2012).

In summary, we currently have enough expertise and equipment to tackle the technical issues that limit the application of phage therapy. Therefore, it is only a matter of time that these drawbacks can be overcome. In turn, this information should pave the way for regulatory approval by filling the gaps regarding the efficacy and safety of these new antimicrobials. Meanwhile, we should realize that phage therapy does not necessarily have to be identical to antibiotic therapy; therefore, the peculiarities of this new bacteria control strategy may require a different approach. Given the impotence of clinicians to treat patients suffering from antibiotic-resistant infections, if the price to pay is more in-depth and thorough research, the effort will be well worth it.

AUTHOR CONTRIBUTIONS

PG conceived and designed the work. PG, LF, DG, and AR wrote the paper.

ACKNOWLEDGMENTS

This research study was supported by grants AGL2015-65673-R (MINECO, Program of Science, Technology and Innovation 2013–2017, Spain, EU ANIWHA ERA-NET (BLAAT ID: 67)-PCIN-2017-001 (MINEICO, State Program of Research, Development and Innovation focused to Societal Challenges 2013–2017, Spain). Proyecto Intramural CSIC 201770E016, and GRUPIN14-139 (FEDER EU funds, Principado de Asturias, Spain). PG and AR are members of the bacteriophage network FAGOMA and the FWO Vlaanderen funded Phagebiotics research community (WO.016.14).

REFERENCES

Agún, S., Fernández, L., González-Menéndez, E., Martínez, B., Rodríguez, A., and Garcia, P. (2018). Study of the interactions between bacteriophage phiIPLA-RODI and four chemical disinfectants for the elimination of *Staphylococcus aureus* contamination. *Viruses* 10:E103. doi: 10.3390/v10030103

Atterbury, R. J. (2009). Bacteriophage biocontrol in animals and meat products. *Microb. Biotechnol.* 2, 601–612. doi: 10.1111/j.1751-7915.2009.00089.x

Bari, S. M. N., Walker, F. C., Cater, K., Aslan, B., and Hatoum-Aslan, A. (2017). Strategies for editing virulent *Staphylococcal* phages using CRISPR-Cas10. *ACS Synth. Biol.* 6, 2316–2325. doi: 10.1021/acssynbio.7b00240

Breitbart, M. (2012). Marine viruses: truth or dare. *Ann. Rev. Mar. Sci.* 4, 425–448. doi: 10.1146/annurev-marine-120709-142805

Buttimer, C., McAuliffe, O., Ross, R. P., Hill, C., O'Mahony, J., and Coffey, A. (2017). Bacteriophages and bacterial plant diseases. *Front. Microbiol.* 8:34. doi: 10.3389/fmicb.2017.00034

Carlton, R. M. (1999). Phage therapy: past history and future prospects. *Arch. Immunol. Ther. Exp.* 47, 267–274.

Carvalho, C., Costa, A. R., Silva, F., and Oliveira, A. (2017). Bacteriophages and their derivatives for the treatment and control of food-producing animal infections. *Crit. Rev. Microbiol.* 43, 583–601. doi: 10.1080/1040841X.2016.1271309

Clokie, M. R., Millard, A. D., Letarov, A. V., and Heaphy, S. (2011). Phages in nature. *Bacteriophage* 1, 31–45. doi: 10.4161/bact.1.1.14942

Dimitrov, D. S. (2012). Therapeutic proteins. *Methods Mol. Biol.* 899, 1–26. doi: 10.1007/978-1-61779-921-1_1

Doss, J., Culbertson, K., Hahn, D., Camacho, J., and Barekzi, N. (2017). A review of phage therapy against bacterial pathogens of aquatic and terrestrial organisms. *Viruses* 9:E50. doi: 10.3390/v9030050

Duarte, J., Pereira, C., Moreirinha, C., Salvio, R., Lopesa, A., Wang, D., et al. (2018). New insights on phage efficacy to control *Aeromonas salmonicida* in aquaculture systems: an *in vitro* preliminary study. *Aquaculture* 495, 970–982. doi: 10.1016/j.aquaculture.2018.07.002

Fan, J., Zeng, Z., Mai, K., Yang, Y., Feng, J., Bai, Y., et al. (2016). Preliminary treatment of bovine mastitis caused by *Staphylococcus aureus*, with trx-SA1, recombinant endolysin of *S. aureus* bacteriophage IME-SA1. *Vet. Microbiol.* 191, 65–71. doi: 10.1016/j.vetmic.2016.06.001

Filatova, L. Y., Donovan, D. M., Ishnazarova, N. T., Foster-Frey, J. A., Becker, S. C., Pugachev, V. G., et al. (2016). A chimeric LysK-lysostaphin fusion enzyme lysing *Staphylococcus aureus* cells: a study of both kinetics of inactivation and specifics of interaction with anionic polymers. *Appl. Biochem. Biotechnol.* 180, 544–557. doi: 10.1007/s12010-016-2115-7

Fischetti, V. A. (2010). Bacteriophage endolysins: a novel anti-infective to control Gram-positive pathogens. *Int. J. Med. Microbiol.* 300, 357–362. doi: 10.1016/j.ijmm.2010.04.002

García, P., Martínez, B., Obeso, J. M., and Rodríguez, A. (2008). Bacteriophages and their application in food safety. *Lett. Appl. Microbiol.* 47, 479–485. doi: 10.1111/j.1472-765X.2008.02458.x

García, P., Rodríguez, L., Rodríguez, A., and Martínez, B. (2010). Food biopreservation: promising strategies using bacteriocins, bacteriophages and endolysins. *Trends Food Sci. Technol.* 21, 373–382. doi: 10.1016/j.tifs.2010.04.010

Gerstmans, H., Criel, B., and Briers, Y. (2017). Synthetic biology of modular endolysins. *Biotechnol. Adv.* 36, 624–640. doi: 10.1016/j.biotechadv.2017.12.009

Gutiérrez, D., Fernández, L., Rodríguez, A., and García, P. (2018). Are phage lytic proteins the secret weapon to kill *Staphylococcus aureus*? *MBio.* 9:e01923–17. doi: 10.1128/mBio.01923-17

Gutiérrez, D., Rodríguez-Rubio, L., Martínez, B., Rodríguez, A., and García, P. (2016). Bacteriophages as weapons against bacterial biofilms in the food industry. *Front. Microbiol.* 7:825. doi: 10.3389/fmicb.2016.00825

Gutiérrez, D., Vandenheuvel, D., Martínez, B., Rodríguez, A., Lavigne, R., and García, P. (2015). Two phages, phiIPLA-RODI and phiIPLA-C1C, lyse mono- and dual-species *Staphylococcal* biofilms. *Appl. Environ. Microbiol.* 81, 3336–3348. doi: 10.1128/AEM.03560-14

Hernández, A., Ruiz, F. M., Romero, A., and Martínez, J. L. (2011). The binding of triclosan to SmeT, the repressor of the multidrug efflux pump SmeDEF, induces antibiotic resistance in *Stenotrophomonas maltophilia*. *PLoS Pathog.* 7:e1002103. doi: 10.1371/journal.ppat.1002103

Jassim, S. A., Limoges, R. G., and El-Cheikh, H. (2016). Bacteriophage biocontrol in wastewater treatment. *World J. Microbiol. Biotechnol.* 32, 70. doi: 10.1007/s11274-016-2028-1

Jonczyk, E., Kłak, M., Miedzybrodzki, R., and Górski, A. (2011). The influence of external factors on bacteriophages. *Folia Microbiol.* 56, 191–200. doi: 10.1007/s12223-011-0039-8

Jones, J. B., Vallad, G. E., Iriarte, F. B., Obradović, A., Wernsing, M. H., Jackson, L. E., et al. (2012). Considerations for using bacteriophages for plant disease control. *Bacteriophage* 2, 208–214. doi: 10.4161/bact.23857

Jun, S. Y., Jung, G. M., Yoon, S. J., Choi, Y. J., Koh, W. S., Moon, K. S., et al. (2014). Preclinical safety evaluation of intravenously administered SAL200 containing the recombinant phage endolysin SAL-1 as a pharmaceutical ingredient. *Antimicrob. Agents Chemother.* 58, 2084–2088. doi: 10.1128/AAC.02232-13

Kutter, E. M., Kuhl, S. J., and Abedon, S. T. (2015). Re-establishing a place for phage therapy in western medicine. *Future Microbiol.* 10, 685–688. doi: 10.2217/fmb.15.28

Ly-Chatain, M. H. (2014). The factors affecting effectiveness of treatment in phages therapy. *Front. Microbiol.* 5:51. doi: 10.3389/fmicb.2014.00051

Manrique, P., Dills, M., and Young, M. J. (2017). The human gut phage community and its implications for health and disease. *Viruses* 9:E141. doi: 10.3390/v9060141

Oechslin, F. (2018). Resistance development to bacteriophages occurring during bacteriophage therapy. *Viruses* 10:E351. doi: 10.3390/v10070351

Oliveira, A., Leite, M., Kluskens, L. D., Santos, S. B., Melo, L. D., and Azeredo, J. (2015). The first *Paenibacillus larvae* bacteriophage endolysin (PlyPl23) with high potential to control American foulbrood. *PLoS ONE* 10:e0132095. doi: 10.1371/journal.pone.0132095

Richards, G. P. (2014). Bacteriophage remediation of bacterial pathogens in aquaculture: a review of the biotechnology. *Bacteriophage* 4:e975540. doi: 10.4161/21597081.2014.975540

Rodríguez-Rubio, L., Gerstmans, H., Thorpe, S., Mesnage, S., Lavigne, R., and Briers, Y. (2016). DUF3380 domain from a *Salmonella* phage endolysin shows potent N-acetylmuramidase activity. *Appl. Environ. Microbiol.* 82, 4975–4981. doi: 10.1128/AEM.00446-16

Rodríguez-Rubio, L., Martínez, B., Donovan, D. M., Rodríguez, A., and García, P. (2013). Bacteriophage virion-associated peptidoglycan hydrolases: potential new enzybiotics. *Crit. Rev. Microbiol.* 39, 427–434. doi: 10.3109/1040841X.2012.723675

Silva, Y. J., Moreirinha, C., Pereira, C., Costa, L., Rocha, R. J. M., Cunha, A., et al. (2016). Biological control of *Aeromonas salmonicida* infection in juvenile Senegalese sole (*Solea senegalensis*) with Phage AS-A. *Aquaculture* 450, 225–233. doi: 10.1016/j.aquaculture.2015.07.025

Stoffels, L., Taunt, H. N., Charalambous, B., and Purton, S. (2017). Synthesis of bacteriophage lytic proteins against *Streptococcus pneumoniae* in the chloroplast of *Chlamydomonas reinhardtii*. *Plant Biotechnol. J.* 15, 1130−1140. doi: 10.1111/pbi.12703

Sulakvelidze, A., and Morris, J. G. Jr. (2001). Bacteriophages as therapeutic agents. *Ann. Med.* 33, 507–509. doi: 10.3109/07853890108995959

Swift, S. M., Seal, B. S., Garrish, J. K., Oakley, B. B., Hiett, K., Yeh, H. Y., et al. (2015). A thermophilic phage endolysin fusion to a *Clostridium perfringens*-specific cell wall binding domain creates an anti-*Clostridium* antimicrobial with improved thermostability. *Viruses* 7, 3019–3034. doi: 10.3390/v7062758

Valério, N., Oliveira, C., Jesus, V., Branco, T., Pereira, C., Moreirinha, C., et al. (2017). Effects of single and combined use of bacteriophages and antibiotics to inactivate *Escherichia coli*. *Virus. Res.* 240, 8–17. doi: 10.1016/j.virusres.2017.07.015

Van Boeckel, T. P., Brower, C., Gilbert, M., Grenfell, B. T., Levin, S. A., Robinson, T. P., et al. (2015). Global trends in antimicrobial use in food animals. *Proc. Natl. Acad. Sci. U.S.A.* 112, 5649–5654. doi: 10.1073/pnas.1503141112

Verbeken, G., Huys, I., Pirnay, J. P., Jennes, S., Chanishvili, N., Scheres, J., et al. (2014). Taking bacteriophage therapy seriously: a moral argument. *Biomed Res. Int.* 2014:621316. doi: 10.1155/2014/621316

Wang, Y., Sun, J. H., and Lu, C. P. (2009). Purified recombinant phage lysin LySMP: an extensive spectrum of lytic activity for swine *Streptococci*. *Curr. Microbiol.* 58, 609–615. doi: 10.1007/s00284-009-9379-x

Wernicki, A., Nowaczek, A., and Urban-Chmiel, R. (2017). Bacteriophage therapy to combat bacterial infections in poultry. *Virol. J.* 14:179. doi: 10.1186/s12985-017-0849-7

Conflict of Interest Statement: The authors declare that the research was conducted in the absence of any commercial or financial relationships that could be construed as a potential conflict of interest.

frontiers in Cellular and Infection Microbiology

ORIGINAL RESEARCH
published: 10 September 2018
doi: 10.3389/fcimb.2018.00316

Antimicrobial Activity of Gallium Compounds on ESKAPE Pathogens

Sarah Hijazi[1], *Daniela Visaggio*[1], *Mattia Pirolo*[1], *Emanuela Frangipani*[1], *Lawrence Bernstein*[2] *and Paolo Visca*[1]*

[1] Department of Science, Roma Tre University, Rome, Italy, [2] Terrametrix, Menlo Park, CA, United States

ESKAPE bacteria are a major cause of multidrug-resistant infections, and new drugs are urgently needed to combat these pathogens. Given the importance of iron in bacterial physiology and pathogenicity, iron uptake and metabolism have become attractive targets for the development of new antibacterial drugs. In this scenario, the FDA-approved iron mimetic metal Gallium [Ga(III)] has been successfully repurposed as an antimicrobial drug. Ga(III) disrupts ferric iron-dependent metabolic pathways, thereby inhibiting microbial growth. This work provides the first comparative assessment of the antibacterial activity of $Ga(NO_3)_3$ (GaN), Ga(III)-maltolate (GaM), and Ga(III)-protoporphyrin IX (GaPPIX), belonging to the first-, second- and third-generation of Ga(III) formulations, respectively, on ESKAPE species, including reference strains and multidrug-resistant (MDR) clinical isolates. In addition to the standard culture medium Mueller Hinton broth (MHB), iron-depleted MHB (DMHB) and RPMI-1640 supplemented with 10% human serum (HS) (RPMI-HS) were also included in Ga(III)-susceptibility tests, because of their different nutrient and iron contents. All ESKAPE species were resistant to all Ga(III) compounds in MHB and DMHB (MIC $> 32\,\mu M$), except *Staphylococcus aureus* and *Acinetobacter baumannii*, which were susceptible to GaPPIX. Conversely, the antibacterial activity of GaN and GaM was very evident in RPMI-HS, in which the low iron content and the presence of HS better mimic the *in vivo* environment. In RPMI-HS about 50% of the strains were sensitive (MIC < 32) to GaN and GaM, both compounds showing a similar spectrum of activity, although GaM was more effective than GaN. In contrast, GaPPIX lost its antibacterial activity in RPMI-HS likely due to the presence of albumin, which binds GaPPIX and counteracts its inhibitory effect. We also demonstrated that the presence of multiple heme-uptake systems strongly influences GaPPIX susceptibility in *A. baumannii*. Interestingly, GaN and GaM showed only a bacteriostatic effect, whereas GaPPIX exerted a bactericidal activity on susceptible strains. Altogether, our findings raise hope for the future development of Ga(III)-based compounds in the treatment of infections caused by multidrug-resistant ESKAPE pathogens.

Keywords: antibacterial, ESKAPE, gallium maltolate, gallium nitrate, gallium protoporphyrin IX, iron uptake

OPEN ACCESS

Edited by:
Rodolfo García-Contreras, Universidad Nacional Autónoma de México, Mexico

Reviewed by:
Rolf Kümmerli, Universität Zürich, Switzerland
Gian Maria Rossolini, Università degli Studi di Firenze, Italy

***Correspondence:**
Paolo Visca
paolo.visca@uniroma3.it

Received: *01 June 2018*
Accepted: *20 August 2018*
Published: *10 September 2018*

Citation:
Hijazi S, Visaggio D, Pirolo M, Frangipani E, Bernstein L and Visca P (2018) Antimicrobial Activity of Gallium Compounds on ESKAPE Pathogens. Front. Cell. Infect. Microbiol. 8:316. doi: 10.3389/fcimb.2018.00316

INTRODUCTION

ESKAPE species (*Enterococcus faecium*, *Staphylococcus aureus*, *Klebsiella pneumoniae*, *Acinetobacter baumannii*, *Pseudomonas aeruginosa*, and *Enterobacter* species) are among the most common bacterial pathogens in nosocomial infections, causing extensive morbidity and mortality, especially in critically ill and immunocompromised patients (Rice, 2010). All these species are characterized by a high level of antibiotic resistance (Pendleton et al., 2013), which recently prompted the World Health Organization to list ESKAPE pathogens among the greatest threats to human health, and to boost research on new effective drugs for treatment of antibiotic-resistant infections (World Health Organization, 2017). Among Gram-negative ESKAPE species, *K. pneumoniae*, *A. baumannii* and *P. aeruginosa* have reached an alarmingly high level of resistance, causing infections which are no longer treatable with conventional antibiotic therapies (Deplano et al., 2005; Elemam et al., 2009; Nowak et al., 2017). Depriving bacteria of essential nutrients, such as iron, is a viable strategy for the development of new antibacterials. Iron is a key nutrient for nearly all forms of life, including bacteria, being a cofactor of many vital enzymes (e.g., those involved in cellular respiration, DNA synthesis, and defense against reactive oxygen species) (Andrews et al., 2003). During infection, bacteria are faced with iron scarcity in body fluids, and must gain access to iron bound to transferrins (e.g., transferrin and lactoferrin) and/or heme-containing proteins (e.g., hemoglobin and myoglobin) (Weinberg, 2009). To counteract iron-limitation, bacteria have developed high-affinity iron-uptake strategies, such as: (i) the production of low-molecular-weight compounds, called siderophores, which bind Fe(III) and actively transport the metal into the cell (Miethke and Marahiel, 2007); (ii) the ability to utilize heme iron, by producing hemophores and/or specific transport systems for heme and heme-binding proteins (Wandersman and Delepelaire, 2004); and (iii) the active transport of Fe(II) through the cytoplasmic membrane *via* the Feo system (Cartron et al., 2006). Given the essential role of iron in bacterial physiology and pathogenicity, iron uptake and metabolism have become attractive targets for the development of new antibacterials (Ballouche et al., 2009; Foley and Simeonov, 2012). In this regard, the ferric iron [Fe(III)] mimetic ion gallium [Ga(III)] has been shown to inhibit the growth of many bacterial and fungal species by interfering with iron-dependent metabolic pathways (Bastos et al., 2010; Minandri et al., 2014). Given the chemical similarity between Fe(III) and Ga(III), microorganisms cannot easily distinguish between these two ions, so that Ga(III) competes with Fe(III) for incorporation into essential proteins and enzymes. However, unlike Fe(III), Ga(III) cannot be reduced under physiological conditions, resulting in the inhibition of several iron-dependent redox pathways (Bernstein, 1998).

For more than three decades, Ga(III) compounds have been employed as diagnostic tools in medicine. Radioactive ^{67}Ga allows localization of malignant cells and inflammatory or infective foci (Edwards and Hayes, 1969). Citrated $Ga(NO_3)_3$ (GaN, brand name Ganite®, Genta, NJ, USA) was approved by the US FDA for the treatment of cancer-associated hypercalcemia, though it is no longer available. Recently, there has been an expansion in the number of Ga(III) compounds showing therapeutic potential, sometimes categorized in first, second, and third generations, and ranging from simple salts such as $GaCl_3$ and GaN, through metal-organic complexes such as Ga(III)-maltolate (GaM) (Bernstein et al., 2000) and Ga(III)-protoporphyrin IX (GaPPIX) (Chitambar, 2017) (**Figure 1**). It is noted that GaN has very low oral bioavailability and must be parenterally administered, whereas GaM has high oral bioavailability and has been safely administered orally to people (Bernstein et al., 2000).

At present, neither standard protocols nor reference media for Ga(III)-susceptibility testing have been defined, though several lines of evidence indicate that iron irreversibly suppresses the antibacterial properties of Ga(III) (Kaneko et al., 2007; Antunes et al., 2012). Moreover, there are no comparative data on the activity of different Ga(III) compounds against ESKAPE species under standard test conditions, representing a major pitfall to the repurposing of Ga(III) as last-resort antibacterial agent.

In this study, the antibacterial activity of three compounds belonging to the first-, second-, and third-generation Ga(III) formulations, i.e., GaN, GaM, and GaPPIX, was tested on ESKAPE pathogens in culture media characterized by different iron content, namely Mueller-Hinton broth (MHB), iron-deprived MHB (DMHB) (Hackel et al., 2018) and RPMI-1640 tissue culture medium supplemented with 10% complement-free human serum (RPMI-HS), to better mimic the *in vivo* environment (Antunes et al., 2012; Thompson et al., 2012; Bonchi et al., 2015). ESKAPE bacteria resulted more susceptible to Ga(III) compounds in RPMI-HS than in MHB and DMHB. However, the presence of serum albumin in RPMI-HS and the type and number of bacterial heme-uptake systems strongly influenced GaPPIX susceptibility. Intriguingly, GaPPIX exerted a bactericidal activity on some strains, whereas GaN and GaM invariably exhibited bacteriostatic effects.

MATERIALS AND METHODS

Bacterial Strains and Culture Conditions

Bacterial strains used in this work are listed in **Table S1**. Bacteria were routinely cultured for 18 h in Tryptic Soy Broth (TSB, Acumedia) with vigorous shaking. When required, tetracycline (Tc), gentamicin (Gm), and 5-bromo-4-chloro-3-indolyl-β-D-galactopyranoside (X-Gal, Sigma) were added to the media. For *A. baumannii*, 50 μg/ml Tc, and 100 μg/ml Gm were used. For *Escherichia coli* 10 μg/ml Gm and 40 μg/ml X-Gal were used. When vitamins (Vit) were required, 19 μg /ml of nicotinic acid (Sigma-Aldrich), and 2 μg /ml of pyridoxal hydrochloride (MERCK) were added to the media. Bovine hemin chloride (Sigma-Aldrich) was freshly prepared in 10 mM NaOH. Bovine serum albumin (BSA, Sigma-Aldrich) was freshly prepared and added to the media at the final concentration of 5 mg/ml.

Media and Ga(III) Compounds

Three media have been used in this study: (i) BBL Mueller Hinton II (Cation-Adjusted) Broth (MHB, Becton Dickinson) was prepared according to the manufacturer's instructions; (ii)

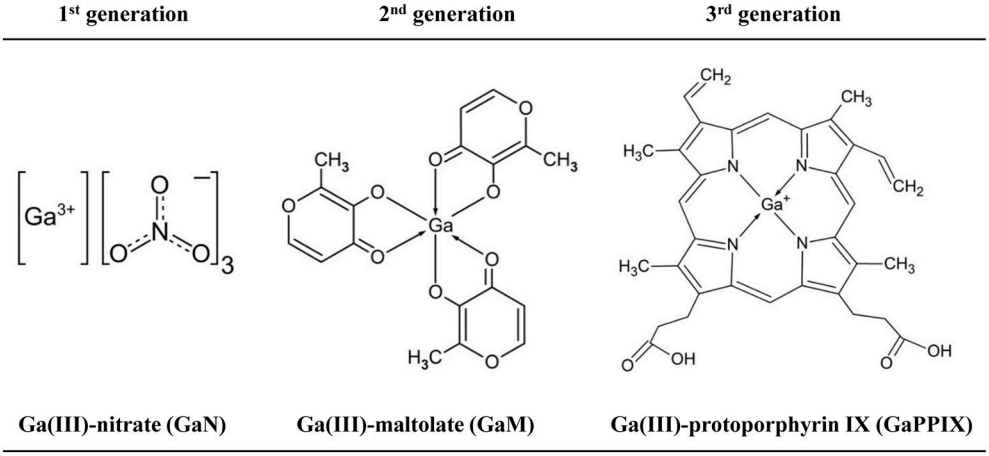

FIGURE 1 | Chemical structures of the three Ga(III) compounds used in this study.

DMHB was prepared following the approved CLSI protocol for antimicrobial susceptibility testing (Hackel et al., 2018). Briefly, MHB was treated for 16 h at 4°C with 100 g/l of the metal-chelating Chelex® 100 resin (Bio-Rad) under moderate stirring, then filtered through Whatman no. 1 filter paper and pH adjusted to 7.3. After autoclaving, $CaCl_2$ and $MgSO_4$ were added to DMHB at the final concentrations of 22.5 and 11.25 μg/ml, respectively; and (iii) RPMI-1640 (Sigma-Aldrich) supplemented with 10% complement-free human serum (RPMI-HS). Human serum was collected from 140 healthy donors, pooled, filtered, and inactivated (30 min, 56°C), as previously described (Antunes et al., 2012). Bulk serum chemistry was: total serum proteins 80 mg/ml; total iron 0.70 μg/ml; ferritin 0.243 μg/ml; transferrin 2.63 mg/ml; total iron binding capacity 4.27 mg/ml (20% transferrin saturation).

Three Ga(III) compounds were used in this study: (i) GaN ($Ga(NO_3)_3 \times 6H_2O$, Sigma-Aldrich; quality tested), freshly prepared as a 100 mM stock solution in water; (ii) GaM (NORAC Pharma, provided by Dr. Bernstein), freshly prepared as a 22 mM stock solution in water; and (iii) GaPPIX (Frontier Scientific), prepared as a 25 mM stock solution in dimethyl sulfoxide (DMSO), and stored at 4°C in the dark.

Iron Content Measurement, Siderophore Production, and β-Galactosidase (LacZ) Activity Assays

The iron concentration of MHB, DMHB, and RPMI-HS was measured by inductively coupled plasma optical emission spectrometry (ICP-OES) using an ICP-OES 710 Varian Spectrometer (Agilent Technologies). Briefly, the medium was mixed with 5% HNO_3, heated for 1 h at 90°C, and filtered through a Millipore membrane (pore size 0.45 μm) prior to ICP-OES analysis.

Siderophore production was determined by the chrome azurol S-Fe(III)-hexadecyltrimethylammonium bromide method (Schwyn and Neilands, 1987). Activity of the *basA*::*lacZ* reporter gene fusion carried by plasmid pMP220::P*basA* (Antunes et al., 2012) was tested in the reference strain *A. baumannii* ATCC 17978, and β-galactosidase levels were expressed as Miller units (Miller, 1972).

Susceptibility Testing of Ga(III) Compounds

The inhibitory activity of Ga(III) compounds on ESKAPE pathogens was assessed by the microdilution method (Clinical Laboratory Standards Institute, 2015), with minor modifications. Bacteria were grown for 18 h in TSB, then washed in saline and diluted to obtain *ca.* 5×10^5 CFU/ml in 200 μl of MHB, DMHB, or RPMI-HS, in the presence of increasing concentrations (0 to 128 μM) of each Ga(III) compound [GaN or GaM or GaPPIX], using 96-well microtiter plates. Plates were incubated for 24 h at 37°C with orbital shaking (110 rpm). The MIC of Ga(III) compounds was determined as the lowest concentration that completely inhibited bacterial growth as detected by the unaided eye (Clinical Laboratory Standards Institute, 2015). To test the effect of Fe(III) and hemin on GaPPIX antibacterial activity, freshly prepared $FeCl_3$ (Sigma-Aldrich) or bovine hemin chloride (Sigma-Aldrich) were added at the indicated final concentrations, into 200 μl of MHB inoculated with *ca.* 5×10^5 CFU/ml, in the presence of GaPPIX supplied at the MIC. Microtiter plates were incubated for up to 24 h at 37°C and bacterial growth {optical density at 600 nm [OD_{600}]} was periodically measured using SPARK 10M TECAN reader.

The antibacterial activity of GaPPIX on *A. baumannii* strains was also assessed by disk diffusion assays. Briefly, 18 h cultures in TSB were washed and diluted in saline to $OD_{600} = 0.1$, then seeded with a sterile swab on the surface of RPMI-HS supplemented with 15 g/l agar (Acumedia). Sterile 6-mm blank disks (ThermoFisher-Oxoid) soaked with 10 μl of a 15 mM solution of GaPPIX were deposited on the agar surface, and the growth inhibition halo was detected after 18 h incubation at 37°C.

Time-Kill Assays

Time-kill kinetic assays of Ga(III) compounds were performed on eleven ESKAPE pathogens according to a previously described procedure (Principe et al., 2009), with minor modifications.

Briefly, tubes containing 1 ml of RPMI-HS supplemented with 28 μM of GaN, GaM or GaPPIX were inoculated with bacteria to a density *ca.* 5×10^5 CFU/ml, and incubated at 37°C with gentle shaking (120 rpm). Aliquots were removed at time 0, 3, 6, and 24 h post-inoculation, and serially diluted in saline for determination of viable counts on Luria Bertani (LB) agar plates.

Identification and Cloning of the Heme-Utilization Gene Clusters in *A. baumannii*

Previously described oligonucleotides and PCR conditions were used to check the presence of genes belonging to the heme iron-uptake gene cluster 2 (hereafter termed *hemT* cluster), and the heme iron-uptake gene cluster 3 (Antunes et al., 2011), which includes the *hemO* gene, hence named *hemO* cluster (Ou et al., 2015).

The 9,833 bp DNA fragment encompassing eight genes of the *hemO* cluster of ACICU (from ACICU_00873 to ACICU_00880 locus) was obtained by PCR amplification using primers HemO_FW (5′-CATTTGGTTTCCGAGTCTCG-3′) and HemO_RV (5′-CCATGATGCGTACCATGCA-3′). The PCR product was purified by the PCR Clean-Up System (Promega) and blunt-end ligated to the SmaI site of pVRL1 (Lucidi et al., 2018), yielding plasmid pVRL1*hemO*. The pVRL1*hemO* plasmid was introduced in *A. baumannii* ATCC 17978 by electroporation according to published procedures (Yildirim et al., 2016). Transformants were selected on LB agar plates supplemented with 100 μg/ml Gm.

RESULTS

DMHB and RPMI-HS Are Iron-Poor Media That Support the Growth of ESKAPE Species

For a comparative assessment of the antibacterial effect of the three Ga(III) compounds, a representative collection of ESKAPE species was used, including reference strains and multidrug-resistant (MDR) clinical isolates (**Table S1**). Since Ga(III) is an Fe(III)-mimetic acting as a metabolic competitor of Fe(III), its antibacterial activity depends on the iron concentration in the test medium, being enhanced by conditions of relative iron scarcity (Minandri et al., 2014). Therefore, both chemical analyses and functional assays were performed to probe iron content and availability in MHB, DMHB, and RPMI-HS media, prior to Ga(III)-susceptibility testing. ICP-OES measurements (**Figure S1**) showed that the iron concentrations in DMHB (0.43 μM) and RPMI-HS (1.95 μM) were lower than in MHB (3.38 μM). The relatively high iron concentration of RPMI-HS can be ascribed to partially (*ca.* 20%) iron-saturated transferrin in human serum, since only iron traces (0.11 μM) are present in serum-free RPMI-1640 (data not shown). To evaluate whether DMHB and RPMI-HS are perceived by bacteria as iron-poor media, both siderophore production and iron-repressible gene expression were investigated by using *A. baumannii* ATCC 17978 as a biosensor organism. Notably, high siderophore levels were produced in both DMHB and RPMI-HS, as opposed to MHB (**Figure S1**). Moreover, a transcriptional fusion between the promoter of the iron-repressible *basA* gene and the reporter *lacZ* gene (Antunes et al., 2012) was expressed by *A. baumannii* ATCC 17978 at higher levels in DMHB and RPMI-HS than in MHB (**Figure S1**). These data indicate that DMHB and RPMI-HS are low-iron media that induce an iron-starvation response during bacterial growth. ESKAPE pathogens share similar iron-mediated regulatory mechanisms of gene expression, all possessing the Ferric uptake regulator protein Fur, which drives the expression of iron-repressible genes, including those for siderophore-biosynthesis (i.e., *basA*). Therefore, it can be assumed that the *basA*::*lacZ* transcriptional fusion provides an indirect estimate of the intracellular iron levels of ESKAPE bacteria grown in different media (Ochsner and Vasil, 1996; Achenbach and Yang, 1997; Haley and Skaar, 2012; Mortensen and Skaar, 2013; Carpenter and Payne, 2014; Latorre et al., 2018). The ability of ESKAPE pathogens to grow in DMHB and RPMI-HS was then tested for the reference strains of each species (**Figure S2**). For all strains tested, evident growth reduction (12–60%) was observed in DMHB compared with MHB. Addition of 3 μM $FeCl_3$ to DMHB (i.e., restoring the iron concentration of MHB before Chelex® 100 treatment) rescued the growth of all strains, except *E. faecium* ATCC 19434 and *S. aureus* ATCC 25923 (**Figure S2A**). For these two species, the residual growth reduction observed in iron-replete DMHB is likely due to the removal of other metabolically relevant metals, besides iron. Moreover, all but one strain grew in RPMI-HS, although at different rates (**Figure S2B**). The only exception was *E. faecium* ATCC 19434, whose growth was rescued by the addition of two vitamins, namely nicotinic acid and pyridoxal hydrochloride. These cofactors were added to RPMI-HS to allow Ga-susceptibility testing of *E. faecium* (**Figure S2C**). These preliminary experiments allowed us to establish iron-poor culture conditions in conventional media that support the growth of all ESKAPE strains tested, thus being suitable for comparative testing of the antibacterial activity of Ga(III) compounds.

Susceptibility of ESKAPE Pathogens to Ga(III) Compounds

The activity of the three Ga(III) compounds was tested on a total of 24 ESKAPE strains in three selected media (**Table 1**). Arbitrarily assuming the resistance breakpoint at MIC > 32 μM, which roughly corresponds to the peak serum concentration of Ga(III) achievable during human therapy (Bernstein, 1998; Collery et al., 2002), all strains were resistant to the three Ga(III) compounds tested in MHB and DMHB, except *S. aureus* and *A. baumannii*, which were susceptible to GaPPIX (MIC ≤ 32 μM). Notably, the MIC of GaPPIX for *S. aureus* was extremely low in both MHB and DMHB (0.06–0.12 μM). Moreover, no differences in MIC values for *S. aureus* and *A. baumannii* were observed between MHB and DMHB, in spite of their different iron content, and thus of the different iron starvation status of bacteria (**Figure S1**). This suggests a mechanism of action of GaPPIX that is not responsive to iron. In fact, addition to MHB of 100 μM $FeCl_3$, i.e., in excess over GaPPIX, did not abrogate the growth inhibitory effect of GaPPIX for all *S. aureus*

TABLE 1 | MIC (μM) of Ga(III) compounds for ESKAPE strains.

Bacterial strain	MHB			DMHB			RPMI-HS[b]		
	GaN	GaM	GaPPIX	GaN	GaM	GaPPIX	GaN	GaM	GaPPIX
E. faecalis ATCC 29212	>128	>128	>128	>128	>128	>128	>128	64	>128
E. faecalis ATCC 700802	>128	>128	>128	>128	>128	>128	>128	128	>128
E. faecium[T] ATCC 19434	>128	>128	>128	>128	>128	>128	>128	64	>128
E. faecium BM4147	>128	>128	>128	>128	>128	>128	ND	ND	ND
S. aureus ATCC 25923	>128	>128	**0.12**	>128	>128	**0.06**	>128	>128	>128
S. aureus ATCC 43300	>128	>128	**0.12**	>128	>128	**0.06**	>128	128	>128
S. aureus Sau117[a]	>128	>128	**0.06**	>128	>128	**0.06**	>128	128	>128
S. aureus UD95[a]	>128	>128	**0.12**	>128	>128	**0.12**	>128	128	>128
K. pnemoniae ATCC 27736	>128	>128	>128	>128	>128	>128	>128	>128	>128
K. pnemoniae Kp3[a]	>128	>128	>128	>128	>128	>128	>128	>128	>128
K. pnemoniae 17830[a]	>128	>128	>128	>128	>128	>128	**4**	**2**	>128
K. pnemoniae 16855[a]	>128	>128	>128	>128	>128	>128	**16**	**16**	>128
A. baumannii ATCC 17978	>128	>128	**16**	> 128	> 128	**16**	**1**	**1**	128
A. baumannii AYE[a]	>128	>128	**32**	>128	>128	**32**	**2**	**1**	128
A. baumannii ACICU[a]	>128	>128	**16**	>128	>128	**16**	**2**	**1**	**1**
A. baumannii C13-373[a]	>128	>128	**32**	>128	>128	**32**	**2**	**1**	**0.25**
P. aeruginosa ATCC 15692 (PAO1)	>128	>128	>128	64	>128	>128	**8**	**4**	128
P. aeruginosa PA14	>128	>128	>128	64	>128	>128	**16**	**8**	128
P. aeruginosa LesB58[a]	>128	>128	>128	>128	>128	>128	**0.5**	**0.5**	**8**
P. aeruginosa SP-13[a]	>128	>128	>128	64	>128	>128	**8**	**4**	128
E. aerogenes[T] ATCC 13048	>128	>128	>128	>128	>128	>128	>128	>128	>128
E. aerogenes 84-6792	>128	>128	>128	>128	>128	>128	>128	>128	>128
E.cloacae[T] ATCC 13047	>128	>128	>128	>128	>128	>128	>128	>128	>128
E. cloacae 78-6303	>128	>128	>128	>128	>128	>128	**8**	**8**	>128

[T], type strain; ND, not determined due to the poor growth. [a], MDR strain; [b], only in the case of Enterococcus species, RPMI-HS was supplemented with nicotinic acid and pyridoxine to allow bacterial growth. Arbitrarily assuming the resistance breakpoint at MIC > 32 μM, the MIC values for susceptible isolates are shown in bold type.

and *A. baumannii* strains tested (**Figure 2**), while 100 μM $FeCl_3$ alone, used as control in MHB, did not influence bacterial growth (data not shown). Since GaPPIX is likely to exert its antibacterial effect by acting as a heme analog (Stojiljkovic et al., 1999; Hijazi et al., 2017), we wondered whether hemin might counteract bacterial GaPPIX susceptibility. To verify this hypothesis, several concentrations of hemin (from 5 to 400 μM) were added to MHB together with GaPPIX, provided at the MIC (**Table 1**). The addition of 5 μM hemin was sufficient to completely abrogate the activity of GaPPIX against all *S. aureus* strains, except *S. aureus* UD95, for which a higher hemin concentration (50 μM) was required (**Figure 2A**). Conversely, not even the highest hemin concentration tested (400 μM) was able to fully reverse the growth-inhibitory effect of GaPPIX in *A. baumannii* (**Figure 2B**). Of note, also $FeCl_3$ provided at 400 μM (i.e., equimolar with the highest hemin concentration tested) did not rescue the growth of all *A. baumannii* strains tested.

Surprisingly, a dramatic loss of GaPPIX activity was observed in RPMI-HS for *S. aureus* and *A. baumannii* (MICs $\geq$ 128 μM for 4/4 and 2/4 strains, respectively), as opposed to the activity of GaN and GaM which was enhanced for almost all species tested in RPMI-HS, compared with MHB or DMHB (**Table 1**). Non-fermenting Gram-negative species, *P. aeruginosa* and *A. baumannii*, showed low MIC values for both GaN and GaM (0.5 μM < MIC < 16 μM) with some intra-species variability. Intriguingly, the hypervirulent *P. aeruginosa* LesB58 (Liverpool strain) showed the lowest MIC values for all Ga(III) compounds, and was the only GaPPIX-sensitive *P. aeruginosa* strain (**Table 1**). Interestingly, half of *K. pneumoniae* strains and one isolate of *E. cloacae* were also susceptible to GaN and GaM in RPMI-HS (MIC $\leq$ 16 μM). Moreover, no GaPPIX MIC could be determined in RPMI-HS for all Enterobacteriaceae tested (MIC > 128 μM) (**Table 1**). Of note, Ga(III) susceptibility was not limited to antibiotic-sensitive ESKAPE strains, but also exerted on MDR clinical isolates (**Table 1**).

Bactericidal Activity of Ga(III) Compounds

A bactericidal activity has previously been reported for GaN and GaPPIX on *P. aeruginosa* and *A. baumannii*, respectively. However, previous killing assays were conducted in rich laboratory media, which do not mimic the condition encountered *in vivo* by infecting pathogens (Kaneko et al., 2007; Arivett et al., 2015). For this reason, we devised to assess the bactericidal activity of the three Ga(III) compounds in RPMI-HS, i.e., under conditions that trend to mimic biological fluids. Only susceptible strains showing MIC values < 32 μM (**Table 1**) were selected for bactericidal activity

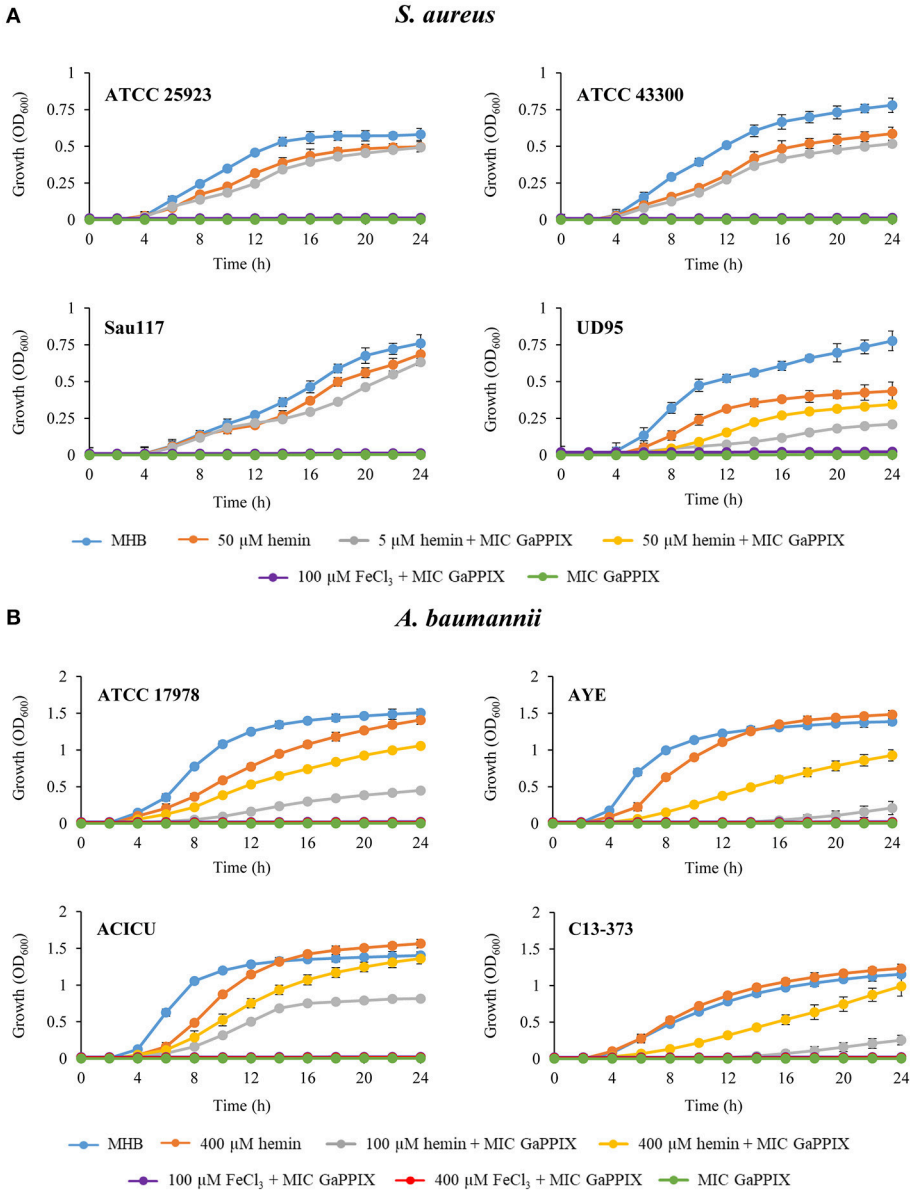

FIGURE 2 | Effect of iron and hemin on the inhibitory activity of GaPPIX. Strains were grown in MHB supplemented or not with GaPPIX at the MIC. Hemin and $FeCl_3$ were supplied at different concentrations, either alone or in combination with GaPPIX, as indicated. **(A)** *S. aureus* ATCC 25923, ATCC 43300, Sau117, UD95, and **(B)** *A. baumannii* strains ATCC17978, AYE, ACICU and C13–373. OD_{600} was monitored periodically for up to 24 h. Data are the mean ± standard deviation of triplicate experiments.

testing of GaN, GaM and GaPPIX, all provided at 28 µM, which corresponds to the peak serum concentration of Ga(III) achievable during human therapy (Bernstein, 1998; Collery et al., 2002). Interestingly, GaN and GaM showed only a bacteriostatic effect (**Figure S3**, **Figure 3**), whereas the response to GaPPIX varied among the susceptible strains (**Figure 3**). The presence of 28 µM GaPPIX caused 2–3 log reduction of viable cells (CFU counts) of *A. baumannii* ACICU, *A. baumannii* C13-373, and *P. aeruginosa* LesB58 after 6 h of incubation at 37°C (**Figure 3**), indicating a bactericidal effect of GaPPIX in RPMI-HS.

Serum Albumin Counteracts the Activity of GaPPIX

In many bacterial pathogens, severe iron limitation induces the expression of heme-uptake systems, therefore increasing the susceptibility to GaPPIX (Stojiljkovic et al., 1999; Hijazi et al., 2017). Intriguingly, *S. aureus* was very sensitive to GaPPIX in both MHB and DMHB, while no MIC was determined for GaPPIX in RPMI-HS (**Table 1**), even though RPMI-HS is iron-poor and induces an iron-starvation response in bacteria (**Figure S1**). Likewise, *A. baumannii* ATCC 17978 and AYE were much more susceptible to GaPPIX in MHB and DMHB than in

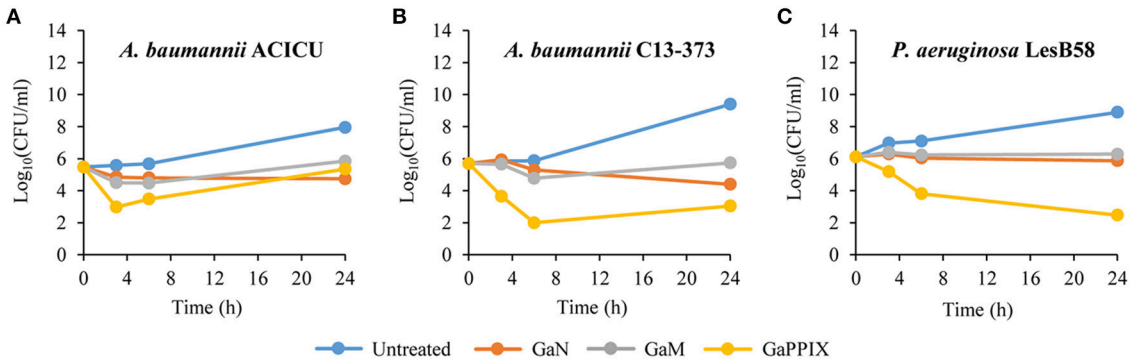

FIGURE 3 | Bactericidal activity of Ga(III) compounds on susceptible strains. GaN, GaM, and GaPPIX time-kill kinetics were determined by plate counts after 0-, 3-, 6-, and 24-h incubation in RPMI-HS supplemented with 28 μM of each Ga(III) compound. **(A)** *A. baumannii* ACICU, **(B)** *A. baumannii* C13-373 and **(C)** *P. aeruginosa* LesB58. Panels show one representative experiment of three independent replicates yielding similar results.

TABLE 2 | Effect of BSA on the MIC (μM) of GaPPIX for *S. aureus* and *A. baumannii*.

Bacterial strains	MHB		RPMI-1640	
	no BSA	5 mg/ml BSA	no BSA	5 mg/ml BSA
S. aureus ATCC 25923	0.12	32	0.12	8
S. aureus ATCC 43300	0.12	16	0.12	32
S. aureus Sau117	0.06	16	0.25	16
S. aureus UD95	0.12	64	0.12	64
A. baumannii ATCC 17978	16	> 128	8	128
A. baumannii AYE	32	> 128	8	128
A. baumannii ACICU	16	> 128	ND	ND
A. baumannii C13-373	32	> 128	16	128

ND, not determined due to the poor bacterial growth.

RPMI-HS (**Table 1**). However, while all *S. aureus* strains were resistant to GaPPIX in RPMI-HS (MIC > 128 μM, **Table 1**), they became extremely sensitive to GaPPIX in RPMI-1640 without HS (MIC ≤ 0.25 μM, **Table 2**). Likewise, *A. baumannii* ATCC 17978 and AYE became sensitive to GaPPIX in RPMI-1640 without HS (MIC = 8 μM, **Table 2**), although showing high GaPPIX MIC in RPMI-HS (128 μM, **Table 1**). These results argue for the presence of HS compound(s) capable of counteracting the antibacterial activity of GaPPIX. Since human serum albumin (HSA), the most abundant plasma protein, binds a variety of ligands including heme (Adams and Berman, 1980), we hypothesized that HSA could bind GaPPIX, due to its chemical similarity with heme, thus impairing its translocation across the cell membrane *via* heme-uptake systems. To test this hypothesis, the susceptibility of *S. aureus* and *A. baumannii* to GaPPIX was determined in MHB and RPMI-1640 supplemented or not with BSA, a protein sharing 76% sequence identity and the same heme-binding properties as HSA (Goncharova et al., 2013). The amount of added BSA was 5 mg/ml, equaling the final concentration of HSA in RPMI-HS. Consistent with our hypothesis, addition of 5 mg/ml BSA to RPMI-1640 dramatically increased (67 to 533 fold) the MICs of GaPPIX on both *S. aureus* and *A. baumannii* (**Table 2**). A similar effect was also observed upon addition of BSA to MHB (**Table 2**). Taken together, these results suggest that the poor susceptibility to GaPPIX observed for *S. aureus* and *A. baumannii* in RPMI-HS is due to the presence of HSA which binds GaPPIX and neutralizes its inhibitory effect.

Multiple Heme-Uptake Systems Influence *A. baumannii* Susceptibility to GaPPIX

The wide range of GaPPIX susceptibility observed among *A. baumannii* isolates led us to hypothesize that the presence of different GaPPIX-uptake capabilities could be the source of this variability. GaPPIX is known to exploit heme-uptake routes to enter bacterial cells (Stojiljkovic et al., 1999; Hijazi et al., 2017), and all *A. baumannii* strains sequenced so far, including ATCC 17978, AYE and ACICU, possess the *hemT* heme-uptake cluster (homolog of the iron-uptake gene cluster 2 in Antunes et al., 2011). Interestingly, *A. baumannii* ACICU possesses an additional heme-uptake cluster, named *hemO* (iron-uptake gene cluster 3 in Antunes et al., 2011) (**Figure 4A**). Since *A. baumannii* ACICU showed an extremely low GaPPIX MIC (1 μM), we hypothesized that the presence of *hemO* could be responsible for the increased GaPPIX susceptibility, likely providing a more efficient GaPPIX uptake route. Indeed, PCR analysis revealed the presence of both *hemO* and *hemT* clusters in *A. baumannii* C13-373 (data not shown), another strain showing very low GaPPIX MIC (0.25 μM), similar to *A. baumannii* ACICU (**Figure 4B**). To shed more light on the relationship between heme uptake and the antibacterial activity of GaPPIX in *A. baumannii*, the whole *hemO* cluster of strain ACICU (9,833 bp), was cloned and expressed *in trans* in *A. baumannii* ATCC 17978. GaPPIX susceptibility of *A. baumannii* ATCC 17978 expressing the whole *hemO* cluster from plasmid pVRL1*hemO* or harboring the empty vector (pVRL1) was then assessed in both solid and liquid RPMI-HS (**Figure 4B**). In RPMI-HS agar plates, a much larger growth inhibition halo was observed around the GaPPIX-soaked disk for *A. baumannii* ATCC 17978 (pVRL1*hemO*), compared with *A. baumannii* ATCC 17978 (pVRL1), indicating that expression of the *hemO* cluster from a multicopy plasmid *in trans* greatly

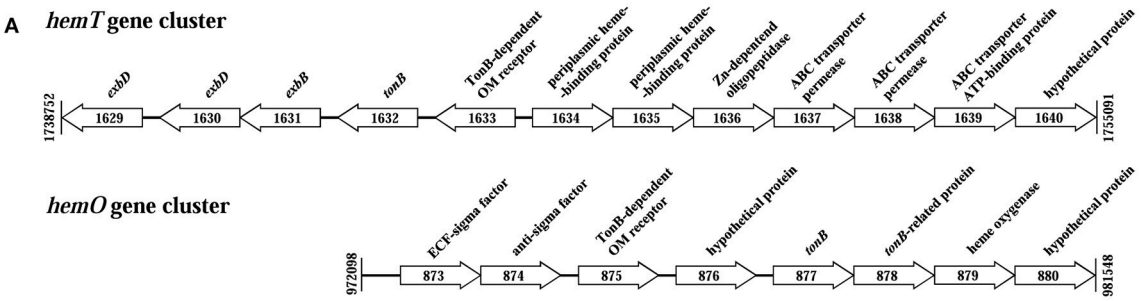

B

A. baumannii strain	ATCC 17978	AYE	ACICU	C13-373	ATCC 17978 pVRL1	ATCC 17978 pVRL1*hemO*
Heme utilization cluster						
hemT	+	+	+	+	+	+
hemO	-	-	+	+	-	++
GaPPIX disk diffusion assay	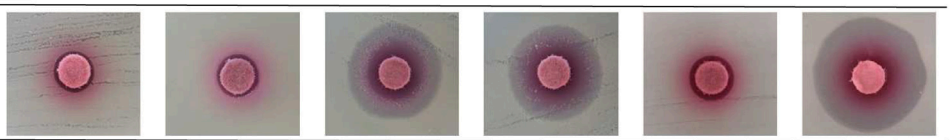					
GaPPIX MIC (μM)						
RPMI-HS	128	128	1	0.25	128	0.25

FIGURE 4 | Influence of heme-uptake systems on *A. baumannii* susceptibility to GaPPIX. **(A)** Schematic representation of the two gene clusters for heme uptake, *hemT* and *hemO,* of *A. baumannii* ACICU. Coding sequences are shown as arrows (not to scale) oriented according to the predicted direction of transcription. **(B)** Top; presence (+) or absence (-) of heme clusters in different *A. baumannii* strains (++, overexpression from the multicopy plasmid pVRL1*hemO*). Middle; GaPPIX disk diffusion assay in RPMI-HS agar plates inoculated with different *A. baumannii* strains. Bottom; MICs of GaPPIX for different *A. baumannii* strains in RPMI-HS.

increases *A. baumannii* ATCC 17978 susceptibility to GaPPIX (**Figure 4B**). As expected, the presence of the empty vector pVRL1 did not affect the susceptibility of *A. baumannii* ATCC 17978 to GaPPIX (**Figure 4B**). In line with the results of the disk diffusion assay, MIC data confirmed that *A. baumannii* ATCC 17978 (pVRL1*hemO*) is more susceptible to GaPPIX than *A. baumannii* ATCC 17978 (pVRL1), the former showing a MIC of 0.25 μM in RPMI-HS (**Figure 4B**). Altogether, these data indicate that the susceptibility of *A. baumannii* to GaPPIX is increased by the presence of the *hemO* gene cluster.

DISCUSSION

Antimicrobial resistance has become one of the most challenging problems of the healthcare system. The spread of antimicrobial-resistant pathogens has dramatic repercussions on mortality and morbidity rates, hence on global medical costs (Friedman et al., 2016). ESKAPE pathogens rank among the most prevalent causative agents of healthcare-associated infections, and pose a serious therapeutic challenge due to their resistance to available antibiotics (Boucher et al., 2009). However, while new antibiotics are urgently needed, the pipeline of antibiotic discovery is almost dry (Luepke and Mohr, 2017). Iron uptake and metabolism are regarded as druggable targets for new antibacterial strategies (Ballouche et al., 2009; Foley and Simeonov, 2012). In this context, the iron mimetic metal Ga(III) has been shown to inhibit bacterial growth, by interfering with iron-dependent metabolic pathways (Minandri et al., 2014).

In this work, we report the first comparative evaluation of the antibacterial properties of three Ga(III) compounds on ESKAPE species in conventional susceptibility testing media characterized by different iron concentrations and nutrient compositions.

Our data demonstrate that the bacterial susceptibility to Ga(III) compounds varies among species and among strains within the same species, and is influenced by the iron concentration and nutrient composition of the medium. Ga(III)-susceptibility tests conducted in MHB and DMHB showed elevated MIC values ($> 32\,\mu M$) for all species, except *S. aureus* and *A. baumannii*, which were sensitive to GaPPIX only. Conversely, Ga(III) testing in RPMI-HS gave a better response, with an overall higher susceptibility to GaN and GaM for *K. pneumoniae*, *A. baumannii*, *P. aeruginosa*, and *E. cloacae* (MIC $\leq 16\,\mu M$ for 50 to 100% of strains tested). Among the

ESKAPE bacteria tested, aerophilic species, which preferentially adopt a respiratory metabolism, namely *A. baumannii* and *P. aeruginosa*, were in general more susceptible to Ga(III) in RPMI-HS than fermenting species, such as Enterobacteriaceae, *S. aureus* and enterococci. This is probably due to Ga(III)-dependent impairment of iron-demanding processes, such as respiration and response to oxidative stress (Stojiljkovic et al., 1999; Hijazi et al., 2017). Moreover, GaN and GaM showed a similar spectrum of activity, although GaM was more potent than GaN in 9 out of 13 isolates for which a MIC could be determined. Previous experiments in a mouse burn wound model infection are in line with this observation, given that much lower GaM concentrations were needed to prevent *P. aeruginosa* and *A. baumannii* proliferation, compared with GaN (DeLeon et al., 2009). The solubility of GaM in both water and lipids, allowing for the penetration of cell walls and membranes, as opposed to the lack of lipophylicity of GaN, probably accounts for much of the difference in biologic effects between the two compounds (Bernstein et al., 2000; DeLeon et al., 2009). Although the presence of non-selective entrance routes for Ga(III) cannot be excluded, Ga(III) mainly exploits iron-uptake systems to enter bacterial cells (Minandri et al., 2014). Therefore, the variable susceptibility to GaN and GaM observed for *K. pneumoniae* and *E. cloacae* in RPMI-HS could be explained by the variable number and type of iron-acquisition systems in these two species (Podschun et al., 1992; Koczura and Kaznowski, 2003) and perhaps their varying growth rates. This holds true also in *P. aeruginosa*, where siderophores, either pyoverdine (PVD) or pyochelin (PCH), have opposite effects on Ga(III) activity; while PCH shuttles Ga(III) into *P. aeruginosa* cells, PVD sequesters it away in the periplasmic space, therefore protecting bacterial cells from Ga(III)-mediated toxicity (Kaneko et al., 2007; Frangipani et al., 2014).

GaPPIX deserves a special comment. As documented for various bacterial species, GaPPIX exerts its activity when transported into the cell, implying that the presence and/or expression level of heme-uptake genes have a major impact on GaPPIX activity (Stojiljkovic et al., 1999; Hijazi et al., 2017). The *A. baumannii hemO* gene cluster encodes a very efficient heme-utilization system, responsible for an increased translocation of GaPPIX in the cell (de Léséleuc et al., 2014). Results presented here suggest a major role for the *hemO* system also in GaPPIX susceptibility, given that only strains possessing both *hemT* and *hemO* gene clusters were severely inhibited by GaPPIX in RPMI-HS (MIC 0.25–1.0 μM), whereas those possessing only the *hemT* cluster were not (MIC > 128 μM) (**Tables 1**, **2**). Notably, this phenomenon was only observed in RPMI-HS, where GaPPIX is bound by HSA, but not in MHB or DMHB where no albumin is present. This suggests that gene products of the *A. baumannii hemO* cluster efficiently withdraw HSA-bound GaPPIX and deliver it to its intracellular targets. On the other hand, the HemT and Isd heme-uptake systems, which are present in *A. baumannii* and *S. aureus*, respectively (Ascenzi et al., 2015), appear by themselves unable to confer GaPPIX susceptibility in RPMI-HS (but not in MHB and DMHB), probably because these two systems cannot efficiently extract HSA-bound GaPPIX for transport into the cell. These observations are in line with a previous report showing that the addition of 10% HS to MHB caused a 3-fold increase of the GaPPIX MIC for *A. baumannii* (Arivett et al., 2015). Intriguingly, the activity of GaPPIX against *S. aureus* and *A. baumannii* was independent of the iron content of the medium, given that: (i) it was similar in MHB and DMHB media, irrespective of their different iron content, and, (ii) amendment of MHB with an exceedingly high $FeCl_3$ concentration did not neutralize the antibacterial activity of GaPPIX (**Figure 2**), in agreement with previous reports (Stojiljkovic et al., 1999; Arivett et al., 2015). Interestingly, the addition of hemin partially reversed the antibacterial activity of GaPPIX in MHB, albeit in one *S. aureus* and in all *A. baumannii* strains tested not even a molar excess of hemin completely abrogated the effect of GaPPIX (**Figure 2**). This means that incorporation of GaPPIX in vital bacterial enzymes is only in part reversed by competition with hemin. This observation could have significant clinical implications, since the release of heme and/or iron from red blood cells and iron-binding proteins during inflammatory processes is unlikely to undermine the antibacterial activity of GaPPIX *in vivo*. These observations, together with the previously reported low toxicity of GaPPIX (Stojiljkovic et al., 1999; Arivett et al., 2015; Chang et al., 2016), support the potential use of GaPPIX as a therapeutic option to treat some bacterial infections. It should be noted that, different from GaN and GaM which exploit multiple routes to enter bacteria (Minandri et al., 2014), making the selection of Ga(III)-resistant cells less likely to occur compared with conventional antibiotic treatments (Ross-Gillespie et al., 2014), GaPPIX enters the cell through specialized heme-uptake systems (Stojiljkovic et al., 1999; Hijazi et al., 2017). While this could imply more frequent emergence of GaPPIX-resistant cells through loss of heme (hence GaPPIX) uptake capabilities, the preferential use of heme as iron source by bacterial pathogens *in vivo* argues against a dispensable role of these systems during infection.

In conclusion, we have determined suitable test conditions to assess the antibacterial activity of Ga(III) compounds *in vitro*. The presence of human serum (HS) in RPMI-HS reduces iron availability thanks to the presence of transferrin, thereby providing a more realistic milieu for testing the antibacterial activity of iron-mimetic compounds. Moreover, in RPMI-HS the presence of serum albumin, which interferes with GaPPIX but not of GaN or GaM, indicates that, among the three Ga(III)-compounds tested, the FDA-approved GaN and the orally active GaM were the most effective under conditions that mimic the *in vivo* environment, i.e., in RPMI-HS. With respect to the clinical repositioning of Ga(III) as an antibacterial agent, one should consider that the recommended dosing regimen of citrated GaN for the treatment of cancer patients (200 to 300 mg/m^2 body surface area, i.v. administration) ensures a peak serum concentration of Ga(III) of *ca.* 28 μM (Bernstein, 1998; Collery et al., 2002). Notably, we found that in RPMI-HS much lower GaN concentrations are needed to inhibit the growth of *A. baumannii*, *P. aeruginosa* and some Enterobacteriaceae. Ongoing clinical trials on patients with cystic fibrosis (IGNITE study, ClinicalTrials.gov Identifier: NCT02354859) will provide

important insights into *P. aeruginosa* inhibition during i.v. GaN treatment of chronic lung infection, hence on the actual potential of Ga(III) as an antibacterial agent. It is also noted that topical or other localized means of administration can readily provide millimolar levels of Ga(III) to sites of infection, including burn-associated infections (DeLeon et al., 2009). In fact, the topic use of Ga(III)-citrate has been shown to improve healing, reduce inflammation and favor reepithelization in a murine wound model of *K. pneumoniae* infection (Thompson et al., 2015).

Interestingly, we found that pre-existing resistance to multiple antibiotics in MDR strains did not compromise Ga(III) susceptibility, likely as a consequence of Ga(III) molecular targets (iron-binding proteins) being different from those of common antibiotics, toward which resistance has been selected. In conclusion, Ga(III) could represent a drug of last resort to combat infections sustained by otherwise untreatable pan-resistant bacteria.

AUTHOR CONTRIBUTIONS

DV and PV conceived and designed the experiments. SH and MP performed the experiments. SH, DV, EF, and PV analyzed the data. SH wrote the draft manuscript. SH, DV, MP, EF, LB, and PV revised the manuscript.

FUNDING

This work was supported by grants from the Italian Cystic Fibrosis Research Foundation (grants FFC#21/2015 and FFC#18/2017).

ACKNOWLEDGMENTS

We wish to thank Prof. Gian Maria Rossolini (Department of Experimental Medicine and Clinic, University of Florence, Italy) for providing *Enterobacter* strains, and Dr. Annalisa Pantosti (Department of Infectious, Parasitic and Immuno-mediated Diseases, Istituto Superiore di Sanità, Rome, Italy) for providing *S. aureus* and *K. pneumoniae* strains. We are also grateful to Dr. Federica Runci and the personnel of Policlinico Umberto I, Sapienza University of Rome, for collecting blood samples from healthy donors. The Grant of Excellence Departments, MIUR-Italy (ARTICOLO 1, COMMI 314–337 LEGGE 232/2016) is gratefully acknowledged.

SUPPLEMENTARY MATERIAL

The Supplementary Material for this article can be found online at: https://www.frontiersin.org/articles/10.3389/fcimb.2018.00316/full#supplementary-material

REFERENCES

Achenbach, L. A., and Yang, W. (1997). The fur gene from *Klebsiella pneumoniae*: characterization, genomic organization and phylogenetic analysis. *Gene* 185, 201–207. doi: 10.1016/S0378-1119(96)00642-7

Adams, P. A., and Berman, M. C. (1980). Kinetics and mechanism of the interaction between human serum albumin and monomeric haemin. *Biochem. J.* 191, 95–102. doi: 10.1042/bj1910095

Andrews, S. C., Robinson, A. K., and Rodríguez-Quiñones, F. (2003). Bacterial iron homeostasis. *FEMS Microbiol. Rev.* 27, 215–237. doi: 10.1016/S0168-6445(03)00055-X

Antunes, L. C., Imperi, F., Minandri, F., and Visca, P. (2012). *In vitro* and *in vivo* antimicrobial activities of gallium nitrate against multidrug-resistant *Acinetobacter baumannii*. *Antimicrob. Agents Chemother.* 56, 5961–5970. doi: 10.1128/AAC.01519-12

Antunes, L. C., Imperi, F., Towner, K. J., and Visca, P. (2011). Genome-assisted identification of putative iron-utilization genes in *Acinetobacter baumannii* and their distribution among a genotypically diverse collection of clinical isolates. *Res. Microbiol.* 162, 279–284. doi: 10.1016/j.resmic.2010.10.010

Arivett, B. A., Fiester, S. E., Ohneck, E. J., Penwell, W. F., Kaufman, C. M., Relich, R. F., et al. (2015). Antimicrobial activity of gallium protoporphyrin IX against *Acinetobacter baumannii* strains displaying different antibiotic resistance phenotypes. *Antimicrob. Agents Chemother.* 59, 7657–7665. doi: 10.1128/AAC.01472-15

Ascenzi, P., di Masi, A., Leboffe, L., Frangipani, E., Nardini, M., Verde, C., et al. (2015). Structural biology of bacterial haemophores. *Adv. Microb. Physiol.* 67, 127–176. doi: 10.1016/bs.ampbs.2015.09.002

Ballouche, M., Cornelis, P., and Baysse, C. (2009). Iron metabolism: a promising target for antibacterial strategies. *Recent Pat. Anti Infect. Drug Discov.* 4, 190–205. doi: 10.2174/157489109789318514

Bastos, T.de O., Soares, B. M., Cisalpino, P. S., Mendes, I. C., dos Santos, R. G., and Beraldo, H. (2010). Coordination to gallium(III) strongly enhances the potency of 2-pyridineformamide thiosemicarbazones against *Cryptococcus* opportunistic fungi. *Microbiol. Res.* 165, 573–577. doi: 10.1016/j.micres.2009.10.005

Bernstein, L. R. (1998). Mechanisms of therapeutic activity for gallium. *Pharmacol. Rev.* 50, 665–682.

Bernstein, L. R., Tanner, T., Godfrey, C., and Noll, B. (2000). Chemistry and pharmacokinetics of gallium maltolate, a compound with high oral gallium bioavailability. *Met. Based Drugs* 7, 33–47. doi: 10.1155/MBD.2000.33

Bonchi, C., Frangipani, E., Imperi, F., and Visca, P. (2015). Pyoverdine and proteases affect the response of *Pseudomonas aeruginosa* to gallium in human serum. *Antimicrob. Agents Chemother.* 59, 5641–5646. doi: 10.1128/AAC.01097-15

Boucher, H. W., Talbot, G. H., Bradley, J. S., Edwards, J. E., Gilbert, D., Rice, L. B., et al. (2009). Bad bugs, no drugs: no ESKAPE! An update from the infectious diseases society of America. *Clin. Infect. Dis.* 48, 1–12. doi: 10.1086/595011

Carpenter, C., and Payne, S. M. (2014). Regulation of iron transport systems in Enterobacteriaceae in response to oxygen and iron availability. *J. Inorg. Biochem.* 133, 110–117. doi: 10.1016/j.jinorgbio.2014.01.007

Cartron, M. L., Maddocks, S., Gillingham, P., Craven, C. J., and Andrews, S. C. (2006). Feo-transport of ferrous iron into bacteria. *Biometals* 19, 143–157. doi: 10.1007/s10534-006-0003-2

Chang, D., Garcia, R. A., Akers, K. S., Mende, K., Murray, C. K., Wenke, J. C., et al. (2016). Activity of gallium meso- and protoporphyrin IX against biofilms of multidrug-resistant *Acinetobacter baumannii* isolates. *Pharmaceuticals* 9:E16. doi: 10.3390/ph9010016

Chitambar, C. R. (2017). The therapeutic potential of iron-targeting gallium compounds in human disease: from basic research to clinical application. *Pharmacol. Res.* 115, 56–64. doi: 10.1016/j.phrs.2016.11.009

Clinical and Laboratory Standards Institute (2015). *Methods for Dilution Antimicrobial Susceptibility Tests for Bacteria That Grow Aerobically*. 10th edn. Wayne, PA: CLSI (Approved standard M07–A10).

Collery, P., Keppler, B., Madoulet, C., and Desoize, B. (2002). Gallium in cancer treatment. *Crit. Rev. Oncol. Hematol.* 42, 283–296. doi: 10.1016/S1040-8428(01)00225-6

de Léséleuc, L., Harris, G., KuoLee, R., Xu, H. H., and Chen, W. (2014). Serum resistance, gallium nitrate tolerance and extrapulmonary dissemination are linked to heme consumption in a bacteremic strain of *Acinetobacter baumannii*. *Int. J. Med. Microbiol.* 304, 360–369. doi: 10.1016/j.ijmm.2013.12.002

DeLeon, K., Balldin, F., Watters, C., Hamood, A., Griswold, J., Sreedharan, S., et al. (2009). Gallium maltolate treatment eradicates *Pseudomonas aeruginosa* infection in thermally injured mice. *Antimicrob. Agents Chemother.* 53, 1331–1337. doi: 10.1128/AAC.01330-08

Deplano, A., Denis, O., Poirel, L., Hocquet, D., Nonhoff, C., Byl, B., et al. (2005). Molecular characterization of an epidemic clone of panantibiotic-resistant *Pseudomonas aeruginosa*. *J. Clin. Microbiol.* 43, 1198–1204. doi: 10.1128/JCM.43.3.1198-1204.2005

Edwards, C. L., and Hayes, R. L. (1969). Tumor scanning with ^{67}Ga citrate. *J. Nucl. Med*. 10, 103–105.

Elemam, A., Rahimian, J., and Mandell, W. (2009). Infection with panresistant *Klebsiella pneumoniae*: a report of 2 cases and a brief review of the literature. *Clin. Infect. Dis.* 49, 271–274. doi: 10.1086/600042

Foley, T. L., and Simeonov, A. (2012). Targeting iron assimilation to develop new antibacterials. *Expert. Opin. Drug Discovery* 7, 831–847. doi: 10.1517/17460441.2012.708335

Frangipani, E., Bonchi, C., Minandri, F., Imperi, F., and Visca, P. (2014). Pyochelin potentiates the inhibitory activity of gallium on *Pseudomonas aeruginosa*. *Antimicrob. Agents Chemother.* 58, 5572–5575. doi: 10.1128/AAC.03154-14

Friedman, N. D., Temkin, E., and Carmeli, Y. (2016). The negative impact of antibiotic resistance. *Clin. Microbiol. Infect.* 22, 416–422. doi: 10.1016/j.cmi.2015.12.002

Goncharova, I., Orlov, S., and Urbanová, M. (2013). The location of the high- and low-affinity bilirubin-binding sites on serum albumin: ligand-competition analysis investigated by circular dichroism. *Biophys. Chem.* 180–181, 55–65. doi: 10.1016/j.bpc.2013.06.004

Hackel, M. A., Tsuji, M., Yamano, Y., Echols, R., Karlowsky, J. A., and Sahm, D. F. (2018). *In vitro* activity of the siderophore cephalosporin, cefiderocol, against carbapenem-non-susceptible and multidrug-resistant isolates of gram-negative *Bacilli* collected worldwide in 2014 to 2016. *Antimicrob. Agents Chemother.* 62:e01968-17. doi: 10.1128/AAC.01968-17

Haley, K. P., and Skaar, E. P. (2012). A battle for iron: host sequestration and *Staphylococcus aureus* acquisition. *Microbes Infect.*14, 217–227. doi: 10.1016/j.micinf.2011.11.001

Hijazi, S., Visca, P., and Frangipani, E. (2017). Gallium-protoporphyrin IX inhibits *Pseudomonas aeruginosa* growth by targeting cytochromes. *Front. Cell. Infect. Microbiol.* 7:12. doi: 10.3389/fcimb.2017.00012

Kaneko, Y., Thoendel, M., Olakanmi, O., Britigan, B. E., and Singh, P. K. (2007). The transition metal gallium disrupts *P.* aeruginosa iron metabolism and has antimicrobial and antibiofilm activity. *J. Clin. Invest.* 117, 877–888. doi: 10.1172/JCI30783

Koczura, R., and Kaznowski, A. (2003). Occurrence of the *Yersinia* high-pathogenicity island and iron uptake systems in clinical isolates of *Klebsiella pneumoniae*. *Microb. Pathog.* 35, 197–202. doi: 10.1016/S0882-4010(03)00125-6

Latorre, M., Quenti, D., Travisany, D., Singh, K. V., Murray, B. E., Maass, A., et al. (2018). The role of Fur in the transcriptional and iron homeostatic response of *Enterococcus faecalis*. *Front. Microbiol.* 9:1580. doi: 10.3389/fmicb.2018.01580

Lucidi, M., Runci, F., Rampioni, G., Frangipani, E., Leoni, L., and Visca, P. (2018). New shuttle vector for gene cloning and expression in multi-drug resistance *Acinetobacter* species. *Antimicrob. Agents Chemother.* 62:e02480-17. doi: 10.1128/AAC.02480-17

Luepke, K. H., and Mohr, J. F. (2017). The antibiotic pipeline: reviving research and development and speeding drugs to market. *Expert Rev. Anti Infect. Ther.* 15, 425–433. doi: 10.1080/14787210.2017.1308251

Miethke, M., and Marahiel, M. A. (2007). Siderophore-based iron acquisition and pathogen control. *Microbiol. Mol. Biol. Rev.* 71, 413–451. doi: 10.1128/MMBR.00012-07

Miller, J. H. (1972). *Experiments in Molecular Genetics.* New York, NY: Cold Spring Harbor Laboratory.

Minandri, F., Bonchi, C., Frangipani, E., Imperi, F., and Visca, P. (2014). Promises and failures of gallium as an antibacterial agent. *Future Microbiol.* 9, 379–397. doi: 10.2217/fmb.14.3

Mortensen, B. L., and Skaar, E. P. (2013). The contribution of nutrient metal acquisition and metabolism to *Acinetobacter baumannii* survival within the host. *Front. Cell. Infect. Microbiol.* 3:95. doi: 10.3389/fcimb.2013.00095

Nowak, J., Zander, E., Stefanik, D., Higgins, P. G., Roca, I., Vila, J., et al. (2017). High incidence of pandrug-resistant *Acinetobacter baumannii* isolates collected from patients with ventilator-associated pneumonia in Greece, Italy and Spain as part of the MagicBullet clinical trial. *J. Antimicrob. Chemother.* 72, 3277–3282. doi: 10.1093/jac/dkx322

Ochsner, U. A., and Vasil, M. L. (1996). Gene repression by the ferric uptake regulator in *Pseudomonas aeruginosa*: cycle selection of iron-regulated genes. *Proc. Natl. Acad. Sci. U.S.A.* 93, 4409–4414. doi: 10.1073/pnas.93.9.4409

Ou, H. Y., Kuang, S. N., He, X., Molgora, B. M., Ewing, P. J., Deng, Z., et al. (2015). Complete genome sequence of hypervirulent and outbreak-associated *Acinetobacter baumannii* strain LAC-4: epidemiology, resistance genetic determinants and potential virulence factors. *Sci. Rep.* 5:8643. doi: 10.1038/srep08643

Pendleton, J. N., Gorman, S. P., and Gilmore, B. F. (2013). Clinical relevance of the ESKAPE pathogens. *Expert Rev. Anti Infect. Ther.* 3, 297–308. doi: 10.1586/eri.13.12

Podschun, R., Fischer, A., and Ullmann, U. (1992). Siderophore production of *Klebsiella* species isolated from different sources. *Zentralbl. Bakteriol.* 276, 481–486. doi: 10.1016/S0934-8840(11)80673-0

Principe, L., D'Arezzo, S., Capone, A., Petrosillo, N., and Visca, P. (2009). *In vitro* activity of tigecycline in combination with various antimicrobials against multidrug resistant *Acinetobacter baumannii*. *Ann. Clin. Microbiol. Antimicrob.* 8:18. doi: 10.1186/1476-0711-8-18

Rice, L. B. (2010). Progress and challenges in implementing the research on ESKAPE pathogens. *Infect. Control Hosp. Epidemiol.* 1, S7–S10. doi: 10.1086/655995

Ross-Gillespie, A., Weigert, M., Brown, S. P., and Kümmerli, R. (2014). Gallium-mediate siderophore quenching as an evolutionarily robust antibacterial treatment. *Evol. Med. Public Health* 2014, 18–29. doi: 10.1093/emph/eou003

Schwyn, B., and Neilands, J. B. (1987). Universal chemical assay for the detection and determination of siderophores. *Anal. Biochem.* 160, 47–56. doi: 10.1016/0003-2697(87)90612-9

Stojiljkovic, I., Kumar, V., and Srinivasan, N. (1999). Non-iron metalloporphyrins: potent antibacterial compounds that exploit haem/Hb uptake systems of pathogenic bacteria. *Mol. Microbiol.* 31, 429–442. doi: 10.1046/j.1365-2958.1999.01175.x

Thompson, M. G., Corey, B. W., Si, Y., Craft, D. W., and Zurawski, D. V. (2012). Antibacterial activities of iron chelators against common nosocomial pathogens. *Antimicrob. Agents Chemother.* 56, 5419–5421. doi: 10.1128/AAC.01197-12

Thompson, M. G., Truong-Le, V., Alamneh, Y. A., Black, C. C., Anderl, J., Honnold, C. L., et al. (2015). Evaluation of gallium citrate formulations against a multidrug-resistant strain of *Klebsiella pneumoniae* in a murine wound model of infection. *Antimicrob. Agents Chemother.* 59, 6484–6493. doi: 10.1128/AAC.00882-15

Wandersman, C., and Delepelaire, P. (2004). Bacterial iron sources: from siderophores to hemophores. *Annu. Rev. Microbiol.* 58, 611–647. doi: 10.1146/annurev.micro.58.030603.123811

Weinberg, E. D. (2009). Iron availability and infection. *Biochem. Biophys. Acta* 1790, 600–605. doi: 10.1016/j.bbagen.2008.07.002

World Health Organization (2017). *List of Antibiotic Resistant Priority Pathogens*. Available online at: http://www.who.int/mediacentre/news/releases/2017/bacteria-antibiotics-needed/en/

Yildirim, S., Thompson, M. G., Jacobs, A. C., Zurawski, D. V., and Kirkup, B. C. (2016). Evaluation of parameters for high efficiency transformation of *Acinetobacter baumannii*. *Sci. Rep.* 6:22110. doi: 10.1038/srep22110

Conflict of Interest Statement: LB holds several patents for possible applications of GaM in human and veterinary medicine and is affiliated with a company (Gallixa LLC) that would like to obtain regulatory approval for topical gallium maltolate as a therapeutic agent. LB did not participate in data collection for this study.

The remaining authors declare that the research was conducted in the absence of any commercial or financial relationships that could be construed as a potential conflict of interest.

frontiers in Cellular and Infection Microbiology

ORIGINAL RESEARCH
published: 03 October 2018
doi: 10.3389/fcimb.2018.00348

Synergistic Activity of Niclosamide in Combination With Colistin Against Colistin-Susceptible and Colistin-Resistant *Acinetobacter baumannii* and *Klebsiella pneumoniae*

Rafael Ayerbe-Algaba[1], *María Luisa Gil-Marqués*[1], *Manuel Enrique Jiménez-Mejías*[1], *Viviana Sánchez-Encinales*[1], *Raquel Parra-Millán*[1], *María Eugenia Pachón-Ibáñez*[1], *Jerónimo Pachón*[1,2]* *and Younes Smani*[1]*

[1] Clinic Unit of Infectious Diseases, Microbiology and Preventive Medicine, Institute of Biomedicine of Seville (IBiS), University Hospital Virgen del Rocío/CSIC/University of Seville, Seville, Spain, [2] Department of Medicine, University of Seville, Seville, Spain

Colistin is among the few antibiotics effective against multidrug-resistant *Acinetobacter baumannii* and *Klebsiella pneumoniae* clinical isolates. However, in the last few years, colistin-resistant *A. baumannii* and *K. pneumoniae* strains have emerged. Therefore, combination therapies, between colistin and other old drugs, restoring the activity of colistin are required. The main objective of this study was to analyse the activity of niclosamide, an anthelmintic drug, in combination with colistin against colistin-susceptible (Col-S) and colistin-resistant (Col-R) *A. baumannii* and *K. pneumoniae*. The MIC were determined by microdilution assay and the time-kill curves were performed. The zeta potential of Col-S and Col-R of *A. baumannii* and *K. pneumoniae* in presence of niclosamide was assessed. Niclosamide in combination with colistin showed improved activity against Col-S and Col-R *A. baumannii* and *K. pneumoniae*. Time-killing curves showed synergic activity between niclosamide and colistin against Col-S and Col-R *A. baumannii* and *K. pneumoniae*, especially when niclosamide or colistin was added for second time at 4 h of the 24 h killing curve. Col-R *A. baumannii* and *K. pneumoniae* in presence of niclosamide exhibited a greater negative charge (-34.95 ± 0.35 mV and -38.85 ± 0.92 mV; $P < 0.05$) than Col-R *A. baumannii* and *K. pneumoniae* in absence of niclosamide (-26.85 ± 3.65 mV and -35.27 ± 0.72 mV). These data suggest that niclosamide might be combined with colistin, being a potential alternative for treatment of Col-R Gram-negative bacilli infections.

Keywords: repurposing drug, niclosamide, colistin, synergistic effect, *Acinetobacter baumannii*, *Klebsiella pneumoniae*

OPEN ACCESS

Edited by:
Rodolfo García-Contreras, Universidad Nacional Autónoma de México, Mexico

Reviewed by:
Rafael Franco, Instituto Nacional de Rehabilitación, Mexico
Yael González Tinoco, Centro de Investigación Científica y de Educación Superior de Ensenada (CICESE), Mexico
Riti Sharan, Texas A&M Health Science Center, United States

***Correspondence:**
Jerónimo Pachón
pachon@us.es
Younes Smani
ysmani-ibis@us.es

Received: *09 August 2018*
Accepted: *11 September 2018*
Published: *03 October 2018*

Citation:
Ayerbe-Algaba R, Gil-Marqués ML, Jiménez-Mejías ME, Sánchez-Encinales V, Parra-Millán R, Pachón-Ibáñez ME, Pachón J and Smani Y (2018) Synergistic Activity of Niclosamide in Combination With Colistin Against Colistin-Susceptible and Colistin-Resistant Acinetobacter baumannii and Klebsiella pneumoniae. Front. Cell. Infect. Microbiol. 8:348. doi: 10.3389/fcimb.2018.00348

INTRODUCTION

A number of infections caused by multidrug-resistant *Acinetobacter baumannii* and *Klebsiella pneumoniae* required the use of colistin, but both pathogens may rapidly acquire specific resistance mechanisms against colistin (Bonnin et al., 2013; Ah et al., 2014). Nowadays, the rates of colistin resistance worldwide vary between 3 and 28% for *A. baumannii*, and 2.8 and 10.5% for *K. pneumoniae* (Fernández-Cuenca et al., 2013; Ah et al., 2014). In this context, combination therapies between colistin and other drugs are among the new promising strategies to treat bacterial infections (Vila and Pachón, 2012; Cassir et al., 2014).

Classical combinations between colistin and other antimicrobial agents to which the isolate is resistant have been reported (Vila and Pachón, 2012; Paul et al., 2014). Their use has remained wide *in vitro* and in animal experimental model of infections (Vila and Pachón, 2012; Zusman et al., 2013). Few randomized controlled trials examining specific combinations have been completed or are ongoing, and are not sufficient to guide clinical practice (Paul et al., 2014; Poulikakos et al., 2014). This joins with the relatively short window of therapeutic application for severely ill patients for some combinations, and for the rapid emergence of drug resistance (Poulikakos et al., 2014).

In this context, "repurposing drugs," defined as investigating new uses for already existing drugs, have gained renewed interest, as reflected by several recent studies (Chopra et al., 2010; Younis et al., 2015; Tharmalingam et al., 2018), and using them associated with colistin (Antunes et al., 2012; Zemke et al., 2014).

Niclosamide is an anthelmintic drug widely used for treating tape worm infection in humans and has lately been shown to possess anti-cancer and anti-diabetic activities (Tao et al., 2014; Ye et al., 2014). Niclosamide has also been identified as a potent anti-bacterial drug against *Helicobacter pylori* (Tharmalingam et al., 2018) and *Pseudomonas aeruginosa* by the inhibition of *quorum sensing* and various virulence genes, and by the reduction of elastase and pyocyanin levels (Imperi et al., 2013; Costabile et al., 2015). Moreover, Rajamuthiah et al., have reported that niclosamide present bacteriostatic activity against *Staphylococcus aureus* probably due the damage in their bacterial membrane but not against *A. baumannii*, *P. aeruginosa*, *E. coli,* and *K. pneumoniae* (Rajamuthiah et al., 2015; Gwisai et al., 2017). Currently there is no study regarding the combination between colistin and niclosamide to restore the activity of colistin against Gram-negative bacilli.

The aim of this study was to determine the *in vitro* activity of niclosamide in combination with colistin against colistin-susceptible and colistin-resistant *A. baumannii* and *K. pneumoniae* strains.

MATERIALS AND METHODS

Bacterial Strains

Reference colistin-susceptible (Col-S) *A. baumannii* ATCC 17978 strain (Baumann et al., 1968), and 13 clinical colistin-resistant (Col-R) *A. baumannii* strains isolated from an hospital outbreak in 2000 in Spain (Valencia et al., 2009) were used in this study. We also used reference Col-S *K. pneumoniae* CECT 997 strain (Reading and Cole, 1977), one Col-S and 2 Col-R clinical *K. pneumoniae* strains (Pachón-Ibáñez et al., 2018).

Pmra, *Pmrb*, *Mgrb*, *Phop,* and *Phoq* Genes Amplification and Sequencing

In order to investigate the possible contribution of *pmrAB*, *mgrB,* and *phoPQ* to the colistin resistance in *A. baumannii* and *K. pneumoniae*, these genes were analyzed to detect any genetic alteration. DNA samples were obtained from the isolates by heating the colonies in water at 96°C. The genes were amplified using the primers listed in **Table 1**. The obtained bands were purified with the kit MEGAquick-spin plus (iNtRON Biotechnology, USA) and sequenced at the Institute of Biomedicine of Seville. The nucleotide and deduced protein sequences were analyzed using the Serial Cloner program (http://serialbasics.free.fr/Serial_Cloner.html).

In vitro Susceptibility Testing

MIC of colistin (Sigma, Spain), MIC of niclosamide (Sigma, Spain), and MIC of colistin in presence of different concentrations of niclosamide (between 0.5 and 4 μM) against Col-S and Col-R references and clinical *A. baumannii* and *K. pneumoniae* strains were determined in two independent experiments by broth microdilution assay according to CLSI recommendations for *A. baumannii* and EUCAST recommendations for *K. pneumoniae* (Clinical and Laboratory Standards Institute, 2016 European Committee on Antimicrobial Susceptibility European Committee on Antimicrobial Susceptibility Testing [EUCAST], 2016). The initial inoculum of 5 x 10^5 CFU/mL for each strain was used in microtiter plates V (Deltlab, Spain) in presence of colistin, niclosamide, or colistin plus niclosamide, and incubated for 16–18 h at 37°C. *Escherichia coli* ATCC 25922 was used as control strain.

Time-Kill Kinetic Assays

Time-kill curves of *A. baumannii* ATCC 17978 and Col-R #11 strains and *K. pneumoniae* CECT 997 and KPc21 strains with starting inoculum of 1 × 10^6 CFU/mL, conducted on Mueller Hinton broth cation-adjusted, in presence of 2 μM niclosamide and colistin (sub-MIC) alone or in combination were performed in two independent experiments as previously described (Smani et al., 2011).

Moreover, in some conditions niclosamide was added for a second time 4 h after bacterial inoculation in order to avoid the antagonism effect of niclosamide with colistin observed in the first 4 h. In the same way colistin was added for a second time 4 h after bacterial inoculation because the half-life of colistin in bacterial culture broth is 4 h (Owen et al., 2007; Bergen et al., 2010). Bacterial cultures without drugs were carried out in parallel as controls. Tubes of each condition were incubated at 37°C with shaking and samples were taken at 0, 2, 4, 8, and 24 h and serially diluted. Viable counts were determined by plating 100 μL of control, test cultures, or dilutions at the indicated times onto sheep blood agar plates (Beckton Dickinson, USA). Plates were incubated for

TABLE 1 | Primers list used in this study.

Pathogen	Gene	Primer name	Sequence	Amplicon size (bp)	References
A. baumannii	*pmrAB*	pmrAB-F	ATGACAAAAATCTTGATGAT	1,335	López-Rojas et al., 2011
		pmrAB-R	TCACGCTCTTGTTTCATGTA		López-Rojas et al., 2011
K. pneumoniae	*pmrAB*	pmrA-F	CGCAGGATAATCTGTTCTCCA	808	Haeili et al., 2017
		pmrA-R	GGTCCAGGTTTCAGTTGCAA		Haeili et al., 2017
		pmrB-F1	GCGAAAAGATTGGCAAATCG	659	Haeili et al., 2017
		pmrB-R1	GGAAATGCTGGTGGTCATCTGA		Haeili et al., 2017
		pmrB-F2	CCCTGAATCAGTTGGTTTC	714	Haeili et al., 2017
		pmrB-R2	ATCAATGGGTGCTGACGTT		Haeili et al., 2017
	mgrB	mgrB-extF	AAGGCGTTCATTCTACCACC	253	Poirel et al., 2015
		mgrB-extR	TTAAGAAGGCCGTGCTATCC		Poirel et al., 2015
	phoPQ	phoP-F	GAGCGTCAGACTACTATCGA	912	Haeili et al., 2017
		phoP-R	GTTTTCCCATCTCGCCAGCA		Haeili et al., 2017
		phoQ-F1	CCACAGGACGTCATCACCA	636	Haeili et al., 2017
		phoQ-R1	AGCTCCACACCATATAGCTG		This study
		phoQ-F2	GAACAGGGCGACGACTCTG	617	This study
		phoQ-R2	TGAGAGCGGAAGTCAGGCT		This study
		phoQ-F3	GATGCTGGAGCAGATAAGCC	621	This study
		phoQ-R3	GCAGGTGTCTGACAGGGATT		This study

24 h, and after colony counts, the log of viable cells (CFU/mL) was determined. Synergy was defined as a reduction $\geq$ 2 log CFU/mL with the combination respect to the more active drug (Pachón-Ibáñez et al., 2018). Thus, niclosamide was considered synergistic when in combination with colistin reduced the bacterial concentration $\geq$ 2 log CFU/mL with respect to colistin alone.

Zeta Potential Measurements

Zeta potential measurements were performed as previously described with minor modifications (Soon et al., 2011). Briefly, the bacterial surface was cleansed by washing twice with Milli-Q water, resuspended in Milli-Q water at 10^8 CFU/mL, and diluted 10-fold in the same medium immediately prior to zeta potential measurement. The resulting suspensions were used to fill clear disposable folded capillary zeta cells (Malvern, UK).

To examine the effect of niclosamide treatment on Col-S and Col-R *A. baumannii* and *K. pneumoniae* strains, 2 μM niclosamide was added to 5 mL of bacterial culture at 10^8 CFU/mL, then incubated in a shaking bath (37°C, 180 rpm) for 20 min and prepared for zeta potential analysis as described above. The zeta potential measurement (mV) of bacterial cells was measured at 25°C with a zeta potential analyzer at 150 V (Zetasizer Nano ZS; Malvern Instruments, Malvern, UK).

Statistical Analysis

Group data are presented as mean ± SEM. Student *t*-test was used to determine differences between means. Differences were considered significant at $P < 0.05$. The SPSS (version 17.0) statistical package was used (SPSS Inc.).

RESULTS

Colistin MIC and Resistance Mechanisms

The MIC for the Col-R *A. baumannii* and *K. pneumoniae* strains ranged from 32 to > 256 μg/mL, while those for the susceptible reference strains were 0.5 μg/mL. The analysis of the *pmrA*, *pmrB*, *mgrB*, *phoP,* and *phoQ* sequences showed that Col-R *A. baumannii* strains presented only different amino acids substitution in *pmrB* (López-Rojas et al., 2016). Col-R *K. pneumoniae* strains presented IS1 transposase insertion in *mgrB* or different amino acids substitution in *pmrA* and *pmrB*, without substituting amino acid in *phoP* and *phoQ* (**Table 2**).

In vitro Activity of Niclosamide in Combination With Colistin Against Col-S and Col-R *A. baumannii* and *K. pneumoniae*

Niclosamide alone or in combination with colistin was tested against reference and clinical Col-S and Col-R *A. baumannii* and *K. pneumoniae* strains. The MIC is shown in **Table 3**. Niclosamide alone showed a range of MIC from 6.25 to 400 μM for Col-S and Col-R *A. baumannii* strains, and from 400 to >800 μM for Col-S and Col-R *K. pneumoniae* strains.

Niclosamide at 1, 2, and 4 μM in combination with colistin increased significantly the activity of colistin against all Col-S and Col-R strains. In contrast niclosamide, at 0.5 μM in combination with colistin didn't increased the activity of colistin against most of Col-R *A. baumannii*. For the rest of experiments, we chose 2 μM as niclosamide optimal concentration.

Time-Killing Curves

We examined the ability of niclosamide in combination with colistin to kill Col-S and Col-R *A. baumannii* strains (ATCC

TABLE 2 | Colistin MICs and description of Col-S and Col-R *A. baumannii* and *K. pneumoniae* strains used in this study.

Pathogen	Strain	Reference/Source	Description	Colistin MIC (μg/ml)
A. baumannii	ATCC 17978	Baumann et al., 1968	Colistin-susceptible reference strain	0.5
	#1	Valencia et al., 2009; López-Rojas et al., 2016	PDR clinical isolate with A236E amino acid substitution of *pmrB*	256
	#10	Valencia et al., 2009; López-Rojas et al., 2016	PDR clinical isolate with F387Y and S403F amino acids substitution of *pmrB*	>256
	#11	Valencia et al., 2009; López-Rojas et al., 2016	PDR clinical isolate with R263C amino acid substitution of *pmrB*	256
	#14	Valencia et al., 2009; López-Rojas et al., 2016	PDR clinical isolate with R263C amino acid substitution of *pmrB*	256
	#16	Valencia et al., 2009; López-Rojas et al., 2016	PDR clinical isolate with S403F amino acid substitution of *pmrB*	>256
	#17	Valencia et al., 2009; López-Rojas et al., 2016	PDR clinical isolate with R263C amino acid substitution of *pmrB*	64
	#19	Valencia et al., 2009; López-Rojas et al., 2016	PDR clinical isolate with T13A and S17G amino acids substitution of *pmrB*	>256
	#20	Valencia et al., 2009; López-Rojas et al., 2016	PDR clinical isolate with A227V and M308T amino acids substitution of *pmrB*	>256
	#21	Valencia et al., 2009; López-Rojas et al., 2016	PDR clinical isolate with P170Q amino acid substitution of *pmrB*	256
	#22	Valencia et al., 2009; López-Rojas et al., 2016	PDR clinical isolate with P170Q amino acid substitution of *pmrB*	>256
	#24	Valencia et al., 2009; López-Rojas et al., 2016	PDR clinical isolate with R263C amino acid substitution of *pmrB*	64
	#99	Valencia et al., 2009; López-Rojas et al., 2016	PDR clinical isolate with A227V amino acid substitution of *pmrB*	>256
	#113	Valencia et al., 2009; López-Rojas et al., 2016	PDR clinical isolate with L5S, R207C and G426S amino acids substitution of *pmrB*	>256
K. pneumoniae	CECT 997	Reading and Cole, 1977	Colistin-susceptible reference strain	0.5
	KPc07	Pachón-Ibáñez et al., 2018	Colistin-susceptible clinical isolate	0.5
	KPc21	Pachón-Ibáñez et al., 2018	Clinical isolate containing IS1 transposase insertion at nucleotide 22 of *mgrB*	64
	KPc29	Pachón-Ibáñez et al., 2018	Clinical isolate with a G56E and M215I amino acids substitution of *pmrA*, and R63P; S68N and R255G amino acids substitution of *pmrB*	32

17978 and #11) and Col-S and Col-R *K. pneumoniae* strains (CECT 997 and KPc21) in time course assays. Two micromolar niclosamide in combination with 0.25 μg/mL colistin, a colistin sub-MIC of ATCC 17978 strain, showed in the first 4 h no synergistic activity with respect to colistin alone, followed by later synergistic activity decreasing the bacterial cell count by 3.14 log CFU/mL with respect to colistin alone at 24 h (**Figure 1A**). Combination of 2 μM niclosamide with 8 μg/mL colistin, a colistin sub-MIC of #11 strain, showed higher synergistic activity, decreasing the bacterial cell count with respect to colistin alone by 5.93 log CFU/mL at 24 h (**Figure 1A**).

In the case of *K. pneumoniae*, 2 μM niclosamide in combination with 0.25 μg/mL colistin, a colistin sub-MIC of CECT 997 strain, didn't showed synergistic effect with colistin during 24 h (**Figure 1B**). In contrast, 2 μM niclosamide in combination with 32 μg/mL colistin, a colistin sub-MIC of KPc21 strain, showed synergistic activity with respect to colistin alone decreasing the bacterial cell count by 3.38 log CFU/mL at 24 h (**Figure 1B**). In a control experiment, 2 μM niclosamide had no effect on the growth of Col-S and Col-R *A. baumannii* and *K. pneumoniae* strains (**Figure 1A,B**).

With these results, since the half-life of colistin in bacterial culture broth is 4 h (Owen et al., 2007; Bergen et al., 2010) and can be degraded during time-kill curve experiments (Mohamed et al., 2014), we cannot rule out the possibility that the absence of synergistic activity of niclosamide in combination with colistin observed especially with *K. pneumoniae* CECT 997 strain (**Figure 1B**) would be due to colistin degradation in the bacterial culture broth.

Consequently, to maintain the colistin concentration in the medium, in the following experiments we added 0.25 μg/mL colistin after 4 h post-incubation with the initial 2 μM niclosamide and 0.25 μg/mL colistin, or with 0.25 μg/mL colistin alone. This approach produced synergy between niclosamide and colistin, decreasing the bacterial cell count of CECT 997 strain by 4.62 log CFU/mL with respect to colistin plus

TABLE 3 | Determination of MIC of niclosamide and colistin alone or in combination against Col-S and Col-R *A. baumannii* and *K. pneumoniae*.

Pathogen	Strain	Nicl MIC (μM)	Col MIC (μg/ml)	Col MIC (μg/ml)			
				+ Nicl 4 μM	+ Nicl 2 μM	+ Nicl 1 μM	+ Nicl 0.5 μM
A. baumannii	ATCC 17978	25	0.5	<0.03	<0.03	<0.03	0.25
	#1	25	256	**0.06**	**0.5**	256	>256
	#10	400	>256	**0.03**	**0.5**	32	ND
	#11	200	256	**0.06**	**0.25**	32	>256
	#14	6.25	256	**0.06**	**0.25**	32	256
	#16	50	>256	**0.03**	**0.5**	64	ND
	#17	12.5	64	**<0.03**	**0.125**	8	64
	#19	12.5	>256	**0.125**	**2**	128	>256
	#20	12.5	>256	**0.125**	**1**	64	>256
	#21	200	256	**<0.03**	**<0.03**	8	16
	#22	200	>256	**<0.03**	**<0.03**	**0.5**	16
	#24	64	64	**0.06**	**0.125**	8	64
	#99	400	>256	**0.03**	**0.5**	16	>256
	#113	400	>256	**0.06**	**1**	8	256
K. pneumoniae	CECT 997	>800	0.5	**0.06**	**0.06**	**0.125**	**0.125**
	KPc07	400	0.5	**0.06**	**0.06**	**0.125**	**0.125**
	KPc21	>800	64	**<0.015**	**<0.015**	**0.15**	32
	KPc29	800	32	**0.25**	**0.5**	**1**	4

Values in bold indicate the condition in which the presence of niclosamide changed the bacterial colistin susceptibility from resistant to susceptible. One micromolar of niclosamide correspond to 0.33 μg/ml. Nicl, niclosamide; Col, colistin; ND, not determined.

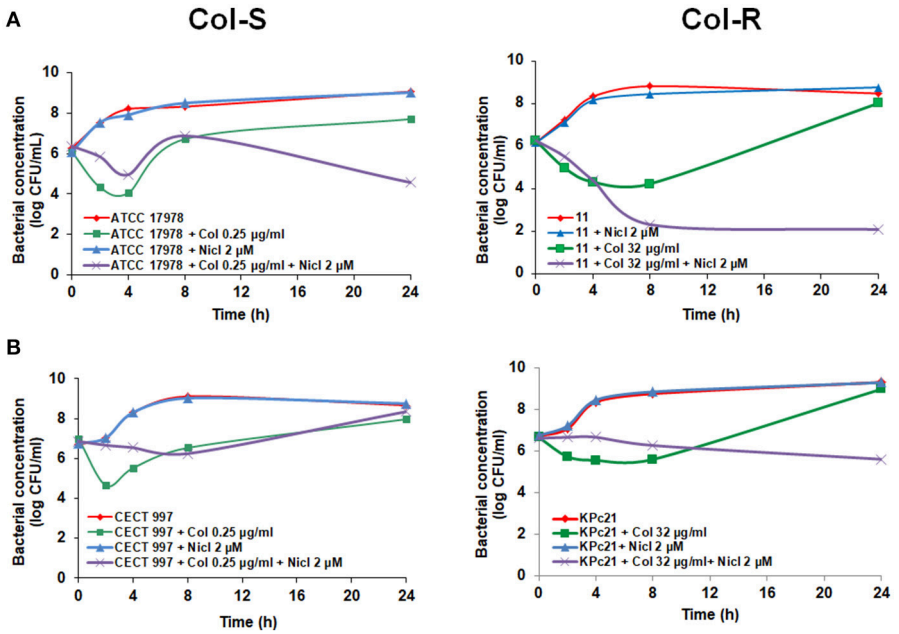

FIGURE 1 | Early addition of niclosamide potentiates the colistin activity against Col-S and Col-R *A. baumannii* and *K. pneumoniae* strains. Time-kill curves of *A. baumannii* ATCC 17978 and #11 strains **(A)** and *K. pneumoniae* CECT 997 and KPc21 strains **(B)** in presence of niclosamide (0 or 2 μM), and colistin (sub-MIC) alone or in combination with niclosamide for 24 h. 1 μM of niclosamide correspond to 0.33 μg/ml. Nicl, niclosamide, Col, colistin.

colistin at 24 h (**Figure 2B**). Similarly, the addition of 32 μg/mL colistin after 4 h post-incubation with niclosamide and 32 μg/mL colistin decreased the growth of KPc21 strain by 4.38 log CFU/mL with respect to colistin plus colistin at 24 h (**Figure 2B**).

In the case of *A. baumannii* ATCC 17978 strain, the addition of colistin for second time at 4 h increased the synergy between niclosamide and colistin plus colistin decreasing the bacterial cell count by 2.37 log CFU/mL with respect to niclosamide plus

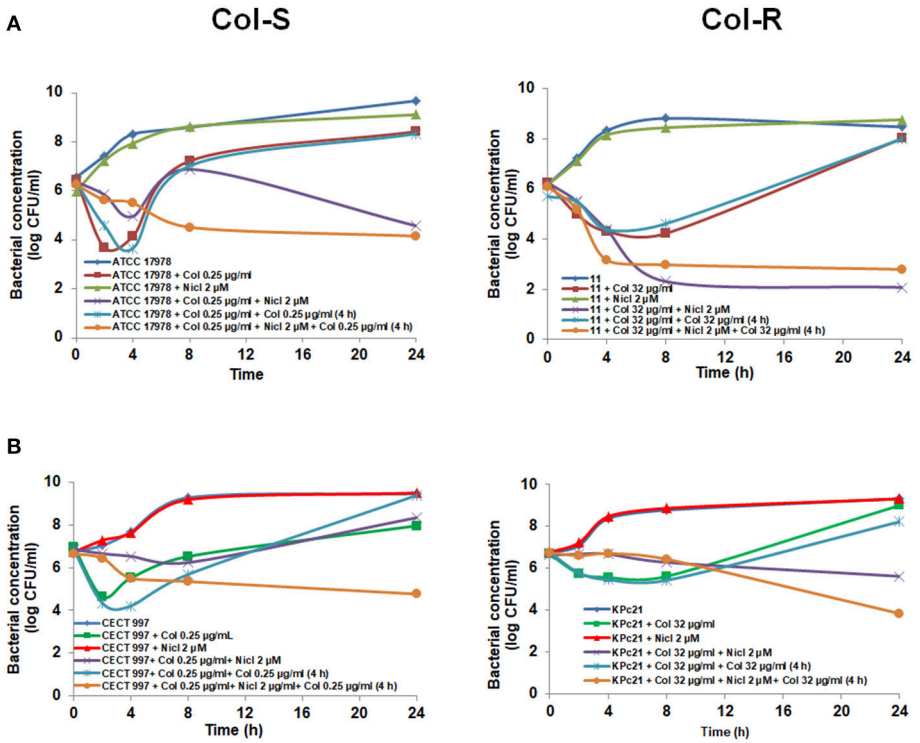

FIGURE 2 | Niclosamide potentiates the colistin activity against Col-S and Col-R *A. baumannii* and *K. pneumoniae* strains after second time addition of colistin. Time-kill curves of *A. baumannii* ATCC 17978 and #11 strains **(A)**, *K. pneumoniae* CECT 997 and KPc21 strains **(B)**, in presence of 2 μM niclosamide and colistin (sub-MIC) alone, or in combination with or without addition of colistin for second time 4 h after bacterial addition. One micromolar of niclosamide correspond to 0.33 μg/ml. Nicl, niclosamide; Col, colistin.

colistin, without the addition of colistin at 4 h, at 8 h (**Figure 2A**). In contrast, with #11 strain the addition of colistin for second time did not improve the synergy between niclosamide and colistin observed in the (**Figures 1**, **2A**).

Furthermore, to avoid the antagonism effect of niclosamide with colistin observed in the first 4 h (**Figures 1**, **2**), we added 2 μM niclosamide after 4 h post-incubation with 0.25 and 8 μg/mL colistin, sub-MIC of *A. baumannii* ATCC 17978 and #11 strains, respectively. We observed a decrease in the growth of ATCC 17978 and #11 strains by 5.06 and 3.38 log CFU/mL, respectively, with respect to colistin alone at 24 h (**Figure 3A**).

In the case of *K. pneumoniae*, we added 2 μM niclosamide after 4 h post-incubation with 0.25 and 32 μg/mL colistin, sub-MIC of CECT 997 and KPc21 strains, respectively. We observed a decrease in the growth of CECT 997 and KPc21 strain by 3.89 and 4.98 log CFU/mL, respectively, with respect to colistin alone at 24 h (**Figure 3B**). In the control experiment, addition of 2 μM niclosamide after 4 h post-bacterial incubation had no effect on the growth of Col-S and Col-R *A. baumannii* and *K. pneumoniae* strains (**Figures 3A**, **3B**).

Zeta Potential

Figure 4 illustrates the zeta potential of *A. baumannii* ATCC 17978 and #11 strains in presence and absence of niclosamide. Analysis of zeta potential revealed that treatment of ATCC 17978 and #11 strains with 2 μM niclosamide exhibited significantly high negative surface charge by −35.62 ± 1.32 mV and −34.95 ± 0.35 mV, respectively with respect to ATCC 17978 and #11 strains without treatment with niclosamide, −32.33 ± 0.63 and −26.85 ± 3.65 mV, respectively. Similarly, analysis of zeta potential revealed that treatment of *K. pneumoniae* CECT 997 and KPc21 strains with 2 μM niclosamide exhibited significantly high negative surface charge by −40.23 ± 0.88 mV and −38.85 ± 0.93 mV, respectively with respect to CECT 997 and KPc21 strains without treatment with niclosamide, −36.7 ± 0.88 and −35.27 ± 0.72 mV, respectively (**Figure 4**).

DISCUSSION

Colistin resistance, although uncommon, is increasingly being reported among clinical Gram-negative bacilli isolates, and an understanding of its impact on the activity of antimicrobials is now evolving (Olaitan et al., 2014). Modification of LPS is one of the colistin resistance mechanisms in Gram negative bacilli that result in the increase of positive surface charge of the bacterial outer membrane (Olaitan et al., 2014).

Niclosamide's ability to carrier proton has been previously used to investigate the potential of niclosamide for blocking the acidification of endosomes in eukaryotic cells (Jurgeit et al., 2012). Thus, the use of niclosamide to carrier the

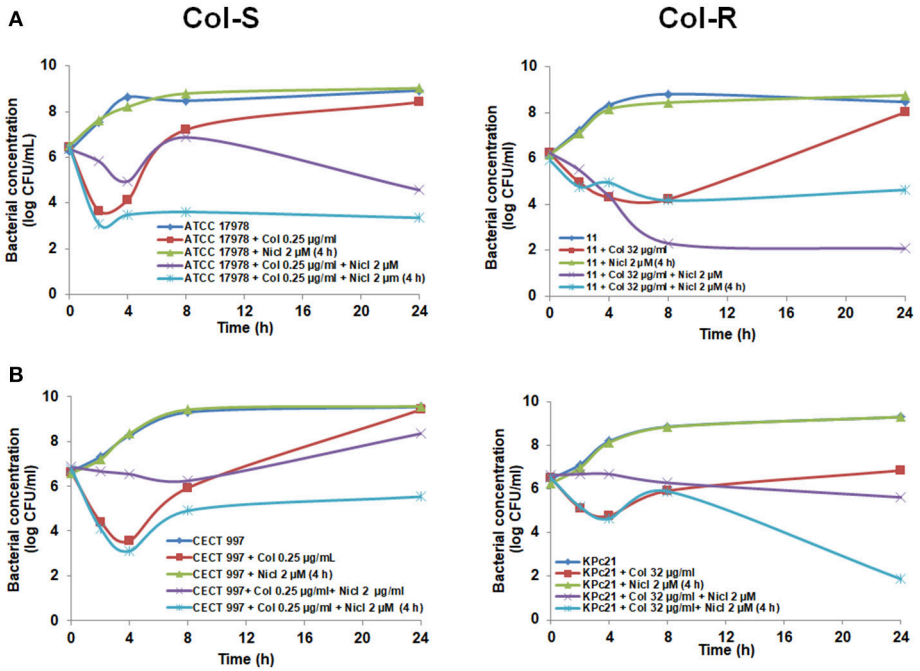

FIGURE 3 | Late addition of niclosamide potentiates the colistin activity against Col-S and Col-R *A. baumannii* and *K. pneumoniae* strains. Time-kill curves of *A. baumannii* ATCC 17978 and #11 strains **(A)**, *K. pneumoniae* CECT 997 and KPc21 strains **(B)**, in presence of colistin (sub-MIC) alone with or without addition of 2 µM niclosamide 4 h after bacterial addition. One micromolar of niclosamide correspond to 0.33 µg/ml. Nicl, niclosamide; Col, colistin.

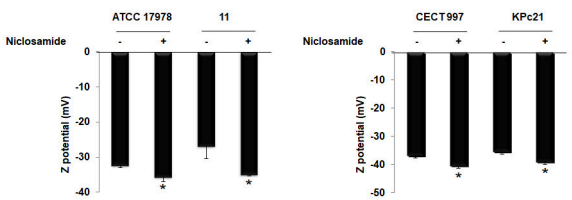

FIGURE 4 | Zeta potential of Col-S and Col-R *A. baumannii* and *K. pneumoniae* strains in presence and absence of niclosamide. Data are the mean ± SEM. *$P < 0.05$ untreated vs. treated with niclosamide.

proton in the outer membrane of Col-R strains could be helpful to restore the activity of colistin against Gram negative bacilli.

In the present study, the combination of niclosamide with colistin potentiates the activity of colistin against Col-S and especially Col-R *A. baumannii* and *K. pneumoniae* strains at 24 h, despite of the antagonist effect of niclosamide on the antibacterial effect of colistin against these strains in the first 4 h. Similar results regarding the antagonism of the colistin effect were observed in the first 4–8 h when colistin was combined with doripenem or ertapenem against a clinical isolate of *K. pneumoniae* resistant to colistin, doripenem, and ertapenem (Hong et al., 2013), and with levofloxacin against a clinical isolate of *A. baumannii* resistant to levofloxacin (Safarika et al., 2015). In the present study, this antagonism has been corrected when niclosamide was added 4 h after bacterial and colistin incubation.

It is noteworthy to mention that the use of niclosamide alone did not affect the growth of Col-S and Col-R *A. baumannii* and *K. pneumoniae* strains, which is consistent with previously published data in which niclosamide was not effective against Gram-negative bacilli including *A. baumannii* and *K. pneumoniae* (Rajamuthiah et al., 2015). In addition, the synergy between niclosamide and colistin was increased when colistin was added for second time 4 h post-bacterial due to a possible compensation of colistin degradation in the broth culture (Owen et al., 2007; Bergen et al., 2010).

It is well known that niclosamide does not cause significant bacterial cell envelope damage in Gram-positive pathogens (Rajamuthiah et al., 2015), and Gram-negative bacilli may have intrinsic resistance to niclosamide due to their functional and structural characteristics (Blair et al., 2014). Interestingly, despite the fact that niclosamide does not appear to inhibit *A. baumannii* and *K. pneumoniae* growth, we demonstrated, for the first time, that niclosamide increased the negative surface charge of Col-S and Col-R *A. baumannii* and *K. pneumoniae* strains. This effect was higher with Col-R than with Col-S *A. baumannii* and *K. pneumoniae* strains. This fact would be due to the proportion of negative and positive surface charge in these strains. Indeed, we observed that Col-R strains contain less negative surface charges than Col-S strains. These data are consistent with previously published reports, showing less negative surface charges in Col-R *A. baumannii* and *K. pneumoniae* (Soon et al., 2011; Velkov et al., 2014). Recently, it was reported that salicylanilide analogs inhibit *Clostridioides difficile* growth via membrane depolarization by

dissipation of the bacterial membrane potential (Gooyit and Janda, 2016).

Furthermore, we showed that Col-R *A. baumannii* strain did not improve the synergy with niclosamide while adding the second colistin dose. A explanation for this data would be that the binding of colistin to the cell wall of this strain is saturated after the first addition of colistin in medium. Indeed, this strain, in presence of niclosamide, has presented lower zeta potential level (-34.95 ± 0.35 mV) than with *K. pneumoniae* CECT 997 strain (-40.23 ± 0.88 mV), *K. pneumoniae* KPc21 strain (-38.85 ± 0.93 mV), and *A. baumannii* ATCC 17978 strain (-35.62 ± 1.32 mV) which suggest the colistin binding saturation.

We have not shown that the incubation of *A. baumannii* and *K. pneumoniae* with niclosamide affect their OMPs profiles (data not shown). Thus, further investigations, including the integrity of bacterial membrane by transmission electron microscopy, are necessary to better understand how niclosamide acts synergistically with colistin against Col-S and Col-R *A. baumannii* and *K. pneumoniae* strains.

Concerning future developments of niclosamide as potent synergic drug with colistin, niclosamide derivative or same structural class of niclosamides, i.e., the salicylanilide oxyclozanide, need to be evaluated in combination with colistin. Previous studies showed that oxyclozanide present same activities as niclosamide against *P. aeruginosa* and *S. aureus* (Imperi et al., 2013; Rajamuthiah et al., 2015). Furthermore, It should be a very interesting exercise to assay *in vitro* the anti-quorum sensing of niclosamide (Imperi et al., 2013; Costabile et al., 2015) in combination with colistin and *in vivo* the colistin niclosamide combination in an infection model like the silk worm *Galleria mellonella*.

CONCLUSIONS

Niclosamide has potentiated the effect of colistin against Col-S and Col-R *A. baumannii* and *K. pneumoniae* strains. This effect might be due to the alteration of negative surface charge proportion in the outer membrane of these strains. The results of this study provide new insights into the use of niclosamide in combination with colistin to treat the infections by Gram negative bacilli.

AUTHOR CONTRIBUTIONS

JP and YS conceived the study. RA-A, MG-M, VS-E, RP-M, and MP-I carried out the experiments. RA-A and YS analyzed the data. MJ-M, MP-I, and JP have reviewed the manuscript and the experiments. RA-A and YS wrote the manuscript. All authors read and approved the final manuscript.

FUNDING

This study was supported by the Instituto de Salud Carlos III, Proyectos de Investigación en Salud (grant PI16/01378). YS is supported by the Subprograma Miguel Servet Tipo I from the Ministerio de Economía y Competitividad of Spain (CP15/01358).

ACKNOWLEDGMENTS

We thank Dr. Alvaro Pascual for the kind gift of the *K. pneumoniae* strains KPc07, KPc21 and KPc29. We thank Dr. Javier Sánchez-Cespedes for helping with anthelmintic drug screening.

REFERENCES

European Committee on Antimicrobial Susceptibility Testing [EUCAST] (2016). *European Society of Clinical Microbiology and Infectious Diseases*. Clinical Breakpoints. Bochum: EUCAST.

Ah, Y. M., Kim, A. J., and Lee, J. Y. (2014). Colistin resistance in *Klebsiella pneumoniae*. *Int. J. Antimicrob. Agents* 44, 8–15. doi: 10.1016/j.ijantimicag.2014.02.016

Antunes, L. C., Imperi, F., Minandri, F., and Visca, P. (2012). *in vitro* and *in vivo* antimicrobial activities of gallium nitrate against multidrug-resistant *Acinetobacter baumannii*. *Antimicrob. Agents Chemother.* 56, 5961–5970. doi: 10.1128/AAC.01519-12

Baumann, P., Doudoroff, M., and Stanier, R. Y. (1968). A study of the Moraxella grouP. II. Oxidative-negative species (genus Acinetobacter). *J. Bacteriol.* 95, 1520–1541.

Bergen, P. J., Bulitta, J. B., Forrest, A., Tsuji, B. T., Li, J., and Nation, R. L. (2010). Pharmacokinetic/pharmacodynamic investigation of colistin against *Pseudomonas aeruginosa* using an *in vitro* model. *Antimicrob. Agents Chemother.* 54, 3783–3789. doi: 10.1128/AAC.00903-09

Blair, J. M., Webber, M. A., Baylay, A. J., Ogbolu, D. O., and Piddock, L. J. V. (2014). Molecular mechanisms of antibiotic resistance. *Nat. Rev. Microbiol.* 13, 42–51. doi: 10.1038/nrmicro3380

Bonnin, A. R., Nordmann, P., and Poirel, L. (2013). Screening and deciphering antibiotic resistance in *Acinetobacter baumannii*: a state of the art. *Expert Rev. Anti. Infect. Ther.* 11, 571–583. doi: 10.1586/eri.13.38

Cassir, N., Rolain, J. M., and Brouqui, P. (2014). A new strategy to fight antimicrobial resistance: the revival of old antibiotics. *Front. Microbiol.* 5:551. doi: 10.3389/fmicb.2014.00551

Chopra, S., Torres-Ortiz, M., Hokama, L., Madrid, P., Tanga, M., Mortelmans, K., et al. (2010). Repurposing FDA-approved drugs to combat drug-resistant *Acinetobacter baumannii*. *J. Antimicrob. Chemother.* 65, 2598–2601. doi: 10.1093/jac/dkq353

Clinical and Laboratory Standards Institute (2016). *Performance Standards for Antimicrobial Susceptibility Testing. Twenty-Sixth Informational Supplement. Document M100-S26. CLSI*. Wayne, PA: Clinical and Laboratory Standards Institute.

Costabile, G., d'Angelo, I., Rampioni, G., Bondi, R., Pompili, B., Ascenzioni, F., et al. (2015). Towards repositioning niclosamide for anti-virulence therapy of *Pseudomonas aeruginosa* lung infections: development of inhalable formulations through nanosuspension technology. *Mol. Pharm.* 12, 2604–2617. doi: 10.1021/acs.molpharmaceut.5b00098

Fernández-Cuenca, F., Tomás-Carmona, M., Caballero-Moyano, F., Bou, G., Martínez-Martínez, L., Vila, J., et al. (2013). *in vitro* activity of 18 antimicrobial agents against clinical isolates of *Acinetobacter* spp.: multicenter national study GEIH-REIPI-Ab 2010. *Enferm Infecc Microbiol. Clin.* 31, 4–9. doi: 10.1016/j.eimc.2012.06.010

Gooyit, M., and Janda, K. M. (2016). Reprofiled anthelmintics bate hypervirulent stationary-phase *Clostridium difficile*. *Sci. Rep.* 6:33642. doi: 10.1038/srep33642

Gwisai, T., Hollingsworth, N. R., Cowles, S., Tharmalingam, N., Mylonakis, E., Burgwyn Fuchs, B., et al. (2017). Repurposing niclosamide as a versatile

antimicrobial surface coating against device-associated. Hospital-acquired bacterial infections. *Biomed. Mater*. 12:045010. doi: 10.1088/1748-605X/aa7105

Haeili, M., Javani, A., Moradi, J., Jafari, Z., Feizabadi, M. M., and Babaei, E. (2017). MgrB alterations mediate colistin resistance in *Klebsiella pneumoniae* isolates from Iran. *Front. Microbiol*. 8, 1–8. doi: 10.3389/fmicb.2017.02470

Hong, J. H., Clancy, C. J., Cheng, S., Shields, R. K., Chen, L., Doi, Y., et al. (2013). Characterization of porin expression in *Klebsiella pneumoniae* Carbapenemase (KPC)-producing *K.* pneumoniae identifies isolates most susceptible to the combination of colistin and carbapenems. *Antimicrob. Agents Chemother.* 57, 2147–2153. doi: 10.1128/AAC.02411-12

Imperi, F., Massai, F., Ramachandran Pillai, C., Longo, F., Zennaro, E., Rampioni, G., et al. (2013). New life for an old drug: the anthelmintic drug niclosamide inhibits *Pseudomonas aeruginosa* quorum sensing. *Antimicrob. Agents Chemother.* 57, 996–1005. doi: 10.1128/AAC.01952-12

Jurgeit, A., McDowell, R., Moese, S., Meldrum, E., Schwendener, R., and Greber, U. F. (2012). Niclosamide is a proton carrier and targets acidic endosomes with broad antiviral effects. *PLoS Pathog.* 8:e1002976. doi: 10.1371/journal.ppat.1002976

López-Rojas, R., Domínguez-Herrera, J., McConnell, M. J., Docobo-Peréz, F., Smani, Y., Fernández-Reyes, M., et al. (2011). Impaired virulence and *in vivo* fitness of colistin-resistant *Acinetobacter baumannii*. *J. Infect. Dis*. 203, 545–548. doi: 10.1093/infdis/jiq086

López-Rojas, R., García-Quintanilla, M., Labrador-Herrera, G., Pachón, J., and McConnell, M. J. (2016). Impaired growth under iron-limiting conditions associated with the acquisition of colistin resistance in *Acinetobacter baumannii*. *Int. J. Antimicrob. Agents* 47, 473–477. doi: 10.1016/j.ijantimicag.2016.03.010

Mohamed, A. F., Cars, O., and Friberg, L. E. (2014). A pharmacokinetic/pharmacodynamic model developed for the effect of colistin on Pseudomonas aeruginosa *in vitro* with evaluation of population pharmacokinetic variability on simulated bacterial killing. *J. Antimicrob. Chemother*. 69, 1350–1361. doi: 10.1093/jac/dkt520

Olaitan, A. O., Morand, S., and Rolain, J. M. (2014). Mechanisms of polymyxin resistance: acquired and intrinsic resistance in bacteria. *Front. Microbiol.* 5:643. doi: 10.3389/fmicb.2014.00643

Owen, R. J., Li, J., Nation, R. L., and Spelman, D. (2007). *in vitro* pharmacodynamics of colistin against *Acinetobacter baumannii* clinical isolates. *J. Antimicrob. Chemother.* 59, 473–477. doi: 10.1093/jac/dkl512

Pachón-Ibáñez, M. E., Labrador-Herrera, G., Cebrero-Cangueiro, T., Díaz, C., Smani, Y., Del Palacio, J. P., et al. (2018). Efficacy of colistin and its combination with rifampin *in vitro* and in experimental models of infection caused by carbapenemase-producing clinical isolates of *Klebsiella pneumoniae*. *Front. Microbiol.* 9:912. doi: 10.3389/fmicb.2018.00912

Paul, M., Carmeli, Y., Durante-Mangoni, E., Mouton, J. W., Tacconelli, E., Theuretzbacher, U., et al. (2014). Combination therapy for carbapenem-resistant Gram-negative bacteria. *J. Antimicrob. Chemother.* 69, 2305–2309. doi: 10.1093/jac/dku168

Poirel, L., Jayol, A., Bontron, S., Villegas, M.,V., and Ozdamar, R., Tükkoglu, S., et al. (2015). The *mgrB* gene as a key target for acquired resistance to colistin in *Klebsiella pneumoniae*. *J. Antimicrob. Chemother*. 70, 75–80. doi: 10.1093/jac/dku323

Poulikakos, P., Tansarli, G. S., and Falagas, M. E. (2014). Combination antibiotic treatment versus monotherapy for multidrug-resistant, extensively drug-resistant, and pandrug-resistant *Acinetobacter* infections: a systematic review. *Eur. J. Clin. Microbiol. Infect. Dis.* 33, 1675–1685. doi: 10.1007/s10096-014-2124-9

Rajamuthiah, R., Fuchs, B. B., Conery, A. L., Kim, W., Jayamani, E., Kwon, B., et al. (2015). Repurposing Salicylanilide anthelmintic drugs to combat drug resistant *Staphylococcus aureus*. *PLoS ONE* 10:e0124595. doi: 10.1371/journal.pone.0124595

Reading, C., and Cole, M. (1977). Clavulanic acid: a beta-lactamase-inhibiting beta-lactam from Streptomyces clavuligerus. *Antimicrob. Agents Chemother*. 11, 852–857. doi: 10.1128/AAC.11.5.852

Safarika, A., Galani, I., Pistiki, A., and Giamarellos-Bourboulis, E. J. (2015). Time-kill effect of levofloxacin on multidrug-resistant *Pseudomonas aeruginosa* and *Acinetobacter baumannii*: synergism with imipenem and colistin. *Eur. J. Clin. Microbiol. Infect. Dis.* 34, 317–323. doi: 10.1007/s10096-014-2231-7

Smani, Y., Domínguez-Herrera, J., and Pachón, J. (2011). Rifampin protects human lung epithelial cells against cytotoxicity induced by clinical multi and pandrug-resistant *Acinetobacter baumannii*. *J. Infect. Dis.* 203, 1110–1119. doi: 10.1093/infdis/jiq159

Soon, R. L., Nation, R. L., Cockram, S., Moffatt, J. H., Harper, M., Adler, B., et al. (2011). Different surface charge of colistin-susceptible and -resistant *Acinetobacter baumannii* cells measured with zeta potential as a function of growth phase and colistin treatment. *J. Antimicrob. Chemother*. 66, 126–133. doi: 10.1093/jac/dkq422

Tao, H., Zhang, Y., Zeng, X., Shulman, G. I., and Jin, S. (2014). Niclosamide ethanolamine-induced mild mitochondrial uncoupling improves diabetic symptoms in mice. *Nat. Med.* 20, 1263–1269. doi: 10.1038/nm.3699

Tharmalingam, N., Port, J., Castillo, D., and Mylonakis, E. (2018). Repurposing the anthelmintic drug niclosamide to combat *Helicobacter pylori*. *Sci. Rep*. 8:3701. doi: 10.1038/s41598-018-22037-x

Valencia, R., Arroyo, L. A., Conde, M., Aldana, J. M., Torres, M. J., Fernández-Cuenca, F., et al. (2009). Nosocomial outbreak of infection with pan-drug-resistant *Acinetobacter baumannii* in a tertiary care university hospital. *Infect. Control HosP. Epidemiol.* 30, 257–263. doi: 10.1086/595977

Velkov, T., Deris, Z. Z., Huang, J. X., Azad, M. A., Butler, M., Sivanesan, S., et al. (2014). Surface changes and polymyxin interactions with a resistant strain of *Klebsiella pneumoniae*. *Innate Immun.* 20, 350–363. doi: 10.1177/1753425913493337

Vila, J., and Pachón, J. (2012). Therapeutic options for *Acinetobacter baumannii* infections: an update. *Expert Opin. Pharmacother.* 13, 2319–2336. doi: 10.1517/14656566.2012.729820

Ye, T., Xiong, Y., Yan, Y., Xia, Y., Song, X., Liu, L., et al. (2014). The anthelmintic drug niclosamide induces apoptosis, impairs metastasis and reduces immunosuppressive cells in breast cancer model. *PLoS ONE* 9:e85887. doi: 10.1371/journal.pone.0085887

Younis, W., Thangamani, S., and Seleem, M. N. (2015). Repurposing Non-antimicrobial drugs and clinical molecules to treat bacterial infections. *Curr. Pharm. Des.* 21, 4106–41011. doi: 10.2174/1381612821666150506154434

Zemke, A. C., Shiva, S., Burns, J. L., Moskowitz, S. M., Pilewski, J. M., Gladwin, M. T., et al. (2014). Nitrite modulates bacterial antibiotic susceptibility and biofilm formation in association with airway epithelial cells. *Free Radic. Biol. Med.* 77, 307–316. doi: 10.1016/j.freeradbiomed.2014.08.011

Zusman, O., Avni, T., Leibovici, L., Adler, A., Friberg, L., Stergiopoulo, T., et al. (2013). Systematic review and meta-analysis of *in vitro* synergy of polymyxins and carbapenems. *Antimicrob. Agents Chemother.* 57, 5104–5111. doi: 10.1128/AAC.01230-13

Conflict of Interest Statement: The authors declare that the research was conducted in the absence of any commercial or financial relationships that could be construed as a potential conflict of interest.

frontiers in Cellular and Infection Microbiology

ORIGINAL RESEARCH
published: 18 October 2018
doi: 10.3389/fcimb.2018.00363

In vitro Activity of Pentamidine Alone and in Combination With Aminoglycosides, Tigecycline, Rifampicin, and Doripenem Against Clinical Strains of Carbapenemase-Producing and/or Colistin-Resistant Enterobacteriaceae

Tania Cebrero-Cangueiro [1,2], Rocío Álvarez-Marín [1,2], Gema Labrador-Herrera [1,2], Younes Smani [1,2], Elisa Cordero-Matía [1,2], Jerónimo Pachón [1,3] and María Eugenia Pachón-Ibáñez [1,2]*

[1] Clinical Unit of Infectious Diseases, Microbiology, and Preventive Medicine, University Hospital Virgen del Rocío, CSIC, University of Seville, Seville, Spain, [2] Institute of Biomedicine of Seville, University Hospital Virgen del Rocío, CSIC, University of Seville, Seville, Spain, [3] Department of Medicine, University of Seville, Seville, Spain

OPEN ACCESS

Edited by:
Maria Tomas, Complexo Hospitalario Universitario A Coruña, Spain

Reviewed by:
Robson Souza Leão, Rio de Janeiro State University, Brazil
Naybi Muñoz, Centro de Investigación Científica de Yucatán, Mexico

***Correspondence:**
Jerónimo Pachón
pachon@us.es

Received: *13 August 2018*
Accepted: *01 October 2018*
Published: *18 October 2018*

Citation:
Cebrero-Cangueiro T, Álvarez-Marín R, Labrador-Herrera G, Smani Y, Cordero-Matía E, Pachón J and Pachón-Ibáñez ME (2018) In vitro Activity of Pentamidine Alone and in Combination With Aminoglycosides, Tigecycline, Rifampicin, and Doripenem Against Clinical Strains of Carbapenemase-Producing and/or Colistin-Resistant Enterobacteriaceae. Front. Cell. Infect. Microbiol. 8:363. doi: 10.3389/fcimb.2018.00363

Enterobacteriaceae cause different types of community- and hospital-acquired infections. Moreover, the spread of multidrug-resistant Enterobacteriaceae is a public health problem and the World Health Organization pointed them among the pathogens in which the search of new antibiotics is critical. The objective of this study was to analyze the *in vitro* activity of pentamidine alone and in combination with gentamicin, tobramycin, amikacin, tigecycline, rifampicin, or doripenem against eight clinical strains of carbapenemase-producing and/or colistin-resistant Enterobacteriaceae: five carbapenemase-producing *Klebsiella pneumoniae*, one carbapenemase-producing *Escherichia coli,* and two colistin-resistant *Enterobacter cloacae*. MIC and MBC were determined following standard protocols. MIC results were interpreted for all the antibiotics according to the EUCAST breakpoints but for rifampicin in which the French FSM breakpoint was used. Bactericidal and synergistic activity of pentamidine alone and in combination with antibiotics at concentrations of 1xMIC was measured by time-kill curves. For one selected strain, *K. pneumoniae* OXA-48/CTX-M-15 time-kill curves were performed also at 1/2xMIC of pentamidine. All studies were performed in triplicate. Pentamidine MIC range was 200–800 μg/mL. The 50, 12.5, 62.5, 87.5, and 62.5% of the strains were susceptible to gentamicin, tobramycin, amikacin, tigecycline, and doripenem, respectively. Only the two *E. cloacae* strains were susceptible to rifampicin. Pentamidine alone at 1xMIC showed bactericidal activity against all strains, except for the *E. cloacae* 32 strain. The bactericidal activity of pentamidine alone was also observed in combination. The combinations of pentamidine were synergistic against *E. cloacae*

32 with amikacin and tobramycin at 24 h and with tigecycline at 8 h. Pentamidine plus rifampicin was the combination that showed synergistic activity against more strains (five out of eight). Pentamidine plus doripenem did not show synergy against any strain. At 1/2xMIC, pentamidine was synergistic with all the studied combinations against the K. pneumoniae OXA-48/CTX-M-15 strain. In summary, pentamidine alone and in combination shows *in vitro* activity against carbapenemase-producing and/or colistin-resistant Enterobacteriaceae. Pentamidine appears to be a promising option to treat infections caused by these pathogens.

Keywords: Enterobacteriaceae, colistin-resistant, carbapenemase producers, pentamidine, *in vitro* activity

INTRODUCTION

Carbapenem-resistance in *Enterobacteriaceae* is a world health problem that has made the World Health Organization (WHO) to point it as a priority in the list of bacteria for which new antibiotics are urgently needed (World Health Organization, 2017). Moreover, these pathogens have spread globally in the past years, and are associated with carbapenemase production as the most important resistance mechanism (Cantón et al., 2012). Therapeutic options for infections caused by these kinds of pathogens are scarce and colistin is often the only remaining treatment option. However, the appearance of colistin-resistant strains has risen dramatically in the last decade due to antibiotic pressure in both human treatment and its use in agriculture (Kempf et al., 2016; Olaitan et al., 2016). In a recently published study (Hong et al., 2018), the *in vitro* activity of colistin was analyzed against 356 clinical strains of *Enterobacter* spp. from eight Korean hospitals, founding that 23.9 and 4.2% of *E. cloacae* and *E. aerogenes* strains, respectively, were resistant to colistin.

In this context, clinical experience on the most effective treatment for infections caused by these pathogens is still scarce (Akova et al., 2012). Currently, the majority of clinical studies conclude that the combined treatment with two or more antimicrobials is the better option in terms of increase the survival (Trecarichi and Tumbarello, 2017). Numerous studies, both *in vitro* and *in vivo*, have tested the efficacy of antimicrobials combinations against these kinds of pathogens (Pachón-Ibáñez et al., 2018; Wang et al., 2018). Nevertheless, the best combination depends on the susceptibility pattern of the strains and there is no one combination that we could qualify as optimal.

Therefore, the increase in the rates of antimicrobial resistance, the difficulty to find an optimal and effective treatment for infections caused by these pathogens, and the lack of the development of new families of antimicrobials by the pharmaceutical industry (Spellberg and Rex, 2013), make urgent the search for new approaches to combat the problem caused by multi-resistant strains of Gram-negative bacilli (GNB) and, specifically, by carbapenemase-producing and/or colistin-resistant Enterobacteriaceae.

As a new treatment strategy, the repurposing of drugs for the treatment of infections caused by these kinds of pathogens seems especially interesting (Younis et al., 2015). This new approach reduces the time, cost, and risk associated with the development of antimicrobial molecules *de novo*. In addition, its effectiveness has been demonstrated in different medical areas, such as infectious diseases (Debnath et al., 2012). Despite of that several drugs have been recycled for other clinical indications; none has been used for the treatment of bacterial infections.

Pentamidine (in the form of isethionate) is an antiprotozoal agent effective in trypanosomiasis, leishmaniasis, and some fungal infections (Nguewa et al., 2005). To our knowledge, pentamidine has never been used in clinic as antimicrobial agent. Nevertheless, in a recent study Stokes et al. found that pentamidine is able to disturb the outer membrane of GNB, due to the interaction with membrane lipopolysaccharides (Stokes et al., 2017). Moreover, they concluded that pentamidine in combination with antimicrobials typically used for Gram-positive cocci had synergistic activity *in vitro* against different GNB and in a mice sepsis model by *Acinetobacter baumannii*.

The aim of this study was to evaluate *in vitro* the activity of pentamidine alone and in combination with different antimicrobials against clinical strains of carbapenemase-producing and/or colistin-resistant Enterobacteriaceae.

MATERIALS AND METHODS

Bacterial Strains

Eight clinical strains of carbapenemase-producing and/or colistin-resistant Enterobacteriaceae were studied: (1) five strains of carbapenemase-producing *Klebsiella pneumoniae*: Kp07, a VIM-1 ST 1603 clone producer from Spain (Miró et al., 2013); Kp21, co-producing VIM-1 and AmpC type beta-lactamase DHA-1 ST 11 clone from Spain (Miró et al., 2013); Kp28, co-producing OXA-48 ST11 clone and the extended spectrum beta-lactamase (ESBL) CTX-M-15 from Spain (Oteo et al., 2015); a Kp29, co-producing KPC-3 ST512 clone with the extended spectrum beta-lactamases TEM-1 and SHV-11 from Spain (López-Cerero et al., 2014); Kp1, a NDM-1 producer from Kenya; (2) Ec271, a *Escherichia coli* NDM-1 producer from Australia Docobo-Pérez et al., 2012; (3) two strains of *Enterobacter* spp. from Spain, *E. cloacae* 32 and *E. cloacae* 297, both resistant to colistin. Identification of these isolates was confirmed by a Microflex LT-MALDI Biotyper mass spectrometer (Ruiz-Aragón et al., 2018) (Bruker Daltonics GmbH, Bremen, Germany). The presence of carbapenemase genes, and genes coding for other beta-lactamases was confirmed by PCR and sequencing as described previously.

Drugs

All the drugs tested were used as standard laboratory powders (Sigma-Aldrich, Madrid, Spain): pentamidine, aminoglycosides (gentamicin, tobramycin, and amikacin), tigecycline, rifampicin, and doripenem.

Antimicrobial Susceptibility Testing

The minimal inhibitory concentration (MIC) and minimal bactericidal concentration (MBC) values were tested. MICs of antibiotics were determined by broth microdilution as recommended by the (Clinical and Laboratory Standards Institute, 2012), using Mueller Hinton broth II (MHB) (Becton Dickinson & Co., Sparks, MD, United States). MIC results were interpreted according to the European Committee on Antimicrobial Susceptibility Testing (http://www.eucast.org/clinical_breakpoints/) breakpoints for all antibiotics (European Committee on Antimicrobial Susceptibility Testing, 2018), but rifampicin, for which the French Society for Microbiology breakpoint was used (Soussy, 2012). Pentamidine has not susceptibility breakpoints defined.

The MIC value was the lowest concentration of antimicrobials that completely inhibited the bacterial growth. To determine the MBC values, 5-μL aliquots from the wells with no visible growth were spread on agar plates. The MBC value was the lowest concentration at which no colony formation occurred. Heteroresistance in the studied strains was also evaluated by reading the MIC at 24 and 48 h of incubation. Heteroresistance was defined when a fraction of the inoculum was able to grow two dilutions above the MIC value previously determined (Ferreira et al., 2015). All assays were performed in triplicates to ensure reproducibility.

Time-Kill Curves

The concentrations used for pentamidine and the different antimicrobials tested corresponded to the MIC value obtained by microdilution. Moreover, with the Kp28 OXA-48/CTX-M-15 strain the assay was also performed at 1/2xMIC of pentamidine. Experiments were carried out with a starting inoculum of 5×10^5 cfu/mL and the drugs alone or in combination. Tubes were incubated at 37°C, with shaking, and samples were taken at 0, 2, 4, 8, and 24 h, serially diluted and plated (Pournaras et al., 2011; Souli et al., 2011). Bactericidal activities of single drugs or combination were defined as a decrease $\geq$ 3 $\log_{10}$ cfu/mL from the starting inoculum, bacteriostatic effect was defined as no change respect to the initial bacterial concentration during the 24 h. Synergy was defined as a decrease $\geq$ 2 $\log_{10}$ cfu/mL for the drugs combination compared with the most active single agent (Pachón-Ibáñez et al., 2018). Experiments were performed three times on separate occasions.

In vitro Selection of Resistant Mutants

Time–kill curves were used. Strains elected strains were incubated with drugs at concentrations 1×MIC, and Kp28 OXA-48/CTX-M-15 also at pentamidine concentration of 1/2×MIC. Furthermore, the possible combinations of pentamidine plus the different studied antimicrobials were tested. Tubes with 20 mL of MHB with an inoculum of 5×10^5 cfu/mL of each one of the strains were used. Tubes with the bacterial inoculum and without drugs were used as growth controls. The bacterial growth was counted at 0 and 24 h after incubation at 37°C. Ten-fold dilutions were made and 100 μL was plated on sheep blood agar and incubated for 24 h at 37°C. For the detection of resistant mutants, the MIC of each one of the studied drugs was carried out in triplicate for a maximum of five colonies at each time-point.

RESULTS

MIC/MBC and Heteroresistance

Individual MIC/MBC of each drug tested for the different clinical strains are shown in **Table 1**. All the strains were multidrug-resistant (MDR) (Magiorakos et al., 2012) except Kp28 OXA-48/CTX-M-15 which was resistant to rifampicin and fosfomycin. Heteroresistance was observed with tigecycline for the Kp1 NDM-1 (1 mg/L) and Kp21 VIM-1/DHA-1 strains (1 mg/L) and with doripenem for *E. cloacae* 32 (1 mg/L). The antibiotic susceptibility profiles are included in the **Supplementary material**.

TABLE 1 | MIC/MBC of the different drugs for the eight carbapenemase-producing and/or colistin-resistant *Enterobacteriaceae* clinical strains.

Clinical strains	MIC/MBC (mg/L)						
	PEN	GEN	AMK	TOB	RIF	TGC	DOR
Kp07 VIM-1	400	4/16	1/1	4/4	32/32	0.5/1	1/2
Kp21 VIM-1/DHA-1	400	2/2	2/4	8 /16	> 256/> 256	0.25/> 4	> 4/> 4
Kp28 OXA-48 /CTX-M-15	400	0.25/0.25	1/1	0.5/0.5	16/16	1/4	0.5/0.5
Kp29 KPC-3	800	2/2	64/64	0.25/0.25	32/64	1/>8	> 4 / > 4
Kp1 NDM-1	400	>32/>32	> 128/> 128	> 32/> 32	> 256/> 256	0.25/> 4	1/2
Ec271 NDM-1	200	>32/>32	> 128/> 128	> 32/> 32	> 256/> 256	1/1	> 4/> 4
E. cloacae 32	800	8/16	2/4	4/8	8/8	0.5/> 4	0.25/> 4
E. cloacae 297	400	0.5/4	0.5/1	8/8	8/256	2/> 8	0.25/0.25

*PEN, pentamidine; GEN, gentamicin; AMK, amikacin; TOB, tobramycin; TGC, tigecycline; RIF, rifampicin; DOR, doripenem; * Pentamidine breakpoints are not defined; GEN and TOB: * Susceptible, MIC ≤ 2 mg/L and resistant MIC > 4 mg/L; AMK, Susceptible, MIC ≤ 8 mg/L and resistant MIC > 16 mg/L; TGC and DOR; Susceptible, MIC ≤ 1 mg/L and resistant MIC > 2 mg/L and RIF: and resistant MIC > 16 mg/L.*

Time-Kill Curves

The bactericidal activity of the drugs alone is shown in **Table 2**. Pentamidine alone at 1xMIC was bactericidal from 2 to 24 h against six of the strains and from 4 to 24 h against Kp21 VIM-1/DHA-1; however, pentamidine alone was no bactericidal against *E. cloacae* 32. Doripenem showed bactericidal activity against three strains, and gentamycin, tobramycin, and amikacin were bactericidal against two strains each. Tigecycline alone was the only antimicrobial that showed not bactericidal effect against any strain.

The *in vitro* activity of pentamidine in combination with antimicrobials is shown in **Table 3**. The bactericidal activity of pentamidine alone was also observed in combination. The combinations of pentamidine were synergistic against *E. cloacae 32* with amikacin, tobramycin and rifampicin at 24 h. Pentamidine plus rifampicin was the combination that showed synergistic activity against more strains: Kp21 VIM-1/DHA-1, Kp29 KPC-3 and *E. cloacae* 297 at 2 h and *E. cloacae* 32 at 24 h. Pentamidine plus doripenem did not show synergy against any strain.

The activity of pentamidine at 1/2xMIC in combination with antimicrobials against Kp28 OXA-48/CTX-M-15 is showed in **Figure 1**. Pentamidine 1/2xMIC plus antimicrobials showed synergism at 24 h, but the combination with

TABLE 2 | Bactericidal activity of drugs alone against eight of carbapenemase-producing and/or colistin-resistant *Enterobacteriaceae* clinical strains.

Clinical strains	PEN	GEN	AMK	TOB	RIF	TGC	DOR
Kp07 VIM-1	B (2–24 h)	–	B (4–8 h)	–	–	–	B (4 h)
Kp21 VIM-1/DHA-1	B (4–24 h)	B (4–24 h)	–	–	–	–	–
Kp28 OXA-48 /CTX-M-15	B (2–24 h)	–	–	–	–	–	–
Kp29 KPC-3	B (2–24 h)	B (2–24 h)	B (4–8 h)	B (2–8 h)	–	–	–
Kp1 NDM-1	B (2–24 h)	–	–	–	–	–	–
Ec271 NDM-1	B (2–24 h)	–	–	–	–	–	–
E. cloacae 32	–	B (24 h)	–	–	–	–	B (8–24 h)
E. cloacae 297	B (4–24 h)	–	–	B (8h)	–	–	B (8 h)

PEN, pentamidine; GEN, gentamicin; AMK, amikacin; TOB, tobramycin; TGC, tigecycline; RIF, rifampicin; DOR, doripenem; B, Bactericidal; –: no bactericidal activity found; (): time frame in hours of the in vitro activity found.

TABLE 3 | *In vitro* activity of pentamidine in combination with antimicrobials against eight of carbapenemase-producing and/or colistin-resistant *Enterobacteriaceae* clinical strains.

Clinical strains	PEN + GEN	PEN + AMK	PEN + TOB	PEN + TGC	PEN + RIF	PEN + DOR
Kp07 VIM-1	B (2–24 h)	B (2–24 h)	B (4–24 h)	B (2–24 h)	B (2–24 h)	B (2–24 h)
Kp21 VIM-1/DHA-1	B (2–24 h)	B (8–24 h)	B (8–24 h)	B (4–24 h)	B + S (2–24 h) + (2 h)	B (2–24 h)
Kp28 OXA-48/CTX-M-15	B (2–24 h)	B (2–24 h)	B (2–24 h)	B (2–24 h)	B (2–24 h)	B (2–24 h)
Kp29 KPC-3	B (2–24 h)	B (2–24 h)	B (2–24 h)	B (2–24 h)	B + S (2–24 h) + (2 h)	B (2–24 h)
Kp1 NDM-1	B (2–24 h)	B (2–24 h)	B (2–24 h)	B (2–24 h)	B (2–24 h)	B (2–24 h)
Ec271 NDM-1	B (4–24 h)	B (4–24 h)	B (4–24 h)	B (2–24 h)	B (2–24 h)	B (2–24 h)
E. cloacae 32	B (24 h)	B + S (8–24 h) + (24 h)	S (24 h)	–	B + S (24 h) + (24 h)	B (8–24 h)
E. cloacae 297	B (4–24 h)	B (2–24 h)	B (4–24 h)	B (4–24 h)	B + S (2–24 h) + (2 h)	B (4–24 h)

PEN, pentamidine; GEN, gentamicin; AMK, amikacin; TOB, tobramycin; TGC, tigecycline; RIF, rifampicin; DOR, doripenem; B, bactericidal; S, synergistic; –: no in vitro activity found; (): time frame in hours of the in vitro activity found.

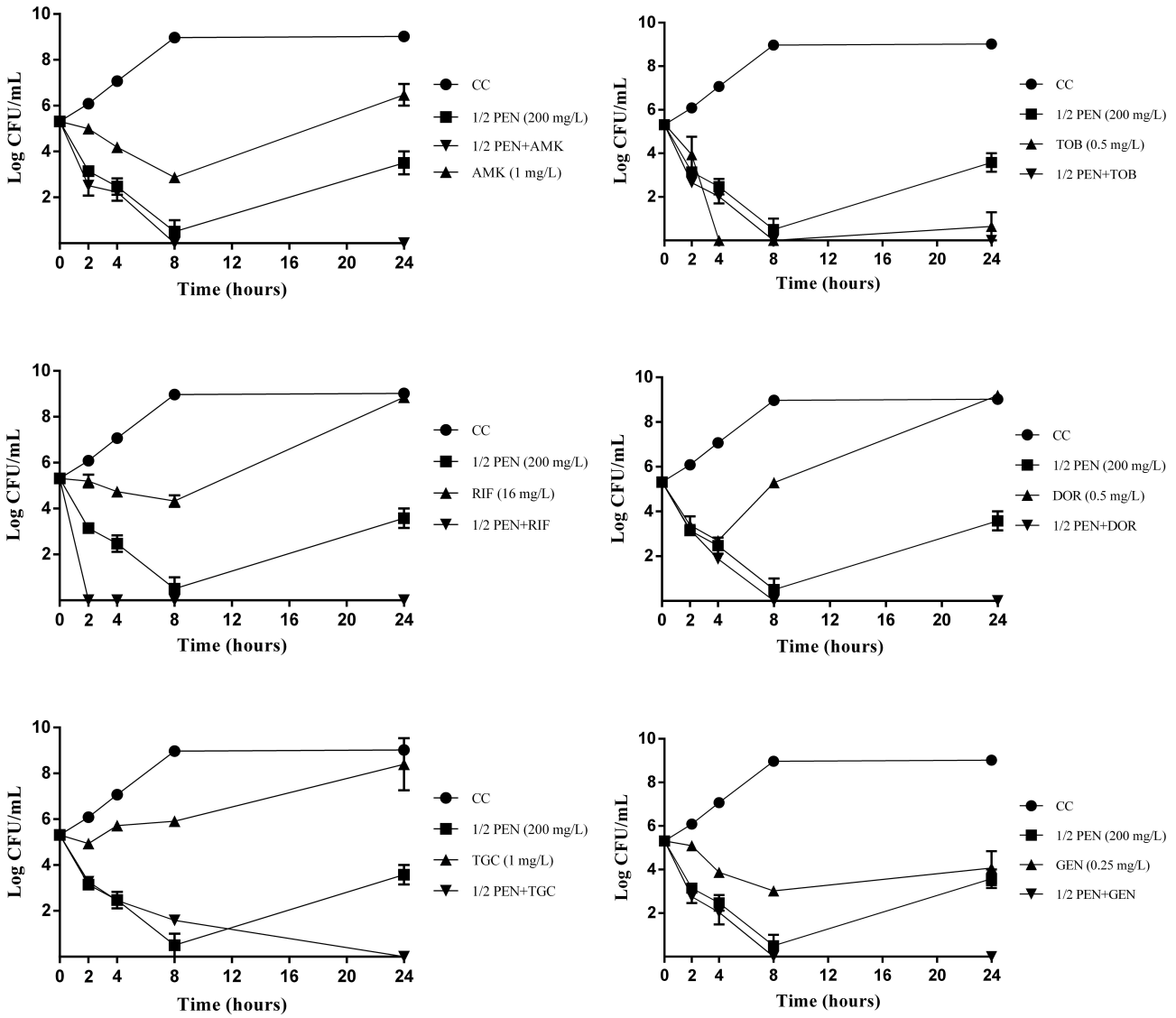

FIGURE 1 | Time-kill curves for pentamidine (PEN) at 1/2xMIC in combination with antimicrobials against the clinical strain Kp28 OXA-48/CTX-M-15. CC: growth control, filled circles; PEN (1/2xMIC), filled squares; antimicrobials (1xMIC), filled triangles, combination of PEN + antimicrobial, filled inverted triangles.

tobramycin due to the high bactericidal activity of tobramycin at 24 h.

In vitro Selection of Resistant Mutants

The high bactericidal activity of pentamidine in combination with antimicrobials, achieving bacterial concentrations close to 0 log cfu/mL did not allow to analyze the selection of resistant mutants after 24 h incubation.

DISCUSSION

This study evaluates the use of pentamidine as antimicrobial agent against clinical strains of carbapenemase-producing and/or colistin-resistant Enterobacteriaceae, finding a strong *in vitro* activity both with pentamidine alone and combined with other antimicrobials, as aminoglycosides, tigecycline, doripenem, and rifampicin. Additionally, pentamidine was synergistic against selected strains in combination with some of these antimicrobials, especially when was studied combined with rifampicin.

Pentamidine showed a MIC rage against eight clinical strains of carbapenemase-producing and/or colistin-resistant Enterobacteriaceae from 200 to 800 mg/L. Due to its use as an antiprotozoal agent (Nguewa et al., 2005), no susceptibility breakpoints for pentamidine are defined. However, the MIC values obtained are in accordance to those reported analyzing the *in vitro* activity of pentamidine and five pentamidine analogs against a *E. coli* strain, with MIC values ranging from 100 to

> 200 mg/L (Stokes et al., 2017). Moreover, we found that pentamidine at MIC concentration is bactericidal against seven of the eight tested strains; furthermore, at 1/2xMIC was bactericidal against the Kp28 OXA-48/CTX-M-15 producer strain.

Besides the robust bactericidal effect found with pentamidine alone, more important is that its combinations with the different antimicrobials tested potentiates the effect of these antimicrobials alone against the clinical strains using the time-kill assay. The *in vitro* activity observed with pentamidine in combination with antibiotics suggests there is strong possibility to repurpose it for antibacterial use against these difficult to treat MDR GNB (Pachón-Ibáñez et al., 2018; Rodríguez-Baño et al., 2018). These results are in accordance to the ones reported by Stokes et al. in which they found that the combination of pentamidine with rifampicin, novobiocin, erythromycin, or vancomycin potentiated the antimicrobials alone against a wild-type *E. coli* strain using chequerboard broth microdilution assays (Stokes et al., 2017). It is noteworthy that synergistic activity was observed when pentamidine was combined with amikacin, tobramycin, tigecycline, and/or rifampicin against the colistin-resistant *E. cloacae* 32, strain against which pentamidine alone did not show bactericidal activity. We would also like to mention, that no more synergistic effect with pentamidine in combination was observed due to the excellent bactericidal activity found with pentamidine alone at MIC concentration.

Pentamidine plus rifampicin was the combination that showed synergism against more of the tested strains (five out of eight). This excellent activity was also pointed out in the Stokes et al. study, in which pentamidine synergized with rifampicin against a wide phylogenetic distribution of antibiotic-resistant strains, including naturally polymyxin-resistant *Serratia* species (Stokes et al., 2017). The combination of rifampicin with other antimicrobials has been proved to be useful, both *in vitro* and *in vivo*, against other MDR GNB as *Acinetobacter baumannii* (Pachón-Ibáñez et al., 2010), as other example of repurposing a drug, such as rifampicin, previously used in staphylococcal and mycobacterial infections.

In summary, these results suggest that pentamidine, alone or in combination, may be a new alternative for the treatment of infections caused by carbapenemase-producing and/or colistin-resistant Enterobacteriaceae. To investigate further the possible usefulness of pentamidine new data from pharmacokinetics and pharmacodynamics and *in vivo* efficacy in experimental models of infection, including the dosage and safety, are required.

AUTHOR CONTRIBUTIONS

MP-I has planned and coordinated the experiments, analyzed the results, and written the manuscript. GL-H and TC-C had performed the *in vitro* experiments. YS had reviewed the manuscript. RÁ-M, EC-M, and JP had reviewed the manuscript and the experiments.

FUNDING

This work was supported by Plan Nacional de I+D+i 2013-2016 and Instituto de Salud Carlos III, Subdirección General de Redes y Centros de Investigación Cooperativa, Ministerio de Economía, Industria y Competitividad, Spanish Network for Research in Infectious Diseases (REIPI RD16/0016/0009)—co-financed by European Development Regional Fund A way to achieve Europe, Operative program Intelligent Growth 2014-2020.

SUPPLEMENTARY MATERIAL

The Supplementary Material for this article can be found online at: https://www.frontiersin.org/articles/10.3389/fcimb.2018.00363/full#supplementary-material

REFERENCES

Akova, M., Daikos, G. L., Tzouvelekis, L., and Carmeli, Y. (2012). Interventional strategies and current clinical experience with carbapenemase-producing Gram-negative bacteria. *Clin. Microbiol. Infect.* 18, 439–448. doi: 10.1111/j.1469-0691.2012.03823.x

Cantón, R., Akóva, M., Carmeli, Y., Giske, C. G., Glupczynski, Y., Gniadkowski, M., et al. (2012). Rapid evolution and spread of carbapenemases among Enterobacteriaceae in Europe. *Clin. Microbiol. Infect.* 18, 413–431. doi: 10.1111/j.1469-0691.2012.03821.x

Clinical and Laboratory Standards Institute (2012). *Methods for Dilution Antimicrobial Susceptibility Tests for Bacteria That Grow Aerobically; Approved Standard—Ninth Edition*. CLSI document M07-A9. Wayne, PA: Clinical and Laboratory Standards Institute.

Debnath, A., Parsonage, D., Andrade, R. M., He, C., Cobo, E. R., Hirata, K., et al. (2012). A high-throughput drug screen for *Entamoeba histolytica* identifies a new lead and target. *Nat. Med.* 18, 956–960. doi: 10.1038/nm.2758

Docobo-Pérez, F., Nordmann, P., Dominguez-Herrera, J., Lopez-Rojas, R., Smani, Y., Poirel, L., et al. (2012). Efficacies of colistin and tigecycline in mice with experimental pneumonia due to NDM-1-producing strains of *Klebsiella pneumoniae* and *Escherichia coli*. *Int. J. Antimicrob. Agents* 39, 251–254. doi: 10.1016/j.ijantimicag.2011.10.012

European Committee on Antimicrobial Susceptibility Testing (2018). *European Society of Clinical Microbiology and Infectious Diseases. Clinical Breakpoints*. EUCAST.

Ferreira, G. F., Santos, J. R., Costa, M. C., Holanda, R. A., Denadai, A. M., Freitas, G. J., et al. (2015). Heteroresistance to itraconazole alters the morphology and increases the virulence of *Cryptococcus gattii*. *Antimicrob. Agents Chemother.* 59, 4600–4609. doi: 10.1128/AAC.00466-15

Hong, Y. K., Lee, J. Y., and Ko, K. S. (2018). Colistin resistance in *Enterobacter* spp. isolates in Korea. *J. Microbiol.* 56, 435–440. doi: 10.1007/s12275-018-7449-0

Kempf, I., Jouy, E., and Chauvin, C. (2016). Colistin use and colistin resistance in bacteria from animals. *Int. J. Antimicrob. Agents* 48, 598–606. doi: 10.1016/j.ijantimicag.2016.09.016

López-Cerero, L., Egea, P., Gracia-Ahufinger, I., Gonzalez-Padilla, M., Rodriguez-Lopez, F., Rodriguez-Bano, J., et al. (2014). Characterisation of the first ongoing outbreak due to KPC-3-producing *Klebsiella pneumoniae* (ST512) in Spain. *Int. J. Antimicrob. Agents* 44, 538–540. doi: 10.1016/j.ijantimicag.2014.08.006

Magiorakos, A. P., Srinivasan, A., Carey, R. B., Carmeli, Y., Falagas, M. E., Giske, C. G., et al. (2012). Multidrug-resistant, extensively drug-resistant and pandrug-resistant bacteria: an international expert proposal for interim standard definitions for acquired resistance. *Clin Microbiol Infect.* 18, 268–281. doi: 10.1111/j.1469-0691.2011.03570.x

Miró, E., Aguero, J., Larrosa, M. N., Fernandez, A., Conejo, M. C., Bou, G., et al. (2013). Prevalence and molecular epidemiology of acquired AmpC beta-lactamases and carbapenemases in Enterobacteriaceae isolates from

35 hospitals in Spain. *Eur. J. Clin. Microbiol. Infect. Dis.* 32, 253–259. doi: 10.1007/s10096-012-1737-0

Nguewa, P. A., Fuertes, M. A., Cepeda, V., Iborra, S., Carrion, J., Valladares, B., et al. (2005). Pentamidine is an antiparasitic and apoptotic drug that selectively modifies ubiquitin. *Chem. Biodivers.* 2, 1387–1400. doi: 10.1002/cbdv.200590111

Olaitan, A. O., Morand, S., and Rolain, J. M. (2016). Emergence of colistin-resistant bacteria in humans without colistin usage: a new worry and cause for vigilance. *Int. J. Antimicrob. Agents* 47, 1–3. doi: 10.1016/j.ijantimicag.2015.11.009

Oteo, J., Ortega, A., Bartolome, R., Bou, G., Conejo, C., Fernandez-Martinez, M., et al. (2015). Prospective multicenter study of carbapenemase-producing Enterobacteriaceae from 83 hospitals in Spain reveals high *in vitro* susceptibility to colistin and meropenem. *Antimicrob. Agents Chemother.* 59, 3406–3412. doi: 10.1128/AAC.00086-15

Pachón-Ibáñez, M. E., Docobo-Perez, F., Lopez-Rojas, R., Domínguez-Herrera, J., Jimenez-Mejias, M. E., García-Curiel, A., et al. (2010). Efficacy of rifampin and its combinations with imipenem, sulbactam, and colistin in experimental models of infection caused by imipenem-resistant *Acinetobacter baumannii*. *Antimicrob Agents Chemother.* 54, 1165–1172. doi: 10.1128/AAC.00367-09

Pachón-Ibáñez, M. E., Labrador-Herrera, G., Cebrero-Cangueiro, T., Diaz, C., Smani, Y., Del Palacio, J. P., et al. (2018). Efficacy of colistin and its combination with rifampin *in vitro* and in experimental models of infection caused by carbapenemase-producing clinical isolates of *Klebsiella pneumoniae*. *Front. Microbiol.* 9:912. doi: 10.3389/fmicb.2018.00912

Pournaras, S., Vrioni, G., Neou, E., Dendrinos, J., Dimitroulia, E., Poulou, A., et al. (2011). Activity of tigecycline alone and in combination with colistin and meropenem against *Klebsiella pneumoniae* carbapenemase (KPC)-producing Enterobacteriaceae strains by time-kill assay. *Int. J. Antimicrob. Agents* 37, 244–247. doi: 10.1016/j.ijantimicag.2010.10.031

Rodríguez-Baño, J., Gutiérrez-Gutiérrez, B., Machuca, I., and Pascual, A. (2018). Treatment of infections caused by extended-spectrum-beta-lactamase-, ampc-, and carbapenemase-producing enterobacteriaceae. *Clin. Microbiol. Rev.* 31, e00079–e00017. doi: 10.1128/CMR.00079-17

Ruiz-Aragón, J., Ballestero-Téllez, M., Gutiérrez-Gutiérrez, B., de Cueto, M., Rodríguez-Baño, J., and Pascual, Á. (2018). Direct bacterial identification from positive blood cultures using matrix-assisted laser desorption/ionization time-of-flight (MALDI-TOF) mass spectrometry: A systematic review and meta-analysis. *Enferm. Infecc. Microbiol. Clin.* 36, 484–492. doi: 10.1016/j.eimc.2017.08.012

Souli, M., Galani, I., Boukovalas, S., Gourgoulis, M. G., Chryssouli, Z., Kanellakopoulou, K., et al. (2011). *In vitro* interactions of antimicrobial combinations with fosfomycin against KPC-2-producing *Klebsiella pneumoniae* and protection of resistance development. *Antimicrob. Agents Chemother.* 55, 2395–2397. doi: 10.1128/AAC.01086-10

Soussy, C. J. (2012). *Antibiogram Committee of the French Society for Microbiology, Recommendations*. Available online at: http://www.sfm-microbiologie.org/UserFiles/files/casfm/CASFM_2012.pdf

Spellberg, B., and Rex, J. H. (2013). The value of single-pathogen antibacterial agents. *Nat. Rev. Drug Discov.* 12:963. doi: 10.1038/nrd3957-c1

Stokes, J. M., MacNair, C. R., Ilyas, B., French, S., Cote, J. P., Bouwman, C., et al. (2017). Pentamidine sensitizes Gram-negative pathogens to antibiotics and overcomes acquired colistin resistance. *Nat. Microbiol.* 2:17028. doi: 10.1038/nmicrobiol.2017.28

Trecarichi, E. M., and Tumbarello, M. (2017). Therapeutic options for carbapenem-resistant Enterobacteriaceae infections. *Virulence* 8, 470–484. doi: 10.1080/21505594.2017.1292196

Wang, J., He, J. T., Bai, Y., Wang, R., and Cai, Y. (2018). Synergistic activity of colistin/fosfomycin combination against carbapenemase-Producing *Klebsiella pneumoniae* in an *in vitro* pharmacokinetic/pharmacodynamic model. *Biomed Res. Int.* 2018:5720417. doi: 10.1155/2018/5720417

World Health Organization (2017). Global *Priority List of Antibiotic-resistant Bacteria to Guide Research, Discovery, and Development of New Antibiotics*. Available online at: http://www.who.int/medicines/publications/global-priority-list-antibiotic-resistant-bacteria/en/

Younis, W., Thangamani, S., and Seleem, M. N. (2015). Repurposing non-antimicrobial drugs and clinical molecules to treat bacterial infections. *Curr. Pharm. Des.* 21, 4106–4111. doi: 10.2174/1381612821666150506154434

Conflict of Interest Statement: The authors declare that the research was conducted in the absence of any commercial or financial relationships that could be construed as a potential conflict of interest.

frontiers in Cellular and Infection Microbiology

ORIGINAL RESEARCH
published: 23 October 2018
doi: 10.3389/fcimb.2018.00365

Identification of Anti-staphylococcal and Anti-biofilm Compounds by Repurposing the Medicines for Malaria Venture Pathogen Box

Vasundhra Bhandari, Shalini Chakraborty, Umarani Brahma and Paresh Sharma*

National Institute of Animal Biotechnology, Hyderabad, India

OPEN ACCESS

Edited by:
Maria Tomas, Complexo Hospitalario Universitario A Coruña, Spain

Reviewed by:
Taissa Vila, University of Maryland, Baltimore, United States
Yan Q. Xiong, UCLA David Geffen School of Medicine, United States

***Correspondence:**
Vasundhra Bhandari
vasundhra23@gmail.com;
vasundhra@niab.org.in

Specialty section:
This article was submitted to Molecular Bacterial Pathogenesis, a section of the journal Frontiers in Cellular and Infection Microbiology

Received: *11 May 2018*
Accepted: *01 October 2018*
Published: *23 October 2018*

Citation:
Bhandari V, Chakraborty S, Brahma U and Sharma P (2018) Identification of Anti-staphylococcal and Anti-biofilm Compounds by Repurposing the Medicines for Malaria Venture Pathogen Box. Front. Cell. Infect. Microbiol. 8:365. doi: 10.3389/fcimb.2018.00365

There has been an alarming increase in infections caused by antimicrobial-resistant pathogens. These infections are responsible for more than half a million deaths globally each year. *Staphylococcus aureus* is one of the deadliest bacterial pathogen responsible for nosocomial and community acquired infections. The open-access Pathogen Box (PBox) provides a potential platform to identify new treatment options against antibiotic-resistant bacteria by repurposing it. In this study, we have screened the PBox library comprised of ∼400 compounds to identify novel anti-staphylococcal compounds. *in vitro* antimicrobial screening using *S. aureus* isolates, ATCC 29213 (methicillin-sensitive) and ATCC 700699 (methicillin-resistant) revealed 13 compounds which showed highly potent antibacterial activity against both planktonic and biofilm state. The 13 compounds were not found cytotoxic to mouse macrophage cell line, RAW264.7. Out of the 13 compounds, only MMV687251 and MMV676477 revealed structural similarity with vancomycin by comparing their atomic pair fingerprints using Tanimoto coefficient method. The structural similarities may indicate similar mode of action like vancomycin for the two compounds. Our result showed that PBox compounds offer a promising lead for the development of new anti-staphylococcal treatment options.

Keywords: anti-staphylococcal, anti-biofilm, repurposing, antimicrobial resistance, open source drug discovery

INTRODUCTION

Staphylococcus aureus is an opportunistic pathogen, which contributes to a significant health problem in both the clinical and community settings, especially methicillin-resistant *S. aureus* (MRSA) (Diep et al., 2008). MRSA causes mild to severe infection of various body tissues, and frequently progress to life-threatening diseases (Otto, 2012). MRSA infections represent a mortality rate of 20% and are challenging to treat due to limited treatment options (Klevens et al., 2007). The World Health Organization has kept *S. aureus* under the list of high priority pathogen against

which new treatments options are required (World health Organization (WHO report)., 2017). *S. aureus* is also known to cause substantial proportions of infections in patients with indwelling medical devices (catheter, implants etc.), due to its ability to form biofilms (LaPlante and Mermel, 2009). Biofilm provides bacteria with an added benefit to evade immune responses and antibiotic effect resulting in much complicated and challenging treatment.

Reports of isolates with reduced susceptibility and resistance to vancomycin, the traditional choice of treatment against MRSA has further raised the concern about the scarcity of new treatment options (Hiramatsu et al., 1997; Howden et al., 2010). Most traditional antibiotics have significantly reduced antimicrobial activities in biofilm-associated infections (LaPlante and Mermel, 2009). Therefore, we have screened the diverse library of compounds (400 drug-like compounds) assembled by Medicine for Malaria Venture (MMV) referred as Pathogen Box® (PBox), to find new treatment option against *S. aureus* (Medicines for Malaria Venture, 2011).

The PBox compounds have been categorized into pathogen-specific subsets, the majority of the compounds have activity against *Plasmodium*, followed by tuberculosis and other Kinetoplastids. Very few compounds with activity against others pathogens: Helminths, *Toxoplasma*, *Dengue* and *Cryptosporidium* are also present in the PBox. The PBox compounds have not been tried against the other pathogens and therefore provides researchers with an opportunity to screen and identify new leads against pathogens with limited treatment options. The PBox compounds were reported to be 5-fold less cytotoxic against the human cell line in comparison to the pathogen, which is within the acceptable levels (Medicines for Malaria Venture, 2011) (https://www.pathogenbox.org/about-pathogen-box/supporting-information/).

Thus, in the present study, we have utilized this opportunity to identify antibacterial agent by repurposing the MMV PBox against planktonic and biofilm state of *S. aureus*.

MATERIALS AND METHODS

Bacterial and Cell Culture

ATCC 29213 (methicillin-susceptible *S. aureus* Sensitive and CLSI recommended isolate for broth microdilution assay) and ATCC 700699 (methicillin-resistant *S. aureus* with reduced vancomycin susceptibility) were used for antimicrobial susceptibility and anti-biofilm assays. RAW 264.7 mouse macrophage cell line was used for cytotoxicity assay. In all experiments, vancomycin and oxacillin were used as internal control.

Antimicrobial Susceptibility Assay

The broth microdilution assay was performed in accordance with Clinical and Laboratory Standards Institute (CLSI) with minor modification by the use of resazurin dye as described earlier (Elshikh et al., 2016; Mahato et al., 2017). Resazurin dye (blue) is a redox indicator, which changes color from blue to pink (resorufin dye) by the metabolically active cells. The assay was performed for all the PBox compounds ranging from (0 to 100 μM) provided by MMV in a 96 well plate format. After 24 h incubation of the bacterial cells with different dilutions of PBox compounds at 37°C, 30 μl of resazurin dye (0.015 %) was added to all wells, followed by 2–4 h of incubation. The lowest dilution columns with no color change were reported as the MIC value.

All assays were performed at least twice in triplicates.

Anti-biofilm Activity

The activity of PBox compounds was tested on *S. aureus* biofilms by Crystal violet (CV) assay in a 96-well plate-format (Coraça-Huber et al., 2012; Masadeh et al., 2013; Ghosh et al., 2015). An overnight cultures of *S. aureus* (ATCC 29213 and ATCC 700699) was diluted 1:200 in Tryptic Soy Broth (TSB) with 0.25 % glucose. Two hundred microliter /well of the diluted culture was dispensed into 96-well plate. The plate was incubated for 24 h at 37°C and washed thrice with PBS. Compounds ranging from 0 to 100 μM, were added to wells and the plate was further incubated for 24 h at 37°C. The wells were then washed thrice with PBS and methanol fixed for 15 min. The plate was air dried for 30 min and 0.1% CV solution was added to each well and incubated at room temperature for 20 min. After washing with distilled water, 33% acetic acid was added to each well and absorbance was taken at 590 nm using a multimode reader (Enspire, Perkin Elmer). Mean absorbance values of each sample was calculated and compared with the mean value of the control. All assays were performed at least twice in triplicates.

Cell Cytotoxicity

The cell cytotoxicity assay was performed using RAW 264.7 mouse macrophage adherent cell line as described previously with slight modifications (Hua et al., 2018). Cells at a density of 5000 cells per well were seeded in 96 well tissue culture plate and allowed to adhere in DMEM medium (10% FBS) for 24 h at 37°C, 5% CO_2. The adherent cells were treated with different concentrations of PBox compounds (0–250 μM) for another 24 h. After incubation, resazurin dye was added to each well, and the plate was incubated for 6–8 h at 37°C, 5% CO_2. Fluorescence was measured (excitation wavelength = 550 nm and emission wavelength = 590 nm) by using a multimode reader (Enspire, Perkin Elmer). The results were expressed as percent cell viability, compared with untreated cells. All assays were performed thrice in triplicates.

Structural Similarity Measurements

Atom Pair fingerprints (APfp) were used for calculating the structural similarity between the PBox compounds showing good antibacterial activity (Bajusz et al., 2015; O'Boyle and Sayle, 2016). The APfp of the 13 PBox compounds and vancomycin was calculated using the sdf files downloaded from the ChemSpider for each compound. The sdf files were there loaded into the ChemMine tools software for calculating APfp of all compounds (Backman et al., 2011). The APfp were submitted to ChemmineR software for hierarchical clustering analysis (Cao et al., 2008). The Tanimoto coefficient (Tc) method was used for the cluster analysis and drawing a phylogenetic tree for calculating the relationship between the compounds.

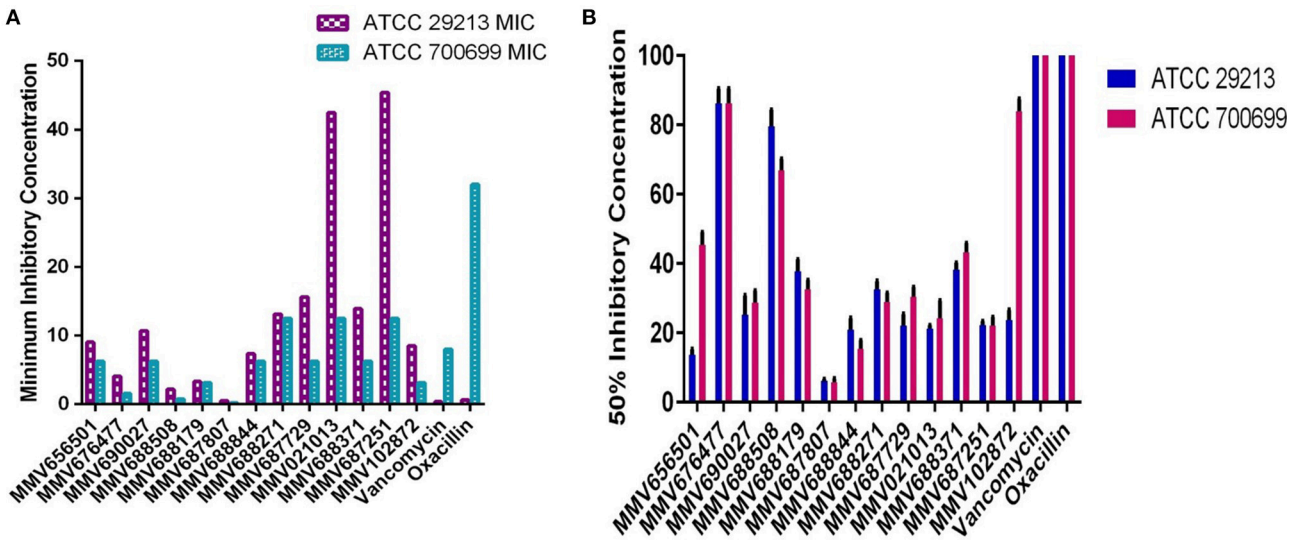

FIGURE 1 | Anti-staphylococcal and anti-biofilm profiling of the 13 PBox compounds. **(A)** Anti-staphylococcal activity was determined by micro-broth dilution assay using ATCC 29213 and ATCC 700699. The bar represents the minimum inhibitory concentration (MIC). **(B)** Anti-biofilm activity was assessed by crystal violet assay against 13 PBox compounds using ATCC 29213 and ATCC 700699. The bar represents mean 50% biofilm reduction concentration ± SD.

RESULTS AND DISCUSSION

The rate at which *S. aureus* has developed antibiotic resistance has raised serious concern for the public health. Further, biofilm infections are more dreadful and challenging to treat. An estimated 10 million deaths due to antimicrobial resistance are predicted by 2050 (Review on Antimicrobial Resistance, 2016) (https://amr-review.org/sites/default/files/160518_Final%20paper_with%20cover.pdf). The unregulated use of antibiotic has resulted in the emergence of "Superbug" such as MRSA which have developed resistance against major antibiotics and become extremely difficult to treat. Therefore, it is crucial to identify new treatment options to tackle resistant bacteria. The PBox by MMV has provided us with the platform to screen approximately 400 compounds and move a step ahead in identifying new treatment options.

We have screened antibacterial activity of the PBox compounds against methicillin sensitive and resistant *S. aureus* planktonic cells using broth microdilution assay (Mahato et al., 2017). Vancomycin and oxacillin were included as the internal controls in every plate. All the compounds were screened using ATCC 29213 and ATCC 700699. Out of ∼400 compounds, we found 13 compounds (**Figure 1**, **Table 1**, **Supplementary Table 1**) with a minimum inhibitory concentration of ≤ 45 μM. These 13 compounds were grouped under Tuberculosis ($n = 9$) and Kinetoplastids (n=4) drugs in the PBox information sheet provided by MMV. Five compounds MMV676477, MMV688179, MMV102872, MMV688508, and MMV687807, showed excellent activity against both methicillin sensitive and resistant *S. aureus* with a MIC value of ≤8.50 μM. Excepting MMV 688179 all the other four compounds belonged to tuberculosis disease set. Therefore, screening of the PBox revealed new compounds with anti-staphylococcal activity which were not reported earlier. Similarly, the free availability of the PBox compounds to researchers has also resulted in the identification of compounds like MMV688271, MMV688768, MMV687273 and MMV687807 showing an excellent activity against fungal pathogens (Vila and Lopez-Ribot, 2016; Mayer and Kronstad, 2017). More research into the PBox compounds also revealed compounds with anti-plasmodium activity which were not initially reported in PBox and were listed under tuberculosis or schistosomiasis (Duffy et al., 2017).

Biofilm infections are more challenging to treat due to increased tolerance to antibiotics and host defense mechanism. Therefore, it is crucial to investigate the anti-biofilm activity of the compounds showing anti-staphylococcal activity for a better treatment option in the future. Hence, the anti-biofilm activity of the 13 compounds was determined by using crystal violet (CV) assay as described previously, using ATCC 29213 and 700699. Out of the 13 compounds tested 6 compounds showed a 50% reduction in biofilm mass at ≤30 μM (**Figure 1**, **Table 1**). Overall, five compounds (MMV656501, MMV687807, MMV688844, MMV687729, and MMV102872) showed good activity against both planktonic and biofilm cells. MMV687807 showed excellent activity against planktonic cells with a MIC of 0.5 μM and anti-biofilm activity with an IC_{50} value of 6. 20 ± 0.54 μM and 5.73 ± 1.10 μM for methicillin-sensitive and resistant isolate respectively. However, the same compound showed a weaker inhibition of biofilm formed by *Candida albicans* (Mayer and Kronstad, 2017). Interestingly, there were two compounds (MMV021013 and MMV 687251) which were more active against biofilm as compared to planktonic cells.

Cytotoxicity assay using RAW 264.7 mouse macrophage cell line showed all compounds to be less cytotoxic than vancomycin except MMV688371 which has comparable cytotoxicity (**Table 1**). The low cytotoxicity levels of these compounds reveal

TABLE 1 | Anti-staphylococcal, anti-biofilm and cytotoxicity of the 13 PBox Compounds.

S. No	Compound ID	MMV Disease set	MIC (μM)		Biofilm mass of 50% (μM)		Cytotoxicity (IC_{50} μM)
			ATCC 29213	ATCC 700699	ATCC 29213 *	ATCC 700699*	
1	MMV656501	Tuberculosis	9.02	18.05	13.81 ± 1.45	45.46 ± 3.56	>250
2	MMV676477	Tuberculosis	4.06	4.06	98.44 ± 6.44	86.24 ± 4.23	>250
3	MMV690027	Kinetoplastids	10.68	10.68	25.26 ± 5.56	28.68 ± 3.45	109.32 ± 2.45
4	MMV688508	Tuberculosis	2.18	2.18	79.53 ± 4.84	66.89 ± 3.23	>250
5	MMV688179	Kinetoplastids	3.28	6.56	37.69 ± 3.49	32.54 ± 2.69	152 ± 5.41
6	MMV687807	Tuberculosis	0.50	0.50	6.20 ± 0.54	5.73 ± 1.10	>250
7	MMV688844	Tuberculosis	7.35	14.71	20.90 ± 3.40	15.43 ± 2.45	>250
8	MMV688271	Kinetoplastids	13.11	26.21	32.50 ± 2.49	28.91 ± 2.67	126.94 ± 5.52
9	MMV687729	Tuberculosis	15.61	15.61	22.15 ± 3.31	30.34 ± 2.87	169.32 ± 12.37
10	MMV021013	Tuberculosis	42.46	42.46	21.23 ± 0.98	24.27 ± 4.98	>250
11	MMV688371	Kinetoplastids	13.89	13.89	38.24 ± 1.94	43.22 ± 2.65	97.27 ± 3.07
12	MMV687251	Tuberculosis	45.41	45.41	22.23 ± 1.18	22.08 ± 2.48	220.99 ± 3.77
13	MMV102872	Tuberculosis	8.50	8.50	23.74 ± 2.90	83.98 ± 3.45	>250
14	Vancomycin	Internal Control	0.35	5.52	>100	>100	110 ± 4.66
15	Oxacillin	Internal Control	0.63	> 100	>100	>100	>250

*Vancomycin and oxacillin were used as internal controls. *Significant difference was observed in the antibiofilm activity among each MMV compound and the controls (Vancomycin and Oxacillin) with $p < 0.05$.*

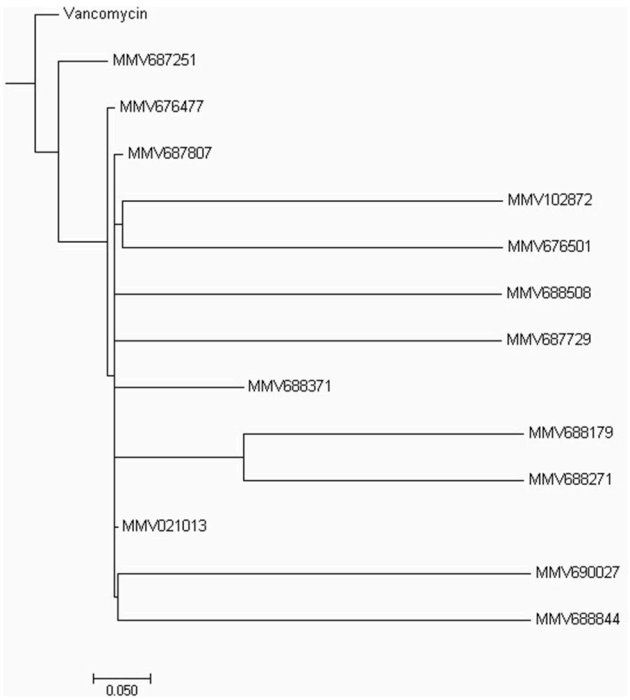

FIGURE 2 | Hierarchical clustering analysis. The Hierarchical clustering analysis was performed using ChemmineR software which highlights the structural similarities between the 13 PBox compounds and vancomycin concerning their Tanimoto coefficients (Tc).

good potential to be taken up for *in vivo* testing in animal models in future. Additionally, to understand whether the 13 compounds shared any structural similarity, the ChemMine tools software was used, and the reference drug vancomycin was also included. The hierarchical clustering analysis (HCA) using the T_C method showed levels of similarities between the identified compounds ranging from 0 to 1 with higher values corresponding to greater similarities. The compounds having the T_C values of 1 did not imply identical compounds, however, can be predicted to have similar structural fingerprints. The HCA analysis resulted in the formation of 5 major clusters with vancomycin showing maximum structural similarity with the compounds MMV687251 and MMV676477 with T_C values of 0.993 and 0.960 respectively (**Figure 2**). The subsequent nearest clusters consist of compounds MMV687807, MMV102872 and MMV676501 (II cluster), MMV688508 and MMV687729 (III Cluster), MMV688371, MMV688179 and MMV688271 (IV Cluster) and MMV021013, MMV690027 and MMV68844 in cluster V based on the analysis. Compounds falling under different clusters indicate structural dissimilarity among them and in comparison, with vancomycin indicating a probable different antibacterial mechanism.

Therefore, our study has highlighted the identification of PBox compounds with bactericidal activity against both planktonic and biofilm cells of *S. aureus*. These compounds have the potential to be developed as a treatment option for biofilm infections, against which vancomycin also has reduced efficacy (LaPlante and Mermel, 2009).

CONCLUSION

The screening of the PBox compounds has opened avenues resulting in the identification of new compounds with antimicrobial activity. These preliminary studies will help us to prioritize the compounds, to be studied at a greater depth for establishing them as a new treatment option for staphylococcal infections.

AUTHOR CONTRIBUTIONS

VB conceived and designed the experiments. VB, SC, and UB performed the experiments. VB and PS analyzed the data. PS and VB contributed reagents, materials, and analysis tools. PS and VB wrote the paper.

ACKNOWLEDGMENTS

We would like to thank Medicines for Malaria Venture (MMV, Switzerland) for support and supply of the Pathogen Box. VB acknowledges Department of Science and Technology-India for the INSPIRE Faculty Award (INSPIRE/04/2015/000242).

SUPPLEMENTARY MATERIAL

The Supplementary Material for this article can be found online at: https://www.frontiersin.org/articles/10.3389/fcimb.2018.00365/full#supplementary-material

Supplementary Table 1 | Minimum Inhibitory concentration against all MMV Pathogen box compounds.

REFERENCES

Backman, T. W., Cao, Y., and Girke, T. (2011). ChemMine tools: an online service for analyzing and clustering small molecules. *Nucleic. Acids. Res.* 39, W486–W491. doi: 10.1093/nar/gkr320

Bajusz, D., Rácz, A., Héberger, K. (2015). Why Tanimoto index is an appropriate choice for fingerprint based similarity calculations? *J. Cheminformatics*. 7:20. doi: 10.1186/s13321-015-0069-3

Cao, Y., Charisi, A., Cheng, L. C., Jiang, T., and Girke, T. (2008). ChemmineR: a compound mining framework for R. *Bioinformatics* 24, 1733–1744. doi: 10.1093/bioinformatics/btn307

Coraça-Huber, D. C., Fille, M., Hausdorfer, J., Pfaller, K., Nogler, M. (2012). *Staphylococcus aureus* biofilm formation and antibiotic susceptibility tests on polystyrene and metal surfaces. *J. Appl. Microbiol*. 112, 1235–1243. doi: 10.1111/j.1365-2672.2012.05288.x

Diep, B. A., Chambers, H. F., Graber, C. J., Szumowski, J. D., Miller, L. G., Han, L. L., et al. (2008). Emergence of multidrug-resistant, community-associated, methicillin resistant *Staphylococcus aureus* clone USA300 in men who have sex with men. *Ann. Intern. Med*.148, 249–257. doi: 10.7326/0003-4819-148-4-200802190-00204

Duffy, S., Sykes, M. L., Jones, A. J., Shelper, T. B., Simpson, M., Lang, R., et al. (2017). Screening the Medicines for Malaria Venture Pathogen Box across multiple pathogens reclassifies starting points for open source drug discovery. *Antimicrob. Agents Chemother*. 61, e00379–e00317. doi: 10.1128/AAC.00379-17

Elshikh, M., Ahmed, S., Funston, S., Dunlop, P., McGaw, M., Marchant, R., et al. (2016). Resazurin-based 96-well plate microdilution method for the determination of minimum inhibitory concentration of biosurfactants. *Biotechnol. Lett.* 38, 1015–1019. doi: 10.1007/s10529-016-2079-2

Ghosh, C., Manjunath, G. B., Konai, M. M., Uppu, D. S., Hoque, J., Paramanandham, K., et al. (2015). Aryl-Alkyl Lysines: agents that kill planktonic cells, Persister cells, Biofilms of MRSA and protect mice from skin infections. *PLoS. ONE*. 10:e0144094. doi: 10.1371/journal.pone.0144094

Hiramatsu, K., Hanaki, H., Ino, T., Yabuta, K., Oguri, T., and Tenover, F. C. (1997). Methicillin-resistant *Staphylococcus aureus* clinical strain with reduced vancomycin susceptibility. *J. Antimicrob. Chemother*. 40, 135–136. doi: 10.1093/jac/40.1.135

Howden, B. P., Davies, J. K., Johnson, P. D., Stinear, T. P., and Grayson, M. L. (2010). Reduced vancomycin susceptibility in *Staphylococcus aureus*, including vancomycin-intermediate and heterogeneous vancomycin-intermediate strains: resistance mechanisms, laboratory detection, and clinical implications. *Clin. Microbiol. Rev*. 23, 99–139. doi: 10.1128/CMR.00042-09

Hua, X., Yang, Q., Zhang, W., Doug, Z., Yu, S., Schwarz, S., et al. (2018). Antibacterial activity and mechanism of action of Aspinidol against multidrug resistant Methcillin resistant *Staphylococcus aureus*. *Front. Pharmacol*. 9:619. doi: 10.3389/fphar.2018.00619

Klevens, R. M., Morrison, M. A., Nadle, J., Petit, S., Gershman, K., Ray, S., et al. (2007). Invasive methicillin-resistant Staphylococcus aureus infections in the United States. *JAMA* 298, 1763–1771. doi: 10.1001/jama.298.15.1763

LaPlante, K. L., and Mermel, L. A. (2009). *In vitro* activities of Telavancin and vancomycin against biofilm-producing *Staphylococcus aureus*, S. *epidermidis,* and *Enterococcus faecalis* strains. *Antimicrob Agents Chemother*. 53, 3166–3169. doi: 10.1128/AAC.01642-08

Mahato, S., Mistry, H. U., Chakraborty, S., Sharma, P., Saravanan, R., and Bhandari, V. (2017). Identification of variable traits among the methicillin resistant and sensitive coagulase negative *Staphylococci* in milk samples from mastitic cows in india. *Front. Microbiol*. 8:1446. doi: 10.3389/fmicb.2017.01446

Masadeh, M. M., Mhaidat, N. M., Alzoubi, K. H., Hussein, E. I., and Al-Trad, E. I. (2013). *In vitro* determination of the antibiotic susceptibility of biofilm-forming *Pseudomonas aeruginosa* and *Staphylococcus aureus*: possible role of proteolytic activity and membrane lipopolysaccharide. *Infect. Drug. Resist*. 6, 27–32. doi: 10.2147/IDR.S41501

Mayer, F. L., and Kronstad, J. W. (2017). Discovery of a novel antifungal agent in the Pathogen Box. *mSphere*. 2, e00120–e00117. doi: 10.1128/mSphere.00120-17

Medicines for Malaria Venture (2011). The Pathogen Box. Available online at: https://www.pathogenbox.org/about-pathogen-box/supporting-information/

O'Boyle, N. M., and Sayle, R. A. (2016). Comparing structural fingerprints using a literature based similarity benchmark. *J. Cheminformatics*. 8, 2206–2219. doi: 10.1186/s13321-016-0148-0

Otto, M. (2012). MRSA virulence and spread. *Cell. Microbiol*. 14, 1513–1521. doi: 10.1111/j.1462-5822.2012.01832.x

Review on Antimicrobial Resistance (2016). *Tackling Drug-Resistant Infections Globally: Final Report And Recommendations*. Availabe online at: https://amr-review.org/sites/default/files/160518_Final%20paper_with%20cover.pdf

Vila, T., and Lopez-Ribot, J. L. (2016). Screening the "Pathogen Box" for the identification of *Candida albicans* biofilm inhibitors. *Antimicrob. Agents Chemother*. 61, e02006–e02016. doi: 10.1128/AAC.02006-16

World health Organization (WHO report). (2017). *Global Priority List of Antibiotic-Resistant Bacteria to Guide Research, Discovery, and Development of New Antibiotics*. Geneva: WHO.

Conflict of Interest Statement: The authors declare that the research was conducted in the absence of any commercial or financial relationships that could be construed as a potential conflict of interest.

frontiers in Cellular and Infection Microbiology

MINI REVIEW
published: 23 October 2018
doi: 10.3389/fcimb.2018.00376

Bacteriophage Therapy: Clinical Trials and Regulatory Hurdles

Lucy L. Furfaro[1]*, *Matthew S. Payne*[1] *and Barbara J. Chang*[2]

[1] *Division of Obstetrics and Gynecology, School of Medicine, The University of Western Australia, Crawley, WA, Australia,*
[2] *The Marshall Centre for Infectious Diseases Research and Training, School of Biomedical Sciences, The University of Western Australia, Crawley, WA, Australia*

Increasing reports of antimicrobial resistance and limited new antibiotic discoveries and development have fuelled innovation in other research fields and led to a revitalization of bacteriophage (phage) studies in the Western world. Phage therapy mainly utilizes obligately lytic phages to kill their respective bacterial hosts, while leaving human cells intact and reducing the broader impact on commensal bacteria that often results from antibiotic use. Phage therapy is rapidly evolving and has resulted in cases of life-saving therapeutic use and multiple clinical trials. However, one of the biggest challenges this antibiotic alternative faces relates to regulations and policy surrounding clinical use and implementation beyond compassionate cases. This review discusses the multi-drug resistant Gram-negative pathogens of highest critical priority and summarizes the current state-of-the-art in phage therapy targeting these organisms. It also examines phage therapy in humans in general and the approaches different countries have taken to introduce it into clinical practice and policy. We aim to highlight the rapidly advancing field of phage therapy and the challenges that lie ahead as the world shifts away from complete reliance on antibiotics.

Keywords: bacteriophage, phage therapy, regulations, clinical trials, antimicrobial resistance, alternative treatments

OPEN ACCESS

Edited by:
Maria Tomas,
Complexo Hospitalario Universitario A Coruña, Spain

Reviewed by:
Katrine L. Whiteson,
University of California, Irvine, United States
Jose Ramos-Vivas,
Instituto de Investigación Marques de Valdecilla (IDIVAL), Spain

***Correspondence:**
Lucy L. Furfaro
lucy.furfaro@uwa.edu.au

Received: *11 August 2018*
Accepted: *05 October 2018*
Published: *23 October 2018*

Citation:
Furfaro LL, Payne MS and Chang BJ (2018) Bacteriophage Therapy: Clinical Trials and Regulatory Hurdles. Front. Cell. Infect. Microbiol. 8:376. doi: 10.3389/fcimb.2018.00376

THE CHALLENGE OF MULTI-DRUG RESISTANT BACTERIA

In 2017 the World Health Organization published a list of global priority pathogens comprising 12 species of bacteria categorized into critical, high and medium priority based on their level of resistance and available therapeutics (Tacconelli et al., 2018). The current rate of resistance development far exceeds the level of antibiotic discovery and development and represents a global public health challenge. Estimates have suggested that upwards of 10 million people could die each year due to antimicrobial resistance by 2050 (O'neill, 2014). While this is a contentious figure (De Kraker et al., 2016), it nonetheless highlights the serious problem we face regarding therapeutic options for multi-drug resistant (MDR) bacterial infections (Bassetti et al., 2017). The natural predators of bacteria are the bacterial viruses known as bacteriophages or phages. Found ubiquitously, these organisms are estimated to be present at numbers equivalent to a trillion per grain of sand on Earth (Keen, 2015). Evolving in parallel with bacteria, phages are potential antibacterial therapeutic agents against such MDR pathogens (Burrowes et al., 2011). Here we focus on three critical priority pathogens, *Acinetobacter baumannii*, *Pseudomonas aeruginosa*, and members of the *Enterobacteriaceae* (Tacconelli et al., 2018) and the current advances in phage therapy research to target these organisms, as well as exploring more general issues of clinical trials and regulatory complexities of phage therapy.

Acinetobacter baumannii

A. baumannii is recognized as a critical priority pathogen due to the increasing incidence of antimicrobial resistance and significant role in nosocomial infections (Mcconnell et al., 2013). Around 20 years after an early trial of anti-*A. baumannii* phage therapy in mice (Soothill, 1992), a surge in reports of *A. baumannii* lytic phage isolation and their *in vitro* activity occurred, as reviewed by Garcia-Quintanilla et al. (2013). Since this time, significant advances have been made with further *in vitro* studies (Liu et al., 2016; Ghajavand et al., 2017) and numerous *in vivo* animal studies (Kusradze et al., 2016; Regeimbal et al., 2016; Yin et al., 2017; Zhou et al., 2018). Phage therapy evaluation in a mouse model of *A. baumannii* infection resulted in 2.3-fold increased survival in the phage-treated group compared to control groups (Cha et al., 2018).

A novel lysin from *A. baumannii* prophages with the capacity to kill clinical MDR isolates and rescue mice from lethal infections has also been characterized (Lood et al., 2015). The use of these enzymatic compounds is not a new concept; and although lysin use has been restricted in Gram-negative bacteria due to their outer membrane barrier, a rise in the literature suggests that this no longer poses a constraint on lysin use in Gram-negatives (Thandar et al., 2016; Peng et al., 2017; Larpin et al., 2018).

Advances have also been made in human phage therapy trials. A key case in the United States involved the first intravenous administration of phage therapy and resulted in the successful treatment and recovery of a patient with *A. baumannii* pancreatic pseudocyst infection (Schooley et al., 2017). This has led to increased phage therapy exposure to the public and arguably increased clinical awareness regarding this alternative therapeutic. More recently another case study involving infection at a craniectomy site with a MDR-*A. baumannii*, applied a personalized phage cocktail intravenously in an attempt to improve patient outcomes (Lavergne et al., 2018). Unfortunately, the patient passed away after life support efforts were ceased following the family's request. In cases such as this it is difficult to navigate the regulatory issues in a timely manner; while personalized therapy is ideal to adapt to patient needs it can be a challenge.

Pseudomonas aeruginosa

P. aeruginosa is a major opportunistic pathogen and cause of nosocomial infections (Lyczak et al., 2000; Breidenstein et al., 2011). It is also a frequent cause of chronic lung infections in cystic fibrosis patients and as such has been assessed as a target for phage therapy (Olszak et al., 2015). Phage therapy for *P. aeruginosa* infections dates back more than 50 years (Bertoye et al., 1959; Soothill, 2013), but recent developments in use of both phage lysins and live phage are very promising. A review by Rossitto and colleagues describes the current literature in this field and the challenges associated with phage therapy in cystic fibrosis, in particular they suggest that future studies include testing on both mucoid and non-mucoid *P. aeruginosa* isolates and the use of both pulmonary and non-pulmonary host models (Rossitto et al., 2018). Spray-dried formulations of phages have also been thoroughly tested for inhaled application against *P. aeruginosa* lung infection (Chang et al., 2017, 2018). Immunogenicity data has been assessed using an *in vitro* human lung model and demonstrated an increase in IL-6 and TNF-a for one of two phages (Shiley et al., 2017). The human immune response is an important consideration when assessing therapeutic phage application (Krut and Bekeredjian-Ding, 2018) however, beneficial effects of the immune response conducive to positive phage therapy outcomes have also been reported (Roach et al., 2017).

A cocktail of six phages was observed to successfully treat respiratory *P. aeruginosa* infection in mice and, additionally, sepsis in *Galleria mellonella* models (Forti et al., 2018). Ability of some phages to penetrate *P. aeruginosa* biofilms is another major advantage over conventional treatments (Fong et al., 2017; Waters et al., 2017), while co-administration of phages and antibiotics has been reported as a mechanism of restoring antibiotic sensitivity (Chan et al., 2016). In the latter case, where phages utilize components of multidrug efflux pump systems as receptors, mutation to confer phage-resistance alters the pump mechanism, leading to antibiotic re-sensitization. A case study of aortic prosthetic graft infection by *P. aeruginosa* with direct administration to the graft of a combination of phage and ceftazidime was successful in resolving and possibly eradicating infection (Chan et al., 2018). Finally, phage lysin research is also on the increase: Guo et al. described a novel endolysin with *in vitro* activity against *P. aeruginosa* and other Gram-negative bacteria on the critical priority pathogens list (Guo et al., 2017), with similar reports from other groups (Larpin et al., 2018).

Enterobacteriaceae

Within the family *Enterobacteriaceae*, *Escherichia coli,* and *Klebsiella* spp. ranked highest in the WHO critical priority list of antibiotic-resistant bacteria followed by *Enterobacter*, *Serratia* and *Proteus* spp. (Tacconelli et al., 2018). While occupying many commensal niches, *E. coli* isolates include significant intestinal and extraintestinal pathogens (Bolocan et al., 2016). The majority of early phage research was undertaken with coliphages (phages that infect *E. coli*), particularly T4 (Stahl, 1989; Edgar, 2004), evidenced by numerous studies, some of which are summarized by Bolocan et al. (2016). More recently, *in vitro* and *in vivo* studies have shown promising results, for example control of enteropathogenic *E. coli* in mice with hospital sewage-isolated phage (Vahedi et al., 2018) and effect of coliphages against planktonic and biofilm-associated infections (Tkhilaishvili et al., 2018).

Klebsiella spp. are frequent nosocomial and community-acquired pathogens recognized for their MDR status. Cao et al. administered intranasal phage to treat *K. pneumoniae* lung infection in mice, resulting in protection against lethal infection and lower inflammatory cytokine levels in the lung (Cao et al., 2015). Similarly, in a burn wound mouse model of *K. pneumoniae* infection, topical phage application resulted in a significant reduction in mortality (Kumari et al., 2011) and a liposome loaded phage cocktail enhanced bacterial clearance and rate of healing (Chadha et al., 2017).

Other phage therapeutic uses include prevention of biofilm formation. Depolymerase producing *K. pneumoniae* phage, in

combination with iron antagonizing agents, showed ability to eradicate early biofilms of *K. pneumoniae*: a promising preventative strategy (Chhibber et al., 2013). Progress has also been made in lysin research: Yan et al. described a novel fusion protein that combines the receptor binding domains of colicin A with an *E. coli* phage lysin to overcome the blocking effect of the Gram-negative outer membrane, with successful control of *E. coli* both *in vitro* and in a mouse model (Yan et al., 2017).

While many studies have addressed phage therapy *in vitro* and *in vivo*, there is much further work required for translation into humans. Case reports have been discussed, but lack the robust evidence of clinical trials.

PHAGE THERAPY IN HUMANS

Phage use in Eastern Europe and the former Soviet Union has been widespread since their discovery; as a result therapeutic phage use is integrated within their health care systems. However, this potential therapy is only recently being investigated according to rigorous scientific standards (Kutter et al., 2010; Villarroel et al., 2017). Abedon has presented a list of key criteria that should be thoroughly considered and reported in phage therapy studies (Abedon, 2017). Information critical to the success of clinical trials includes the adequate characterization and selection of phages as well as of the subjects (humans) and the target bacteria. Additional data are also required such as formulations, dosing and efficacy, however, without the foundation of characterized and well-planned targets these are of no value. Detailed reporting would improve the quality of future research and enable replication and extension of previous studies. Another consideration is the choice of appropriate disease targets for phage therapy (Harper, 2018). For example, the species specificity characteristic of most phages is generally highly desirable in monomicrobial diseases, however, this specificity can be a major limitation in cases of polymicrobial infections unless, perhaps, the phage is administered in combination with a suitable antibiotic. Such considerations are imperative for patient safety in clinical trials, as removal of one pathogen and consequent overgrowth of a second could potentially have fatal consequences (Harper, 2018). On the other hand, it may be that broad-host-range phages are more common than is currently believed, due in part to biases in phage isolation methods (De Jonge et al., 2018): this disparity deserves much further research.

CLINICAL TRIALS INVOLVING PHAGES

One of the current challenges of progressing phage therapy into the clinic is the lack of validated and adequately controlled clinical trials. Additional care should be taken in the planning and design of such trials as, while clinical trial design for phage therapy will naturally share many parallels with standard drug clinical trials, there are several factors that are unique to phages. These include pharmacological considerations such as the dosage (Payne and Jansen, 2003). As these are self-replicating viruses, their dose has the potential to exponentially increase upon reaching the bacteria of interest. This leads to another consideration of application: phages require direct contact with the bacteria and if distributed too broadly they will be less efficacious. Topical applications have been widely used to address this, however, as mentioned other methods have been used with success. When considering monotherapy or combination therapy approaches, phage cocktails offer broad spectrum activity and reduce the chances of resistance formation, however, it should be noted that combination therapy greatly increases the challenge of assessing inflammatory effects, potential for gene transfer and phage resistance development for all phages in a cocktail (Parracho et al., 2012).

Some have argued that exposure to bacteriophages occurs in humans every day and is evidence of their safety, however, in the context of clinical trials there are a number of considerations that should be addressed. The first of these relates to the sterility and purity of the phage preparation. It is imperative that products exclude toxins and bacterial debris to comply with good manufacturing practice or equivalent quality assurance standards. Parracho et al. described the quality parameters recommended for bacteriophage products from the point of phage identification through to manufacturing processes (Parracho et al., 2012). Secondly, concerns surrounding the potential for the onset of toxic shock as a result of the bactericidal effect of phages must also be addressed. While this has been reported to not be an issue (Speck and Smithyman, 2016) and this method of bacterial killing is shared by bactericidal antibiotics (Dufour et al., 2017), this is a necessary safety consideration prior to clinical trials.

Previous clinical trials involving phage therapy have been described in detail by Kutter et al. and include those undertaken in Georgia and Poland (Kutter et al., 2010). Worth noting are two phage therapy clinical trials that are used as examples throughout the literature, addressing safety of phages for treating venous leg ulcers (Rhoads et al., 2009) and safety and efficacy in chronic otitis (Wright et al., 2009). Rhoads and colleagues reported on safety in a small phase I trial in patients with venous leg ulcers and reported no adverse events with the administration of phages (Rhoads et al., 2009). Wright et al. demonstrated efficacy and safety of anti-Pseudomonal phages against late stage recurrent otitis which was dominated by MDR-*P. aeruginosa*. These are among the first controlled clinical trials in humans conducted in the western world. More recently, a number of clinical trials have been registered (https://clinicaltrials.gov/ and https://globalclinicaltrialdata.com/) as summarized in **Figure 1** (Miedzybrodzki et al., 2012; Sarker et al., 2016; Leitner et al., 2017). At both web sites, use of the search phrase "phage therapy" resulted in 15 studies/trials in the former site, of which nine were phage therapy-related, with a focus on treatment of infection. Two additional studies were identified using the global clinical trials resource. Search results did not all represent standard clinical trials, for example sputum collections for *in vitro* phage testing and expanded access interventional trials were also included. Additional, scientifically sound clinical trials are vital to increasing the western clinical worlds' acceptance of phage therapy applications. While many observational studies have been conducted, these have been limited by small sample sizes and many are poorly controlled. Conversely, promising case

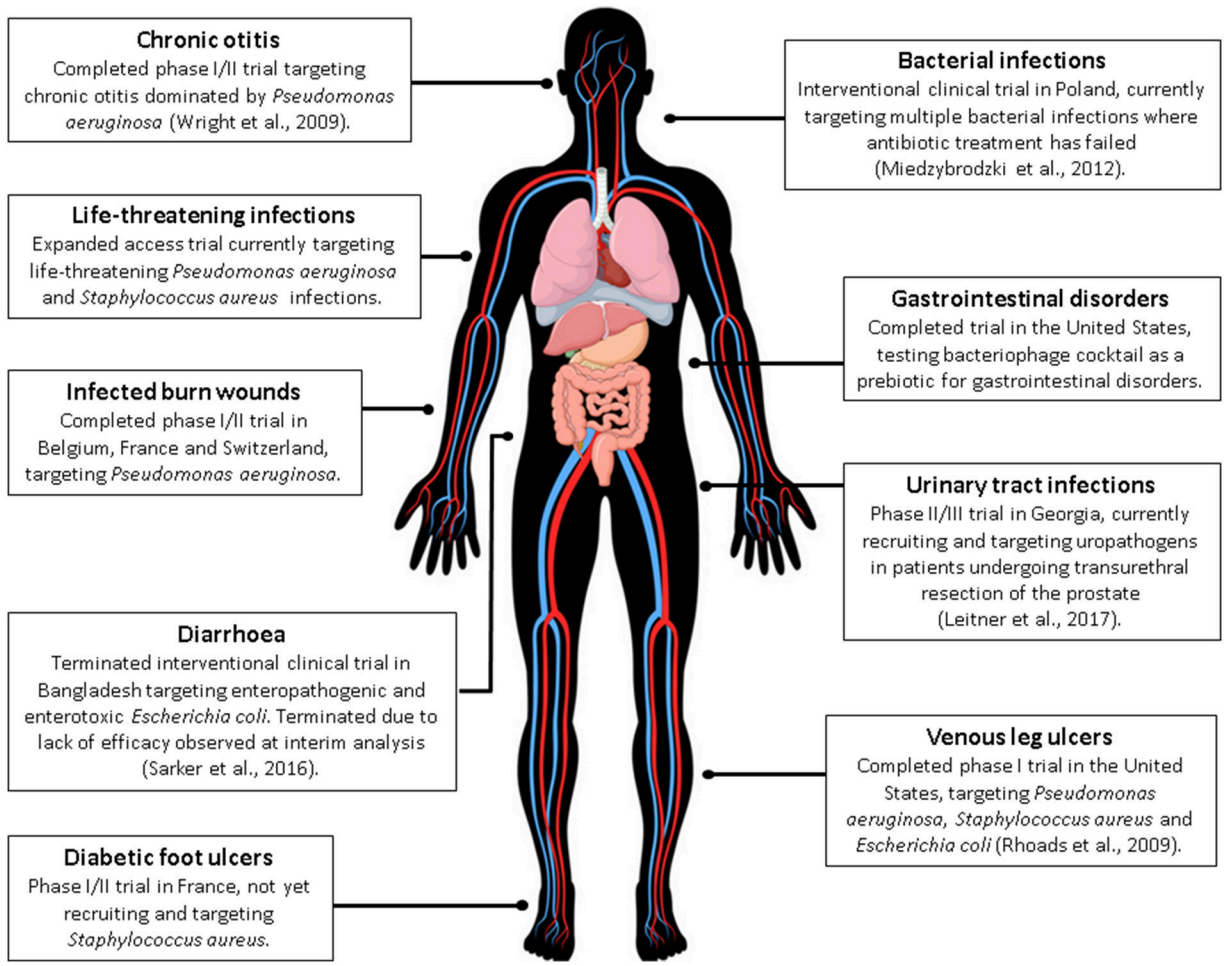

FIGURE 1 | A current summary of human phage therapy trials and the range of target sites/infections (see www.clinicaltrials.gov or https://globalclinicaltrialdata.com/ where citation is not given). This figure includes a licensed image obtained by the authors.

studies do exist, however, robust clinical trial data is what is required by regulators in order to progress clinical guidelines for phage therapy.

REGULATION AND POLICY DEVELOPMENT

No framework currently exists that explicitly defines phages in the context of medicinal products for use in humans, however, in Georgia these are embedded in the healthcare system as a standard medical application (Kutateladze, 2015). Specifically, the Eliava Institute of Bacteriophages, Microbiology and Virology has several phage preparations readily available (over-the-counter) and a broader range of products, specifically supplied to medical practitioners (Kutter et al., 2010; Kutateladze, 2015). Similarly, Poland has the Hirszfeld Institute of Immunology and Experimental Therapy, although this center supplies personalized phage products directly to physicians using a more tailored approach (Kutter et al., 2010). In other parts of the world, however, bacteriophages present a unique regulatory agenda.

Gorski summarizes the current access schemes around the world and identifies the main inclusion of compassionate use cases in most countries as a last resort option (Gorski et al., 2018). Schemes vary, however, all respond to the situation of a critically ill or chronically suffering patient for whom all authorized treatment options have been exhausted. While these schemes are beneficial in the short-term, it has been recognized that a dedicated phage therapy legal framework is essential for the smooth introduction of natural phage therapy into western medicine. Regulatory calls to action have been made in Europe with discussions around regulatory hurdles and future steps required to achieve appropriate phage-based therapeutic guidelines (Huys et al., 2013; Verbeken et al., 2014).

Working Towards a Solution

A thorough analysis of key stakeholder opinions on the regulatory status of phage therapy was reported by Verbeken et al. (2014). Calls for two regulatory pathways were proposed, including product market placement of natural phage-based products and hospital exemption pathways for tailored phage

therapy. The consensus among surveyed stakeholders was the need for a dedicated new regulatory framework for phage therapy and one which acknowledges the specific properties of phages and their interactions, in addition to the role of hospitals as providers of phage therapy (Verbeken et al., 2014). In the same vein, a workshop with the European Medicines Agency (EMA) set out to work together with all stakeholders to provide a solution to regulatory hurdles faced by phage researchers, while maintaining the standards of quality and safety (Pelfrene et al., 2016). Here, the EMA confirmed that none of the current regulations were suitable for phage therapy and discussed options for the way forward.

Magistral Phages

Political progression in Belgium has resulted in a magistral phage regulatory framework: a pragmatic framework to encompass tailored phage therapy (Pirnay et al., 2018). This regulatory framework includes a magistral formula in which non-authorized phage products can be prepared by a pharmacist, given the external quality assessment of the phage preparations. Quality assurance and good manufacturing practice are of extreme importance for any therapeutic agent and considerations for phage banks would include the characterization of all phages so that amongst other parameters, identity, viability, potency and purity are ensured (Pirnay et al., 2015; Pelfrene et al., 2016).

A Therapeutic Classification for Phages

Questions regarding the biological status of phages include whether they are living or not, which highlights the need for defined phage-specific terms of policy. As it currently stands, phage therapy in many cases represents the epitome of personalized medicine as it is a process involving tailor-made phage combinations specific for an individual patient's bacterial infection/s. This presents difficulties in the regulatory pipeline, as this move toward personalized medicine breaks the mold of regulatory conventions. It must be acknowledged that other therapeutics, for example cancer therapy (Daly, 2007), have faced a similar hurdle in the past and refinement is certainly possible. The Food and Drug Administration in the United States has recently provided an opportunity for the new Center for Innovative Phage Applications and Therapeutics (IPATH) to utilize phage therapy via the Emergency Investigational New Drug scheme. These initiatives are likely to improve clinical understanding and acceptance, while also providing supporting evidence of the need for dedicated regulatory guidelines.

A FUTURE FOR PHAGES

There is no doubt that phage therapy is an attractive solution to combating escalating antibiotic resistance. Numerous studies highlight the *in vitro* and *in vivo* potential of therapeutic phages and while a number of clinical trials have taken place over the last decade, further data is needed to present a robust regulatory case for clinical use. There remain obvious challenges ahead for phage therapy, particularly regarding management of regulatory policy. Progression toward novel schemes based around knowledge of phage applications should guide these processes and work toward a reasonable implementation structure. Ideally, regulatory developments should be reached in a standardized and global manner; however, this is understandably a challenge. While the field is rapidly progressing toward therapeutics, fuelled by the evident need for antibiotic alternatives, regulatory processes must be refined and approached from a novel phage-based perspective. One size does not fit all and collaborative efforts to build models that suit phages will surely result in better health outcomes for all. We must also remember that despite the frustrations of legislative parameters, it is of utmost importance to conserve high standards of safety, quality, and efficacy. It is vital that scientists and clinicians continue having these discussions with the appropriate regulatory bodies and move this area forward sooner rather than later.

AUTHOR CONTRIBUTIONS

LF conceived the review topic and focus, drafted the manuscript and approved the final version to be published. Both BC and MP contributed to the structure and content, critically revised the drafted manuscript and approved the final version to be published.

FUNDING

LF is supported by an Australian Government Research Training Program Scholarship and a Professor Gordon King Postgraduate Scholarship, provided by the Women and Infants Research Foundation. MP is supported by an NHMRC project grant [1144040].

REFERENCES

Abedon, S. T. (2017). Information phage therapy research should report. *Pharmaceuticals* 10:E43. doi: 10.3390/ph10020043

Bassetti, M., Poulakou, G., Ruppe, E., Bouza, E., Van Hal, S. J., and Brink, A. (2017). Antimicrobial resistance in the next 30 years, humankind, bugs and drugs: a visionary approach. *Intensive Care Med.* 43, 1464–1475. doi: 10.1007/s00134-017-4878-x

Bertoye, A., Gaillard, L., and Courtieu, A. L. (1959). Adapted bacteriophages in the treatment of infections caused by antibiotic-resistant microorganisms. *J. Med. Lyon* 40, 465–471.

Bolocan, A. S., Callanan, J., Forde, A., Ross, P., and Hill, C. (2016). Phage therapy targeting *Escherichia coli*-a story with no end? *FEMS Microbiol. Lett.* 363:fnw256. doi: 10.1093/femsle/fnw256

Breidenstein, E. B., De La Fuente-Nunez, C., and Hancock, R. E. (2011). *Pseudomonas aeruginosa*: all roads lead to resistance. *Trends Microbiol.* 19, 419–426. doi: 10.1016/j.tim.2011.04.005

Burrowes, B., Harper, D. R., Anderson, J., Mcconville, M., and Enright, M. C. (2011). Bacteriophage therapy: potential uses in the control of antibiotic-resistant pathogens. *Expert Rev. Anti Infect Ther.* 9, 775–785. doi: 10.1586/eri.11.90

Cao, F., Wang, X., Wang, L., Li, Z., Che, J., Wang, L., et al. (2015). Evaluation of the efficacy of a bacteriophage in the treatment of pneumonia induced by multidrug resistance *Klebsiella pneumoniae* in mice. *Biomed. Res. Int.* 2015:752930. doi: 10.1155/2015/752930

Cha, K., Oh, H. K., Jang, J. Y., Jo, Y., Kim, W. K., Ha, G. U., et al. (2018). Characterization of two novel bacteriophages infecting multidrug-resistant (MDR) *Acinetobacter baumannii* and evaluation of their therapeutic efficacy *in vivo*. *Front. Microbiol.* 9:696. doi: 10.3389/fmicb.2018.00696

Chadha, P., Katare, O. P., and Chhibber, S. (2017). Liposome loaded phage cocktail: enhanced therapeutic potential in resolving *Klebsiella pneumoniae* mediated burn wound infections. *Burns* 43, 1532–1543. doi: 10.1016/j.burns.2017.03.029

Chan, B. K., Sistrom, M., Wertz, J. E., Kortright, K. E., Narayan, D., and Turner, P. E. (2016). Phage selection restores antibiotic sensitivity in MDR *Pseudomonas aeruginosa*. *Sci. Rep.* 6:26717. doi: 10.1038/srep26717

Chan, B. K., Turner, P. E., Kim, S., Mojibian, H. R., Elefteriades, J. A., and Narayan, D. (2018). Phage treatment of an aortic graft infected with *Pseudomonas aeruginosa*. *Evol. Med. Public Health* 2018, 60–66. doi: 10.1093/emph/eoy005

Chang, R. Y., Wong, J., Mathai, A., Morales, S., Kutter, E., Britton, W., et al. (2017). Production of highly stable spray dried phage formulations for treatment of *Pseudomonas aeruginosa* lung infection. *Eur. J. Pharm. Biopharm.* 121, 1–13. doi: 10.1016/j.ejpb.2017.09.002

Chang, R. Y. K., Chen, K., Wang, J., Wallin, M., Britton, W., Morales, S., et al. (2018). Proof-of-principle study in a murine lung infection model of antipseudomonal activity of phage PEV20 in a dry-powder formulation. *Antimicrob. Agents Chemother.* 62:e01714–e01717.

Chhibber, S., Nag, D., and Bansal, S. (2013). Inhibiting biofilm formation by *Klebsiella pneumoniae* B5055 using an iron antagonizing molecule and a bacteriophage. *BMC Microbiol.* 13:174. doi: 10.1186/1471-2180-13-174

Daly, A. K. (2007). Individualized drug therapy. *Curr Opin Drug Discov Devel* 10, 29-36.

De Jonge, P. A., Nobrega, F. L., Brouns, S. J. J., and Dutilh, B. E. (2018). Molecular and evolutionary determinants of bacteriophage host range. *Trends Microbiol.* 7:1352. doi: 10.1016/j.tim.2018.08.006

De Kraker, M. E., Stewardson, A. J., and Harbarth, S. (2016). Will 10 million people die a year due to antimicrobial resistance by 2050? *PLoS Med.* 13:e1002184. doi: 10.1371/journal.pmed.1002184

Dufour, N., Delattre, R., Ricard, J. D., and Debarbieux, L. (2017). The lysis of pathogenic *Escherichia coli* by bacteriophages releases less endotoxin than by beta-lactams. *Clin. Infect. Dis.* 64, 1582–1588. doi: 10.1093/cid/cix184

Edgar, B. (2004). The genome of bacteriophage T4: an archeological dig. *Genetics* 168, 575–582.

Fong, S. A., Drilling, A., Morales, S., Cornet, M. E., Woodworth, B. A., Fokkens, W. J., et al. (2017). Activity of bacteriophages in removing biofilms of *Pseudomonas aeruginosa* isolates from chronic rhinosinusitis patients. *Front. Cell Infect. Microbiol.* 7:418. doi: 10.3389/fcimb.2017.00418

Forti, F., Roach, D. R., Cafora, M., Pasini, M. E., Horner, D. S., Fiscarelli, E. V., et al. (2018). Design of a broad-range bacteriophage cocktail that reduces *Pseudomonas aeruginosa* biofilms and treats acute infections in two animal models. *Antimicrob. Agents Chemother.* 62:e02573–17. doi: 10.1128/AAC.02573-17

Garcia-Quintanilla, M., Pulido, M. R., Lopez-Rojas, R., Pachon, J., and Mcconnell, M. J. (2013). Emerging therapies for multidrug resistant *Acinetobacter baumannii*. *Trends Microbiol.* 21, 157–163. doi: 10.1016/j.tim.2012.12.002

Ghajavand, H., Esfahani, B. N., Havaei, A., Fazeli, H., Jafari, R., and Moghim, S. (2017). Isolation of bacteriophages against multidrug resistant *Acinetobacter baumannii*. *Res. Pharm. Sci.* 12, 373–380. doi: 10.4103/1735-5362.213982

Gorski, A., Miedzybrodzki, R., Lobocka, M., Glowacka-Rutkowska, A., Bednarek, A., Borysowski, J., et al. (2018). Phage therapy: what have we learned? *Viruses* 10:E288. doi: 10.3390/v10060288

Guo, M., Feng, C., Ren, J., Zhuang, X., Zhang, Y., Zhu, Y., et al. (2017). A novel antimicrobial endolysin, LysPA26, against *Pseudomonas aeruginosa*. *Front. Microbiol.* 8:293. doi: 10.3389/fmicb.2017.00293

Harper, D. R. (2018). Criteria for selecting suitable infectious diseases for phage therapy. *Viruses* 10:E177. doi: 10.3390/v10040177

Huys, I., Pirnay, J. P., Lavigne, R., Jennes, S., De Vos, D., Casteels, M., et al. (2013). Paving a regulatory pathway for phage therapy. Europe should muster the resources to financially, technically and legally support the introduction of phage therapy. *EMBO Rep.* 14, 951–954. doi: 10.1038/embor.2013.163

Keen, E. C. (2015). A century of phage research: bacteriophages and the shaping of modern biology. *Bioessays* 37, 6–9. doi: 10.1002/bies.201400152

Krut, O., and Bekeredjian-Ding, I. (2018). Contribution of the immune response to phage therapy. *J. Immunol.* 200, 3037–3044. doi: 10.4049/jimmunol.1701745

Kumari, S., Harjai, K., and Chhibber, S. (2011). Bacteriophage versus antimicrobial agents for the treatment of murine burn wound infection caused by *Klebsiella pneumoniae* B5055. *J. Med. Microbiol.* 60, 205–210. doi: 10.1099/jmm.0.018580-0

Kusradze, I., Karumidze, N., Rigvava, S., Dvalidze, T., Katsitadze, M., Amiranashvili, I., et al. (2016). Characterization and testing the efficiency of *Acinetobacter baumannii* phage vB-GEC_Ab-M-G7 as an antibacterial agent. *Front. Microbiol.* 7:1590. doi: 10.3389/fmicb.2016.01590

Kutateladze, M. (2015). Experience of the eliava institute in bacteriophage therapy. *Virol. Sinica* 30, 80–81. doi: 10.1007/s12250-014-3557-0

Kutter, E., De Vos, D., Gvasalia, G., Alavidze, Z., Gogokhia, L., Kuhl, S., et al. (2010). Phage therapy in clinical practice: treatment of human infections. *Curr. Pharm. Biotechnol.* 11, 69–86. doi: 10.2174/138920110790725401

Larpin, Y., Oechslin, F., Moreillon, P., Resch, G., Entenza, J. M., and Mancini, S. (2018). *In vitro* characterization of PlyE146, a novel phage lysin that targets Gram-negative bacteria. *PLoS ONE* 13:e0192507. doi: 10.1371/journal.pone.0192507

Lavergne, S., Hamilton, T., Biswas, B., Kumaraswamy, M., Schooley, R. T., and Wooten, D. (2018). Phage therapy for a multidrug-resistant *Acinetobacter baumannii* craniectomy site infection. *Open Forum Infect. Dis.* 5:ofy064. doi: 10.1093/ofid/ofy064

Leitner, L., Sybesma, W., Chanishvili, N., Goderdzishvili, M., Chkhotua, A., Ujmajuridze, A., et al. (2017). Bacteriophages for treating urinary tract infections in patients undergoing transurethral resection of the prostate: a randomized, placebo-controlled, double-blind clinical trial. *BMC Urol.* 17:90. doi: 10.1186/s12894-017-0283-6

Liu, Y., Mi, Z., Niu, W., An, X., Yuan, X., Liu, H., et al. (2016). Potential of a lytic bacteriophage to disrupt *Acinetobacter baumannii* biofilms *in vitro*. *Future Microbiol.* 11, 1383–1393. doi: 10.2217/fmb-2016-0104

Lood, R., Winer, B. Y., Pelzek, A. J., Diez-Martinez, R., Thandar, M., Euler, C. W., et al. (2015). Novel phage lysin capable of killing the multidrug-resistant Gram-negative bacterium *Acinetobacter baumannii* in a mouse bacteremia model. *Antimicrob Agents Chemother.* 59, 1983–1991. doi: 10.1128/AAC.04641-14

Lyczak, J. B., Cannon, C. L., and Pier, G. B. (2000). Establishment of *Pseudomonas aeruginosa* infection: lessons from a versatile opportunist. *Microbes Infect.* 2, 1051–1060. doi: 10.1016/S1286-4579(00)01259-4

Mcconnell, M. J., Actis, L., and Pachón, J. (2013). *Acinetobacter baumannii*: human infections, factors contributing to pathogenesis and animal models. *FEMS Microbiol. Rev.* 37, 130–155. doi: 10.1111/j.1574-6976.2012.00344.x

Miedzybrodzki, R., Borysowski, J., Weber-Dabrowska, B., Fortuna, W., Letkiewicz, S., Szufnarowski, K., et al. (2012). Clinical aspects of phage therapy. *Adv. Virus Res.* 83, 73–121. doi: 10.1016/B978-0-12-394438-2.00003-7

Olszak, T., Zarnowiec, P., Kaca, W., Danis-Wlodarczyk, K., Augustyniak, D., Drevinek, P., et al. (2015). *In vitro* and *in vivo* antibacterial activity of environmental bacteriophages against *Pseudomonas aeruginosa* strains from cystic fibrosis patients. *Appl. Microbiol. Biotechnol.* 99, 6021–6033. doi: 10.1007/s00253-015-6492-6

O'neill, J. (2014). Antimicrobial resistance: tackling a crisis for the health and wealth of nations. *Rev. Antimicrob. Resist.* Available online at: http://amr-review.org/

Parracho, H. M., Burrowes, B. H., Enright, M. C., Mcconville, M. L., and Harper, D. R. (2012). The role of regulated clinical trials in the development of bacteriophage therapeutics. *J. Mol. Genet. Med.* 6, 279–286. doi: 10.4172/1747-0862.1000050

Payne, R. J., and Jansen, V. A. (2003). Pharmacokinetic principles of bacteriophage therapy. *Clin. Pharmacokinet* 42, 315–325. doi: 10.2165/00003088-200342040-00002

Pelfrene, E., Willebrand, E., Cavaleiro Sanches, A., Sebris, Z., and Cavaleri, M. (2016). Bacteriophage therapy: a regulatory perspective. *J. Antimicrob. Chemother.* 71, 2071–2074. doi: 10.1093/jac/dkw083

Peng, S. Y., You, R. I., Lai, M. J., Lin, N. T., Chen, L. K., and Chang, K. C. (2017). Highly potent antimicrobial modified peptides derived from the *Acinetobacter baumannii* phage endolysin LysAB2. *Sci. Rep.* 7:11477. doi: 10.1038/s41598-017-11832-7

Pirnay, J. P., Blasdel, B. G., Bretaudeau, L., Buckling, A., Chanishvili, N., Clark, J. R., et al. (2015). Quality and safety requirements for sustainable phage therapy products. *Pharm. Res.* 32, 2173–2179. doi: 10.1007/s11095-014-1617-7

Pirnay, J. P., Verbeken, G., Ceyssens, P. J., Huys, I., De Vos, D., Ameloot, C., et al. (2018). The magistral phage. *Viruses* 10:E64. doi: 10.3390/v10020064

Regeimbal, J. M., Jacobs, A. C., Corey, B. W., Henry, M. S., Thompson, M. G., Pavlicek, R. L., et al. (2016). Personalized therapeutic cocktail of wild environmental phages rescues mice from *Acinetobacter baumannii* wound infections. *Antimicrob. Agents Chemother.* 60, 5806–5816. doi: 10.1128/AAC.02877-15

Rhoads, D. D., Wolcott, R. D., Kuskowski, M. A., Wolcott, B. M., Ward, L. S., and Sulakvelidze, A. (2009). Bacteriophage therapy of venous leg ulcers in humans: results of a phase I safety trial. *J. Wound Care* 18, 237–238, 240–233. doi: 10.12968/jowc.2009.18.6.42801

Roach, D. R., Leung, C. Y., Henry, M., Morello, E., Singh, D., Di Santo, J. P., et al. (2017). Synergy between the host immune system and bacteriophage is essential for successful phage therapy against an acute respiratory pathogen. *Cell Host Microbe 22*, 38–47.e34. doi: 10.1016/j.chom.2017.06.018

Rossitto, M., Fiscarelli, E. V., and Rosati, P. (2018). Challenges and promises for planning future clinical research into bacteriophage therapy against *Pseudomonas aeruginosa* in cystic Fibrosis. An argumentative review. *Front. Microbiol.* 9:775. doi: 10.3389/fmicb.2018.00775

Sarker, S. A., Sultana, S., Reuteler, G., Moine, D., Descombes, P., Charton, F., et al. (2016). Oral phage therapy of acute bacterial diarrhea with two coliphage preparations: a randomized trial in children from Bangladesh. *EBioMedicine* 4, 124–137. doi: 10.1016/j.ebiom.2015.12.023

Schooley, R. T., Biswas, B., Gill, J. J., Hernandez-Morales, A., Lancaster, J., Lessor, L., et al. (2017). Development and use of personalized bacteriophage-based therapeutic cocktails to treat a patient with a disseminated resistant *Acinetobacter baumannii* infection. *Antimicrob Agents Chemother.* 61:e00954–17. doi: 10.1128/AAC.00954-17

Shiley, J. R., Comfort, K. K., and Robinson, J. B. (2017). Immunogenicity and antimicrobial effectiveness of *Pseudomonas aeruginosa* specific bacteriophage in a human lung *in vitro* model. *Appl. Microbiol. Biotechnol.* 101, 7977–7985. doi: 10.1007/s00253-017-8504-1

Soothill, J. (2013). Use of bacteriophages in the treatment of *Pseudomonas aeruginosa* infections. *Expert Rev. Anti Infect Ther.* 11, 909–915. doi: 10.1586/14787210.2013.826990

Soothill, J. S. (1992). Treatment of experimental infections of mice with bacteriophages. *J. Med. Microbiol.* 37, 258–261. doi: 10.1099/00222615-37-4-258

Speck, P., and Smithyman, A. (2016). Safety and efficacy of phage therapy via the intravenous route. *FEMS Microbiol. Lett.* 363:fnv242. doi: 10.1093/femsle/fnv242

Stahl, F. (1989). The linkage map of phage T4. *Genetics* 123, 245–248.

Tacconelli, E., Carrara, E., Savoldi, A., Harbarth, S., Mendelson, M., Monnet, D. L., et al. (2018). Discovery, research, and development of new antibiotics: the WHO priority list of antibiotic-resistant bacteria and tuberculosis. *Lancet Infect Dis.* 18, 318–327. doi: 10.1016/S1473-3099(17)30753-3

Thandar, M., Lood, R., Winer, B. Y., Deutsch, D. R., Euler, C. W., and Fischetti, V. A. (2016). Novel engineered peptides of a phage lysin aseffective antimicrobials against multidrug-resistant *Acinetobacter baumannii*. *Antimicrob Agents Chemother.* 60, 2671–2679. doi: 10.1128/AAC.02972-15

Tkhilaishvili, T., Di Luca, M., Abbandonato, G., Maiolo, E. M., Klatt, A. B., Reuter, M., et al. (2018). Real-time assessment of bacteriophage T3-derived antimicrobial activity against planktonic and biofilm-embedded *Escherichia coli* by isothermal microcalorimetry. *Res. Microbiol.* doi: 10.1016/j.resmic.2018.05.010. [Epub ahead of print].

Vahedi, A., Dallal, M. M. S., Douraghi, M., Nikkhahi, F., Rajabi, Z., Yousefi, M., et al. (2018). Isolation and identification of specific bacteriophage against enteropathogenic *Escherichia coli* (EPEC) and *in vitro* and *in vivo* characterization of bacteriophage. *FEMS Microbiol. Lett.* 365:fny136. doi: 10.1093/femsle/fny136

Verbeken, G., Pirnay, J. P., Lavigne, R., Jennes, S., De Vos, D., Casteels, M., et al. (2014). Call for a dedicated European legal framework for bacteriophage therapy. *Arch. Immunol. Ther. Exp.* 62, 117–129. doi: 10.1007/s00005-014-0269-y

Villarroel, J., Larsen, M. V., Kilstrup, M., and Nielsen, M. (2017). Metagenomic analysis of therapeutic PYO phage cocktails from 1997 to 2014. *Viruses* 9:E328. doi: 10.3390/v9110328

Waters, E. M., Neill, D. R., Kaman, B., Sahota, J. S., Clokie, M. R. J., Winstanley, C., et al. (2017). Phage therapy is highly effective against chronic lung infections with *Pseudomonas aeruginosa*. *Thorax* 72:666. doi: 10.1136/thoraxjnl-2016-209265

Wright, A., Hawkins, C. H., Anggard, E. E., and Harper, D. R. (2009). A controlled clinical trial of a therapeutic bacteriophage preparation in chronic otitis due to antibiotic-resistant *Pseudomonas aeruginosa*; a preliminary report of efficacy. *Clin. Otolaryngol.* 34, 349–357. doi: 10.1111/j.1749-4486.2009.01973.x

Yan, G., Liu, J., Ma, Q., Zhu, R., Guo, Z., Gao, C., et al. (2017). The N-terminal and central domain of colicin A enables phage lysin to lyse *Escherichia coli* extracellularly. *Antonie Van Leeuwenhoek* 110, 1627–1635. doi: 10.1007/s10482-017-0912-9

Yin, S., Huang, G., Zhang, Y., Jiang, B., Yang, Z., Dong, Z., et al. (2017). Phage Abp1 rescues human cells and mice from infection by pan-drug resistant *Acinetobacter baumannii*. *Cell Physiol. Biochem.* 44, 2337–2345. doi: 10.1159/000486117

Zhou, W., Feng, Y., and Zong, Z. (2018). Two new lytic bacteriophages of the myoviridae family against carbapenem-resistant *Acinetobacter baumannii*. *Front. Microbiol.* 9:850. doi: 10.3389/fmicb.2018.00850

Conflict of Interest Statement: The authors declare that the research was conducted in the absence of any commercial or financial relationships that could be construed as a potential conflict of interest.

frontiers in Cellular and Infection Microbiology

ORIGINAL RESEARCH
published: 14 November 2018
doi: 10.3389/fcimb.2018.00402

Paradigm Shift in Drug Re-purposing From Phenalenone to Phenaleno-Furanone to Combat Multi-Drug Resistant *Salmonella enterica* Serovar Typhi

Shama Mujawar[1], *Derek Gatherer*[2] *and Chandrajit Lahiri*[1]*

[1] Department of Biological Sciences, Sunway University, Bandar Sunway, Malaysia, [2] Department of Biomedical and Life Sciences, Lancaster University, Lancaster, United Kingdom

OPEN ACCESS

Edited by:
Rodolfo García-Contreras, Universidad Nacional Autónoma de México, Mexico

Reviewed by:
Bernardo Franco, Universidad de Guanajuato, Mexico
Dakshinamurthy Sivakumar, Konkuk University, South Korea

***Correspondence:**
Chandrajit Lahiri
chandrajitl@sunway.edu.my

Specialty section:
This article was submitted to Clinical Microbiology, a section of the journal Frontiers in Cellular and Infection Microbiology

Received: 13 August 2018
Accepted: 24 October 2018
Published: 14 November 2018

Citation:
Mujawar S, Gatherer D and Lahiri C (2018) Paradigm Shift in Drug Re-purposing From Phenalenone to Phenaleno-Furanone to Combat Multi-Drug Resistant Salmonella enterica Serovar Typhi. Front. Cell. Infect. Microbiol. 8:402. doi: 10.3389/fcimb.2018.00402

Over recent years, typhoid fever has gained increasing attention with several cases reporting treatment failure due to multidrug resistant (MDR) strains of *Salmonella enterica* serovar Typhi. While new drug development strategies are being devised to combat the threat posed by these MDR pathogens, drug repurposing or repositioning has become a good alternative. The latter is considered mainly due to its capacity for saving sufficient time and effort for pre-clinical and optimization studies. Owing to the possibility of an unsuccessful repositioning, due to the mismatch in the optimization of the drug ligand for the changed biochemical properties of "old" and "new" targets, we have chosen a "targeted" approach of adopting a combined chemical moiety-based drug repurposing. Using small molecules selected from a combination of earlier approved drugs having phenalenone and furanone moieties, we have computationally delineated a step-wise approach to drug design against MDR *Salmonella*. We utilized our network analysis-based pre-identified, essential chaperone protein, SicA, which regulates the folding and quality of several secretory proteins including the Hsp70 chaperone, SigE. To this end, another crucial chaperone protein, Hsp70 DnaK, was also considered due to its importance for pathogen survival under the stress conditions typically encountered during antibiotic therapies. These were docked with the 19 marketed anti-typhoid drugs along with two phenalenone-furanone derivatives, 15 non-related drugs which showed 70% similarity to phenalenone and furanone derivatives and other analogous small molecules. Furthermore, molecular dynamics simulation studies were performed to check the stability of the protein-drug complexes. Our results showed the best binding interaction and stability, under the parameters of a virtual human body environment, with XR770, a phenaleno-furanone moiety based derivative. We therefore propose XR770, for repurposing for therapeutic intervention against emerging and significant drug resistance conferred by pathogenic *Salmonella* strains.

Keywords: drug repurposing, salmonellosis, multidrug resistance, chaperones, SicA, DnaK

INTRODUCTION

Bacterial infections have been a life threatening problem to the human population throughout the existence of our species. In addition, with the advent of antimicrobial resistance (AMR), this has become an ever-increasing concern, contributing nearly one fifth of total global deaths every year. With a worldwide prevalence of probably five hundred million cases and hundreds of thousands of deaths every year, human salmonellosis or typhoid fever, has become a major cause for concern with the emergence of multidrug-resistance (MDR) serovars and strains of *Salmonella enterica* (Zaidi et al., 2008). The severity of the disease, depends on host factors and the individual emerged MDR serotype of *Salmonella* (Neckers and Tatu, 2008). Thus, it has become imperative to replace conventional anti-typhoid treatment strategies with new ones more suitable for drug-resistant pathogens. However, designing novel effective drugs against the most important virulence protein targets, choosing from the whole genome of *Salmonella* sp., is a highly challenging task.

To encounter the aforementioned threats and challenges of MDR, new strategies like drug repurposing have surfaced as alternative approaches to novel therapeutics (Rangel-Vega et al., 2015). This include computational drug repurposing strategies based on transcriptional signatures, networks, ligands, target structures using chemogenomics, machine learning, and molecular docking techniques (March-Vila et al., 2017). Nevertheless, drug repurposing approach may have some limitations on its successful outcome (Aubé, 2012). For example, the drug might act at the same target but with different outcomes that depend on the new active site of biological action of the repurposed drug (Aubé, 2012). Again, different structure-activity relationship might be possible for old and new drug with different biochemical targets, leading to an obsolete solution to be replaced by further repurposed drugs (Aubé, 2012). However, a screening of drugs identified for repurposing has proven to be useful when used together in combination thereby making it the most competing strategy to adapt the current pharmacopeia for new uses (Aubé, 2012).

To repurpose drug(s) through a network based approach, the technique of computationally analyzing the protein interaction networks for *Salmonella* could be employed (Pan et al., 2015). This pathogen is found to encode a Type III Secretion System (T3SS) within a pathogenicity island that is essential for virulence (Tucker and Galán, 2000). All T3SSs require the function of a family of low-molecular-weight proteins that aid the secretion process by acting as secretion factors (Tucker and Galán, 2000). One such secretion associated protein is the chaperone SicA, identified as a secretion factor from the network based approach of the protein interactome analysis of *Salmonella* pathogenicity islands (SPI) and two component signal transduction systems (TCS) (Lahiri et al., 2014). In summary, chaperones aid in folding, packaging, and secretion of synthesized proteins besides inhibiting aggregation due to stress factors like heat shock, thereby striking a balance between refolding and proteolytic degradation (Liberek et al., 2008). The potential of exploiting pathogenic chaperones as drug targets has also been reported (Neckers and Tatu, 2008). Notably, chaperones that support folding of newly synthesized proteins, namely Hsp60, Hsp70, and Hsp90, have distinct mechanisms of action (Fink, 1999). Most of these heat shock proteins (HSP) are constitutively synthesized but are further induced in response to stress conditions, including antibiotic therapies (Zügel and Kaufmann, 1999). In fact, DnaK, the bacterial homolog of human Hsp70, has been found to play an important role in pathogen survival (Chiappori et al., 2015). Moreover, previous work has shown that the chaperone SicA, is auto-regulated and required for the transcription of *sigE* (Darwin and Miller, 2001). SigE is another Hsp70 molecular chaperone protein required for stabilization of SopB/SigD secretory proteins through prevention of premature association of effectors and their degradation prior to secretion (Darwin et al., 2001). All of these proteins could, therefore, form the new targets for the newly proposed drug for repurposing. Targeting such HSPs may, therefore, help to combat pathogen virulence by reducing its capacity to respond to other treatments (Neckers and Tatu, 2008). Such treatments have been linked to the therapy of inflammatory diseases and cancer which is possible due to the molecular chaperone and antigen-binding properties of the HSPs (Calderwood et al., 2012).

To repurpose drugs through a ligand based approach, a combination of the chemical moieties of individually approved and marketed drugs could be used. Typically, drugs used mostly for treating infectious diseases caused by gram positive pathogens contain phenalenone moieties (March-Vila et al., 2017). Again, furanone moiety-based drugs have gained attention for treating other infectious (Chrystal et al., 2007). To address the pressing need for better treatment alternatives for MDR *Salmonella*, here we have used a combined phenaleno-furanone moiety-based ligand XR770, which was previously shown to be more preferable in performing as dual TCS inhibitor against the catalytic domain of the histidine kinase BaeS and the dimerization domain of the response regulator BaeR (Sivakumar et al., 2013). In summary, using molecular dynamics simulation, we have screened current typhoid drugs, non-typhoidal drugs and Hsp70 modulators to propose XR770 as a drug candidate against plausible chaperone protein targets, namely SicA, DnaK, and SigE compared to our reference TCS protein pairs, SsrA/SsrB and OmpR/EnvZ of the T3SS. We anticipate that targeting such molecular chaperones might help in the rational development of effective drugs for salmonellosis and thus, future control of the pathogenic bacterial growth, in an era of rapidly increasing antibiotic resistance. Furthermore, our combined-moiety ligand-based molecular docking approach via indispensable targets, will likely provide new opportunities of drug repurposing for MDR *Salmonella*.

MATERIALS AND METHODS

Selection of Ligands

Ligand screening was performed with the aim of finding existing drugs for treating systemic infections like typhoid (Kaur et al., 2011). The molecular structures of the 19 typhoid-related drugs were obtained from Drug Bank (Wishart et al., 2017), namely Amoxicillin, Azithromycin, Ceftriaxone, Chloramphenicol,

Ciprofloxacin, Levofloxacin, Ofloxacin, Sulfamethoxazole, Trimethoprim, Rolitetracycline, Auranofin, Imiquimod, Alverine, Lymecycline, Digitoxin, Rimonabant, Isosorbide Mononitrate, Acenocoumarol, Doxycycline. Structures of phenalenone-furanone derivatives XR770 and XR587 were produced using MarvinSketch (Csizmadia, 1999). Furthermore, we constructed a control set of 15 other drugs, not known to cure typhoid, but already used to treat infections caused mostly by gram positive bacteria like *Staphylococcus aureus*, *Streptococcus pneumonia* etc. (**Supplementary Table 2**). The structures of these drugs, containing moieties of either phenalenone or furanone, were obtained from DrugBank *viz.* Moxifloxacin, Grepafloxacin, Lomefloxacin, Gatifloxacin, Sparfloxacin, Temafloxacin, Nemonoxacin, Besifloxacin, Finafloxacin, Cadazolid, Nadifloxacin, Sitafloxacin, Clinafloxacin, Pilocarpine, Matairesinol. The non-typhoidal drugs were found to possess 70% similarity to Phenaleno-furanone derivatives such as XR770 and XR587 (Sivakumar et al., 2013). Also, Hsp70 modulators (analogous to Hsp90 inhibitors) were also used in this study that are known to have significant effects on chaperone function (Patury et al., 2009).

Selection of Targets

The secretion associated chaperone protein, SicA, was selected on the basis of previous work (Lahiri et al., 2014) on the interactome analysis of SPI and TCS. Another chaperone protein, DnaK, of the Hsp70 class, was identified from the top-most centrality ranking protein list of the whole genome protein interaction network analysis of *Salmonella* Typhimurium strain LT2 (Mujawar & Lahiri, unpublished data). For a comparison with these identified targets, a similar Hsp70 chaperone protein, SigE, required for the stabilization of secretory proteins, was selected. These chaperone proteins were compared with the TCS protein pairs of SsrA/B and EnvZ/OmpR as controls for the binding efficacy of the ligand XR770 previously reported to be effective for the TCS pair BaeS/R of *Salmonella* (Sivakumar et al., 2013). As both the serovars of *Salmonella*, namely Typhimurium and Typhi share almost similar genes/proteins, the aforementioned proteins of Typhimurium have been utilized in the context of Typhi as well. The sequences of target chaperone proteins, SicA, DnaK, SigE, and the TCS proteins SsrA, SsrB, OmpR and EnvZ were collected from UniprotKB database with the accession IDs are P69066, Q56073, O30917, Q8ZPP5, O54305, P0AA19, and P0AA20 for *Salmonella* Typhimurium and P69065, Q8Z9R1, Q8Z7R2, Q8Z6K9, Q8XFU4, P08982, and P41406 for *Salmonella* Typhi, respectively.

Target Structure Modeling

As the selected proteins above did not have any solved X-ray crystallographic or NMR 3D structures in Protein Data Bank (PDB), we have generated homology models and validated their structure to pursue further docking studies. We have used Phyre2 (Kelley et al., 2015), SWISS MODEL (Schwede et al., 2003) and I-TASSER (Zhang, 2008) and VERIFY 3D (Bowie et al., 1991) protein modeling servers to generate the structures and evaluated them through Ramachandran plot, Q-mean score, and Z-score listed in SAVES server. Consensus studies of different models generated by above mentioned servers was carried out to identify the best structure. **Table 1** represents the details of protein structures that were used for further docking studies.

Binding Site Identification for Docking

To have an understanding of the binding activity, active sites or binding pockets of the selected proteins were determined by using CASTp server (Computer Atlas of Surface Topology of protein) (Dundas et al., 2006). AutoDock v4.2 was used to generate grid box and map files for docking (Morris et al., 2009). The generated grid coordinates *viz.* X, Y, and Z were stored in a grid parameter file (GPF). The atoms such as Hydrogen (H), chlorine (Cl), bromine (Br), sulfur (S), phosphorus (P), and fluorine (F) were added, as appropriate, to set the map types to generate the grid box that covers the active site. The span of the active sites in the 3D structures of SicA, DnaK, SigE, SsrA, SsrB, OmpR, and EnvZ on X, Y, & Z coordinates were 40, 7, and 17 Å, respectively. The grid dimensions for the receptor for docking were taken as 60, 60, and 60 Å, respectively, to ensure that the search spaces are large enough for the ligands to rotate in. The execution of GPF files using MGLTools v1.5.7 was used to generate the map files of the atoms mentioned above to be used for docking. Upon GPF execution, grid log files (GLG) were generated which consisted of all the atomic map files to be used as the input parameter for docking calculated by the program AUTOGRID (Morris et al., 2009).

Ligand Screening Against Salmonellosis

The aforementioned existing drugs, along with the hypothesized **signal** transduction inhibitors (Chrystal et al., 2007), were used for chaperone protein inhibition as shown in **Figures 1**, **2**. XR770 and XR587 were further analyzed on the basis of Lipinski Rule of five. ADME and Toxicity testing were also done using Schrodinger Software (Friesner et al., 2006).

Lipinski's Rule Prediction of Selected Drugs

To evaluate drug likeness and determine if a chemical compound with a certain pharmacological or biological activity has properties that would make it a likely orally active drug in humans, we have carried out the Lipinski's rule prediction method for the selection of drugs. Comparison of the marketed drugs reflected some deviation to the above rule but are still used for oral administration with the given inhibitory concentration (**Tables 2**, **3**).

Protein-Ligand Docking

To perform the docking process, a genetic algorithm is used to furnish the docking conformations, binding energies, interactions etc. For the docking of ligands into intended protein binding pockets (Kitchen et al., 2004) and to approximate the binding affinities of the ligands, the molecular docking program AutoDock Vina was used (Trott and Olson, 2010). Docking studies were performed on SicA, DnaK, SigE, SsrA, SsrB, OmpR, and EnvZ against 21 typhoid related drugs (**Table 4** and **Supplementary Figure 2**), 15 non-typhoidal drugs (**Table 5** and **Supplementary Figure 3**), and 7 Hsp70 modulators (**Table 6** and

TABLE 1 | Comparison of the 3D structures generated for SicA, DnaK, and SigE using different protein modeling servers.

Protein	Server	Q-mean	Z-score	Favored region(%)	Disallowed region(%)	SASA (A^2)
SicA	**PHYRE2**	**0.765**	**−0.23**	**95.5**	**0.0**	**101**
	SWISSMODEL	0.727	−0.55	94.7	0.0	97
	I-TASSER	0.481	−2.84	87.0	0.0	103
	VERIFY 3D	0.761	−0.26	93.2	0.0	91.6
DnaK	PHYRE2	0.686	−0.86	89.7	0.2	106
	SWISSMODEL	0.621	−0.81	81.0	0.5	105
	I-TASSER	**0.689**	**−0.80**	**90.5**	**0.1**	**106**
	VERIFY 3D	0.692	−0.67	89.4	0.1	106
SigE	PHYRE2	0.712	−0.40	89.2	0.2	91
	SWISSMODEL	0.741	−0.26	80.1	0.2	96
	I-TASSER	**0.622**	**−0.73**	**91.6**	**0.0**	**99.1**
	VERIFY 3D	0.644	−0.23	89.2	0.2	91.3
SsrA	PHYRE2	0.721	−0.43	90.1	0.1	92.3
	SWISSMODEL	0.702	−0.55	89.0	0.1	85
	I-TASSER	**0.753**	**−0.82**	**92.2**	**0.0**	**89.1**
	VERIFY 3D	0.719	−0.56	90.2	0.0	89.2
SsrB	PHYRE2	0.681	−0.81	92.2	0.2	101
	SWISSMODEL	**0.723**	**−0.80**	**90.2**	**0.1**	**89.2**
	I-TASSER	0.695	−0.83	90.0	0.2	88.1
	VERIFY 3D	0.69	−0.81	90.2	0.1	88.2
OmpR	PHYRE2	0.721	−0.29	92.5	0.0	96.1
	SWISSMODEL	**0.786**	**−0.43**	**96.2**	**0.0**	**104.0**
	I-TASSER	0.681	−0.43	94.3	0.0	93.1
	VERIFY 3D	0.732	−0.43	94.9	0.0	101
EnvZ	**PHYRE2**	**0.771**	**−0.36**	**94.6**	**0.0**	**101**
	SWISSMODEL	0.762	−0.33	94.4	0.0	100
	I-TASSER	0.769	−0.33	93.2	0.0	98.3
	VERIFY 3D	0.786	−0.34	94.4	0.0	98.0

Bold values indicates best representative.

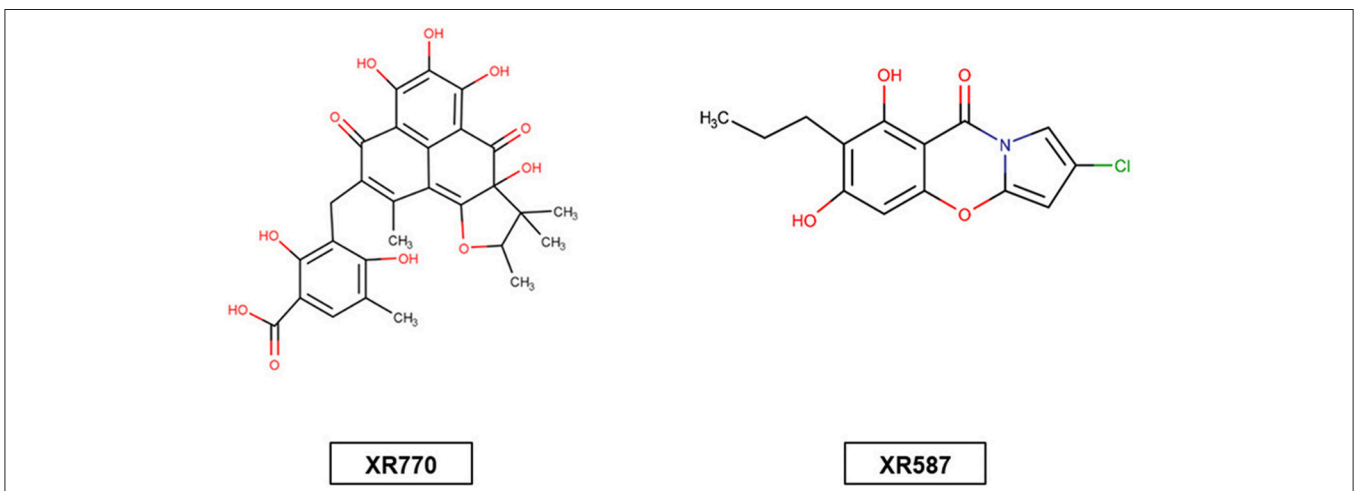

FIGURE 1 | Structure of signal transduction inhibitors XR770 (a phenalenone derivative) produced by Penicillium cf. herquei 20421 and XR587 (streptopyrrole) fermentation product of actinomycete strain.

Figure 2). The protein and the ligand files were changed into the PDBQT format containing the protein atom coordinates, partial charges and deliverance parameters. Auto Grid boxes were predetermined around the active site of the protein based on the Lamarckian Genetic Algorithm (LGA) and the obtained dock scores were reported in kcal/mol. The utilized docking protocol

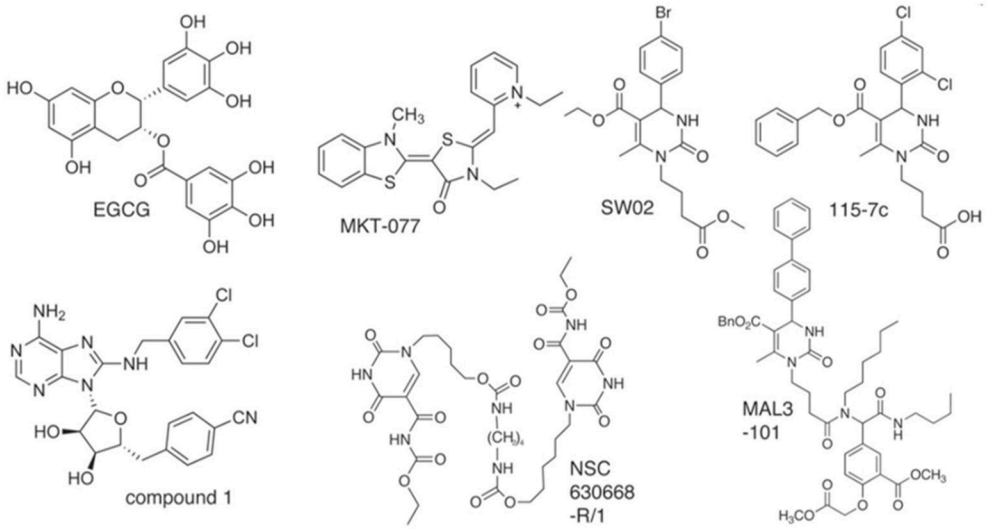

FIGURE 2 | Structures of Hsp70 modulators (analogous to Hsp90 inhibitors) with selective chemical scaffolds that target the varied functions of chaperones.

comprised 35 autonomous iterations per ligand. The docked log files (DLG) calculated by the program AutoDock consisted of detailed information about binding energy, hydrogen bonds, interacting residues etc. which were further used for the docking analysis (Sousa et al., 2006).

Molecular Dynamics Simulation of SicA, DnaK, and SigE Protein Complex From *S.* Typhimurium and *S.* Typhi

To study the macromolecular interactions of SicA, DnaK, and SigE with XR770, simulation studies were performed using MOE (Chemical Computing Group, Montreal). Multiple conformations of the SicA, DnaK, and SigE complex were prepared based on minimum binding energy and number of hydrogen bonds. For the SicA-XR770 protein ligand complex, three docked poses were simulated as three replicates. All structures were corrected using the clean protein application in Discovery Studio (DS) 2.5 (Accelrys Inc., San Diego, CA). This preparation of all molecular files followed by Molecular Dynamics (MD) simulations were conducted using the previously described energy minimized files. The all-atom CHARMM 27 force field was assigned to all molecules for topology generation, and the explicit extended simple point charge (SPC/E) SPC216 water model was applied to solvate the molecules. A triclinic box was generated with a minimum of 1.0 nm distance from the edges of the box to maintain periodic boundary conditions throughout the simulations. Adequate counter ions (Cl^- and Na^+) were added to the solvent to keep the system neutral at physiological ionic strength (0.10 M salt concentration). Steepest descent minimization was performed until the maximum force reached below 1,000.0 kJ mol^{-1} nm^{-1}. Before the MD simulations, the systems were equilibrated using position restrained (PR) for 100 ps of isochoric-isothermal (NVT) equilibration at 300K. This was followed by an equilibration under an isothermal-isobaric (NPT) ensemble for 100 ps at the same temperature and 1.0 bar of pressure without position restraints. In NVT and NPT ensembles, the short range non-bonded interactions were defined as van der Waals (VDW) and electrostatic interactions for particles within 1.0 nm. The well-equilibrated systems SicA-XR770, DnaK-XR770, and SigE-XR770 were used to run 100 ns production of MD simulation in three replicates using velocity rescale thermostat. The long-range electrostatic interactions i.e., Particle Mesh Ewald (PME) treatments were also implemented as described in NVT and NPT ensembles (Hansson et al., 2002; Shattuck, 2011).

RESULTS

Docking Analysis

Docking analysis of all the docked complexes of the aforementioned proteins viz. SicA, Dnak, SigE, SsrA, SsrB, OmpR, and EnvZ against the set of 19 typhoid related drugs, 15 non-typhoidal drugs and 7 Hsp70 modulators was performed. The docking outcome was analyzed on the source of ranked clusters of compound conformations with the binding energy values of various ligands as shown in **Tables 4–6**. High affinity is related to a high release of the free energy upon binding. The binding pattern of XR770 and XR587, along with the list of marketed drugs against typhoid and diarrhea, were compared for their efficiency against SicA, DnaK, and SigE**.** Based on the binding pattern of the aforementioned proteins, SicA showed Lys143 as the most consistent residue for all the drugs with the highest binding energy being −9.98 kcal/mol for XR770. For DnaK, the prominent residues were Thr11 and Gly197 showing the highest binding energy (−8.76 kcal/mol) with XR770. Similarly, SigE showed Thr69 and Arg84 to be the residues at the active sites for all the drugs. Interestingly, XR770 showed the highest binding energy of −11.48 kcal/mol with SigE which, notably, was the strongest binding affinity amongst all the proteins compared. Moreover, the chaperone proteins

TABLE 2 | Physicochemical properties of typhoid related drugs and phenaleno-furanone derivatives.

Drugs	Compound_ID	Molecular weight g/mol	XLOGP3	HBond donor	HBond acceptor	Inhibitory conc. (mol/ Kg)
Acenocoumarol	DB01418	353.33	2.5	1	6	2.7869
Alverine	DB01616	281.443	5.3	0	1	2.6539
Amoxicillin	DB01060	365.404	−2.0	4	7	1.7036
Anacardic Acid	167551	348.527	9.5	2	3	NA
Auranofin	DB00995	678.483	NA	0	10	3.1438
Azithromycin	DB00207	748.996	4.0	5	14	2.5423
Ceftriaxone	DB01212	554.571	−1.3	4	13	2.1681
Chloramphenicol	DB00446	323.126	1.1	3	5	2.2247
Ulexone C	14583602	420.461	4.3	2	6	NA
CID_21591963	21591963	438.476	3.4	3	7	NA
Ulexin C	5323553	418.445	4.4	2	6	NA
Osajin	95168	404.462	5.9	2	5	NA
Ciprofloxacin	DB00537	331.347	−1.1	2	7	NA
Digitoxin	DB01396	764.95	2.3	5	13	4.4764
Doxycycline	DB00254	444.44	−0.7	6	9	2.3159
Ergonovine	DB01253	325.412	1.8	3	3	3.3967
Imiquimod	DB00724	240.31	2.6	1	3	2.5683
Isosorbide_Mononitrate	DB01020	191.139	−0.4	1	6	2.0753
Levofloxacin	DB01137	361.373	−0.4	1	8	NA
Lymecycline	DB00256	602.641	−4.4	9	13	2.5422
Ofloxacin	DB01165	361.373	−0.4	1	8	2.1639
Rimonabant	DB06155	463.787	6.5	1	3	2.5418
Rolitetracycline	DB01301	527.574	−0.9	6	10	2.7094
Sulfamethoxazole	DB01015	253.276	0.9	2	6	1.6422
Trimethoprim	DB00440	290.323	0.9	2	7	1.7701
XR587	NA	281.611	−0.5	2	7	NA
XR770	**NA**	**512.301**	**−0.6**	**2**	**8**	**NA**

Bold values indicates best representative.

i.e., SicA, DnaK, and SigE, showing commendable interaction with efficient binding energies with XR770, were considered for further molecular dynamics simulation studies (**Figure 3**).

Binding Interactions Between SicA, DnaK, and SigE With XR770 Protein-Ligand Complex

Protein-ligand interaction depends on some bonded and non-bonded interactions. To make a stable protein-ligand complex, as well as for proper folding of proteins several H-bonds, nonbonded electrostatic and van-der Waals (vdW) interactions (**Table 7** and **Supplementary Figure 5**). Among the amino acid residues of SicA, the residues participating in protein-ligand formation are Lys143 for *S.* Typhimurium and Arg61, Gln86, Lys89 for *S.* Typhi which had more than −70 kJ mol^{-1} total electrostatic and vdW energy terms. Similarly, in DnaK Thr11, Gly197 for *S.* Typhimurium and Arg167, Asp38, and Ile418 for *S.* Typhi and in SigE Arg84, Thr69 for *S.* Typhimurium and Ala74 for *S.* Typhi are the participating residues. Thus, the amino acid residues from each of the complex i.e., SicA, DnaK, and SigE were maximally involved in the interactions with XR770 throughout MD simulation processes (**Supplementary Figure 4**). In order to analyse the binding interactions between each chaperone protein complex accurately, hydrogen bond pairing during all frames of the MD production run were calculated in MOE with bond pair distances within 3.6 Å and angles at 35°. It was found that, several amino acid residues formed hydrogen bonds in the protein-ligand complex. MD simulation study showed the clear indication of each amino acid interaction with the hydrogen bond formation. Maximum occupancies of the following amino acids were considered separately for each complex. The solvent accessible surface area of the SicA, DnaK, and SigE complex became higher after simulation. The sum of solvent accessible surface area of SicA, DnaK, and SigE complex was 424 nm^2 whereas for the DnaK and SigE complex it was 533 and 460 nm^2, respectively. The spatial changes denote that the XR770 complex with each of the proteins became more accessible for free binding.

DISCUSSION

Multidrug resistance has increased dramatically in the last two decades. Therefore, drug repurposing, is gaining in importance.

TABLE 3 | Physicochemical properties of 70% similar phenalenone-furanone derivatives.

Drugs	Compound_ID	Molecular weight g/mol	XLOGP3	HBond donor	HBond acceptor	Inhibitory Conc. (mol/ kg)
Moxifloxacin	DB00218	401.438	0.6	2	8	2.3267
Grepafloxacin	DB00365	359.401	−0.2	2	7	2.0923
Lomefloxacin	DB00978	351.354	−0.8	2	8	1.9971
Gatifloxacin	DB01044	375.4	−0.7	2	8	2.3029
Sparfloxacin	DB01208	392.407	0.1	3	9	1.9265
Temafloxacin	DB01405	417.388	0.6	2	9	2.0973
Nemonoxacin	DB06600	371.437	0.3	2	7	NA
Besifloxacin	DB06771	393.84	0.7	2	6	2.3263
Finafloxacin	DB09047	398.394	−0.5	2	8	NA
Cadazolid	DB11847	585.561	1.4	3	10	NA
Nadifloxacin	DB12447	360.385	0.8	2	6	NA
Sitafloxacin	DB13261	873.68	0.2	2	6	NA
Clinafloxacin	DB14025	365.79	0.3	2	6	NA
Pilocarpine*	DB01085	208.256	1.1	0	3	2.6826
Matairesinol*	DB04200	358.385	2.7	2	5	2.4961

The asterisk (*) indicate the furanone derivatives.

TABLE 4 | Interaction pattern of SicA, DnaK and SigE with the corresponding interacting residues and Binding energy against typhoid related drugs.

Drugs	SASA	Interacting residues			Binding energy			H bonds		
	(A^2)	SicA	DnaK	SigE	SicA	DnaK	SigE	SicA	DnaK	SigE
Amoxicillin	249	Lys143	Thr11,Lys70	Arg84,Thr69	−4.97	−6.91	−8.24	1	2	2
Azithromycin	225	Lys143	NA	Thr69	−5.74	NA	−7.07	1	NA	1
Ceftriaxone	167	Lys143	Thr11,Lys70	Arg84,Thr69	−2.96	−6.2	−7.2	1	2	2
Chloramphenicol	197	Lys143	Thr11,Gly197	Arg84,Thr69	−5.73	−6.85	−6.49	1	2	2
Ciprofloxacin	201	Lys143	Thr12,Lys270	Arg84,Thr69	−5.38	−8.18	−6.92	1	2	2
Digitoxin	236	Lys143	NA	Arg84,Tyr83	−9.89	NA	−8.07	2	NA	2
Ergonovine	240	NA	Thr11,Lys70,Gly197	Arg84,Tyr83	NA	−8.03	−7.63	NA	3	2
Imiquimod	155	NA	Gly197	Arg84,Thr69	NA	−6.69	−7.16	NA	1	2
Isosorbide Mononitrate	172	NA	Thr11,Gly197	Arg84,Thr69	NA	−5.94	−4.84	NA	2	2
Levofloxacin	159	Lys143	Thr11,Lys70,Gly197	Arg84,Thr69	−5.49	−7.05	−7.39	1	3	2
Lymecycline	285	NA	Thr11,Lys70	Arg84,Thr69	NA	−8.05	−9.29	NA	2	2
Ofloxacin	174	Lys143	Thr11,Lys70,Gly197	Arg84,Thr69	−5.4	−7.69	−7.53	1	3	2
Rimonabant	104	NA	NA	Arg84	NA	NA	−9.21	NA	NA	1
Rolitetracycline	223	NA	NA	Arg84,Thr69	NA	NA	−9.45	NA	NA	2
Sulfamethoxazole	201	Lys143	Thr11,Lys70,Gly197	Arg84,Thr69	−5.22	−7.22	−8.29	1	3	2
Trimethoprim	263	Lys143	Thr11, Thr12, Lys55	Arg84,Thr69	−4.24	−7.4	−6.55	1	3	2
XR770	**197**	**Lys143**	**Thr11,Gly197**	**Arg84,Thr69**	**-9.98**	**-8.76**	**-11.48**	**1**	**2**	**2**
XR587	129	NA	Thr11,Lys70,Gly197	Thr69	NA	−7.04	−7.69	NA	3	1

Bold values indicates best representative.

The analysis and prediction of the activity of existing and novel drug ligands for new protein targets is based on the concept that similar compounds tend to have similar biological properties. Similarly, incorporating a structure based approach focusses on obtaining proteins likely to have similar functions and/or to recognize similar ligands. Thus, in the field of drug repurposing, protein comparison is used as a method to identify secondary targets of an approved drug. To hypothesize a new target for treating MDR *Salmonella*, we have explored the results of a network based approach (Lahiri et al., 2014) to identify the most indispensable proteins important for available as well as next generation drugs. The present study further develops this work at a structural level.

TABLE 5 | Interaction pattern of SicA, DnaK, and SigE with the corresponding interacting residues and binding energy against non-typhoidal drugs.

Drugs	SASA	Interacting residues			Binding energy			H bonds		
	(A^2)	SicA	DnaK	SigE	SicA	DnaK	SigE	SicA	DnaK	SigE
Moxifloxacin	265	Lys143	Lys70	Arg84	−5.21	−6.02	−6.30	1	1	1
Grepafloxacin	187	Lys143,Thr21	Thr11,Gly197	Thr69,Arg84	−6.42	−6.38	−6.31	1	2	2
Lomefloxacin	148	Lys143	Lys70, Thr11	Arg84	−5.96	−6.22	−7.24	1	2	1
Gatifloxacin	214	Lys143,Thr21	Thr11,Gly197	NA	−6.76	−6.98	−6.67	2	2	NA
Sparfloxacin	216	Lys143	Thr11,Lys70	Thr69,Arg84	−5.18	−6.82	−5.23	1	2	2
Temafloxacin	191	Lys143	Gly197	Arg84	−6.11	−6.06	−6.15	1	1	1
Nemonoxacin	230	Thr21	Thr11, Lys70	Thr69	−6.48	−6.32	−6.33	1	2	1
Besifloxacin	228	Lys143	NA	NA	−4.20	NA	NA	1	NA	NA
Finafloxacin	165	NA	Gly197, Lys70	NA	−5.28	NA	NA	NA	2	NA
Cadazolid	214	Lys143,Thr21	Thr11, Gly197	Arg84	−5.94	−6.00	−5.32	2	2	1
Nadifloxacin	148	Lys143	NA	Arg84,Thr69	−7.21	NA	−6.29	1	NA	2
Sitafloxacin	**191**	**Lys143,Thr21**	**Thr11,Lys70,Gly197**	**Arg84,Thr69**	**-7.57**	**-7.84**	**-7.39**	**2**	**3**	**2**
Clinafloxacin	264	NA	Thr11, Gly197	NA	NA	−7.66	NA	NA	2	NA
Pilocarpine	165	Lys143	Thr11, Gly197	Arg84	−6.60	−6.85	−6.08	1	2	1
Matairesinol	255	Lys143	Thr11,Gly197	Arg84	−6.51	−6.73	−7.52	1	2	2

Bold values indicates best representative.

TABLE 6 | Interaction pattern of SicA, DnaK, and SigE with the corresponding interacting residues and Binding energy against Hsp70 modulators.

Drugs	SASA	Interacting residues			Binding energy			H bonds		
	(A^2)	SicA	DnaK	SigE	SicA	DnaK	SigE	SicA	DnaK	SigE
EGCG	151	Lys143	Gly197,Thr11	Arg84,Thr69	−6.93	−10.54	−10.87	1	2	2
MKT-077	189	NA	Lys121	Arg84	NA	−7.24	−9.07	NA	2	1
SW02	143	NA	Lys70	Arg84,Thr69	NA	−7.95	−8.21	NA	2	1
115–7c	146	Lys143	Gly197,Thr12	Arg84,Thr69	−7.31	−8.69	−9.86	1	2	2
Compound 1	**229**	**Lys143**	**Thr12**	**Arg84,Thr69**	**−8.35**	**−8.39**	**−10.51**	**1**	**1**	**1**
NSC-630668	183	NA	NA	Arg84,Thr69	NA	NA	−8.02	NA	NA	NA
MAL3-101	158	Lys143	NA	Arg84,Thr69	−8.69	NA	−6.53	1	NA	NA

Bold values indicates best representative.

Furthermore, recent progress in proteomics has significantly increased the plausible number of macromolecular targets as candidates for drug discovery. Molecular docking studies have been successfully exploited in drug repurposing. Such techniques are used to predict the geometry and binding energy of the interaction of a protein in complex with a small-molecule ligand. Therefore, the method can be used to predict if a given drug is potentially able to bind other targets. The ability of such target proteins to be bound by the approved drugs shows the druggability of these proteins and indicates their potential as drug targets for the treatment of disease. Additionally, the binding between these proteins and the drugs could also probably indicate their involvement in the mechanism of action of the drugs. Such mechanism might entail inhibition of the drugs, which is exhibited computationally through the efficiency of docking between proteins and ligands, and largely depends upon the binding energy. Through molecular simulation studies, we have observed the stability in the binding energy of the target-ligand complexes and consistency of their interacting residues.

We therefore gain an insight into the ligand specificity of a protein which depends on the consistently binding active site residues of the target proteins. Thus, the homology models of SicA, DnaK, SigE, SsrA, SsrB, EnvZ, and OmpR were used for further docking studies (**Table 1**). Among the selected drugs *viz.* 19 typhoid related, 15 non-typhoidal, and 7 Hsp70 modulators, some do not obey Lipinski's rule of 5 but are still in the market and thus, were further considered for drug repositioning (**Tables 2**, **3**). Blind docking was performed for all the chaperones and TCS proteins. This was done to avoid any bias of predictive binding sites of homology modeled proteins and yet, eventually confirm the binding pockets through the same binding residues of each different ligands at the same site, yielding good binding energy against each chaperone and TCS protein. To confirm the binding pocket with the same residues of interaction, loop docking was performed with 35 conformations. To this end, structural alignment of the pockets was also performed for chaperone and TCS proteins against the selected pockets (**Supplementary Figure 1**). The structural

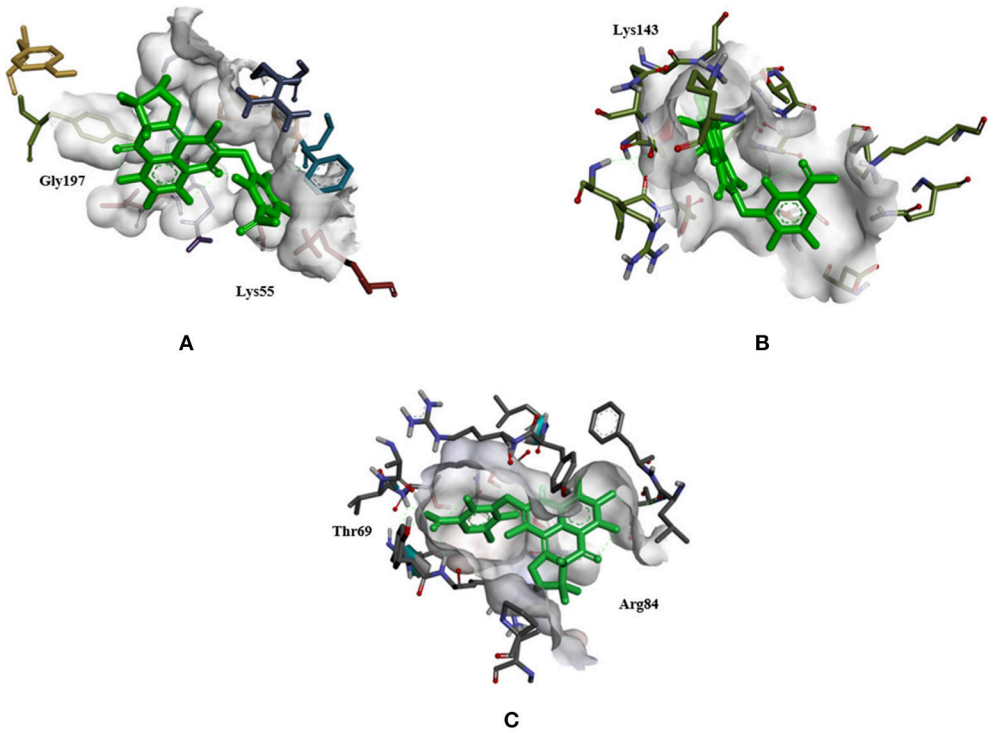

FIGURE 3 | The best docked complex of DnaK, SicA, and SigE with XR770, a histidine kinase inhibitor. **(A)** DnaK with XR770, interacts with −8.76 binding energy, the target residues being Gly197 and Lys55. **(B)** SicA with XR770, interacts with −9.78 binding energy, the target residue being Lys143. **(C)** SigE with XR770, interacts with −11.48 binding energy, the target residues being Thr69 and Arg84.

TABLE 7 | Representative parametric values for predocked and postdocked conformations with respect to temperature, potential energy, pressure and RMSD.

Protein 3D structure (predocked)	Temperature (300K)	Potential energy(Kcal/mol)	Pressure (bar)	RMSD (A^0)
SicA	298	−2942.36	130.0	1.15
DnaK	299	−2761.78	139.2	1.21
SigE	298	−2789.245	125	1.17
Protein-ligand complex (postdocked)	**Temperature (300K)**	**Potential energy(Kcal/mol)**	**Pressure (bar)**	**RMSD (A^0)**
SicA-XR770	299	−2301.36	145.5	1.32
DnaK–XR770	296	−2263.78	160.10	1.19
SigE–XR770	298	−2298.245	170	1.26

alignment results showed the proper fitting of the pockets as each protein has the same binding site, though the sequence length varies from protein to protein. However, the docking sites of each proteins are different, making it difficult to interpret the difference between them emerging from the structural alignment of the proteins (**Supplementary Figure 1**).

To have an insight of the same, the most effective conformation, with the highest binding energy for every ligand, was chosen from 30 assigned iterations with the formation of hydrogen bonds between the ligand and protein. Our docking results with XR770 showed hydrogen bond formation with Lys143 of SicA having −9.78 kcal/mol binding energy. Moreover, hydrogen bonds with Lys55 and Gly197 of DnaK (−8.76 kcal/mol) and those with Arg84 and Thr69 of SigE (−11.48 kcal/mol) were observed in *S.* Typhimurium (**Figure 3**). Similarly, *S.* Typhi showed hydrogen bond interactions with Arg61, Gln86, and Lys89 of SicA, Arg167, Asp388, and Ile418 of DnaK and Ala74 of SigE, with respective binding energies of −9.85, −9.57, and −7.35 kcal/mol (**Tables 4**, **5**). These interacting residues showed consistency and thus, ligand specificity, conferring highest binding energy from the available conformations. Notably, XR770, Sitafloxacin and Compound 1 topped the best in the individual set amongst the three sets of drugs i.e., 19 typhoid related, 15 non-typhoidal, and 7 Hsp70 modulators, respectively. Again, XR587 showed comparatively slightly less binding energy than XR770, which has the probability

to show better results if explored against different selected targets. Even though functions of some of the non-typhoidal drugs are unknown (**Supplementary Table 2**), they show interaction against the selected proteins with lower binding energies compared to XR770. We have also incorporated pharmacophore based prediction to analyse the common features that reveal the activity of the drugs. However, pharmacophore based screening was not performed because our objective was to check the available marketed typhoidal and non-typhoidal drugs against the target proteins selected i.e., chaperone and TCS. The common pharmacophore features for the best binding drugs are shown in **Supplementary Figure 6**. These observations might help us to delineate the broader perspective of typhoid drug repositioning by either considering XR770 with the fused phenaleno-furanone moiety as the repurposed ligand or the chaperone proteins like SicA, DnaK, and /or SigE as the network based new targets and pose them for experimental studies for revealing potential side-effects, if any.

To determine the efficacy of inhibition, a comparative account of the aforementioned binding patterns of XR770 showed it to be conferring the greatest binding affinity among the selected anti-typhoid drugs, like Amoxicillin and Ciprofloxacin (**Table 2**). In fact, resistance to the approved drugs, like Amoxicillin and Ciprofloxacin, in systemic infection, has been known in patients with typhoid and diarrhea (Cui et al., 2008). Besides, these drugs are also known to cause many unpleasant side effects, such as stomach pain, nausea, vomiting, vaginal itching or discharge, headache etc. (Leegaard et al., 1996). The toxicity for patients against typhoidal and non-typhoidal drugs is given in **Supplementary Tables 3**, **4**.

Notably, XR770 in comparison to other drugs in this study showed more consistent amino acid residues and highest binding affinity toward the target proteins. Moreover, the greater number of hydrogen bonding formed suggests more stability of the binding interactions as are also conceived through molecular dynamics simulation. Furthermore, in order to address the issue about specificity, the parameters like relatively high difference in binding energy and binding to specific active site residues in the protein has been considered to project XR770 as the potential candidate.

Pertaining to the above results observed, thus, proving the effectiveness of the aforementioned selected proteins as drug targets could be the real challenge. To cater to this need, we have incorporated other known virulent TCS proteins of *Salmonella* to be compared with the chaperones. In all the cases, XR770 turned out to be the promising chemical ligand in inhibiting the selected targets *viz*. SicA, DnaK, SigE, SsrA, SsrB, EnvZ, and OmpR. Based on the least energy score, best docked complex was compared with the interaction pattern of XR770. Comparative study of docking interaction pattern of the above listed proteins was also performed in *Salmonella* typhi as well as shown in **Supplementary Table 1** which revealed similar results.

Potency of a drug does not depend solely on its overall binding affinity with the target(s). On the contrary, it is a result of the complex interaction of the drug binding efficacy, namely the ability of the drug to exhibit a biological response upon interaction with the target protein. This interaction may be an agonist or antagonist depending on the physiological response. Based on the docking energy scores and ADME properties, it was found that XR770 has lower energy scores revealing higher binding affinity toward the active site. The binding follows Lipinski's rule of five with a little higher molecular weight which is acceptable when compared to several marketed drugs.

The binding free energies for the stable protein-ligand complexes with XR770 for SicA, DnaK, and SigE were −2301.36, −2263.78, and −2298.245 kJ mol^{-1}, which also denote stability with respect to temperature and pressure (**Supplementary Figure 5** and **Table 7**). The results of the MD simulation run clearly indicated that these protein-ligand complexes were held together by strong intermolecular non-covalent forces. These strong binding interactions between the XR770 and chaperone proteins make the complexes highly stable and fit for possible involvement in various reactions (**Supplementary Figure 4**).

Despite having such exemplary computational binding activities against the chaperone and TCS proteins, it is worthwhile to mention that XR770 has been reported to have only inhibitory effect on NRII (or NtrB) histidine kinase from *E. coli* but no effect is reported for the whole cell bacteria (Chrystal et al., 2007; Bem et al., 2014). However, in the absence of proper knowledge of the assay done to check for the activity of XR770, it can be considered as the main caveat of this study.

CONCLUSION

From our study, chaperone proteins SicA, DnaK, and SigE along with the TCS proteins SsrA SsrB, EnvZ, and OmpR have been demonstrated to be potential druggable targets for the new phenaleno-furanone based ligand XR770.Thus, XR770 confers high binding affinity toward all the target proteins with a binding affinity comparable to the approved drugs. Hence, XR770 might prove to be potent inhibitor for the chaperone proteins. However, pharmacological studies are required to confirm the inhibitory activity of XR770 against the chaperones as effective drug targets.

AUTHOR CONTRIBUTIONS

CL conceived the concepts, planned, and designed the layout of the work. The work was conducted by SM under the primary supervision of CL with additional supervisory input from DG. Figures were created by SM. SM wrote the paper, with textual revisions by CL and DG.

ACKNOWLEDGMENTS

The authors wish to acknowledge the support from Department of Biological Sciences at Sunway University, Malaysia for the provision of computational facilities.

SUPPLEMENTARY MATERIAL

The Supplementary Material for this article can be found online at: https://www.frontiersin.org/articles/10.3389/fcimb.2018.00402/full#supplementary-material

REFERENCES

Aubé, J. (2012). Drug repurposing and the medicinal chemist. *ACS Med. Chem. Lett.* (2012) 3, 442–444. doi: 10.1021/ml300114c

Bem, A. E., Velikova, N., Pellicer, M. T., Baarlen, P. V., Marina, A., and Wells, J. M. (2014). *Bacterial histidine* kinases as novel antibacterial drug targets. *ACS Chem. Biol.* 10, 213–224. doi: 10.1021/cb5007135

Bowie, J. U., Luthy, R., and Eisenberg, D. (1991). A method to identify protein sequences that fold into a known three-dimensional structure. *Science* 253, 164–170.

Calderwood, S. K., Stevenson, M. A., and Murshid, A. (2012). Heat shock proteins, autoimmunity, and cancer treatment. *Autoimmune Dis.* 2012:486069. doi: 10.1155/2012/486069

Chiappori, F., Fumian, M., Milanesi, L., and Merelli, I. (2015). DnaK as antibiotic target: hot spot residues analysis for differential inhibition of the bacterial protein in comparison with the human HSP70. *PLoS ONE* 10:e0124563. doi: 10.1371/journal.pone.0124563

Chrystal, E. J., Wrigley, S. K., Thomas, R., Nicholson, N., and Hayes, M. (eds.). (2007). *Biodiversity: New Leads for the Pharmaceutical and Agrochemical Industries*. Cambridge, UK: Royal Society of Chemistry.

Csizmadia, P. (1999). "MarvinSketch and MarvinView: molecule applets for the World Wide Web," in *Proceedings of ECSOC-3, the Third International Electronic Conference on Synthetic Organic Chemistry, September 1a30* (Basel), 367–369.

Cui, S., Li, J., Sun, Z., Hu, C., Jin, S., Guo, Y., et al. (2008). Ciprofloxacin-resistant *Salmonella enterica* serotype Typhimurium, China. *Emerg. Infect. Dis.* 14:493. doi: 10.3201/eid1403.070857

Darwin, K. H., and Miller, V. L. (2001). Type III secretion chaperone-dependent regulation: activation of virulence genes by SicA and InvF in Salmonella typhimurium. *EMBO J.* 20, 1850–1862. doi: 10.1093/emboj/20.8.1850

Darwin, K. H., Robinson, L. S., and Miller, V. L. (2001). SigE is a chaperone for the *Salmonella enterica* serovar Typhimurium invasion protein SigD. *J. Bacteriol.* 183, 1452–1454. doi: 10.1128/JB.183.4.1452-1454.2001

Dundas, J., Ouyang, Z., Tseng, J., Binkowski, A., Turpaz, Y., and Liang, J. (2006). CASTp: computed atlas of surface topography of proteins with structural and topographical mapping of functionally annotated residues. *Nucleic Acids Res.* 34(Suppl. 2), W116–W118. doi: 10.1093/nar/gkl282

Fink, A. L. (1999). Chaperone-mediated protein folding. *Physiol. Rev.* 79, 425–449. doi: 10.1152/physrev.1999.79.2.425

Friesner, R. A., Murphy, R. B., Repasky, M. P., Frye, L. L., Greenwood, J. R., Halgren, T. A., et al. (2006). Extra precision glide: Docking and scoring incorporating a model of hydrophobic enclosure for protein– ligand complexes. *J. Med. Chem.* 49, 6177–6196. doi: 10.1021/jm051256o

Hansson, T., Oostenbrink, C., and van Gunsteren, W. (2002). Molecular dynamics simulations. *Curr. Opin. Struct. Biol.* 12, 190–196. doi: 10.1016/S0959-440X(02)00308-1

Kaur, S. P., Rao, R., and Nanda, S. (2011). Amoxicillin: a broad spectrum antibiotic. *Int. J. Pharm. Pharm. Sci.* 3, 30–37.

Kelley, L. A., Mezulis, S., Yates, C. M., Wass, M. N., and Sternberg, M. J. (2015). The Phyre2 web portal for protein modeling, prediction and analysis. *Nat. Protoc.* 10:845. doi: 10.1038/nprot.2015.053

Kitchen, D. B., Decornez, H., Furr, J. R., and Bajorath, J. (2004). Docking and scoring in virtual screening for drug discovery: methods and applications. *Nat. Rev. Drug Discov.* 3:935. doi: 10.1038/nrd1549

Lahiri, C., Pawar, S., Sabarinathan, R., Ashraf, M. I., Chand, Y., and Chakravortty, D. (2014). Interactome analyses of Salmonella pathogenicity islands reveal SicA indispensable for virulence. *J. Theor. Biol.* 363, 188–197. doi: 10.1016/j.jtbi.2014.08.013

Leegaard, T. M., Van Gestel, M. H., Petit, P. L. C., and Van De Klundert, J. A. M. (1996). Antibiotic resistance mechanisms in Salmonella species causing bacteraemia in Malawi and Kenya. *Apmis* 104, 302–306. doi: 10.1111/j.1699-0463.1996.tb00721.x

Liberek, K., Lewandowska, A., and Zietkiewicz, S. (2008). Chaperones in control of protein disaggregation. *EMBO J.* 27, 328–335. doi: 10.1038/sj.emboj.7601970

March-Vila, E., Pinzi, L., Sturm, N., Tinivella, A., Engkvist, O., Chen, H., et al. (2017). On the integration of *in silico* drug design methods for drug repurposing. *Front. Pharmacol.* 8:298. doi: 10.3389/fphar.2017.00298

Morris, G. M., Huey, R., Lindstrom, W., Sanner, M. F., Belew, R. K., Goodsell, D. S., et al. (2009). AutoDock4 and AutoDockTools4: automated docking with selective receptor flexibility. *J. Comput. Chem.* 30, 2785–2791. doi: 10.1002/jcc.21256

Neckers, L., and Tatu, U. (2008). Molecular chaperones in pathogen virulence: emerging new targets for therapy. *Cell Host Microbe* 4, 519–527. doi: 10.1016/j.chom.2008.10.011

Pan, A., Lahiri, C., Rajendiran, A., and Shanmugham, B. (2015). Computational analysis of protein interaction networks for infectious diseases. *Brief. Bioinformatics* 17, 517–526. doi: 10.1093/bib/bbv059

Patury, S., Miyata, Y., and Gestwicki, J. E. (2009). Pharmacological targeting of the Hsp70 chaperone. *Curr. Top. Med. Chem.* 9, 1337–1351. doi: 10.2174/156802609789895674

Rangel-Vega, A., Bernstein, L. R., Mandujano Tinoco, E. A., García-Contreras, S. J., and García-Contreras, R. (2015). Drug repurposing as an alternative for the treatment of recalcitrant bacterial infections. *Front. Microbiol.* 6:282. doi: 10.3389/fmicb.2015.00282

Schwede, T., Kopp, J., Guex, N., and Peitsch, M. C. (2003). SWISS-MODEL: an automated protein homology-modeling server. *Nucleic Acids Res.* 31, 3381–3385. doi: 10.1093/nar/gkg520

Shattuck, T. W. (2011). *Colby College Molecular Mechanics Exercises MOE (Molecular Operating Environment) Exercises.* Montreal, QC: Chemical Computing Group ULC.

Sivakumar, D., Lahiri, C., and Chakravortty, D. (2013). Computational studies on histidine kinase protein BaeS to target multidrug-resistant Salmonella. *Med. Chem. Res.* 22, 1804–1811. doi: 10.1007/s00044-012-0188-6

Sousa, S. F., Fernandes, P. A., and Ramos, M. J. (2006). Protein–ligand docking: current status and future challenges. *Proteins Struct. Funct. Bioinformatics* 65, 15–26. doi: 10.1002/prot.21082

Trott, O., and Olson, A. J. (2010). AutoDock Vina: improving the speed and accuracy of docking with a new scoring function, efficient optimization, and multithreading. *J. Comput. Chem.* 31, 455–461. doi: 10.1002/jcc.21334

Tucker, S. C., and Galán, J. E. (2000). Complex function for SicA, a *Salmonella enterica* serovar typhimurium type III secretion-associated chaperone. *J. Bacteriol.* 182, 2262–2268. doi: 10.1128/JB.182.8.2262-2268.2000

Wishart, D. S., Feunang, Y. D., Guo, A. C., Lo, E. J., Marcu, A., Grant, J. R., et al. (2017). DrugBank 5.0: a major update to the DrugBank database for 2018. *Nucleic Acids Res.* 46, D1074–D1082. doi: 10.1093/nar/gkx1037

Zaidi, M. B., Calva, J. J., Estrada-Garcia, M. T., Leon, V., Vazquez, G., Figueroa, G., et al. (2008). Integrated food chain surveillance system for Salmonella spp. in Mexico. *Emerg. Infect. Dis.* 14:429. doi: 10.3201/eid1403.071057

Zhang, Y. (2008). I-TASSER server for protein 3D structure prediction. *BMC Bioinformatics* 9:40. doi: 10.1186/1471-2105-9-40

Zügel, U., and Kaufmann, S. H. (1999). Role of heat shock proteins in protection from and pathogenesis of infectious diseases. *Clin. Microbiol. Rev.* 12, 19–39.

Conflict of Interest Statement: The authors declare that the research was conducted in the absence of any commercial or financial relationships that could be construed as a potential conflict of interest.

frontiers in Cellular and Infection Microbiology

ORIGINAL RESEARCH
published: 04 January 2019
doi: 10.3389/fcimb.2018.00438

Repurposing Screen Identifies Unconventional Drugs With Activity Against Multidrug Resistant *Acinetobacter baumannii*

*Yu-Shan Cheng[1], Wei Sun[1], Miao Xu[1], Min Shen[1], Mozna Khraiwesh[2], Richard J. Sciotti[2] and Wei Zheng[1]**

[1] National Center for Advancing Translational Sciences, National Institutes of Health, Bethesda, MD, United States,
[2] Experimental Therapeutics Branch, Walter Reed Army Institute of Research, Silver Spring, MD, United States

Antibiotic-resistant nosocomial infections are an emerging public health issue; carbapenem-resistant gram-negative bacteria such as *Acinetobacter baumannii* are among the pathogens against which new therapeutic agents are desperately needed. Drug repurposing has recently emerged as an alternative approach to rapidly identifying effective drugs and drug combinations to combat drug resistant bacteria. We performed a drug repurposing screen against a highly virulent, multidrug resistant, *Acinetobacter baumannii* strain AB5075. This strain, isolated from a patient, is resistant to 25 first-line antibiotics for gram-negative bacteria. A compound screen using a bacterial growth assay led to identification and confirmation of 43 active compounds. Among these confirmed compounds, seven are approved drugs or pharmacologically active compounds for non-antimicrobial indications. Three of these drugs, 5-fluorouracil, fluspirilene, and Bay 11-7082 resensitized strain AB5075 to azithromycin and colistin in a two-drug combination format. The approach using a drug repurposing screen with a pathogen sample isolated from a patient and a high throughput bacterial growth assay led to the successful identification of new drug combinations to overcome a multidrug resistant bacterial infection.

Keywords: *Acinetobacter baumannii*, multidrug resistance, drug repositioning, drug repurposing screen, synergistic drug combination, nosocomial infections, non-antimicrobial drugs

OPEN ACCESS

Edited by:
Rodolfo García-Contreras, National Autonomous University of Mexico, Mexico

Reviewed by:
Attilio Vittorio Vargiu, Università degli Studi di Cagliari, Italy
Bernardo Franco, Universidad de Guanajuato, Mexico

***Correspondence:**
Wei Zheng
wzheng@mail.nih.gov

Specialty section:
This article was submitted to Clinical Microbiology, a section of the journal Frontiers in Cellular and Infection Microbiology

Received: *14 August 2018*
Accepted: *10 December 2018*
Published: *04 January 2019*

Citation:
Cheng Y-S, Sun W, Xu M, Shen M, Khraiwesh M, Sciotti RJ and Zheng W (2019) Repurposing Screen Identifies Unconventional Drugs With Activity Against Multidrug Resistant Acinetobacter baumannii. Front. Cell. Infect. Microbiol. 8:438. doi: 10.3389/fcimb.2018.00438

INTRODUCTION

The emergence and dissemination of drug-resistant bacterial infections are a public health issue. *Acinetobacter baumannii* is one of the major causes for the nosocomial infections in critically ill patients. Treatment of *Acinetobacter baumannii* can be extremely difficult, especially for the carbapenem resistant strains. Colistin and tigecycline are the last resorts for carbapenem resistant *Acinetobacter baumannii*. However, colistin and tigecycline resistant strains have been reported worldwide (Deng et al., 2014; Oikonomou et al., 2015). In light of the rapid expansion of imipenem resistance in 35 countries, increasing from 24 to 74% in just 11 years (Xie et al., 2018), the development of novel drugs to combat *Acinetobacter baumannii* infections is an urgent need.

Antibiotic development mainly relies on two strategies, a target-based approach and isolation of bioactive secondary metabolites from microorganisms (Demain, 1999; Marinelli, 2009). New antibiotic drug development is a long-term process; for example, a target-based method takes time to go through the steps of target selection, lead discovery and optimization, preclinical

development, then clinical trials before the FDA gives approval for marketing for a new indication. Drug repurposing and drug combinations have emerged as promising alternative approaches to provide novel therapeutic options for multidrug resistant bacteria (Zheng et al., 2018). Drug repurposing of approved drugs bypasses the need for novel molecules in nature or from a synthetic chemical library, and alleviates the need for preclinical development and phase I clinical trials as the data for pre-clinical experiments, human pharmacokinetics, and drug safety are already established. Thus, drug repurposing accelerates the drug development process and reduces the development costs. In addition, drug combination therapy with a synergistic effect of two or three drugs in combination can overcome drug resistance by inhibiting multiple targets and reducing occurrence of further drug resistance.

A multidrug resistant *Acinetobacter baumannii* clinical isolate, *Acinetobacter baumannii* 5075 (AB5075) (Jacobs et al., 2014), was used in this study. Strain AB5075 was first isolated from the osteomyelitis of a patient's tibia bone in 2008. The detailed genomic analysis of AB5075 in 2015 unveiled some antibiotic resistant mechanisms (Gallagher et al., 2015). Briefly, AB5075 carries 133 genes that likely cause resistance to broad-spectrum β-lactams (for example, penicillins, cephalosporins, and carbapenems), aminoglycosides, chloramphenicol, quinolones, tetracycline, trimethoprim, sulfonamides, macrolides, and other toxic agents. We report here the identification of seven non-antimicrobial drugs that suppressed AB5075 growth *in vitro* by a drug repurposing screen using the AB5075 strain. The results demonstrate the usefulness of a drug repurposing screen using patient derived pathogens. These newly identified compounds with inhibitory activities against multidrug resistant *Acinetobacter baumannii* can be further studied for use as new therapeutic agents.

MATERIALS AND METHODS

Materials

Tigecycline was obtained from Chem-Impex International (Wood Dale, IL, USA). Doripenem and ertapenem were acquired from Cayman Chemical (Ann Arbor, MI, USA) and TOKU-E (Bellingham, WA, USA), respectively. Other chemicals were purchased from Sigma-Aldrich (St. Louis, MO, USA).

Preparation of Bacterial Stock for High Throughput Screen

Acinetobacter baumannii 5075 (AB5075) was obtained from Walter Reed Army Institute of Research. Individual colonies on agar plates were cultured in tryptic soy broth (TSB, Remel, Thermo Scientific, Waltham, MA, USA) at 37°C. The bacterial cultures were mixed with sterile glycerol in a 9:1 ratio when the optical density at 600 nm (OD_{600}) reached about 0.25–0.3. Bacteria in 10% glycerol were stored in aliquots at −80°C.

Bacterial Growth Experiments

Bacteria were thawed from −80°C and diluted to a desire initial density from 1:200 to 1:1,000 in TSB. Each bacterial culture was grown in TSB at 37°C, 5% CO_2 humidified atmosphere for 2–48 h. Bacterial growth was monitored by measuring the OD_{600} in a PHERAstar plate reader (BMG Labtech, Cary, NC, USA).

Compound Library

A pharmacologically active compound library (LOPAC 1280) was purchased from Sigma-Aldrich (St. Louis, MO, USA). The NCATS Pharmaceutical Collection (NPC) of approved and investigational drug collection was generated in house (Huang et al., 2011). The NPC library consists of 2,816 small molecule compounds, 38.4% approved by U.S. FDA, 22.5% approved in the EU, Canada, or Japan, and 39.0% being used in clinical trials or as research compounds.

Compound Screening and Validation

A quantitative high throughput screen (qHTS) and confirmation assays were performed as previously described in a 1,536-well format (Sun et al., 2016). Briefly, 2.5 μL TSB was first loaded into each well of a black clear bottom microplate by a Multidrop Combi dispenser (Thermo Fisher Scientific, Waltham, MA, USA). An automated pintool station (WAKO Scientific Solutions, San Diego, CA) was then used to transfer 23 nL of compounds from compound plates into assay plates. For the primary screen, each compound was tested at four concentrations. Compound plates were prepared by an Evolution P^3 system (PerkinElmer, Wellesley, MA) as described in a previous publication (Inglese et al., 2006). In the follow-up confirmation assays, dose-effects of the carefully selected compounds were examined as an intraplate 11-point, 3-fold dilution series. Each compound was tested in three biological replicates. Dimethyl sulfoxide (DMSO) served as a negative control and 46 μM of rifampin was the positive control. Bacterial stock diluted in TSB at a ratio 1:500 was added at 2.5 μL/well to make a 1:1000 dilution of initial inoculum density. The assay plates were incubated at 37°C for 20–22 h and placed onto a PHERAstar plate reader (BMG Labtech, Cary, NC, USA) to detect the bacterial growth in response to OD_{600}.

Two Drug Combination Assays

In two drug combination assays, non-antimicrobial drugs (drug 1) resulting from the qHTS were tested in combination with an 11-concentration series of 25 standard treatment drugs (drug 2). The screen was conducted in the same procedure as for qHTS except the TSB media was mixed with drug 1 prior to loading into the assay plates. The final concentrations of drug 1 were one-fourth and one-eighth of the calculated half-maximal inhibitory concentration (IC_{50}) values. The dose-effect curve of drug 2 as a single agent or with a fixed concentration of drug 1 were calculated. A significant synergistic response was defined as a three-fold decrease in IC_{50}. Drug pairs that showed a synergistic response were further validated in a 96-well plate.

Statistics and Data Analysis

The qHTS analysis was designed internally to include three steps: normalization, pattern correction, and curve fitting. Raw plate

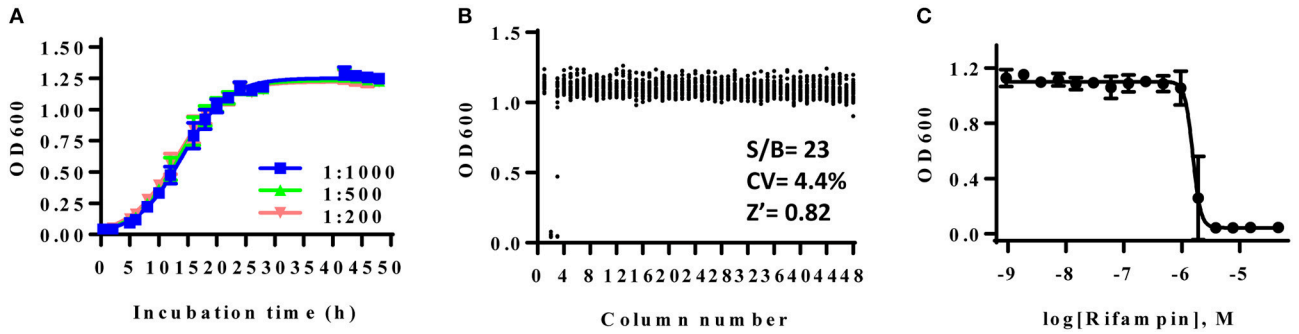

FIGURE 1 | (A) Growth curve of AB5075 in 1536-well plate. AB5075 stock solution was diluted to different starting ratios and incubated at 37°C. Data points represent the mean, and the error bars represent the standard deviation (SD); $n = 128$. **(B)** Scatter plot of the results from a DMSO plate screening. The wells in column 2 of the 1536-well assay plate contained 46 μM rifampin as a positive control (0% viability); the wells in column 3 contained varying doses of rifampin at 1:3 dilution. The wells in the rest of plate contained DMSO as a negative control (100% viability). The signal-to-basal ratio (S/B) in this plate was 23-fold, with a coefficient of variation (CV) of 4.4%, and a Z′ factor of 0.82. **(C)** Dose–response curves for rifampin from column 3. The data points represent the mean, and the error bars represent the SD; $n = 2$.

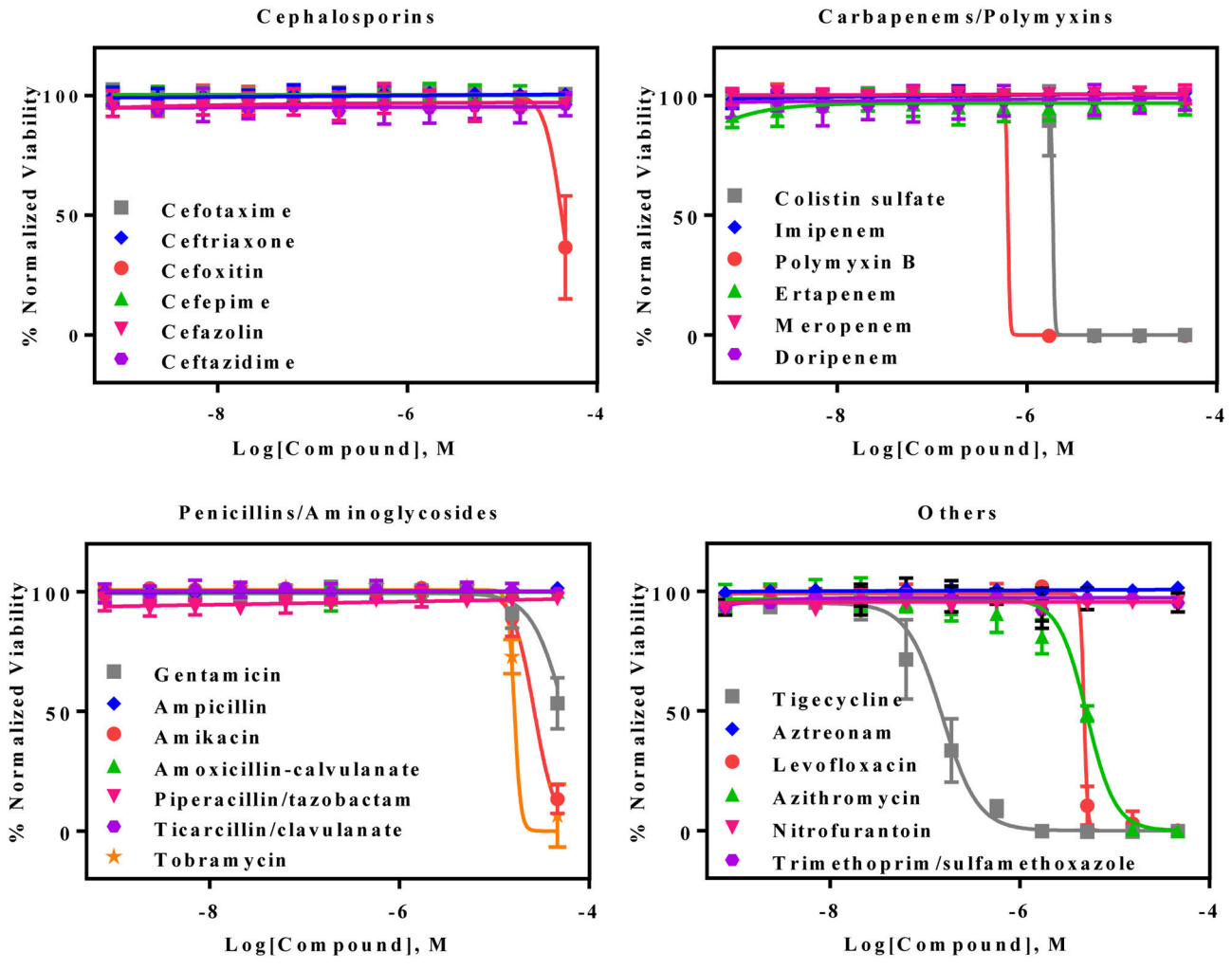

FIGURE 2 | Concentration–response curves of the inhibition of AB5075 growth by 25 standard antibiotics. Data points represent mean, and error bars represent the SD; $n = 3$.

reads were first normalized to relative controls (such that DMSO alone was considered as 100% viability and 46 μM rifampin as 0% viability) using the following equation: % normalized viability = $[(V_{compound} - V_{positive})/(V_{DMSO} - V_{positive})] \times 100$. Next the data underwent a pattern-correction based on information from a DMSO-alone plate. Interplate dose-response data of each compound was processed by a four-parameter Hill equation based grid algorithm to yield the IC_{50}, the maximum response, and the curve class (Wang et al., 2010). IC_{50} and IC_{90} values in the confirmation experiments were calculated with Prism 7 software (GraphPad Software, Inc. San Diego, CA, USA).

RESULTS

Assay Optimization for the High Throughput Bacterial Growth Assay

The high throughput bacterial growth assay (Sun et al., 2016) were adapted to examine antibiotic susceptibility for AB5075. The growth kinetics of AB5075 was monitored in a 1536-well plate format to determine the optimal inoculum density and incubation time. Measurement of OD_{600} of assay plates, reflecting the bacterial growth rate, was recorded at various time points over 48 h (**Figure 1A**). A classical growth kinetic pattern was observed encompassing lag, exponential, and stationary phases; the growth reached stationary phase at 24 h. As suggested by the antimicrobial susceptibility testing guideline for *Acinetobacter* spp. from the Clinical and Laboratory Standards Institute (CLSI), experimental endpoints were setting at 22–24 h for the following studies. All bacterial stock dilutions used for inoculum showed similar signal-to-basal ratios of ∼26-fold. The dilution of 1:1,000 was chosen for use in further experiments.

The DMSO alone plate was used to account for well to well variation. Rifampin was selected to serve as the positive control compound in the experiments. The calculated signal-to-basal ratio was 23-fold, the coefficient of variation (CV) was 4.4%, and the Z′ factor was 0.82, indicating a robust assay for high

TABLE 1 | IC_{50} and MIC data for standard care antibiotics against AB5075.

Antibiotics	IC_{50}	IC_{90}	Reported MIC		Breakpoints for resistance	
Unit	μM	μM	μg/ml	μM	μg/ml	μM
Carbapenems						
Doripenem	>46	>46			2	4.8
Imipenem	>46	>46	8	25.2	2	6.3
Ertapenem	>46	>46			N/A	
Meropenem	>46	>46			2	4.6
Penicillins						
Amoxicillin-clavulanate	>46	>46	≥32	≥87.6	N/A	
Ampicillin	>46	>46	≥32	≥86.2	16	43.1
Ticarcillin-clavulanate	>46	>46			16/2	41.6
Piperacillin-tazobactam	>46	>46	≥128	≥247.3	16/4	30.9
Cephalosporins						
Cefazolin	>46	>46	≥64	≥140.8	N/A	
Cefepime	>46	>46	≥64	≥112.0	8	14.0
Cefotaxime	>46	>46	≥64	≥134.1	8	16.8
Cefoxitin	42.0	66.5	≥64	≥142.4	N/A	
Ceftazidime	>46	>46	≥64	≥100.5	8	12.6
Ceftriaxone	>46	>46	≥64	≥96.7	8	12.1
Aminoglycosides						
Amikacin	26.3	46.8			16	20.5
Gentamicin	54.8	>46	≥16	≥10.8	4	2.7
Tobramycin	16.3	39.4	2	4.3	4	8.6
Polymyxins						
Polymyxin B	0.63	0.69			2	1.4
Colistin sulfate	1.9	2.0			2	1.6
Macrolide						
Azithromycin	5.1	10.8				2.5
Quinolones						
Levofloxacin	4.7	5.2	4–8	11.1–22.1	2	5.4
Folate Pathway Inhibitors						
Trimethoprim-sulfamethoxazole	>46	>46	≥320	≥1102.2	2/38	6.9
Glycylcycline						
Tigecycline	0.15	0.39	≤0.5	≤0.85	N/A	
Other						
Aztreonam	>46	>46	≥64	≥147.0	N/A	
Nitrofurantoin	>46	>46	≥512	≥2149.8	N/A	

throughput screening (**Figure 1B**). The calculated IC_{50} value of rifampin against AB5075 was 0.40 μM (**Figure 1C**).

Activities of Standard Care Antibiotics Against AB5075 Strain

The AB5075 growth assay was evaluated with a set of 25 antibiotics commonly used for infections by gram negative bacteria. Nine compounds showed concentration-dependent inhibition of AB5075 growth including tigecycline, two polymyxins (polymyxin B and colistin sulfate), levofloxacin, azithromycin, three aminoglycosides (amikacin, gentamicin, and tobramycin) and cefoxitin (**Figure 2**, **Table 1**). Among these active antibiotics, tigecycline was the most potent compound with an IC_{50} of 0.15 μM. The other 16 antibiotics were not active (i.e., IC_{50} > 46 μM) against the multidrug resistant AB5075 strain.

Repurposing Screen Using LOPAC and NPC Library

The primary screen assessed 4,096 approved drugs and bioactive compounds to identify compounds inhibiting the growth of AB5075 (**Figure 3A**). Each compound was tested at four concentrations (4.1, 9.2, 20.6, and 46 μM) in the primary screen. The primary hits were selected based on an IC_{50} below 30 μM and an efficacy (maximum inhibition) >70%. Fifty-two compounds meeting these criteria were selected and retested, resulting in 43 confirmed compounds, an 83% confirmation rate (**Table 2**). These confirmed compounds include 30 antibacterial, 2 antifungal, 4 antiseptic, 3 antineoplastic, and 4 other agents (**Figure 3B**). Tetracycline and its analogs were the most potent compounds identified with IC_{50} values of 0.045–0.47 μM. Among the confirmed compounds, seven were drugs categorized as non-antimicrobial agents (**Figure 3C**, **Table 3**).

Synergistic Drug Combinations of Newly Identified Non-antimicrobial Compounds and Standard Care Antibiotics

A drug combination of a standard care antibiotic agent with a newly identified compound from the above confirmed compounds (non-antimicrobial agents) was screened using the same AB5075 growth assay. After additional testing of these individual compounds with 25 standard care antibiotic

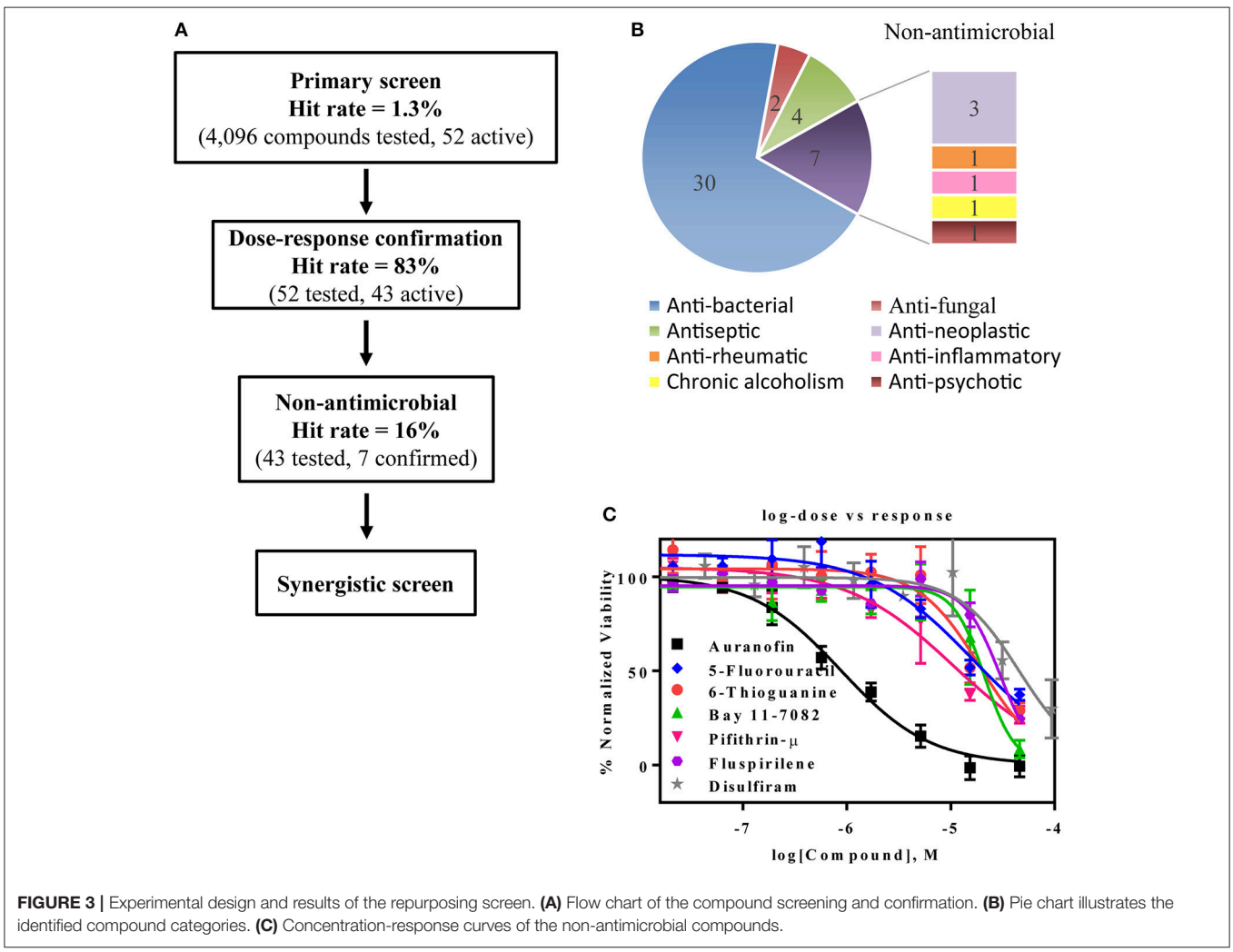

FIGURE 3 | Experimental design and results of the repurposing screen. **(A)** Flow chart of the compound screening and confirmation. **(B)** Pie chart illustrates the identified compound categories. **(C)** Concentration-response curves of the non-antimicrobial compounds.

TABLE 2 | Antagonists identified in the qHTS.

Drug name	IC_{50} (μM)	Maximum response	Primary action
Doxycycline HCl	0.045	109	Antibacterial
Minocycline HCl	0.094	112	Antibacterial
Demeclocycline HCl	0.13	94	Antibacterial
Methacycline HCl	0.13	84	Antibacterial
Sancycline	0.14	104	Antibacterial
Rifampicin	0.45	100	Antibacterial
Tetracycline HCl	0.47	91	Antibacterial
Thimerosal	0.53	92	Antiseptic and germicides
Triclosan	0.93	90	Antibacterial
Auranofin	1.09	106	Antirheumatic
Gatifloxacin	1.37	105	Antibacterial
Sitafloxacin	1.43	97	Antibacterial
Novobiocin sodium	1.53	107	Antibacterial
Diphenyleneiodonium chloride	1.97	101	Antibacterial
Phenylmercuric acetate	2.77	99	Antifungal in agriculture
Sparfloxacin	3.64	106	Antibacterial
Trovafloxacin mesylate	4.18	102	Antibacterial
Erythromycin propionate	4.35	110	Antibacterial
Enrofloxacin	4.88	99	Antibacterial
Malachite green oxalate	5.07	101	Antiseptic in veterinary
Marbofloxacin	5.54	94	Antibacterial
Nitroxoline	5.79	108	Antibacterial
Nitromersol	5.90	94	Antiseptic and disinfectant.
Pifithrin-mu	7.24	82	Antineoplastic (p53 inhibitor)
Chloroxine	7.29	96	Antibacterial
5-Fluorouracil	7.29	79	Antineoplastic
Grepafloxacin HCl	8.03	96	Antibacterial
Ticlatone	8.45	88	Antifungal
Azithromycin dihydrate	8.71	117	Antibacterial
Moxifloxacin HCl	9.35	105	Antibacterial
Garenoxacin mesylate hydrate	9.38	96	Antibacterial
Ofloxacin	9.66	100	Antibacterial
Difloxacin HCl	11.34	117	Antibacterial
Fusidic acid sodium	11.34	124	Antibacterial
6-Thioguanine	11.98	77	Antineoplastic
Tosufloxacin toluenesulfonic acid	14.54	76	Antibacterial
Dipyrithione	16.86	111	Fungicidal and bactericidal
Nadifloxacin	17.30	95	Antibacterial
Alatrofloxacin mesylate	18.06	103	Antibacterial
Fluspirilene	22.74	77	Antipsychotic
Bay 11-7082	23.57	99	Anti-inflammatory
Alexidine dihydrochloride	29.02	111	Antibacterial
Disulfiram	30.08	81	Chronic alcoholism

therapies, three promising drug combination pairs with a synergistic effect against the drug resistant AB5075 strain were identified, including azithromycin/5-fluorouracil, colistin sulfate/fluspirilene, and colistin sulfate/Bay 11-7082. The synergistic effects of all three combination pairs were confirmed in a 96-well format assay. The IC_{50} values of known antibiotics was significantly reduced in the presence of the newly identified non-antibiotic agents. The IC_{50} value of azithromycin was reduced 6-fold, from 6.4 to 1.1 μM in the presence of 1.8 μM 5-fluorouracil (**Figure 4A**). Fluspirilene (11.4 μM) and Bay 11-7082 (11.8 μM) increased the inhibitory activity of colistin sulfate against the drug resistant AB5075 by 30- and 4-fold, respectively. The IC_{50} values of colistin were reduced from 0.22 to 0.0074 and 0.06 μM in the presence of fluspirilene and Bay 11-7082, respectively (**Figures 4B,C**).

DISCUSSION

In this study, we describe the optimization and validation of a high throughput growth assay to measure the viability of a multidrug resistant *Acinetobacter baumannii* strain, AB5075. The 1,536-well format of the bacterial growth assay enabled the quick screening of thousands of compounds and drug combination sets with low reagent costs. The results from 25 known antibiotics revealed that AB5075 is resistant to most β-lactams, aminoglycosides, quinolones, and macrolides. The data agreed with these reported by Jacobs et al. (2014).

Seven non-antimicrobial agents, either approved drugs or in clinical trials, were identified in the compound screening campaign; these were confirmed as novel inhibitors of AB5075. For consideration of potential clinical applications of the newly identified antimicrobial activity of these compounds, the human plasma drug concentration levels should be higher than their IC_{90} values or minimum inhibitory concentrations (MIC). Two drugs, among these seven confirmed antimicrobial agents, 5-fluorouracil and 6-thioguanine, met this criterion; these two drugs are potent anticancer medications. Five-fluorouracil is a fluoropyrimidine and is a broad-spectrum anticancer agent, typically used as a first line chemotherapy agent for colorectal cancer (Longley et al., 2003). The standard treatment dose of 5-fluorouracil for cancer patients is 370 mg/m^2 daily with a reported C_{max} of 48.41 μg/mL (Bocci et al., 2000) which is higher than the IC_{90} (25.22 μg/mL) we found in the AB5075 growth inhibition assay. It has dual inhibition mechanisms including functioning as an alternative substrate resulting in miscoding DNA and RNA and inhibiting thymidylate synthase. The broad spectrum antimicrobial activity of 5-fluorouracil was observed as early as 1985 (Bodet et al., 1985). Anti-microbial activity of 5-fluorouracil has also been confirmed against *S. aureus* and *S. epidermidis* (Gieringer et al., 1986; Rangel-Vega et al., 2015). Mechanistic studies of antimicrobial activity are scant for 5-fluorouracil. However, the antimycotic mechanism of flucytosine suggests that 5-fluorouracil may share the same inhibitory mechanism against pathogens as it has against cancer (Vermes et al., 2000). Flucytosine, a prodrug, is converted into 5-fluorouracil following cell uptake.

TABLE 3 | Active and plasma concentration for non-antimicrobial indication candidates.

Drug name	Chemical structure	IC_{50} (μM)	IC_{90} (μM)	Max response	Primary action	C_{max}	
						μg/mL	μM
Auranofin	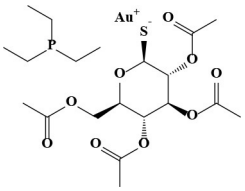	1.09	7.6	106	Antirheumatic	0.68*	1
Pifithrin-μ		7.24	145.8	82	Antineoplastic (p53 inhibitor)	N/A	
5-Fluorouracil	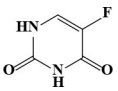	7.29	193.9	79	Antineoplastic	48.41 Bocci et al., 2000	372.2
6-Thioguanine	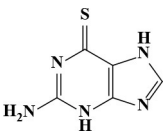	11.98	84.8	77	Antineoplastic	15 Kovach et al., 1986	87
Fluspirilene	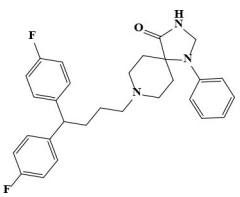	22.74	71.7	77	Antipsychotic	0.2×10^{-3} Swart et al., 1998	0.42×10^{-3}
Bay 11-7082	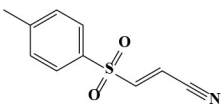	23.57	45.0	99	Anti-inflammatory	N/A	
Disulfiram	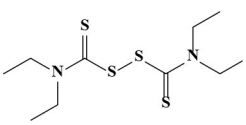	30.08	198.7	81	Chronic alcoholism	0.39×10^{-3}	1.3×10^{-3} Johansson, 1992

http://www.prometheuslabs.com/Resources/PI/Ridaura.pdf.

Six-thioguanine is mainly used as a chemotherapy for myeloid leukemia and myeloid malignancies (Munshi et al., 2014). The recommended dose for acute non-lymphocytic leukemia patients is 2–3 mg/kg daily in an oral form as a single agent, or 75–200 mg/m^2 daily when used as a combination therapy. At a dose of 65 mg/m^2, the mean peak plasma concentration of 6-thioguanine ranges from 6–10 μM (Kovach et al., 1986). Although the plasma concentration of conventional dosage is lower than the IC_{90}, it has been reported that 87 μM in human plasma has been achieved at a larger dose of 800–1200 mg/m^2 (Presant et al., 1984; Kovach et al., 1986). As a guanosine structural analog, 6-thioguanine gets incorporated into DNA and RNA, blocking the biosynthesis of these two essential macromolecules. Additionally, 6-thioguanine hinders purine synthesis by inhibiting hypoxanthine phosphoribosyltransferase (Hprt). The bactericidal effect of 6-thioguanine against *S. aureus* and bacteriostatic effects against for *E. coli* and *S. typhimurium* were reported previously (Soo et al., 2016). Although there is no Hprt homolog in bacteria, the bacterial PRTases [Xanthine-guanine phosphoribosyltranferase (Gpt), hypoxanthine phosphoribosyltransferase (Hpt) and adenine phosphoribosyltransferase (Apt)], show substrate binding-site conservation with Hprt, suggesting that these bacterial PRTases

could be the molecular targets of 6-thioguanine (Wensing et al., 2014).

We have noticed that the majority of non-antimicrobial drugs we found in this repurposing screen are anticancer drugs. Because most anticancer drugs are cytotoxic and have serious side effects, it is a reasonable concern for application of anticancer drugs to treat infectious diseases. However, repositioning of anticancer drugs for infectious diseases has been reported (reviewed in Soo et al., 2016) despite the concerns of potential side effects. For example, miltefosine has been approved to treat leishmaniasis in 2014 (Berman, 2015). The application of gallium compounds to control *P. aeruginosa* in patients with cystic fibrosis is completed its phase II clinical trial (ClinicalTrials.gov[1]). Five-fluorouracil has been implemented as a coating agent for central venous catheters to prevent the bacterial colonization during treatment (Walz et al., 2008). Therefore, treatment needs to balance the therapeutic benefit with potential side effects before considering use of the anticancer drugs for the severe infectious diseases.

Azithromycin has pronounced activity against *H. influenza* as well as most gram-negative bacteria including *Acinetobacter baumannii*. Recently, two important findings support the potential of anti-multidrug resistant *Acinetobacter baumannii* for azithromycin. Azithromycin exhibited better efficacy in cell culture media and animal models than the canonical bacterial culture media (Lin et al., 2015) and it was effective against lipopolysaccharide deficient colistin-resistant strains (García-Quintanilla et al., 2015). The AB5075 strain belongs to the latter case; in our study the minimal inhibitory concentration for 90% inhibition (MIC_{90}) of azithromycin was 8.5 μg/mL, which is lower than the average from 15 clinical isolates of 64 μg/mL (Fernández Cuenca et al., 2003). However, using the breakpoint for *H. influenza*, 4 μg/mL from CLSI, AB5075 is not sensitive to azithromycin. The MIC_{90} value of azithromycin drops to a clinically attainable level through a synergistic effect with 5-fluorouracil in the two-drug combination therapy format.

The appearance of colistin resistance in *Acinetobacter baumannii* infections presents an urgent need for development of new therapeutics. Glycopeptides and hydrophobic compounds such as trimethoprim showed synergistic effects with colistin in an earlier study (Vidaillac et al., 2012). In this study, we identified two non-antimicrobial drugs which can resensitize the AB5075 strain to colistin, lowering the MIC_{90} of colistin to clinically achievable concentrations.

Fluspirilene belongs to the diphenylbutylpiperidine family, which were first-generation antipsychotics. The initial therapeutic dose is 2 mg weekly followed by 1–10 mg weekly injection for maintenance. The C_{max} of fluspirilene at 2 mg is about 200 pg/mL (Swart et al., 1998). Diphenylbutylpiperidines are dopamine D2 receptor antagonists and ameliorate the positive symptoms resulting from the hyperdopaminergic neurotransmission (Seeman, 1980). The finding of antifungal potential of fluspiriline supports a mechanistic study suggesting that fluspirilene likely inhibits the AB5075 growth by blockading the calcium-modulating protein, calmodulin (Butts et al., 2013).

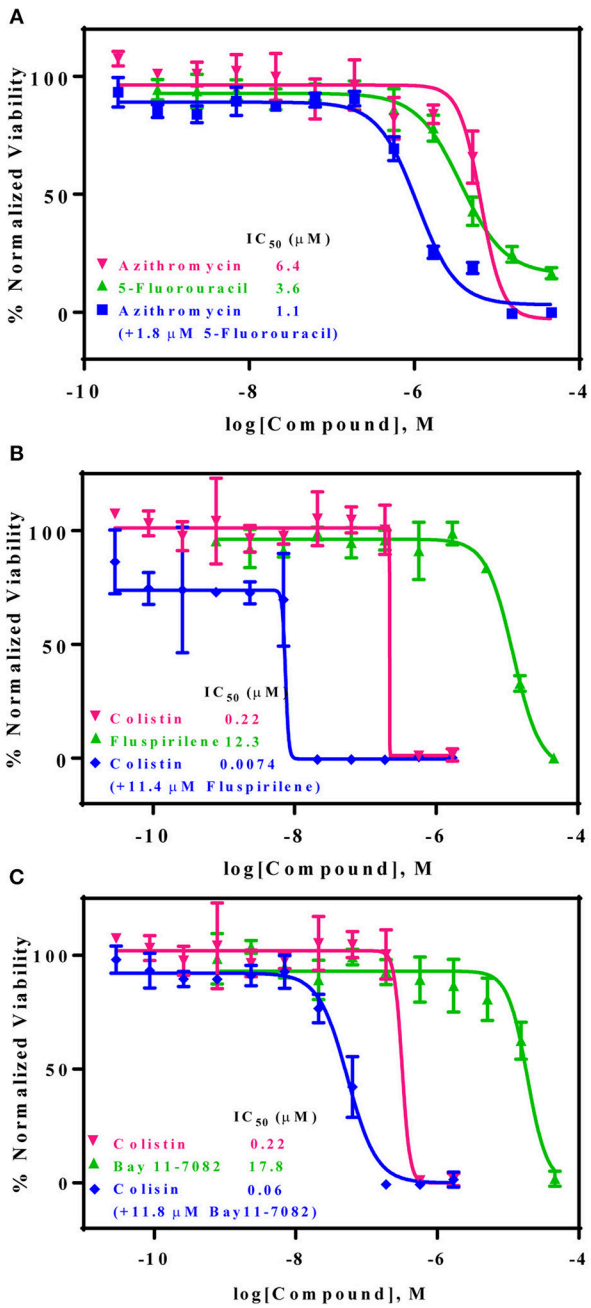

FIGURE 4 | Three non-conventional active compounds resensitize AB5075 to standard care antibiotics. AB5075 was treated with 5-fluorouracil, fluspirilene, or Bay 11-7082 combined with varying concentrations of azithromycin or colistin for 24 h at 37°C before detection of bacterial growth at OD_{600} (blue line). **(A)** In combination with 1.8 μM 5-fluorouracil the IC_{50} of azithromycin decreased ~6-fold (6.4–1.1 μM). **(B)** In combination with 11.4 μM fluspirilene, the IC_{50} of colistin reduced ~30-fold (0.22 μM–7.4 nM). **(C)** In combination with 11.8 μM Bay 11-7082, the IC_{50} of colistin decreased ~4-fold (0.22 μM to 60 nM).

[1]ClinicalTrials.gov. Available online at: https://clinicaltrials.gov/ct2/show/NCT02354859

On the other hand, Bay 11-7082 is widely known as an IκB kinase (IKK) inhibitor. The molecular target of Bay 11-7082 remains unclear. From the chemical structural perspective, Bay 11-7082 is a phenyl vinyl sulfone related compound. The vinyl sulfone in conjugation with a nitrile group makes it a good Michael acceptor to interact with cysteine. The ability to inhibit cysteine proteases through an irreversible Michael addition were demonstrated in a recent study (Kerr et al., 2009). Notably, vinyl sulfone was identified as an anti-parasitic agent through this mechanism, suggesting cysteine proteases could be the molecular target of AB5075 inhibition (Kerr et al., 2009).

In conclusion, we have identified 43 approved drugs or drug candidates that significantly suppressed the growth of the multidrug resistant AB5075 strain including seven non-antimicrobial indication compounds. We also found three pairs of two drug combinations that exhibited synergistic effects with two known antibiotics against the AB5075 strain including azithromycin/5-fluorouracil, colistin sulfate/fluspirilene, and colistin sulfate/Bay 11-7082. These drug pairs are not contraindicated as only minor interactions between azithromycin and 5-fluorouracil have been reported which may be tolerable to patients. While these drug combination pairs may have the potential for clinical trials to treat multidrug resistant *Acinetobacter baumannii* infections, the other drugs found in this study may be useful for identification of new drugs scaffolds or new targets to combat this pathogen.

AUTHOR CONTRIBUTIONS

Y-SC, WS, and WZ conceived and designed the study. Y-SC, WS, and MX performed the experiments. MS performed the statistical analysis. MK and RS contributed materials. Y-SC wrote the first draft of the manuscript. All authors contributed to manuscript revision, read, and approved the submitted version.

FUNDING

This work was supported by the Intramural Research Program of the National Center for Advancing Translational Sciences (NCATS), National Institutes of Health.

ACKNOWLEDGMENTS

We thank the NCATS compound management group for their technical support and Dr. DeeAnn Visk, a medical writer and editor, for editing the manuscript.

REFERENCES

Berman, J. (2015). Miltefosine, an FDA-approved drug for the 'orphan disease', leishmaniasis. *Expert Opin. Orphan Drugs* 3, 727–735. doi: 10.1517/21678707.2015.1039510

Bocci, G., Danesi, R., Di Paolo, A. D., Innocenti, F., Allegrini, G., Falcone, A., et al. (2000). Comparative pharmacokinetic analysis of 5-fluorouracil and its major metabolite 5-fluoro-5,6-dihydrouracil after conventional and reduced test dose in cancer patients. *Clin. Cancer Res.* 6, 3032–3037.

Bodet, C. A., Jorgensen, J. H., and Drutz, D. J. (1985). Antibacterial activities of antineoplastic agents. *Antimicrob. Agents Chemother.* 28, 437–439. doi: 10.1128/AAC.28.3.437

Butts, A., DiDone, L., Koselny, K., Baxter, B. K., Chabrier-Rosello, Y., Wellington, M., et al. (2013). A repurposing approach identifies off-patent drugs with fungicidal Cryptococcal activity, a common structural chemotype, and pharmacological properties relevant to the treatment of Cryptococcosis. *Eukaryot Cell* 12, 278–287. doi: 10.1128/EC.00314-12

Demain, A. L. (1999). Pharmaceutically active secondary metabolites of microorganisms. *Appl. Microbiol. Biotechnol.* 52, 455–463. doi: 10.1007/s002530051546

Deng, M., Zhu, M. H., Li, J. J., Bi, S., Sheng, Z. K., Hu, F. S., et al. (2014). Molecular epidemiology and mechanisms of tigecycline resistance in clinical isolates of *Acinetobacter baumannii* from a Chinese university hospital. *Antimicrob. Agents Chemother.* 58, 297–303. doi: 10.1128/AAC.01727-13

Fernández Cuenca, F., Pascual, A., Martinez Martinez, L., and Perea, E. J. (2003). *In vitro* activity of azithromycin against clinical isolates of *Acinetobacter baumannii*. *Rev. Esp. Quimioter.* 16, 204–208.

Gallagher, L. A., Ramage, E., Weiss, E. J., Radey, M., Hayden, H. S., Held, K. G., et al. (2015). Resources for genetic and genomic analysis of emerging pathogen *Acinetobacter baumannii*. *J. Bacteriol.* 197, 2027–2035. doi: 10.1128/JB.00131-15

García-Quintanilla, M., Carretero-Ledesma, M., Moreno-Martinez, P., Martin-Pena, R., Pachon, J., and McConnell, M. J. (2015). Lipopolysaccharide loss produces partial colistin dependence and collateral sensitivity to azithromycin, rifampicin, and vancomycin in *Acinetobacter baumannii*. *Int. J. Antimicrob. Agents* 46, 696–702. doi: 10.1016/j.ijantimicag.2015.07.017

Gieringer, J. H., Wenz, A. F., Just, H. M., and Daschner, F. D. (1986). Effect of 5-fluorouracil, mitoxantrone, methotrexate, and vincristine on the antibacterial activity of ceftriaxone, ceftazidime, cefotiam, piperacillin, and netilmicin. *Chemotherapy* 32, 418–424. doi: 10.1159/000238445

Huang, R., Southall, N., Wang, Y., Yasgar, A., Shinn, P., Jadhav, A., et al. (2011). The NCGC pharmaceutical collection: a comprehensive resource of clinically approved drugs enabling repurposing and chemical genomics. *Sci. Transl. Med.* 3:80ps16. doi: 10.1126/scitranslmed.3001862

Inglese, J., Auld, D. S., Jadhav, A., Johnson, R. L., Simeonov, A., Yasgar, A., et al. (2006). Quantitative high-throughput screening: a titration-based approach that efficiently identifies biological activities in large chemical libraries. *Proc. Natl. Acad. Sci. U.S.A.* 103, 11473–11478. doi: 10.1073/pnas.0604348103

Jacobs, A. C., Thompson, M. G., Black, C. C., Kessler, J. L., Clark, L. P., McQueary, C. N., et al. (2014). AB5075, a highly virulent isolate of *Acinetobacter baumannii*, as a model strain for the evaluation of pathogenesis and antimicrobial treatments. *MBio* 5, e01076–e01014. doi: 10.1128/mBio.01076-14

Johansson, B. (1992). A review of the pharmacokinetics and pharmacodynamics of disulfiram and its metabolites. *Acta Psychiatr. Scand. Suppl.* 369, 15–26. doi: 10.1111/j.1600-0447.1992.tb03310.x

Kerr, I. D., Lee, J. H., Farady, C. J., Marion, R., Rickert, M., Sajid, M., et al. (2009). Vinyl sulfones as antiparasitic agents and a structural basis for drug design. *J. Biol. Chem.* 284, 25697–25703. doi: 10.1074/jbc.M109.014340

Kovach, J. S., Rubin, J., Creagan, E. T., Schutt, A. J., Kvols, L. K., Svingen, P. A., et al. (1986). Phase I trial of parenteral 6-thioguanine given on 5 consecutive days. *Cancer Res.* 46, 5959–5962.

Lin, L., Nonejuie, P., Munguia, J., Hollands, A., Olson, J., Dam, Q., et al. (2015). Azithromycin synergizes with cationic antimicrobial peptides to exert bactericidal and therapeutic activity against highly multidrug-resistant gram-negative bacterial pathogens. *EBioMedicine* 2, 690–698. doi: 10.1016/j.ebiom.2015.05.021

Longley, D. B., Harkin, D. P., and Johnston, P. G. (2003). 5-fluorouracil: mechanisms of action and clinical strategies. *Nat. Rev. Cancer* 3, 330–338. doi: 10.1038/nrc1074

Marinelli, F. (2009). Chapter 2. From microbial products to novel drugs that target a multitude of disease indications. *Methods Enzymol.* 458, 29–58. doi: 10.1016/S0076-6879(09)04802-2

Munshi, P. N., Lubin, M., and Bertino, J. R. (2014). 6-thioguanine: a drug with unrealized potential for cancer therapy. *Oncologist* 19, 760–765. doi: 10.1634/theoncologist.2014-0178

Oikonomou, O., Sarrou, S., Papagiannitsis, C. C., Georgiadou, S., Mantzarlis, K., Zakynthinos, E., et al. (2015). Rapid dissemination of colistin and carbapenem resistant *Acinetobacter baumannii* in Central Greece: mechanisms of resistance, molecular identification and epidemiological data. *BMC Infect. Dis.* 15:559. doi: 10.1186/s12879-015-1297-x

Presant, C. A., Denes, A. E., Liu, C., and Bartolucci, A. A. (1984). Prospective randomized reappraisal of 5-fluorouracil in metastatic colorectal carcinoma. A comparative trial with 6-thioguanine. *Cancer* 53, 2610–2614. doi: 10.1002/1097-0142(19840615)53:12<2610::AID-CNCR2820531207>3.0.CO;2-9

Rangel-Vega, A., Bernstein, L. R., Mandujano-Tinoco, E. A., García-Contreras, S. J., and García-Contreras, R. (2015). Drug repurposing as an alternative for the treatment of recalcitrant bacterial infections. *Front. Microbiol.* 6:282. doi: 10.3389/fmicb.2015.00282

Seeman, P. (1980). Brain dopamine receptors. *Pharmacol. Rev.* 32, 229–313.

Soo, V. W., Kwan, B. W., Quezada, H., Castillo-Juarez, I., Perez-Eretza, B., Garcia-Contreras, S. J., et al. (2016). Repurposing of anticancer drugs for the treatment of bacterial infections. *Curr. Top. Med. Chem.* 17, 1157–1176. doi: 10.2174/1568026616666160930131737

Sun, W., Weingarten, R. A., Xu, M., Southall, N., Dai, S., Shinn, P., et al. (2016). Rapid antimicrobial susceptibility test for identification of new therapeutics and drug combinations against multidrug-resistant bacteria. *Emerg. Microbes Infect.* 5:e116. doi: 10.1038/emi.2016.123

Swart, K. J., Sutherland, F. C., van Essen, G. H., Hundt, H. K., and Hundt, A. F. (1998). Determination of fluspirilene in human plasma by liquid chromatography-tandem mass spectrometry with electrospray ionisation. *J. Chromatogr. A* 828, 219–227. doi: 10.1016/S0021-9673(98)00635-9

Vermes, A., Guchelaar, H. J., and Dankert, J. (2000). Flucytosine: a review of its pharmacology, clinical indications, pharmacokinetics, toxicity, and drug interactions. *J. Antimicrob. Chemother.* 46, 171–179. doi: 10.1093/jac/46.2.171

Vidaillac, C., Benichou, L., and Duval, R. E. (2012). *In vitro* synergy of colistin combinations against colistin-resistant *Acinetobacter baumannii*, Pseudomonas aeruginosa, and Klebsiella pneumoniae isolates. *Antimicrob. Agents Chemother.* 56, 4856–4861. doi: 10.1128/AAC.05996-11

Walz, J., Luber, J., Reyno, J., Stanford, G., Gitter, R., Longtine, K., et al. (2008). A multicenter randomized controlled clinical trial comparing central venous catheters impregnated with either 5-fluorouracil or chlorhexidine/silver sulfadiazine in preventing catheter colonization. *Crit. Care* 12(Suppl. 2):P40. doi: 10.1186/cc6261

Wang, Y., Jadhav, A., Southal, N., Huang, R., and Nguyen, D. T. (2010). A grid algorithm for high throughput fitting of dose-response curve data. *Curr. Chem. Genomics* 4, 57–66. doi: 10.2174/1875397301004010057

Wensing, A., Gernold, M., Jock, S., Jansen, R., and Geider, K. (2014). Identification and genetics of 6-thioguanine secreted by Erwinia species and its interference with the growth of other bacteria. *Mol. Genet. Genomics* 289, 215–223. doi: 10.1007/s00438-013-0805-1

Xie, R., Zhang, X. D., Zhao, Q., Peng, B., and Zheng, J. (2018). Analysis of global prevalence of antibiotic resistance in *Acinetobacter baumannii* infections disclosed a faster increase in OECD countries. *Emerg. Microbes Infect.* 7:31. doi: 10.1038/s41426-018-0038-9

Zheng, W., Sun, W., and Simeonov, A. (2018). Drug repurposing screens and synergistic drug-combinations for infectious diseases. *Br. J. Pharmacol.* 175, 181–191. doi: 10.1111/bph.13895

Conflict of Interest Statement: The authors declare that the research was conducted in the absence of any commercial or financial relationships that could be construed as a potential conflict of interest.

frontiers in Cellular and Infection Microbiology

REVIEW
published: 18 February 2019
doi: 10.3389/fcimb.2019.00022

Fighting Pathogenic Bacteria on Two Fronts: Phages and Antibiotics as Combined Strategy

Thaysa Leite Tagliaferri[1,2], *Mathias Jansen*[1] and *Hans-Peter Horz*[1]*

[1] Institute of Medical Microbiology, RWTH Aachen University Hospital, Aachen, Germany, [2] Department of Microbiology, Institute of Biological Sciences, Universidade Federal de Minas Gerais, Belo Horizonte, Brazil

With the emerging threat of infections caused by multidrug resistant bacteria, phages have been reconsidered as an alternative for treating infections caused by tenacious pathogens. However, instead of replacing antibiotics, the combination of both types of antimicrobials can be superior over the use of single agents. Enhanced bacterial suppression, more efficient penetration into biofilms, and lowered chances for the emergence of phage resistance are the likely advantages of the combined strategy. While a number of studies have provided experimental evidence in support of this concept, negative interference between phages and antibiotics have been reported as well. Neutral effects have also been observed, but in those cases, combined approaches may still be important for at least hampering the development of resistance. In any case, the choice of phage type and antibiotic as well as their mixing ratios must be given careful consideration when deciding for a dual antibacterial approach. The most frequently tested bacterium for a combined antibacterial treatment has been *Pseudomonas aeruginosa,* but encouraging results have also been reported for *Escherichia coli, Staphylococcus aureus, Klebsiella pneumoniae*, *Acinetobacter baumannii*, *Enterococcus faecalis*, and *Burkholderia cepacia*. Given the immense play area of conceivable phage-antibiotic combinations and their potential excess value, it is time to recapitulate of what has been achieved so far. This review therefore gathers and compares the results from most relevant studies in order to help researchers and clinicians in their strategies to combat multidrug resistant bacteria. Special attention is given to the selected bacterial model organisms, the phage families and genera employed, and the experimental design and evaluation (e.g., *in vitro* vs. *in vivo* models, biofilm vs. planktonic culture experiments, order and frequency of administration etc.). The presented data may serve as a framework for directed further experimental approaches to ultimately achieve a resolute challenge of multidrug resistant bacteria based on traditional antibiotics and phages.

Keywords: antibiotics, phages, phage therapy, phage and antibiotic combination, antimicrobial resistance, phage-antibiotic synergy (PAS), resistance evolution, ESKAPE

OPEN ACCESS

Edited by:
Maria Tomas, Complexo Hospitalario Universitario A Coruña, Spain

Reviewed by:
Christian T. K.-H. Stadtlander, Independent researcher, St. Paul, MN, United States
Lorena Ruiz, Instituto de Productos Lácteos de Asturias (IPLA), Spain

***Correspondence:**
Hans-Peter Horz
hhorz@ukaachen.de

Specialty section:
This article was submitted to Clinical Microbiology, a section of the journal Frontiers in Cellular and Infection Microbiology

Received: *10 October 2018*
Accepted: *22 January 2019*
Published: *18 February 2019*

Citation:
Tagliaferri TL, Jansen M and Horz H-P (2019) Fighting Pathogenic Bacteria on Two Fronts: Phages and Antibiotics as Combined Strategy. Front. Cell. Infect. Microbiol. 9:22. doi: 10.3389/fcimb.2019.00022

INTRODUCTION

In the era of the increasing emergence of multi-drug resistant bacteria, a key question is currently being raised: do bacteriophages represent an alternative to antibiotics (Lin et al., 2017)? Numerous *in vitro* and *in vivo* studies using single or mixed phage types (phage cocktails) have been conducted over the years, however, a clear answer to this question has still not been provided (Nobrega et al., 2015). While in principle promising results have been reported, the establishment of phage therapy in modern Western medicine is a long and stony road, on which a number of hurdles have to be overcome (Pelfrene et al., 2016). Besides complicated regulatory issues and safety concerns, reluctance toward using phages for curing infectious diseases stems from prevailing skepticism about their true therapeutic efficiency, for example because of phage resistance evolution (Chanishvili, 2012). Because of such potential shortcomings of phages, the probably more adequate question would be whether the joint use of phages and antibiotics is the superior strategy for controlling bacterial pathogens. The expected benefit of such a dual approach might be the stronger bacterial suppression and the reduced bacterial capacity of developing phage and/or antibiotic resistance (Torres-Barceló and Hochberg, 2016). In fact, several studies investigating the combined benefit of phages and traditional antibiotics have provided encouraging results. For instance, it has been shown that sub-inhibitory concentrations of antibiotics can foster phage productivity and thus phage-mediated bacterial decline, a phenomenon termed phage-antibiotic synergy, or PAS (e.g., Comeau et al., 2007). This beneficial effect has been observed for some phage/antibiotic combinations (Ryan et al., 2012; Kamal and Dennis, 2015; Uchiyama et al., 2018), but not for others (Gelman et al., 2018; Torres-Barceló et al., 2018). A combined approach can also lead to the restoration of antibiotic sensitivity, for instance, in cases where the phage interacts with the bacterial drug efflux systems (Chan et al., 2016). Given the immense diversity of phages, there still exists a plethora of untapped phage-antibiotic combinations. Furthermore, positive interactions between any two antimicrobial agents may strongly depend on the treatment conditions (e.g., dosage, frequency, time points and order of administration etc.), which offers plenty of room for versatile experimentation. Knowledge and consideration of already tested phage/antibiotic "medleys," whether proofing to be successful or not, may assist in the more directed elucidation of suitable combinations and conditions. This review therefore provides an overview of the most pertinent studies describing dual approaches, which may aid with the conception of optimized antibacterial strategies. We primarily focused on articles that were directed against selected members of the so-called ESKAPE-group, which includes *Enterococcus faecium*, *Staphylococcus aureus*, *Klebsiella pneumoniae*, *Acinetobacter baumannii*, *Pseudomonas aeruginosa*, and *Enterobacter* species (Rice, 2008) or directed against other opportunistic pathogens (such as *Escherichia coli*, *Enterococcus faecalis*, and *Burkholderia cepacia*). Depending on the magnitude of bacterial suppression, desirable positive interactions can be categorized as true synergism, additive effects, or as facilitation, the latter of which indicates that the combined approach is better than the best acting single agent, but worse than the sum of both antimicrobials acting independently (Chaudhry et al., 2017). Given that even facilitation is a desirable outcome, this has probably led to the tentatively broader use of the word "synergy," as many studies use this term without further distinction for any improvement of the combined approach, as long as it is significant. Accordingly, unless otherwise stated, the term "synergy" in this paper refers to a combined antibacterial effect that is stronger compared to the best acting compound (phage or antibiotic) alone.

Figure 1 and **Table 1** provide an overview of the experimental approaches (i.e., *in vitro*/*in vivo* studies, planktonic culture/biofilm studies etc.). **Table 1** includes also additional information about the selection of phage genus, antimicrobial agents, and the potential synergistic combinations. Further details, e.g., antibiotic and phage dosage used in each combination are listed in the **Supplementary Table S1**.

PSEUDOMONAS AERUGINOSA

So far, the majority of phage/antibiotic studies have focused on *P. aeruginosa*, apparently because of its important clinical impact as opportunistic pathogen, which is often involved in cystic fibrosis, burn infections, hospital-acquired pneumonia, urinary tract infections, among others (Sousa and Pereira, 2014). *P. aeruginosa* has a strong colonization capacity on biotic and abiotic surfaces and persists against a wide range of antimicrobials (Kung et al., 2010; Alshalchi and Anderson, 2015). Biofilms and planktonic cultures of *P. aeruginosa* were the major target of many studies using mostly the strain PA01 or other reference strains, such as PA14, CHA, and PAK (De Soyza et al., 2013). Furthermore, a few case reports as well as some *in vivo* studies based on mice or rats as model organisms have been published.

Chaudhry et al. treated a 48-h biofilm of PA14 with the two phages NP1 (*Siphoviridae, NP1Virus*) and NP3 (*Myoviridae*) together or both in combination with five antibiotics (Chaudhry et al., 2017). Each antimicrobial alone showed only moderate anti-biofilm efficacy, however, when applied simultaneously, true synergistic effects *sensu stricto* were observed between phages and ceftazidime at 1x MIC and 8x MIC and for ciprofloxacin at 1x MIC. An improved effect by way of facilitation was also achieved for ciprofloxacin at 8x MIC and for tobramycin at 1x MIC, but interestingly not at 8x MIC (Chaudhry et al., 2017). These findings indicate the dose dependency of simultaneous applications with higher antibiotic concentrations likely removing the minimum bacterial density required for optimal phage replication. No improvement was observed with colistin and gentamicin, the latter of which is somewhat surprising, given that this antibiotic belongs to the same class as tobramycin. The therapeutic outcome differed with time-delayed use of phages and antibiotics. The addition of tobramycin or gentamicin 24 h after phage application led to a significant synergistic effect. Conversely, successive addition of ciprofloxacin or ceftazidime did not lead to a better outcome compared to the simultaneous application. Hence, critical to a successful combined application is the dosage and the time

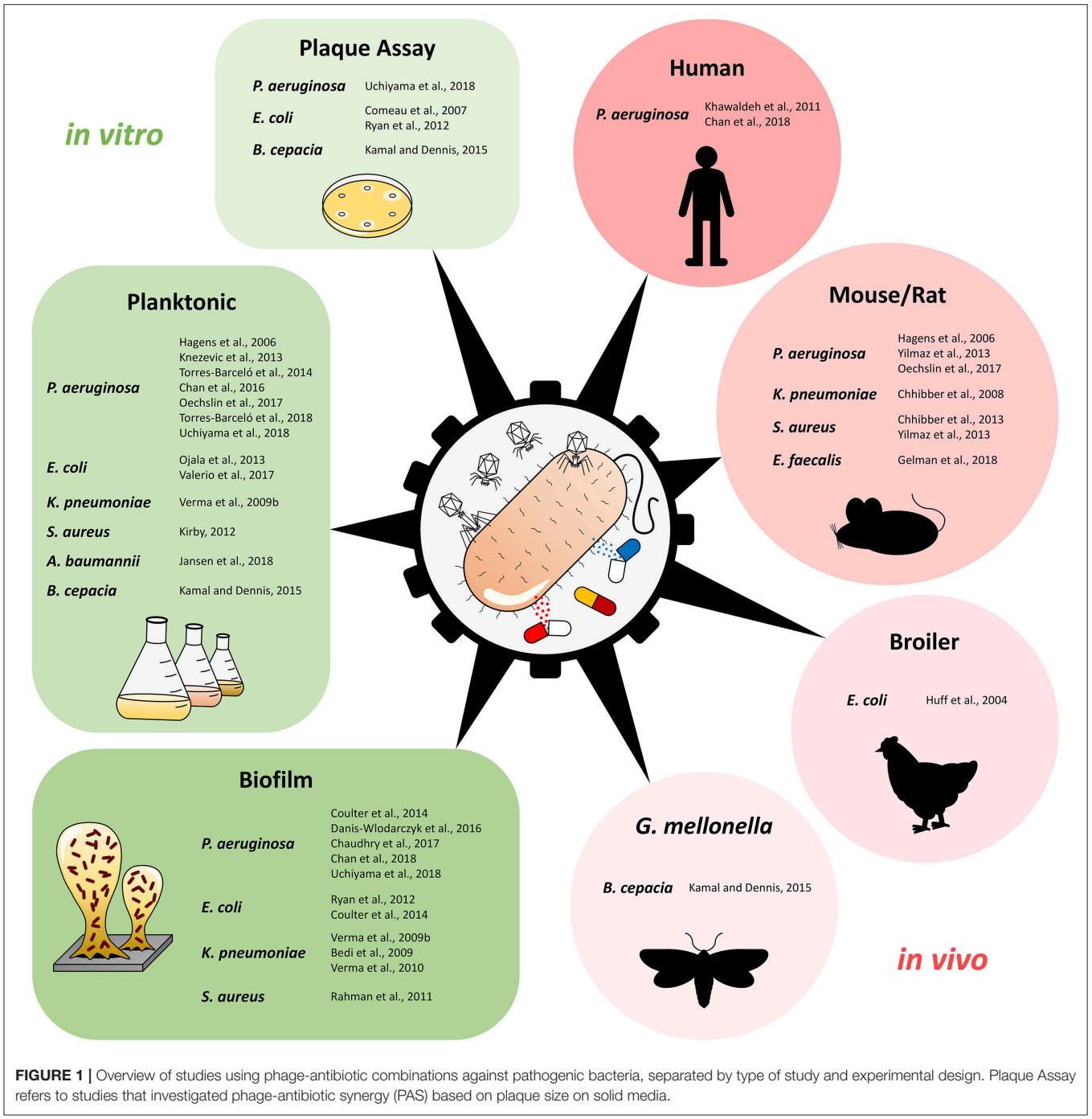

FIGURE 1 | Overview of studies using phage-antibiotic combinations against pathogenic bacteria, separated by type of study and experimental design. Plaque Assay refers to studies that investigated phage-antibiotic synergy (PAS) based on plaque size on solid media.

point of antibiotic addition. Variations in the phage dosage may also impact the antibacterial outcome, which was, however not further evaluated in this study.

Anti-biofilm activity but no synergistic effect was seen when the giant phage KTN4 (*Myoviridae*, *phiKZ-like-virus*) was combined with colistin against strain PAO1 grown for 24, 48, and 72 h *in vitro* (Danis-Wlodarczyk et al., 2016). Both antimicrobials alone achieved already a significant biofilm reduction, and as a possible explanation, the authors presume that colistin could limit phage propagation as it destabilizes the cell membrane. Conversely, phage KTN4 recognizes IV-type pili as receptor and therefore does not interfere positively or negatively with colistin activity (Danis-Wlodarczyk et al., 2016).

Likewise, a 48-h-old biofilm of PAO1 could not be stronger reduced with phage PB-1 (*Myoviridae, Pbunavirus,*) and tobramycin together (Coulter et al., 2014). However, the combination resulted in a significant decrease in the emergence of antibiotic and phage resistant bacterial cells.

TABLE 1 | Overview of phage-antibiotic combinations tested against human pathogenic bacteria[Δ].

Reference	Phage name (*Family*)	Phage genus[+]	Antibiotic classes					
			β-L	AG	FQ	PM	TC	OT
Pseudomonas aeruginosa								
Chaudhry et al. (2017)	NP1 (*S*) + NP3 (*M*)	*NP1Virus* / n.s.l.	**CAZ**	**TOB/GEN**	**CIP**	CST		
Danis-Wlodarczyk et al. (2016)	KTN4 (*M*)	*phiKZ-like-virus*				CST		
Coulter et al. (2014)	PB-1 (*M*)	*Pbunavirus*[1]		TOB*				
Torres-Barceló et al. (2014)	LUZ7 (*P*)	*N4-like virus*[2]		**STR**				
Torres-Barceló et al. (2018)	LKD16 (*P*)	*Phikmvvirus*[1]	**CAZ***		**CIP***			ERY*
	LUZ7 (*P*)	*N4-like virus*[2]	**CAZ***		**CIP***			ERY*
	14/1 (*M*)	*Pbunavirus*[1]	**CAZ***		**CIP***			ERY*
	EL (*M*)	*Elvirus*[1]	**CAZ***		**CIP***			ERY*
Uchiyama et al. (2018)	KPP21 (*P*)	*N4-like virus*[2]	FEP/CZO/**CFP**/CFP+SUL/ CAZ/CTX/CPD/**MOX**/ FMX/CTM/CMZ/PIP/ **MEM** /IPM/ATM	GEN/TOB/AMK	CIP/LVX	CST	MIN	**FOF**/**CHL**/SXT
	KPP22 (*M*)	*Pbunavirus*	**FEP**/**CZO**/**CFP**/**CFP**+**SUL**/ **CAZ**/**CTX**/CPD/**MOX**/ FMX/CTM/CMZ/**PIP**/**MEM** /IPM/**ATM**	**GEN**/**TOB**/**AMK**	CIP/LVX	CST	MIN	**FOF**/CHL/SXT
	KPP23 (*S*)	n.s.l.	FEP/CZO/CFP/**CFP**+**SUL**/ CAZ/CTX/CPD/MOX/ FMX/CTM/CMZ/PIP/MEM /IPM/ATM	GEN/**TOB**/AMK	CIP/LVX	CST	MIN	**FOF**/CHL/SXT
	KPP25 (*P*)	*Kpp25virus*	FEP/CZO/CFP/CFP+SUL/ CAZ/CTX/CPD/MOX/ FMX/CTM/CMZ/PIP/MEM /IPM/ATM	GEN/TOB/AMK	CIP/LVX	CST	MIN	FOF/CHL/SXT
Knezevic et al. (2013)	δ (*P*)	n.s.l.	CRO	GEN	CIP	PMB		
	δ-1 (*S*)	n.s.l.	**CRO**	GEN	CIP	PMB		
	001A (*S*)	n.s.l.	CRO	GEN	CIP	PMB		
Chan et al. (2016)	OMKO1 (*M*)	*phiKZ-like-virus*	**CAZ**		**CIP**		**TET**	**ERY**
Chan et al. (2018)	OMKO1 (*M*)	*phiKZ-like-virus*	**CAZ**		CIP			
Khawaldeh et al. (2011)	Pyophage cocktail	n.s.l.	**MEM**			**CST**		
Oechslin et al. (2017)	PP1131 cocktail	n.s.l.	**MEM***		**CIP***			
Yilmaz et al. (2013)	PAT14 (*P*)	n.s.l.	**IPM**+**CIL**	**AMK**				
Hagens et al. (2006)	Pf3 (*I*)	*Inovirus*[3]	**CAR**	**GEN**			**TET**	**CHL**
	Pf1 (*I*)	*Inovirus*[3]	**CAR**	**GEN**			**TET**	**CHL**
Escherichia coli								
Comeau et al. (2007)	Φ MFP (*S*)	n.s.l.	**CTX**/**ATM**/**CFM**/**CRO**/**CAZ**	**GEN**			**TET**	
	RB32 (*M*)	n.s.l.	**CTX**					
	RB33 (*M*)	n.s.l.	**CTX**					
	T3 (*P*)	*T7virus*[1]	**CTX**					
	T7 (*P*)	*T7virus*[1]	**CTX**					
	T4 (*M*)	*T4virus*[1]	**CTX**/**PIP**/**AMP**/**TIC**		**NAL**			**MTC**
Ryan et al. (2012)	T4 (*M*)	*T4virus*[1]	**CTX**					
Coulter et al. (2014)	T4 (*M*)	*T4virus*[1]		**TOB***				
Valério et al. (2017)	ECA2 (*P*)	n.s.l.	AMP/PIP	KAN	**CIP***		TET	CHL
Ojala et al. (2013)	PRD1 (*T*)	*Tectivirus*[1]		KAN*				RIF*
Huff et al. (2004)	SPR02 + DAF6	n.s.l.			**ENR**			

(Continued)

TABLE 1 | Continued

Reference	Phage name (*Family*)	Phage genus[+]	Antibiotic classes					
			β-L	AG	FQ	PM	TC	OT
Staphylococcus aureus								
Rahman et al. (2011)	SAP-26 (*S*)	*Phietavirus*[1]						VAN/RIF/AZM
Kirby (2012)	SA5 (*M*)	*Kayvirus*[1]		GEN*				
Yilmaz et al. (2013)	Sb-1 (*M*)	*Kayvirus*[1]						TEC
Chhibber et al. (2013)	MR-10 (*M*)	n.s.l.						LZD
Klebsiella pneumoniae								
Verma et al. (2009b) and (2010)	KPO1K2 (*P*)	*T7-like virus*[4]			CIP*			
Bedi et al. (2009)	n.s.l.	n.s.l.	AMX					
Chhibber et al. (2008)	SS (*P*)	n.s.l.		AMK				
Acinetobacter baumannii								
Jansen et al. (2018)	KARL-1 (*M*)	*T4-like virus*	MEM*		CIP	CST		
Enterococcus faecalis								
Gelman et al. (2018)	EFDG1+EFLK1 (*M*)	n.s.l.	AMP*					
Burkholderia cepacia								
Kamal and Dennis (2015)	KS12 (*M*)	n.s.l.	AMP/CAZ/PIP/MEM	KAN	CIP/LVX		TET/MIN	
	KS14 (*M*)	*P2-like-virus*	AMP/CAZ/PIP/MEM	KAN	CIP/LVX		TET/MIN	

[Δ] *Experimental studies appear in the same order as in the main text. Antibiotics in green indicate positive interaction (enhanced bacterial suppression or PAS) with the respective phage; antibiotics in black indicate that positive interactions with respective phage were not observed; Stars behind the antibiotics mark those studies in which resistance evolution was investigated; green stars indicate that the combined approach reduced the emergence of resistant cells; black stars indicate that the emergence of resistant cells was not reduced or the sensitivity level was maintained with the combined approach, respectively. Gray scale: in vitro studies; light red scale: in vivo studies; dark red scale: human case reports.*

[+] Phage genus information was provided by the respective references in the table (left column), except for cases with superscript numbers: [1] Mihara et al. (2016); [2] Shen et al. (2016); [3] Holland et al. (2006); [4] Verma et al. (2009a), which do not represent studies about phage/antibiotic combinations, but provide information about the phage genus.

(M), Myoviridae; (I), Inoviridae; (P), Podoviridae; (S), Siphoviridae; (T), Tectiviridae; n.s.l.: genus not specified in literature; β-L, Beta-Lactam antibiotics/Beta-Lactamase inhibitors; AG, Aminoglycosides; FQ, Fluoroquinolones; PM, Polymyxins; TC, Tetracyclines; OT, Others; AMK, amikacin; AMP, ampicillin; AMX, amoxicillin; ATM, aztreonam; AZM, azithromycin; CAR, carbenicillin; CAZ, ceftazidime; CFM, cefixime; CFP, cefoperazone; CHL, chloramphenicol; CIL, cilastatin; CIP, ciprofloxacin; CMZ, cefmetazole; CPD, cefpodoxime; CRO, ceftriaxone; CST, colistin; CTM, cefotiam; CTX, cefotaxime; CZO, cefozopran; ENR, enrofloxacin; ERY, erythromycin; FEP, cefepime; FMX, flomoxef; FOF, fosfomycin; GEN, gentamicin; IPM, imipenem; KAN, kanamycin; LVX, levofloxacin; LZD, linezolid; MEM, meropenem; MIN, minocycline; MOX, moxalactam (latamoxef); MTC, mitomycin C; NAL, nalidixic acid; PIP, piperacillin; PMB, polymyxin B; RIF, rifampicin; STR, streptomycin; SUL, sulbactam; SXT, trimethoprim/sulfamethoxazole; TEC, teicoplanin; TET, tetracycline; TIC, ticarcillin; TOB, tobramycin; VAN, vancomycin.

Thus, the treatment of biofilms using the dual approach is clearly warranted, despite an apparent lack of a stronger anti-biofilm capacity.

Irrespective of this, the challenge of planktonic cultures of PA01 generally led to more promising results. Torres-Barceló et al. applied phage LUZ7 (*Podoviridae*, *N4-like virus*) in conjunction with streptomycin which reduced the bacterial cell density significantly stronger than each single treatment (Torres-Barceló et al., 2014). Notably, the time point of antibiotic addition mattered (i.e., streptomycin administration 12 h after phage application achieved higher bacterial suppression than after 24 h), the result of which was independent from the streptomycin dosages. Hence, corroborating the findings of Chaudhry et al., there exists a specific time window during which the supplementary delivery of the antibiotic leads to optimal results (Chaudhry et al., 2017). Realization of the ideal time period may be the key for successful future applications.

However, larger time scales must also be taken into consideration. For instance, long-term effects over several days of four unrelated phages were investigated in addition with sub-inhibitory concentrations of ceftazidime, ciprofloxacin, and erythromycin applied against the strain PAO1 (Torres-Barceló et al., 2018). The phages used were LKD16 (*Podoviridae*, *Phikmvvirus*), LUZ7 (*Podoviridae*, *N4-like virus*), 14/1 (*Myoviridae*, *Pbunavirus*), and EL (*Myoviridae*, *Elvirus*). Except for ciprofloxacin, phage density initially decreased in most tested antibiotic-phage combinations, which is somewhat opposing the phenomenon of PAS. Even phage virulence, defined as the capacity to inhibit ancestral bacterial density, was reduced in the co-presence of antibiotics. Those negative effects on the phages were not observed later on (i.e., after 8 days), indicating that phages had adapted to the antibiotic-containing environment. Despite of this, combination treatments stronger controlled bacterial density and particularly ciprofloxacin limited antibiotic resistance evolution. Thus, this study principally encourages combination strategies, but also points at the need for investigations at a prolonged time scale (i.e., several days, comparable to the time window of an infectious disease under treatment) in order to account for—and understand—the clinical importance of evolutionary adaptations during phage therapy.

In an attempt to systematically identify well-working phage/antibiotic combinations, Uchiyama et al. tested PAS, using

four unrelated phages and 25 antibiotics against strain PAO1 and five clinical isolates of *P. aeruginosa* (Uchiyama et al., 2018). The four phages were KPP21 (*Podoviridae*, *N4-like virus*), KPP22 (*Myoviridae*, *Pbunavirus*), KPP23 (*Siphoviridae*), and KPP25 (*Podoviridae*, *Kpp25virus*). While no PAS was observed between KPP25 and any of the antibiotics, the other three phages exhibited PAS with 5, 13, and 3 antibiotics, respectively. Involved in PAS were predominantly cell wall synthesis inhibiting antibiotics including the anti-*Pseudomonas* drugs ceftazidime and piperacillin. PAS was further confirmed for the best scoring phage KPP22 based on time-kill curves and biofilm assays, along with the testing of additional clinical isolates. The study shows that PAS can be observed quite frequently, although the selection of the phage type seems to be a crucial factor. It remains to be demonstrated though, whether PAS automatically qualifies successfully tested combinations for *in vivo* applications. Conversely, it is unclear whether or not those phage/antibiotic pairs, displaying no PAS, are *de facto* unsuitable as potential treatment option. This is an unexplored field and requires further investigation.

The suppressive effect against reference strains other than PA01 was assessed by Knezevic et al., using three unrelated phages (Knezevic et al., 2013). Phages δ (*Podoviridae*), δ-1, and 001A (both *Siphoviridae*) were used against their individual hosts, i.e., PA-4U, ATCC 9027, and PA-M2, respectively, in conjunction with sub-inhibitory concentrations of ciprofloxacin, ceftriaxone, gentamicin, or polymyxin B. Only with ceftriaxone an enhanced reduction of planktonic cultures was observed. In addition, a synergistic effect—*sensu stricto*—occurred only with the combination of phage δ-1. This study again shows, that not every phage-antibiotic combination supresses bacteria stronger. The precise mode of antibiotic action (e.g., cell elongation) and the molecular base of phage/host interactions are important determinants of success. Nonetheless, the emergence of resistant variants might be reduced also with less successful combinations. This latter issue should therefore always be investigated, whenever combination approaches are evaluated.

Encouragement for a clinical approach was fuelled by the *in vitro* observation that the lytic phage OMKO1 (*Myoviridae*, *phiKZ-like-virus*) led to the re-sensitization to several antibiotics of eight *P. aeruginosa* strains including PAO1 (Chan et al., 2016). This phage binds to the outer membrane porin M, which belongs to certain efflux systems responsible for antibiotic resistance. Consequently, efflux pump mechanisms are severely affected by such a phage attack. Apparently, the attempt to evade the phage infection requires mutation adaptation that represents a genetic trade-off between phage resistance and antibiotic sensitivity. Chan et al. (2018) subsequently assessed the efficiency of the combined treatment of phage OMKO1 and antibiotic in a patient with prosthetic vascular graft infection in the aorta artery (Chan et al., 2018). Prior to the human application, the clinical isolate of the patient was tested in an *in vitro* biofilm assay. Both, ceftazidime and ciprofloxacin at 2x MIC were not sufficient to eliminate a 72-h old biofilm. In contrast, phage OMKO1 as single agent significantly reduced mean cell densities, but the biofilm was not stronger reduced by further adding antibiotics. However, since no antagonism was observed and given the aforementioned *in vitro* results (Chan et al., 2016), the patient was treated with a combined phage/antibiotic approach. In fact, following a single application of phage OMKO1 and ceftazidime, the infection appeared to resolve with no signs of recurrence (Chan et al., 2018). However, part of the graft was excised 4 weeks after the treatment due to aortic perforation. Hence, at this point it remains unclear whether the treatment success was due to this intervention, the phage activity alone, or its combination with ceftazidime (Chan et al., 2018).

In another case report Khawaldeh et al. described the successful use of six lytic *P. aeruginosa* phages combined at equal amounts into a Pyophage cocktail (Villarroel et al., 2017), as adjunctive therapy (Khawaldeh et al., 2011). While antibiotics alone failed to cure a recurrent bladder infection in a 67-year-old woman, the combination of the phage cocktail with meropenem and colistin led to symptomatic relief and reduction of the bacterial load, when applying the cocktail every 12 h for 10 days. Interestingly, a decrease in viable bacterial counts was already observed before starting the time-delayed antibiotic therapy which commenced on the sixth day of phage therapy. From then on, the bacterial count further decreased (day 7) until no viable bacteria could be detected anymore from the eighth day. This case report is encouraging, because the treatment was well-tolerated by the patient and because the beneficial effect of successive application of different antimicrobials agrees well with the aforementioned *in vitro* observations (Torres-Barceló et al., 2014).

Oechslin et al. (2017) evaluated the anti-*Pseudomonas* phage cocktail PP1131 containing 12 phages in combination with either 2.5x MIC of ciprofloxacin or meropenem against the *P. aeruginosa* strain CHA *in vitro* (Oechslin et al., 2017). With both antibiotics a significant synergistic effect with PP1131 was observed, and emerging phage-resistant subpopulations could be prevented by co-addition of the antibiotics. This positive effect could subsequently be confirmed when treating an experimental endocarditis model in rats. While a single application of the phage cocktail or ciprofloxacin was equally effective in reducing the bacterial load, a significant synergistic effect was achieved when both antimicrobial agents were jointly used. In this case, 64% of tested rats could be successfully treated. Hence, the combination approach proved to be meaningful in this infection model. However, *P. aeruginosa*-associated endocarditis is relatively rare in humans, which means that it would be interesting to know whether or not more common bacterial causes of this heart disease (e.g., staphylococci or streptococci) can also be treated with phage/antibiotic combinations. To our knowledge this has not been investigated so far.

Rats were also selected for an implant-related infection model using clinical isolates of *P. aeruginosa* followed by a subsequent treatment with phage vB_PsaP PAT14 (*Podoviridae*) in combination with imipenem/cilastatin, and amikacin (Yilmaz et al., 2013). The phage was administered through the skin, directly into the medullary canal, once a day for 3 consecutive days. The antibiotics were applied intraperitoneally once a day for 14 days. While the number of colony-forming units could be significantly stronger reduced during the combination therapy compared to the control group and the two groups receiving

phage or antibiotics only, no significant difference was observed in the final biofilm thickness across the different treatments. Besides a too short follow-up time, failure to reduce the biofilm was ascribed to the selected phage, which apparently was not effective enough for biofilm degradation.

In contrast to the aforementioned studies, which focused on lytic phages, Hagens et al. examined the impact of the filamentous phages Pf3 and Pf1 (*Inoviridae*, *Inovirus*) on the dosage of certain antimicrobials required to inhibit the growth of *P. aeruginosa* strains PAO1 and PAK, respectively (Hagens et al., 2006). Up to 10-fold lower concentrations of antibiotics were needed in the presence of the filamentous phages. Even re-sensitization, despite the carriage of a plasmid containing resistance genes against antibiotics (including gentamicin and tetracycline), could be achieved with those phages. Finally, the authors evaluated the therapeutic effect of gentamicin and phage Pf1 in an intraperitoneal infection mouse model with the PAK strain. As a result, 16 out of 20 mice survived the 7-day observation period, whereas the control groups died within 48 h. As a major mechanism, it is plausible to assume that the extrusion of filamentous phage progenies may weaken the antibiotic-barrier function of the outer membrane of gram-negative bacteria. Thus, the effect of filamentous phages merits further investigation as potential complementation of antibiotics against multi-drug resistant bacteria.

ESCHERICHIA COLI

Although generally being a commensal in the gastrointestinal tract, *E. coli* is also recognized for intestinal and extra intestinal disorders such as diarrhea, colitis, urinary tract infections, bacteremia, as well as sepsis (Blount, 2015; Vila et al., 2016). It has been estimated that until 2050 more than 3 million people will die due to infections caused by multi-drug resistant *E. coli* (O'Neil, 2016).

The term PAS had first been introduced by Comeau et al., based on an uropathogenic strain of *E. coli* (MFP) and a lytic siphovirus, co-isolated from a patient with urinary tract infection (Comeau et al., 2007). It was found that this lytic phage (ΦMFP) benefits from sub-lethal doses of beta-lactams leading to a higher burst size and thus to increased plaques on agar plates (Comeau et al., 2007). This effect was not observed with tetracycline and gentamicin as well as phage ΦMFP. With phage T4 (*Myoviridae, T4virus*) PAS was also detected using quinolone and mitomycin C as well as further beta-lactam antibiotics. Cefotaxime also favored PAS with phages RB32 and RB33 (both *Myoviridae*) against strain MFP. In addition, while PAS could also be demonstrated for the *E. coli* strain AS19 with the phages T4, T3 (*Podoviridae, T7virus*), and T7 (*Podoviridae, T7virus*) the authors found that PAS occurred independently of the bacterial SOS system and was rather due to cellular filamentation upon exposure to respective antibiotics. Hence, there is a wide distribution of PAS across unrelated phages, however, as stated above, the true value of this phenomenon for phage therapy remains to be elucidated.

Complementary results were observed by Ryan et al., who observed PAS with phage T4 (*Myoviridae, T4virus*) and distinct concentrations of cefotaxime against *E. coli* strain ATCC 11303 (Ryan et al., 2012). Besides an increased burst size, along with a reduced latent period of T4, the dual combination had a significantly stronger anti-biofilm capacity compared to the single biofilm treatments. Also, with increasing phage titers, decreasing levels of cefotaxime were needed for the eradication of a 24-h biofilm. Thus, this study demonstrated for the first time that PAS affected bacterial biofilms. Furthermore, decreasing the effective therapeutic level of an antibiotic with phages could be a beneficial strategy to minimize adverse side effects of the antibiotics *in vivo*. By using the same strain and the same phage—this time combined with tobramycin—a 48-h biofilm could nearly be completely eradicated after 24 h of exposure, in contrast to the single treatments (Coulter et al., 2014). Moreover, the combined strategy prevented the occurrence of antibiotic- and phage-resistant cells by 99 and 39%, respectively.

Sub-lethal doses favored synergistic effects between the phage ECA2 (*Podoviridae*) and ciprofloxacin against the *E. coli* strain ATCC 13706 (Valério et al., 2017). Interestingly, this effect was not observed with higher antibiotic concentrations. No synergy was observed with the bacteriostatic antibiotics tetracycline and chloramphenicol and with antibiotics against which the strain was *a priori* resistant, i.e., piperacillin, ampicillin, and kanamycin. In agreement with the synergistic result, the authors also found a lower frequency of resistant mutants when the sub-inhibitory concentration of ciprofloxacin was used. Finally, using identical treatment conditions, the synergistic effect of the dual treatment could be confirmed based on the *in vitro*-simulation of an *E. coli*-driven urinary tract infection with real urine samples.

An elegant and somewhat different approach was described by Ojala et al. Instead of the attempt to maximize bacterial suppression with combined antimicrobials, their goal was the prevention of the spread of drug resistance genes via conjugative plasmids (Ojala et al., 2013). To this end, the phage PRD1 (*Tectiviridae, Tectivirus*), which adsorbs to receptors encoded by conjugative plasmids, was used. The presence of this phage shifted the selective pressure toward *E. coli* strains that were plasmid free and thus became sensitive to certain antibiotics. This positive effect, although less strongly pronounced, was also seen with the co-presence of kanamycin or rifampicin, suggesting that a combination approach is suitable for obtaining plasmid-free cells. Although not performed with clinical strains but with the two reference strains (i.e., *E. coli* K-12 strains JE2571 and HMS174), the study provides proof-of principle that conjugative-plasmid dependent phages might represent a valuable complementation of antimicrobial therapies. Notably, the host range of phage PRD1 is determined by the host range of suitable conjugative plasmids, which means that this phage can be applied against many other gram-negative species as well (Ojala et al., 2013). However, more research is needed, especially for assessing the functionality of this system against clinical isolates and under more complex *in vivo* conditions.

By way of an example of a successfully tested *in vivo* model, Huff et al. treated broiler chicken simultaneously with enrofloxacin (a fluoroquinolone antibiotic used for the treatment of domestic animals), with a mixture of the phages SPR02 and DAF6 and rescued all individuals that were experimentally

infected with an avian pathogenic *E. coli* isolate (Huff et al., 2004). This result was in clear contrast to the single application of phages or enrofloxacin, which led to mortality rates of 15 and 3%, respectively, which were, however, significantly lower than those of untreated chicken (i.e., 68%). Hence, this study demonstrates that phage/antibiotic approaches may have a practical and exploitable value for poultry and animal production systems.

STAPHYLOCOCCUS AUREUS

Although present in about 30% of population as a commensal bacterium, *S. aureus* is a leading cause of bacteraemia as well as infective endocarditis. It is also responsible for osteoarticular-, skin-, and device-related infections, among others (Tong et al., 2015; Oliveira et al., 2018). Importantly, MRSA is responsible for 13% up to 74% of all *S. aureus* infections worldwide, with different incidences around the world (Hassoun et al., 2017). Treatment options are limited for MRSA (Lee et al., 2018) and usually comprise the administration of linezolid, vancomycin, or daptomycin when the infection is invasive (Wunderink et al., 2012; Choo and Chambers, 2016). Therefore, several MRSA preventive strategies are under consideration (Lee et al., 2018), one of which could be the combination of phages and antibiotics.

In order to eradicate the biofilm of the clinical isolate *S. aureus* D43-a, phage SAP-26 (*Siphoviridae, Phietavirus*) was administered simultaneously with azithromycin, vancomycin, or rifampicin (Rahman et al., 2011). A synergistic effect was observed during treatment of the 24-h-old biofilm with SAP-26 and rifampicin leading to around 35% of surviving cells, while phage combinations with azithromycin or vancomycin revealed survival rates of about 40% and 60%, respectively. With phage alone, 72% of the bacteria survived, whereas the survival rate with single rifampicin, azithromycin, or vancomycin application was 60, 75, and 83%, respectively. Biofilm eradication was also demonstrated by field emission scanning electron microscopy, which identified only few bacterial cells, most of which with irregular morphology after combined therapy. Thus, this study showed for the first time that an *S. aureus* biofilm can efficiently be reduced by the use of an appropriate mixture of phage and antibiotic, in this case rifampicin.

By using a continuous culture system, the dual treatment of gentamicin and phage SA5 (*Myoviridae*, *Kayvirus*) was tested against the clinical isolate PS80 (Kirby, 2012). In fact, the combination was more efficacious than single therapies after 72 h of treatment. The synergistic effect was explained by gentamicin leading *S. aureus* cells to assume an aggregate phenotype. And although this phenotype eases biofilm formation (as an attempt to evade antibiotic activity), it is also more susceptible to the phage attack, resulting ultimately in lower cell densities (Kirby, 2012). Even more, no phage resistant cells were identified in the dual approach as opposed to the phage-only treatment. Notably, aggregate formation upon antibiotic exposure has frequently been reported for other strains and species (Kirby, 2012), indicating that this antimicrobial combination may be of broader suitability.

Yilmaz et al. evaluated the therapeutic potential of Phage Sb-1 (*Myoviridae*, *Kayvirus*) and teicoplanin in a rat tibiae infection model induced by a clinical isolate of MRSA (Yilmaz et al., 2013). The antibiotic was applied intraperitoneally once a day for 2 weeks, while the phage was administered through the skin, directly into the medullary canal, once a day for 3 consecutive days. This treatment resulted in more than 3-fold decrease of colony-forming units compared to the single application of the antibiotic and more than 6-fold decrease compared to the application of phage Sb-1 alone. Moreover, the development of a biofilm was only prevented with the combination therapy. For this reason, local phage application as adjunct to antibiotic therapy against MRSA holds great potential for use in orthopedic surgery.

Comparably promising results were obtained by treatment of diabetic mice with MRSA-induced hindpaw foot infections (*S. aureus* strain ATCC 43300). Treatment was performed with a local administration of phage MR-10 (*Myoviridae*) and a simultaneous oral application of linezolid (Chhibber et al., 2013). When assessed after 1, 3, and 5 days, the combination led to the strongest reduction of the bacterial load compared to mono-treatments, which was also verified by a stronger decline of clinical signs, such as lesion score, foot myeloperoxidase activity, and histopathology. Measurements after 7, 9, and 12 days of treatment revealed entire absence of bacteria in the combination treatment, but also in the monotherapy groups. Although the bacterial load did not differ significantly among the different treatment groups, the fact that the overall tissue healing was expedited argues for the combined treatment approach for preventing foot infections with MRSA. Clearly, diabetic foot infections are polymicrobial (Jneid et al., 2018), however, MRSA is highly prevalent and difficult to treat in diabetes patients worldwide. Using phage MR-10 with its reported host range >90% of tested clinical *S. aureus* isolates in combination with antibiotics could therefore at least mitigate the overall complications associated with such infections (Chhibber et al., 2013).

KLEBSIELLA PNEUMONIAE

K. pneumoniae causes serious infections, especially in immunocompromised individuals, including pneumonia, bacteremia, or meningitis (Decré et al., 2011; Paczosa and Mecsas, 2016). However, some hyper-virulent *K. pneumoniae* strains have been reported to affect also healthy individuals (Paczosa and Mecsas, 2016). Allied to this, the ability of this bacterium to resist against a considerable number of antimicrobials asks for alternative strategies to treat *K. pneumoniae* infections.

For instance, the anti-biofilm effect of the combination of the phage KPO1K2 (*Podoviridae, T7-like virus*) and ciprofloxacin did not lead to a significant difference compared to single administrations applied on a 12-h-old biofilm of *K. pneumoniae*

(Verma et al., 2009b). However, there was no negative interference and the frequency of emerging antibiotic or phage resistant cells was significantly lower with the combined approach. Unfortunately, with continued age of the biofilm, the anti-biofilm efficiency of either compound alone and together dropped markedly (Verma et al., 2010). When switching to amoxicillin as the antibiotic complement to the phage, the outcome of the dual approach scored better with minor statistical significance, indicating that beta-lactams are the preferable partner to phages against this species (Bedi et al., 2009). The same group also exploited the combined therapy to treat an experimental lobar pneumonia induced by *K. pneumoniae* B5055 in a mouse model (Chhibber et al., 2008). To this end, an intranasal injection of the podovirus SS (*Podoviridae*) was added together with amikacin. Again, the authors reported no additional advantage with the combined approach, however, they hinted at the different antimicrobial actions of both compounds, which should minimize the emergence of resistance. Unfortunately, this was not further investigated in this study. Given that only one reference strain and only phages from the *Podoviridae* family were tested against *K. pneumoniae* so far, a gallery of combinations still awaits to be explored against this pathogen.

ACINETOBACTER BAUMANNII

A. baumannii is responsible for several outbreaks worldwide (Dijkshoorn et al., 2007) causing a wide spectrum of infections including bacteremia, meningitis, pneumoniae as well as wound- and urinary tract infections (Peleg et al., 2008). Besides a high tolerance against harsh environmental conditions such as desiccation, UV, detergents, and disinfectants, intrinsic and acquired antibiotic resistance mechanisms constitute a major obstacle for controlling this nosocomial pathogen (Wendt et al., 1997; Wisplinghoff et al., 2007; Peleg et al., 2008). Consequently, strong interest in alternative antibacterial strategies exists also for *A. baumannii*. Nevertheless, we are aware of only one study, in which the combined use of antibiotics and phages was investigated.

Jansen et al. tested phage vB_AbaM-KARL-1 (*Myoviridae*, *T4-like virus*) in combination with each of the three antibiotics, meropenem, ciprofloxacin, and colistin against multi-drug resistant clinical isolates (Jansen et al., 2018). Although a complete clearance of planktonic *A. baumannii* cultures was achieved at a phage MOI of 10^{-1} and meropenem, the extent of additional bacterial suppression was most strongly pronounced when the phage titer was very low (i.e., MOI of 10^{-7}). Likewise, significant stronger antibacterial effects were observed with colistin using the phage at an MOI of 10^{-7}. Apparently, at higher phage titers, KARL-1 is already very effective with only little improvement by the co-addition of antibiotics. However, the lack of antibacterial efficiency due to a low amount of phages could be overcome by the addition of meropenem or colistin. Such an effect was not observed with ciprofloxacin. The authors also reported that the emergence of phage resistant variants could at least be hampered with the co-addition of meropenem. Whether or not the development of resistant variants could also be delayed with the other two antibiotics was not further investigated in this study.

ENTEROCOCCUS FAECALIS

E. faecalis is well-known as opportunistic pathogen related to nosocomial infections, endocarditis, and endodontic infections, among others (Fisher and Phillips, 2009; Muller et al., 2015; Madsen et al., 2017). The genetic plasticity of this species allowed it to succeed in the healthcare environment and the high levels of resistance have been compromising clinical treatment with conventional strategies (Miller et al., 2014; Muller et al., 2015).

A phage cocktail consisting of the two phages EFDG1 and EFLK1 (*Myoviridae*), was used in combination with ampicillin for treatment of septic peritonitis in a mouse model with the vancomycin resistant *E. faecalis* (VRE) strain V583, also referred to as ATCC 700802 (Gelman et al., 2018). Sub-optimal concentrations of the antibiotic were used, in order to mimic the PAS-effect. As a result, mouse mortality rates were similar between the dual therapy and single application of phages, but expectedly lower than the antibiotic-alone approach. The bacterial load in intra- and extra abdominal organs, such as liver and heart, was stronger reduced with the combined approach compared to either single therapy. Sensitivity to ampicillin, vancomycin, or to the phage cocktail of cultured bacteria from these organs revealed no difference between the single or dual treatments. Interestingly, recovery of active phages after the treatment revealed lower phage titers with the combined strategy compared to the phage-alone treatment. This result opposes to, what occurs in PAS, in which the antibiotic stimulates the phage production. Therefore, since the combined approach was more successful in reducing the bacterial load, positive antibiotic-phage interactions other than PAS must have determined the clinical outcome. Notably, phage treatment did not lead to an alteration of the gut microbiome as revealed by 16S rRNA amplicon sequencing of mice stool samples. This is valuable ancillary information considering that the potential impact of phage therapy on the natural microflora is poorly understood so far.

BURKHOLDERIA CEPACIA

B. cepacia is an opportunistic pathogen responsible for rare cases of nosocomial infections and is especially related to pulmonary infections in cystic fibrosis patients. The symptoms of *B. cepacia* infections can differ from asymptomatic to respiratory failure and the treatment is problematic considering that this bacteria has an intrinsic resistance to many antibiotics (Horsley et al., 2016; Garcia et al., 2018).

Kamal and Dennis investigated PAS among several antibiotics belonging to four different classes and two distinct phages KS12 (*Myoviridae*) and KS14 (*Myoviridae*, *P2-like virus*) (Kamal and Dennis, 2015). By comparing plaque diameter in two *B. cepacia strains* C6433 and K56-2, PAS was observed with minocycline, levofloxacin, ceftazidime, meropenem, ciprofloxacin, and

tetracycline, of which the three latter compounds produced the strongest results. No PAS was seen with ampicillin, kanamycin, and piperacillin. Cell filamentation occurred under exposure to meropenem and ciprofloxacin, which is in keeping with previous observations that this altered cell morphology favors PAS (Comeau et al., 2007). However, obviously PAS can also occur without filamentation, as tetracycline led to cell clustering, which enabled phages to move across the increased cell surfaces thereby increasing the chance of contacting cell receptors (Kamal and Dennis, 2015).

PAS was further confirmed with phage KS12 and strain K56-2 based on growth/kill curves and using larvae of *Galleria mellonella* as infection model (Kamal and Dennis, 2015). Survival rates of larvae were significantly increased with low-dose of meropenem and phage compared to either single treatment. Thus, the functionality of PAS could again be confirmed *in vivo*. It is known that *B. cepacia* can hardly be cleared from the lungs of patients with cystic fibrosis, for among other reasons, because antibiotics poorly penetrate into the tenacious biofilm. Ironically and fortunately, this could, however, have a practical medical implication, because with low amounts of antibiotics arriving at the bacterial target, optimal conditions for PAS might be realized. It would therefore be a worthwhile endeavor to investigate the therapeutic value of a joint application of antibiotics and phages in humans suffering from cystic fibrosis.

CONCLUDING REMARKS

As a quintessence from the studies described in this review the combined treatment with phage and antibiotic is generally well-appreciated. Better clearance of bacterial cells and reduced evolvement of phage or antibiotic resistance are the major advantages of the joint therapy. Positive interactions between phages and antibiotics against which the pathogen is *a priori* resistant, gives hope that combined treatments will also be successful against the worst case of pandrug-resistant "super bugs" (Magiorakos et al., 2012). Depending on the type of antibiotic and phage, PAS has frequently been observed (e.g., Ryan et al., 2012; Uchiyama et al., 2018). And although representing no ubiquitous mechanism, PAS worked in biofilms as well (Ryan et al., 2012) and first data have demonstrated its occurrence under *in vivo* conditions (Kamal and Dennis, 2015). However, apart from neutral effects, the opposite of PAS has also been observed. The underlying negative interactions between the antimicrobials seem to be, however, only transient and the phages are not further disturbed by the presence of the antibiotic at a later treatment stage (Torres-Barceló et al., 2018). Combination therapies might greatly benefit from the careful choice of dosing and from the time points at which either antimicrobial substance is administered. In future studies particular attention should be given to sequential application, as at least two studies with *P. aeruginosa* demonstrated an improved therapeutic effect, when the antibiotic were introduced after phages had already started to tackle the bacteria (Torres-Barceló et al., 2014; Chaudhry et al., 2017). The attempt to evade the phage attack apparently makes the pathogen more vulnerable toward certain antibiotics. This concept warrants further investigation for other pathogenic bacteria and may ultimately turn out to be superior over simultaneous applications in most cases.

Additional interesting insights of phage/antibiotic combinations have recently been obtained using *Pseudomonas fluorescens*, which is a rare human pathogen, as model organism. Some of the results corroborate and some contradict previous findings with pathogenic bacteria. First, using a combination of kanamycin and phage SBW25Φ2 robustly prevented resistance evolution in *P. fluorescens* strain SBW25, which was not seen with either antimicrobial alone and which is in line with previous findings (Zhang and Buckling, 2012). Second, the sequential addition of rifampicin and the phage SBW25Φ 2 was more effective at reducing *P. fluorescens* SBW25 populations than their simultaneous employment. This is in line with the aforementioned observations of successful sequential treatment, except that this time the antibiotic was given first, followed by the phage. Here, stress induced by rifampicin made the population less able to evolve resistance against the phage (Escobar-Páramo et al., 2012). Lastly, using the same bacteria/phage system, the opposite of PAS was demonstrated. Using sub-MICs of the antibiotic streptomycin (Sm) increased the rate of phage resistance evolution and caused extinction of the phage. The combination also enhanced the evolution of Sm resistance compared with Sm alone (Cairns et al., 2017). Since Sm is a known mutagen, higher mutation rates may have been responsible for this counterintuitive development. However, the data also show that general conclusions about the functionality of phage/antibiotic combinations are difficult to draw. Negative interference might be more common as assumed, and it is possible that such experimental outcomes in the laboratory are less frequently reported than the positive ones. Negative results, however, should be encouraged for publication (Levin, 2014), as it avoids that mistakes are repeated and as it fosters the successful search for suitable phage/antibiotic combinations.

In order to achieve ever more improvements with phage/antibiotic combinations, the key to ultimate success might probably be the use of tailored bio-engineered phages as adjuvants for antibiotics (e.g., Lu and Collins, 2009). However, although we are in the age of synthetic biology (Barbu et al., 2016), the reluctance toward using replicating entities for therapy may be complicated by general public concerns surrounding the use of genetically manipulated compounds within humans (Bawa and Anilakumar, 2013). Nevertheless, bio-engineered phages may become broadly used eventually in the future, but it can be anticipated, that more progress with natural (i.e., genetically unmodified) phages will also be made in the meantime.

We conclude with the note, that at present, there is still a large gap in knowledge regarding the precise mechanisms that drive the phage/antibiotic interactions. Therefore, for now, it remains difficult to predict the optimal combinations for a given bacterial pathogen. Nevertheless, the encouraging results obtained so far suggest that the continued experimentation with phage/antibiotic combinations is an endeavor, which likely will

pay off in future as an ultimate and robust remedy against multi-drug resistant bacteria.

AUTHOR CONTRIBUTIONS

H-PH designed the research. TT and MJ performed the research. TT and MJ analyzed the data and TT, MJ, and H-PH wrote the paper.

ACKNOWLEDGMENTS

TT was supported by CNPq Scholarship—Brazil.

SUPPLEMENTARY MATERIAL

The Supplementary Material for this article can be found online at: https://www.frontiersin.org/articles/10.3389/fcimb.2019.00022/full#supplementary-material

REFERENCES

Alshalchi, S. A., and Anderson, G. G. (2015). Expression of the lipopolysaccharide biosynthesis gene lpxD affects biofilm formation of *Pseudomonas aeruginosa*. *Arch. Microbiol.* 197, 135–145. doi: 10.1007/s00203-014-1030-y

Barbu, E. M., Cady, K. C., and Hubby, B. (2016). Phage therapy in the era of synthetic biology. *Cold Spring Harb. Perspect. Biol.* 8:a023879. doi: 10.1101/cshperspect.a023879

Bawa, A. S., and Anilakumar, K. R. (2013). Genetically modified foods: safety, risks and public concerns—a review. *J. Food Sci. Technol.* 50, 1035–1046. doi: 10.1007/s13197-012-0899-1

Bedi, M. S., Verma, V., and Chhibber, S. (2009). Amoxicillin and specific bacteriophage can be used together for eradication of biofilm of *Klebsiella pneumoniae* B5055. *World J. Microbiol. Biotechnol.* 25, 1145–1151. doi: 10.1007/s11274-009-9991-8

Blount, Z. D. (2015). The unexhausted potential of *E. coli*. *eLife* 4:e05826. doi: 10.7554/eLife.05826

Cairns, J., Becks, L., Jalasvuori, M., and Hiltunen, T. (2017). Sublethal streptomycin concentrations and lytic bacteriophage together promote resistance evolution. *Philos. Trans. R. Soc. B Biol. Sci.* 372:20160040. doi: 10.1098/rstb.2016.0040

Chan, B. K., Sistrom, M., Wertz, J. E., Kortright, K. E., Narayan, D., and Turner, P. E. (2016). Phage selection restores antibiotic sensitivity in MDR *Pseudomonas aeruginosa*. *Sci. Rep.* 6:26717. doi: 10.1038/srep26717

Chan, B. K., Turner, P. E., Kim, S., Mojibian, H. R., Elefteriades, J. A., and Narayan, D. (2018). Phage treatment of an aortic graft infected with Pseudomonas aeruginosa. *Evol. Med. Public Health* 2018, 60–66. doi: 10.1093/emph/eoy005

Chanishvili, N. (2012). Phage therapy—History from twort and d'herelle through soviet experience to current approaches *Adv. Virus Res.* 83, 3–40. doi: 10.1016/B978-0-12-394438-2.00001-3

Chaudhry, W. N., Concepción-Acevedo, J., Park, T., Andleeb, S., Bull, J. J., and Levin, B. R. (2017). Synergy and order effects of antibiotics and phages in killing *Pseudomonas aeruginosa* biofilms. *PLoS ONE* 12:e0168615. doi: 10.1371/journal.pone.0168615

Chhibber, S., Kaur, S., and Kumari, S. (2008). Therapeutic potential of bacteriophage in treating *Klebsiella pneumoniae* B5055-mediated lobar pneumonia in mice. *J. Med. Microbiol.* 57, 1508–1513. doi: 10.1099/jmm.0.2008/002873-0

Chhibber, S., Kaur, T., and Sandeep, K. (2013). Co-therapy using lytic bacteriophage and linezolid: effective treatment in eliminating methicillin resistant *Staphylococcus aureus* (MRSA) from diabetic foot infections. *PLoS ONE* 8:e56022. doi: 10.1371/journal.pone.0056022

Choo, E. J., and Chambers, H. F. (2016). Treatment of methicillin-resistant *Staphylococcus aureus* bacteremia. *Infect. Chemother.* 48, 267. doi: 10.3947/ic.2016.48.4.267

Comeau, A. M., Tétart, F., Trojet, S. N., Prère, M.-F., and Krisch, H. M. (2007). Phage-antibiotic synergy (PAS): β-lactam and quinolone antibiotics stimulate virulent phage growth. *PLoS ONE* 2:e799. doi: 10.1371/journal.pone.0000799

Coulter, L. B., McLean, R. J., Rohde, R. E., and Aron, G. M. (2014). Effect of bacteriophage infection in combination with tobramycin on the emergence of resistance in *Escherichia coli* and *Pseudomonas aeruginosa* biofilms. *Viruses* 6, 3778–3786. doi: 10.3390/v6103778

Danis-Wlodarczyk, K., Vandenheuvel, D., Jang, H. B., Briers, Y., Olszak, T., Arabski, M., et al. (2016). A proposed integrated approach for the preclinical evaluation of phage therapy in *Pseudomonas* infections. *Sci. Rep.* 6:28115. doi: 10.1038/srep28115

De Soyza, A., Hall, A. J., Mahenthiralingam, E., Drevinek, P., Kaca, W., Drulis-Kawa, Z., et al. (2013). Developing an international *Pseudomonas aeruginosa* reference panel. *Microbiologyopen* 2, 1010–1023. doi: 10.1002/mbo3.141

Decré, D., Verdet, C., Emirian, A., Le Gourrierec, T., Petit, J.-C., Offenstadt, G., et al. (2011). Emerging severe and fatal infections due to *Klebsiella pneumoniae* in two university hospitals in France. *J. Clin. Microbiol.* 49, 3012–3014. doi: 10.1128/JCM.00676-11

Dijkshoorn, L., Nemec, A., and Seifert, H. (2007). An increasing threat in hospitals: multidrug-resistant *Acinetobacter baumannii*. *Nat. Rev. Microbiol.* 5, 939–951. doi: 10.1038/nrmicro1789

Escobar-Páramo, P., Gougat-Barbera, C., and Hochberg, M. E. (2012). Evolutionary dynamics of separate and combined exposure of *Pseudomonas fluorescens* SBW25 to antibiotics and bacteriophage: combined exposure to antibiotics and phage. *Evol. Appl.* 5, 583–592. doi: 10.1111/j.1752-4571.2012.00248.x

Fisher, K., and Phillips, C. (2009). The ecology, epidemiology and virulence of Enterococcus. *Microbiology* 155, 1749–1757. doi: 10.1099/mic.0.026385-0

Garcia, B. A., Carden, J. L., Goodwin, D. L., Smith, T. A., Gaggar, A., Leon, K., et al. (2018). Implementation of a successful eradication protocol for *Burkholderia cepacia* complex in cystic fibrosis patients. *BMC Pulm. Med.* 18:35. doi: 10.1186/s12890-018-0594-8

Gelman, D., Beyth, S., Lerer, V., Adler, K., Poradosu-Cohen, R., Coppenhagen-Glazer, S., et al. (2018). Combined bacteriophages and antibiotics as an efficient therapy against VRE *Enterococcus faecalis* in a mouse model. *Res. Microbiol.* 169, 531–539. doi: 10.1016/j.resmic.2018.04.008

Hagens, S., Habel, A., and Bläsi, U. (2006). Augmentation of the antimicrobial efficacy of antibiotics by filamentous phage. *Microb Drug Resist.* 12, 164–168. doi: 10.1089/mdr.2006.12.164

Hassoun, A., Linden, P. K., and Friedman, B. (2017). Incidence, prevalence, and management of MRSA bacteremia across patient populations—a review of recent developments in MRSA management and treatment. *Crit. Care* 21:211. doi: 10.1186/s13054-017-1801-3

Holland, S. J., Sanz, C., and Perham, R. N. (2006). Identification and specificity of pilus adsorption proteins of filamentous bacteriophages infecting *Pseudomonas aeruginosa*. *Virology* 345, 540–548. doi: 10.1016/j.virol.2005.10.020

Horsley, A., Jones, A. M., and Lord, R. (2016). Antibiotic treatment for *Burkholderia cepacia* complex in people with cystic fibrosis experiencing a pulmonary exacerbation. *Cochrane Database Syst. Rev.* CD009529. doi: 10.1002/14651858.CD009529.pub3

Huff, W. E., Huff, G. R., Rath, N. C., Balog, J. M., and Donoghue, A. M. (2004). Therapeutic efficacy of bacteriophage and Baytril (enrofloxacin) individually and in combination to treat colibacillosis in broilers. *Poult. Sci.* 83, 1944–1947. doi: 10.1093/ps/83.12.1944

Jansen, M., Wahida, A., Latz, S., Krüttgen, A., Häfner, H., Buhl, E. M., et al. (2018). Enhanced antibacterial effect of the novel T4-like bacteriophage KARL-1 in combination with antibiotics against multi-drug resistant *Acinetobacter baumannii*. *Sci. Rep.* 8:14140. doi: 10.1038/s41598-018-32344-y

Jneid, J., Cassir, N., Schuldiner, S., Jourdan, N., Sotto, A., Lavigne, J.-P., et al. (2018). Exploring the microbiota of diabetic foot infections with culturomics. *Front. Cell. Infect. Microbiol.* 8:282. doi: 10.3389/fcimb.2018.00282

Kamal, F., and Dennis, J. J. (2015). *Burkholderia cepacia* complex phage-antibiotic synergy (PAS): antibiotics stimulate lytic phage activity. *Appl. Environ. Microbiol.* 81, 1132–1138. doi: 10.1128/AEM.02850-14

Khawaldeh, A., Morales, S., Dillon, B., Alavidze, Z., Ginn, A. N., Thomas, L., et al. (2011). Bacteriophage therapy for refractory *Pseudomonas aeruginosa* urinary tract infection. *J. Med. Microbiol.* 60, 1697–1700. doi: 10.1099/jmm.0.029744-0

Kirby, A. E. (2012). Synergistic Action of gentamicin and bacteriophage in a continuous culture population of *Staphylococcus aureus*. *PLoS ONE* 7:e51017. doi: 10.1371/journal.pone.0051017

Knezevic, P., Curcin, S., Aleksic, V., Petrusic, M., and Vlaski, L. (2013). Phage-antibiotic synergism: a possible approach to combatting *Pseudomonas aeruginosa*. *Res. Microbiol.* 164, 55–60. doi: 10.1016/j.resmic.2012.08.008

Kung, V. L., Ozer, E. A., and Hauser, A. R. (2010). The accessory genome of *Pseudomonas aeruginosa*. *Microbiol. Mol. Biol. Rev.* 74, 621–641. doi: 10.1128/MMBR.00027-10

Lee, A. S., de Lencastre, H., Garau, J., Kluytmans, J., Malhotra-Kumar, S., Peschel, A., et al. (2018). Methicillin-resistant *Staphylococcus aureus*. *Nat. Rev. Dis. Primers* 4, 18033. doi: 10.1038/nrdp.2018.33

Levin, L. (2014). Publishing negative results - sometimes it is more important! *Quintessence Int.* 45, 635. doi: 10.3290/j.qi.a32445

Lin, D. M., Koskella, B., and Lin, H. C. (2017). Phage therapy: an alternative to antibiotics in the age of multi-drug resistance. *World J. Gastrointest. Pharmacol. Ther.* 8, 162. doi: 10.4292/wjgpt.v8.i3.162

Lu, T. K., and Collins, J. J. (2009). Engineered bacteriophage targeting gene networks as adjuvants for antibiotic therapy. *Proc. Natl. Acad. Sci. U.S.A.* 106, 4629–4634. doi: 10.1073/pnas.0800442106

Madsen, K. T., Skov, M. N., Gill, S., and Kemp, M. (2017). Virulence factors associated with infective endocarditis: a mini review. *Open Microbiol. J.* 11, 1–11. doi: 10.2174/1874285801711010001

Magiorakos, A.-P., Srinivasan, A., Carey, R. B., Carmeli, Y., Falagas, M. E., Giske, C. G., et al. (2012). Multidrug-resistant, extensively drug-resistant and pandrug-resistant bacteria: an international expert proposal for interim standard definitions for acquired resistance. *Clin. Microbiol. Infect.* 18, 268–281. doi: 10.1111/j.1469-0691.2011.03570.x

Mihara, T., Nishimura, Y., Shimizu, Y., Nishiyama, H., Yoshikawa, G., Uehara, H., et al. (2016). Linking virus genomes with host taxonomy. *Viruses* 8, 66. doi: 10.3390/v8030066

Miller, W. R., Munita, J. M., and Arias, C. A. (2014). Mechanisms of antibiotic resistance in enterococci. *Expert Rev. Anti Infect. Ther.* 12, 1221–1236. doi: 10.1586/14787210.2014.956092

Muller, C., Cacaci, M., Sauvageot, N., Sanguinetti, M., Rattei, T., Eder, T., et al. (2015). The intraperitoneal transcriptome of the opportunistic pathogen *Enterococcus faecalis* in mice. *PLoS ONE* 10:e0126143. doi: 10.1371/journal.pone.0126143

Nobrega, F. L., Costa, A. R., Kluskens, L. D., and Azeredo, J. (2015). Revisiting phage therapy: new applications for old resources. *Trends Microbiol.* 23, 185–191. doi: 10.1016/j.tim.2015.01.006

Oechslin, F., Piccardi, P., Mancini, S., Gabard, J., Moreillon, P., Entenza, J. M., et al. (2017). Synergistic interaction between phage therapy and antibiotics clears *Pseudomonas aeruginosa* infection in endocarditis and reduces virulence. *J. Infect. Dis.* 215, 703–712. doi: 10.1093/infdis/jiw632

Ojala, V., Laitalainen, J., and Jalasvuori, M. (2013). Fight evolution with evolution: plasmid-dependent phages with a wide host range prevent the spread of antibiotic resistance. *Evol. Appl.* 6, 925–932. doi: 10.1111/eva.12076

Oliveira, D., Borges, A., and Simões, M. (2018). *Staphylococcus aureus* toxins and their molecular activity in infectious diseases. *Toxins* 10:252. doi: 10.3390/toxins10060252

O'Neil, J. (2016). *Tackling Drug-Resistant Infections Globally: Final Report And Recommendations*. Available online at: http://amr-review.org.

Paczosa, M. K., and Mecsas, J. (2016). *Klebsiella pneumoniae*: going on the offense with a strong defense. *Microbiol. Mol. Biol. Rev.* 80, 629–661. doi: 10.1128/MMBR.00078-15

Peleg, A. Y., Seifert, H., and Paterson, D. L. (2008). *Acinetobacter baumannii*: emergence of a successful pathogen. *Clin. Microbiol. Rev.* 21, 538–582. doi: 10.1128/CMR.00058-07

Pelfrene, E., Willebrand, E., Cavaleiro Sanches, A., Sebris, Z., and Cavaleri, M. (2016). Bacteriophage therapy: a regulatory perspective. *J. Antimicrob. Chemother.* 71, 2071–2074. doi: 10.1093/jac/dkw083

Rahman, M., Kim, S., Kim, S. M., Seol, S. Y., and Kim, J. (2011). Characterization of induced Staphylococcus aureus bacteriophage SAP-26 and its anti-biofilm activity with rifampicin. *Biofouling* 27, 1087–1093. doi: 10.1080/08927014.2011.631169

Rice, L. B. (2008). Federal funding for the study of antimicrobial resistance in nosocomial pathogens: No ESKAPE. *J. Infect. Dis.* 197, 1079–1081. doi: 10.1086/533452

Ryan, E. M., Alkawareek, M. Y., Donnelly, R. F., and Gilmore, B. F. (2012). Synergistic phage-antibiotic combinations for the control of *Escherichia coli* biofilms *in vitro*. *FEMS Immunol. Med. Microbiol.* 65, 395–398. doi: 10.1111/j.1574-695X.2012.00977.x

Shen, M., Le, S., Jin, X., Li, G., Tan, Y., Li, M., et al. (2016). Characterization and comparative genomic analyses of *Pseudomonas aeruginosa* phage PaoP5: new members assigned to PAK_P1-like viruses. *Sci. Rep.* 6:34067. doi: 10.1038/srep34067

Sousa, A. M., and Pereira, M. O. (2014). *Pseudomonas aeruginosa* diversification during infection development in cystic fibrosis lungs—A review. *Pathogens* 3, 680–703. doi: 10.3390/pathogens3030680

Tong, S. Y., Davis, J. S., Eichenberger, E., Holland, T. L., and Fowler, V. G. (2015). *Staphylococcus aureus* infections: epidemiology, pathophysiology, clinical manifestations, and management. *Clin. Microbiol. Rev.* 28, 603–661. doi: 10.1128/CMR.00134-14

Torres-Barceló, C., Arias-Sánchez, F. I., Vasse, M., Ramsayer, J., Kaltz, O., and Hochberg, M. E. (2014). A window of opportunity to control the bacterial pathogen *Pseudomonas aeruginosa* combining antibiotics and phages. *PLoS ONE* 9:e106628. doi: 10.1371/journal.pone.0106628

Torres-Barceló, C., Gurney, J., Gougat-Barberá, C., Vasse, M., and Hochberg, M. E. (2018). Transient negative effects of antibiotics on phages do not jeopardise the advantages of combination therapies. *FEMS Microbiol. Ecol.* 94:fiy107. doi: 10.1093/femsec/fiy107

Torres-Barceló, C., and Hochberg, M. E. (2016). Evolutionary rationale for phages as complements of antibiotics. *Trends Microbiol.* 24, 249–256. doi: 10.1016/j.tim.2015.12.011

Uchiyama, J., Shigehisa, R., Nasukawa, T., Mizukami, K., Takemura-Uchiyama, I., Ujihara, T., et al. (2018). Piperacillin and ceftazidime produce the strongest synergistic phage–antibiotic effect in *Pseudomonas aeruginosa*. *Arch. Virol.* 163, 1941–1948. doi: 10.1007/s00705-018-3811-0

Valério, N., Oliveira, C., Jesus, V., Branco, T., Pereira, C., Moreirinha, C., et al. (2017). Effects of single and combined use of bacteriophages and antibiotics to inactivate *Escherichia coli*. *Virus Res.* 240, 8–17. doi: 10.1016/j.virusres.2017.07.015

Verma, V., Harjai, K., and Chhibber, S. (2009a). Characterization of a T7-like lytic bacteriophage of *Klebsiella pneumoniae* B5055: a potential therapeutic agent. *Curr. Microbiol.* 59, 274–281. doi: 10.1007/s00284-009-9430-y

Verma, V., Harjai, K., and Chhibber, S. (2009b). Restricting ciprofloxacin-induced resistant variant formation in biofilm of *Klebsiella pneumoniae* B5055 by complementary bacteriophage treatment. *J. Antimicrob. Chemother.* 64, 1212–1218. doi: 10.1093/jac/dkp360

Verma, V., Harjai, K., and Chhibber, S. (2010). Structural changes induced by a lytic bacteriophage make ciprofloxacin effective against older biofilm of *Klebsiella pneumoniae*. *Biofouling* 26, 729–737. doi: 10.1080/08927014.2010.511196

Vila, J., Sáez-López, E., Johnson, J. R., Römling, U., Dobrindt, U., Cantón, R., et al. (2016). *Escherichia coli* : an old friend with new tidings. *FEMS Microbiol. Rev.* 40, 437–463. doi: 10.1093/femsre/fuw005

Villarroel, J., Larsen, M. V., Kilstrup, M., and Nielsen, M. (2017). Metagenomic analysis of therapeutic PYO phage cocktails from 1997 to 2014. *Viruses* 9, 328. doi: 10.3390/v9110328

Wendt, C., Dietze, B., Dietz, E., and Rüden, H. (1997). Survival of *Acinetobacter baumannii* on dry surfaces. *J. Clin. Microbiol.* 35, 1394–1397.

Wisplinghoff, H., Schmitt, R., Wöhrmann, A., Stefanik, D., and Seifert, H. (2007). Resistance to disinfectants in epidemiologically defined clinical isolates of *Acinetobacter baumannii*. *J. Hosp. Infect.* 66, 174–181. doi: 10.1016/j.jhin.2007.02.016

Wunderink, R. G., Niederman, M. S., Kollef, M. H., Shorr, A. F., Kunkel, M. J., Baruch, A., et al. (2012). Linezolid in methicillin-resistant *Staphylococcus aureus* nosocomial pneumonia: a randomized, controlled study. *Clin. Infect. Dis.* 54, 621–629. doi: 10.1093/cid/cir895

Yilmaz, C., Colak, M., Yilmaz, B. C., Ersoz, G., Kutateladze, M., and Gozlugol, M. (2013). Bacteriophage therapy in implant-related infections: an experimental study. *J. Bone Joint Surg. Am.* 95, 117–125. doi: 10.2106/JBJS.K.01135

Zhang, Q.-G., and Buckling, A. (2012). Phages limit the evolution of bacterial antibiotic resistance in experimental microcosms: phages limit bacterial antibiotic resistance. *Evol. Appl.* 5, 575–582. doi: 10.1111/j.1752-4571.2011.00236.x

Conflict of Interest Statement: The authors declare that the research was conducted in the absence of any commercial or financial relationships that could be construed as a potential conflict of interest.

frontiers in Cellular and Infection Microbiology

ORIGINAL RESEARCH
published: 28 February 2019
doi: 10.3389/fcimb.2019.00037

Auranofin Releasing Antibacterial and Antibiofilm Polyurethane Intravascular Catheter Coatings

Hanyang Liu[1†], Shashank Shukla[1†], Noel Vera-González[1†], Nagendran Tharmalingam[2], Eleftherios Mylonakis[2], Beth Burgwyn Fuchs[2] and Anita Shukla[1]*

[1] Center for Biomedical Engineering, School of Engineering, Institute for Molecular and Nanoscale Innovation, Brown University, Providence, RI, United States, [2] Division of Infectious Diseases, Rhode Island Hospital, Alpert Medical School and Brown University, Providence, RI, United States

OPEN ACCESS

Edited by:
Rodolfo García-Contreras, National Autonomous University of Mexico, Mexico

Reviewed by:
Martijn Riool, Academic Medical Center (AMC), Netherlands
César de la Fuente, Massachusetts Institute of Technology, United States

***Correspondence:**
Anita Shukla
anita_shukla@brown.edu

[†] *These authors have contributed equally to this work and are co-first authors*

Specialty section:
This article was submitted to Clinical Microbiology, a section of the journal Frontiers in Cellular and Infection Microbiology

Received: *27 November 2018*
Accepted: *07 February 2019*
Published: *28 February 2019*

Citation:
Liu H, Shukla S, Vera-González N, Tharmalingam N, Mylonakis E, Fuchs BB and Shukla A (2019) Auranofin Releasing Antibacterial and Antibiofilm Polyurethane Intravascular Catheter Coatings. Front. Cell. Infect. Microbiol. 9:37. doi: 10.3389/fcimb.2019.00037

Intravascular catheter related bloodstream infections (CRBSIs) are a leading cause of hospital-acquired infections worldwide, resulting not only in the burden of cost and morbidity for patients but also in the over-consumption of medical resources for hospitals and health care organizations. In this study, a novel auranofin releasing antibacterial and antibiofilm polyurethane (PU) catheter coating was developed and investigated for future use in preventing CRBSIs. Auranofin is an antirheumatic drug with recently identified antimicrobial properties. The drug carrier, PU, acts as a barrier surrounding the antibacterial agent, auranofin, to extend the drug release profile and improve its long-term antibacterial and antibiofilm efficacy and potentially the length of catheter implantation within a patient. The PU+auranofin coatings developed here were found to be highly stretchable (exhibiting ∼500% percent elongation), which is important for the compliance of the material on a flexible catheter. PU+auranofin coated catheters were able to inhibit the growth of methicillin-resistant *Staphylococcus aureus* (MRSA) for 8 to 26 days depending on the specific drug concentration utilized during the dip coating process. The PU+auranofin coated catheters were also able to completely inhibit MRSA biofilm formation *in vitro*, an effect that was not observed with auranofin or PU alone. Lastly, these coatings were found to be hemocompatible with human erythrocytes and maintain liver cell viability.

Keywords: antimicrobial catheter coating, antibiofilm, auranofin, polyurethane, drug delivery, *Staphylococcus aureus*, catheter-related bloodstream infection

INTRODUCTION

Approximately 150 million intravascular catheters are implanted annually in the United States alone (Shah et al., 2013). Intravascular catheters are used for hemodynamic monitoring, renal replacement therapy, nutritional support, and administration of medications (Alberti et al., 2014). With the use of these intravascular devices comes a risk of catheter-related bloodstream infections (CRBSIs). Over 250,000 CRBSIs are diagnosed annually in the U.S. (Maki et al., 2006), making CRBSIs the most prevalent source of nosocomial bacteremia (Abebe et al., 2014). These infections can prolong hospital stays by ∼10–20 days and increase the cost of care from $4,000 to $56,000 per patient; more importantly, CRBSIs are associated with mortality rates of 12–25% (Maki et al., 2006).

CRBSIs are predominantly caused by Gram-positive bacteria including species of *Staphylococcus aureus* (Abebe et al., 2014). Intravascular catheters can become infected by microorganisms in several ways: the catheter lumen can be contaminated prior to use, the catheter tip and cutaneous tract can be contaminated by the skin microbiome during insertion, contaminated infusate can deliver bacteria, and inserted materials can be exposed to microbes due to an existing systemic infection (Pugach et al., 1999; Abebe et al., 2014). Once bacteria are introduced to the catheter material, they can adhere and begin the process of forming a biofilm, playing a significant role in CRBSI pathogenesis (Donlan, 2002; Raad et al., 2007). Biofilms are complex, surface-attached, three-dimensional microbial colonies, consisting of bacteria embedded within a self-secreted matrix containing proteins, polysaccharides, and extracellular DNA (Donlan, 2002). Once biofilms develop on medical device surfaces they can lead to device failure (Danese, 2002) and may also spread infection by releasing planktonic cells, which can colonize downstream sites (Costerton, 1999; Stewart, 2002; Lewis et al., 2005). Eradication of biofilms is a formidable challenge due to the many sophisticated mechanisms bacteria develop to protect against host defense mechanisms and the prevalence of increased resistance against traditional antibiotic treatments (Stewart, 2002; Flemming et al., 2016; Koo et al., 2017). The biofilm matrix forms a physical barrier hindering penetration and diffusion of antimicrobial agents (Costerton, 1999; Stewart, 2002), while the low metabolic state of biofilm bacteria make them less susceptible to antibiotics (Brown et al., 1988; de la Fuente-Núñez et al., 2013). Additionally, bacteria also coordinate their physiological processes through quorum sensing (Donlan, 2002; Li and Tian, 2016), allowing the cells to communicate by releasing and responding to small molecules aiding in colonization, defense against antimicrobials, and adaptation to the microenvironment (Li and Tian, 2016). The accumulation of biofilm within the catheter can lead to the need for implant removal.

Several methods have been utilized to prevent microbial colonization of catheters. The most common methods involve the use of antimicrobial loaded or antimicrobial coated catheters. Antimicrobial agents such as cefazolin (Kamal et al., 1991), minocycline, rifampin (Raad et al., 1996), chlorhexidine, and silver sulfadiazine (Maki et al., 1997) have been deposited directly on catheter surfaces using dip coating or solvent casting methods (Darouiche et al., 1999). However, these coating strategies often lead to rapid release of the entire antimicrobial payload (Danese, 2002). In order to provide sustained drug release and long-term therapeutic efficacy, antimicrobials can be incorporated on catheters within polymeric surface coatings. Pugach et al. developed a gelatin hydrogel coating encapsulating ciprofloxacin liposomes on silicone Foley catheters, which significantly delayed bacteria colonization *in vivo* compared to uncoated catheters (Pugach et al., 1999). Fischer et al. coated polyurethane catheters with silver nanoparticles embedded in star-shaped poly(ethylene glycol)-heparin hydrogels, achieving catheter hemocompatibility and antimicrobial functionality for up to a week *in vitro* (Fischer et al., 2015). Hook et al. identified a group of polymers capable of reducing bacterial attachment up to 30-fold when compared to a commercial silver hydrogel and successfully coated catheters with these polymers demonstrating *in vivo* antibacterial efficacy (Hook et al., 2012). Fu et al. and Curtin et al. loaded bacteriophage into *Lubri-sil*®, a neutral hydrogel coating, on silicone French Foley catheters. They observed a significant reduction in viable biofilm formation by *Staphylococcus epidermidis* on the catheters over a 24 h *in vitro* exposure period (Curtin and Donlan, 2006; Fu et al., 2010). The antimicrobial efficacy of these previously reported catheter coatings has been limited to a maximum of 2 weeks.

Despite the progress that has been made, the development of drug resistance remains a significant concern while utilizing traditional antibiotic therapeutics in available catheter technologies (Danese, 2002). Thus, we sought to incorporate and examine a recently identified antimicrobial agent with therapeutic potential in a new catheter coating. Auranofin is an FDA approved antirheumatic therapeutic that is a particularly promising antimicrobial candidate, having shown antibacterial and antifungal efficacy (Cassetta et al., 2014; Harbut et al., 2015; Fuchs et al., 2016; Thangamani et al., 2016) along with potent antibiofilm efficacy (Torres et al., 2016; AbdelKhalek et al., 2018). Auranofin exhibits effective antimicrobial activity primarily against Gram-positive pathogenic bacteria including *Mycobacterium tuberculosis*, *Bacillus subtilis*, and *Enterococcus faecalis*, drug-sensitive and drug-resistant *Enterococcus faecium*, and *S. aureus* (Harbut et al., 2015). The minimum inhibitory concentration (MIC) of auranofin against these bacteria is as low as 0.25 μg/mL (Hassanein et al., 2017). Auranofin has a unique mechanism of action that relies on its potent inhibition of bacterial thioredoxin reductase, an important protein in thiol based redox metabolism essential in maintaining cellular processes including protection against reactive oxygen species, protein folding, and DNA synthesis (Lundstrom and Holmgren, 1990; Ritz and Beckwith, 2001; Lu and Holmgren, 2014). Inhibiting the bacterial thioredoxin reductase and disrupting the redox balance results in cell death (Bonilla et al., 2008; Debnath et al., 2012; Tejman-Yarden et al., 2013). This antibacterial drug target has been shown to highly limit the development of drug resistance (Lin et al., 2016; Sweeney et al., 2017).

Localized delivery has the potential to provide rapid antimicrobial activity, while minimizing offsite toxicity and lowering susceptibility to resistance (Brooks and Brooks, 2014). Auranofin has previously been incorporated into polymeric particles for the localized treatment of bacterial infections (Pearson et al., 2015; Díez-Martínez et al., 2016). In this work, we report the development and *in vitro* characterization of an auranofin containing polyurethane (PU) catheter coating that may have the potential to lower the incidence of CRBSIs. To the best of our knowledge, this is the first report of an auranofin containing device coating. PU is an FDA approved polymer that has been used extensively in biomedical devices for over 45 years due to its biocompatibility, mechanical flexibility (Ding et al., 2012; He et al., 2012), and low protein fouling properties (Xue and Greisler, 2003; Wilson, 2004; Maki et al., 2006). Specifically, we utilized a commercially available aromatic polyether-based PU, Texin RxT85A, to develop the auranofin encapsulating coatings reported in this work. Texin RxT85A has been used in a

wide range of medical products including anesthetic connectors, flexible tubing and films, and catheters. It has also been used to fabricate drug delivery materials including nanocomposite films and nanofibers that can encapsulate and control the release of antiseptic drugs (Saha et al., 2014). Here, we demonstrate the sustained release capabilities of auranofin containing PU catheter coatings, leading to antibacterial and antibiofilm efficacy against MRSA.

MATERIALS AND METHODS

Materials

Aromatic polyether-based PU (Texin RxT85A) was supplied by Covestro AG (Leverkusen, Germany). The antibacterial drug, auranofin, was purchased from Santa Cruz Biotechnology (Dallas, TX). All solvents, chemicals, and media, unless otherwise noted, were purchased from MilliporeSigma (St. Louis, MO). Bacto agar was obtained from BD Biosciences (San Jose, CA). Ultrapure deionized water (18.2 MΩ.cm, Milli-Q, EMD Millipore, Taunton, MA) was used in all experiments. Surflo fourteen-gauge Teflon intravenous catheters [2.15 O.D. (1.73 I.D.) × 51 mm] were supplied by Patterson Veterinary (Devens, MA). Polytetrafluoroethylene (PTFE) sheets (AMS 3651) measuring 30 cm by 30 cm with a thickness of 0.38 mm, were obtained from Amazon (Seattle, WA). Tryptic soy broth (Remel), Dulbecco's modified Eagle's medium (DMEM, Gibco), fetal bovine serum (FBS, Gibco), and precleaned microscope glass slides were purchased from Thermo Fisher Scientific (Waltham, MA). MRSA USA300 engineered to express luciferase (USA300 Lac::Lux) was supplied by Dr. Michael Hamblin at Massachusetts General Hospital (Boston, MA) (Dai et al., 2013). For cytotoxicity testing, human red blood cells (hRBCs) and human hepatoma cells (ATCC HB-8065 HepG2) were obtained from Rockland Immunochemicals (Limerick, PA) and Dr. Bryan Fuchs at Massachusetts General Hospital (Boston, MA), respectively. Cell proliferation reagent, WST-1, was obtained from Roche (Mannheim, Germany).

Development of PU Coatings

Auranofin containing PU coatings were developed by first dissolving PU in tetrahydrofuran (THF) at a concentration of 50 mg/mL at 20°C for 24 h. Auranofin was then added to the PU solution and thoroughly mixed. This PU+auranofin mixture was then used to produce films for: (1) thickness measurement, (2) tensile testing, or (3) catheter coating for drug release and *in vitro* efficacy and cytocompatibility testing. For thickness measurements, flat PTFE substrates measuring 16 mm by 16 mm by 0.38 mm were coated via drop casting 1 mL of the PU+auranofin mixture with 0, 3, or 10 mg/mL auranofin; coatings were dried at 20°C until complete THF evaporation was noted, resulting in a dry PU+auranofin coating. For tensile testing, standalone PU+auranofin films were developed similarly to the coatings on PTFE but instead, 2 mL of the PU+auranofin mixture was drop cast onto glass slides measuring 25 mm by 75 mm. These coatings were readily peeled off of the glass and cut into rectangles measuring 12 mm by 38 mm for subsequent testing. For the catheter coatings, catheter segments measuring 10 mm in length were dipped into the PU+auranofin solution (1 catheter segment per 1 mL of PU+auranofin mixture) at auranofin concentrations of 0, 3, 10, 30, or 60 mg/mL for 24 h at 20°C. The catheters were removed from this mixture and the solvent in the coatings was allowed to evaporate at 20°C for 24 h. All coatings were stored at 4°C prior to use. Films with 0 mg/mL auranofin were denoted "PU only" coatings.

Characterization of Coating Morphological and Mechanical Properties

The thicknesses of PU+auranofin and PU only coatings on PTFE were evaluated using a Dektak3 profilometer (Bruker, Santa Barbara, CA). Average step height was measured at three random locations on the coated material. Tensile testing of the standalone films was carried out using an Instron Series 5942 Universal Testing System (Norwood, MA) equipped with a 500 N load cell. An extension rate of 0.1 mm/s was employed until material failure was noted. The pre-yield elastic deformation region (up to 15% extension) of the engineering stress vs. strain curve was used to determine the tensile elastic modulus of the film. The interior and outer coating surfaces on the coated catheters along with non-coated catheters were imaged using a LEO Gemini 1530 scanning electron microscope (SEM, Carl Zeiss, Oberkochen, Germany). Prior to SEM imaging, the catheters were sputter coated with gold and palladium. Coated and non-coated catheters were also imaged using an inverted tissue culture trinocular microscope (AmScope, Irvine, CA) equipped with an AmScope MU500 eyepiece camera (5.1 MP Aptina Color CMOS) and 4× objective lens.

Quantifying Auranofin Release *in vitro*

Auranofin release from PU+auranofin coated catheters was monitored by incubating each coated catheter in 1.98 mL of tryptic soy broth supplemented with 0.25% glucose (TSBG) at 37°C with shaking at 110 rpm. Glucose supplementation of TSB has previously been shown to promote biofilm formation (Heilmann et al., 1996; Lim et al., 2004). Every 24 h, the release solutions were collected and completely replaced with fresh medium. A microdilution assay, as described previously (Shukla and Shukla, 2018), was used to determine the amount of auranofin contained in the media release samples by comparing the antibacterial activity to that of known concentrations of non-coating incorporated auranofin. Briefly, 150 μL of each TSBG release sample was transferred to 96-well plates in triplicate and serially diluted 1:1 (v/v) with TSBG. Controls of non-coating incorporated auranofin were treated similarly. MRSA USA300 (10 μL) at a final concentration of 10^5 CFU/mL in the exponential growth phase (as determined by optical density) was added to these wells. Negative controls of media with no bacteria and positive controls of TSBG with USA300 in the absence of drug were included. Plates were incubated at 37°C with shaking at 110 rpm for ∼18 h. Subsequently, the optical density (OD) of the samples was read at 600 nm using a Cytation3 microplate reader (BioTek, Winooski, VT). The normalized bacteria density

was calculated using Equation (1).

$$\text{Normalized bacteria density} = \frac{\text{sample OD} - \text{negative control OD}}{\text{positive control OD} - \text{negative control OD}} \quad (1)$$

The MIC of the auranofin control against USA300 was determined as the concentration range of auranofin needed to observe a statistically significant transition of normalized bacteria density from zero to greater than zero. The amount of auranofin in the PU coating release media was then estimated by determining how many dilutions of the release media were required to reach this MIC transition point and computing a high and low estimate for the concentration of auranofin in the release solution (set by the MIC concentration range of non-coating incorporated auranofin).

Auranofin release was also monitored in water (pH 6) at 37°C for PU+auranofin coated catheters formulated with auranofin at 3 and 10 mg/mL. These coated catheters were incubated in 1 mL of water at 37°C with shaking at 110 rpm. Every 24 h, the release solutions were collected and completely replaced with fresh water. Auranofin in the water release samples was quantified using inductively coupled plasma optical emission spectroscopy (ICP-OES, Thermo Fisher, Waltham, MA). ICP-OES can detect the presence of the gold (Au) atom in the auranofin molecule. Briefly, the release samples were diluted 1:4 (v/v) with water for a total sample volume of 5 mL. This sample was injected into the ICP-OES with a radial plasma view configuration for concentrations above 1 ppm of auranofin and with an axial plasma view configuration for concentrations below 1 ppm. The concentration of auranofin in the release solutions was calculated by comparing the intensity of the signal obtained at the characteristic wavelength range of Au (242.79–242.80 nm) against that of a known auranofin standard examined concurrently.

Assessing Coating Antibacterial and Antibiofilm Efficacy *in vitro*

Antibacterial and antibiofilm activity of PU+auranofin catheter coatings was examined against USA300, a community-associated MRSA strain. Kirby-Bauer and broth bacteria survival assays on the coated catheters and on their release solutions were conducted, respectively. For the Kirby-Bauer assay, USA300 in its exponential growth phase at a concentration of 10^8 CFU/mL was spread on tryptic soy agar plates. PU+auranofin coated and uncoated catheters were cut in half lengthwise using a scalpel. Both the inner and outer surfaces of the catheters were placed in direct contact with the bacteria seeded agar and incubated for 24 h at 37°C. These plates were then photographed using a Canon PowerShot S110 digital camera (Tokyo, Japan).

Long-term antibacterial activity of the coated catheters was confirmed using MRSA microdilution assays as described in the section Quantifying Auranofin Release *in vitro*. The efficacy of these coatings against a greater MRSA challenge than a standard microdilution assay (2 x 10^6 CFU/mL vs. 10^5 CFU/mL, respectively) was investigated. Coated catheters were incubated in 1.98 mL of TSBG medium with shaking at 110 rpm at 37°C. The release medium was collected every 24 h and replaced with fresh TSBG medium. A 20 μL suspension of USA300 was added to the release solution to obtain a final bacteria concentration of 2×10^6 CFU/mL. This bacterial suspension was incubated with shaking at 110 rpm at 37°C for 24 h. The OD of the samples was measured at 600 nm using a Thermo Scientific Spectronic 2000 Visible Spectrophotometer (Waltham, MA). Negative controls of media with no bacteria and positive controls of TSBG with USA300 in the absence of drug were included. A normalized bacteria density was computed using Equation (1) for all test samples. Additional release samples were tested for bacterial growth inhibition until no inhibition of bacterial growth was observed. An identical assay was conducted to examine the effect of coating time on antibacterial activity over time. For this study, coatings were formulated as described in section Development of PU Coatings, except that coating times were varied (5 s, 1 h, 1 day, or 7 days).

The antibiofilm activity of PU+auranofin coatings was also examined. PU+auranofin coatings with 3 or 10 mg/mL auranofin utilized in the coating process, along with PU only coatings and variations of these coatings, in which vancomycin replaced auranofin, or only auranofin (3 mg/mL) was used without any PU, were examined in these studies. Vancomycin coated catheters were first dip coated in an ethanol solution containing the drug at either 3 or 10 mg/mL for 24 h at 20°C. These catheters were then removed from the ethanol solution and allowed to dry for 24 h at 20°C. The catheters were subsequently dip coated in 50 mg/mL PU in THF for 24 h at 20°C, followed by a complete drying of these coatings at 20°C. Coated or uncoated catheter segments were placed in 1 mL USA300 bacterial suspensions at a concentration of 10^4 CFU/mL in TSBG at 37°C with shaking at 110 rpm for 2 h. The samples were then removed from this suspension and rinsed 3 times with fresh TSBG to remove any unattached bacteria. The rinsed catheter segments were placed in new sterile vials containing 5 mL of fresh TSBG every 12 h. After 2 days, the bacterial burden on the catheters was evaluated by examining the level of bacterial bioluminescence on the catheters using an *in vivo* imaging system (IVIS Lumina III, PerkinElmer, Waltham, MA). Following IVIS imaging, the biofilms were disrupted by placing the catheter segments in 5 mL of 1× phosphate buffered saline (PBS) and subjected to sonication at ∼40 kHz for 7 min (Fisher Scientific FS30) followed by vortexing for 1 min. The samples were serially diluted in TSBG, plated on tryptic soy agar, and the colony forming units (CFUs) were counted.

Examining Coating Biocompatibility *in vitro*

The biocompatibility of PU+auranofin coatings and controls was evaluated by examining erythrocyte lysis and human hepatoma cell (ATCC HB-8065 HepG2) viability upon exposure to coated catheters or catheter incubated media, respectively. Hemolysis was examined as previously described (Gwisai et al., 2017; Zhou et al., 2017) by incubating hRBCs with PU+auranofin coated catheters (3, 10, 30, and 60 mg/mL auranofin coating concentration), PU only coatings, auranofin only coatings (3 mg/mL coating concentration), and uncoated catheters. Catheters were incubated with 1 mL of 2% (v/v) hRBCs in 24-well

plates for 1 h at 37°C. Negative controls containing no catheter and only hRBCs were also included. Positive controls of the 2% hRBCs suspension incubated with 0.1% v/v Triton X-100 were included. After incubation, the plates were centrifuged at 500 × g for 5 min. A 50 μL aliquot of the supernatant from each well was transferred to a 96-well plate. Absorbance at 540 nm was quantified using a SpectraMax M2 plate reader (Molecular Devices, San Jose, CA) to measure hemolysis. Normalized hemolysis was calculated using Equation (2).

$$\textit{Normalized hemolysis} = \frac{\textit{sample abs} - \textit{negative control abs}}{\textit{positive control abs} - \textit{negative control abs}} \quad (2)$$

The viability of HepG2 cells exposed to PU+auranofin coating release solutions was assessed using a colorimetric assay with WST-1. HepG2 cells were maintained in DMEM supplemented with 10% FBS at 37°C with 5% CO_2. PU+auranofin coated catheters (3 mg/mL auranofin coating concentration), PU only coatings, and uncoated catheters were incubated in HepG2 culture media for 24 h at 37°C. HepG2 cells were seeded at a density of 3.125×10^6 cells/cm^2 in polystyrene tissue-culture treated 96-well plates (Corning, Corning, NY) and immediately incubated with 100 μL of the different catheter incubation medias at 37°C with 5% CO_2. Non-coating incorporated auranofin was also included at concentrations of 0.5–32 μg/mL. After 20 h, 10 μL of WST-1 was added to each well and the plates were incubated for 4 h at 37°C with 5% CO_2. The absorbance (abs) of each well was measured at 450 nm using a SpectraMax M2 UV-Vis microplate reader (Molecular Devices, San Jose, CA). Normalized cell viability was calculated using Equation (3).

$$\textit{Normalized cell viability} = \frac{\textit{sample abs} - \textit{negative control abs}}{\textit{positive control abs} - \textit{negative control abs}} \quad (3)$$

Statistical Analysis

All experiments were conducted in triplicate at minimum. All data is reported as mean ± standard deviation. Statistical significance was calculated using GraphPad Prism with either a two-tailed *t*-test or one- or two-way analysis of variance (ANOVA) with Tukey's *post-hoc* analysis, as appropriate. Data was considered statistically significant for $p < 0.05$.

RESULTS AND DISCUSSION

In vitro Auranofin Release From Coated Catheters and Antibacterial Efficacy

In this work, PU+auranofin catheter coatings were developed to combat complications such as bacteria attachment, infection, and biofilm development that can occur with extended catheter use (Trautner and Darouiche, 2004). To the best of our knowledge, auranofin has not previously been used in device coatings. We sought to determine if auranofin was released from PU coatings at concentrations effective against planktonic MRSA. Initial investigations were performed with PU+auranofin coated catheters formulated from four concentrations of auranofin coating solution (3, 10, 30, and 60 mg/mL). Auranofin, unlike many other antimicrobial agents such as vancomycin, which has a measurable absorbance (Shukla and Shukla, 2018), is not readily detectable via absorbance or fluorescence spectroscopy without modification. Therefore, MRSA growth inhibition in a microdilution assay was utilized to estimate the concentrations of auranofin present in coated catheter release solutions. In this technique, serial dilutions of the release samples are made and incubated with MRSA. The most diluted solution able to inhibit bacterial growth is considered the upper range of the MIC of the drug in the release sample. By multiplying the dilution factor used to reach this concentration with the measured MIC of the drug, a concentration of drug in the release solution can be estimated.

Figure S1 shows normalized MRSA density over a range of concentrations for non-coating incorporated auranofin. The MIC of non-coating incorporated auranofin against USA300 was determined to be 0.063 μg/mL, consistent with previous reports (Harbut et al., 2015; Fuchs et al., 2016; Thangamani et al., 2016). We observed a transition of MRSA growth to no growth between auranofin concentrations of 0.031 and 0.063 μg/mL. Using this concentration range for non-coating incorporated auranofin and assuming no change in auranofin activity caused by the coating process, the auranofin release profile from the PU+auranofin catheter coatings was determined. **Figure 1** shows the release profile of all PU+auranofin coatings tested as a range estimated by the dilution factor required to reach MIC values. Catheters with coatings formulated using 3 and 10 mg/mL auranofin solutions exhibited effective drug release above MIC values over a period of 8 days. Raising the drug concentration in the coatings during formulation to 30 or 60 mg/mL extended auranofin release from 8 days to 11 and 26 days, respectively. A large auranofin release was observed for all coating formulations in the first 24 h followed by a slow extended release. As shown in **Figure 1**, for the 3 mg/mL auranofin coating concentration, ∼90% of the total auranofin eluted by 8 days was released in the first day. Interestingly, 10, 30, and 60 mg/mL PU+auranofin samples all had similar percentages of auranofin released in the first day (∼65, 66, and 62% of the total auranofin released by 8, 11, and 26 days, respectively). The similar burst release for the higher auranofin coating concentrations suggests that at these concentrations, the burst release of auranofin is independent of the amount of auranofin loaded on the catheters. The cumulative release of auranofin was increased from ∼7 μg for a 3 mg/mL auranofin coating concentration to ∼37 μg for a 10 and 30 mg/mL auranofin coating concentration and 78 μg for a 60 mg/mL auranofin coating concentration. Given that the bacterial MIC is reached with the lowest auranofin formulation concentration, it is perceivable that this formulation could be effective in inhibiting bacterial accumulation on the implant material.

It is possible that the final auranofin release values do not represent the total auranofin loading in a single 10 mm catheter segment and that some auranofin may still release below MIC values which are not readily detectable. ICP-OES, which is capable of detecting the gold atom in auranofin molecules in non-complex solvents (e.g., water rather than PBS or media), was utilized to evaluate auranofin release in deionized water (pH 6) at 37°C from PU+auranofin catheters

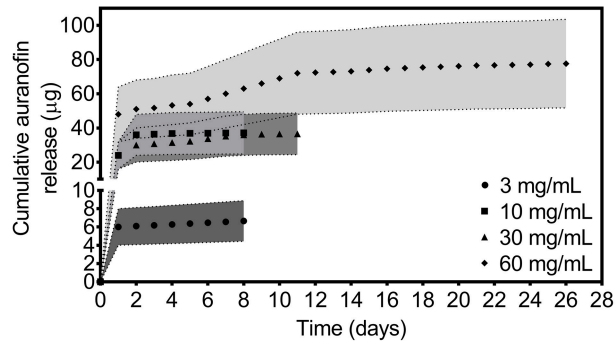

FIGURE 1 | *In vitro* release profile of auranofin in TSBG medium for PU+auranofin coated catheters formulated at 4 different auranofin coating concentrations (3, 10, 30, and 60 mg/mL). Release was evaluated by examining MRSA USA300 inhibition. Data is represented as a range set by the upper and lower limits of the auranofin MIC for each day at which the release solution auranofin concentration was above MIC for USA300 ($n = 3$).

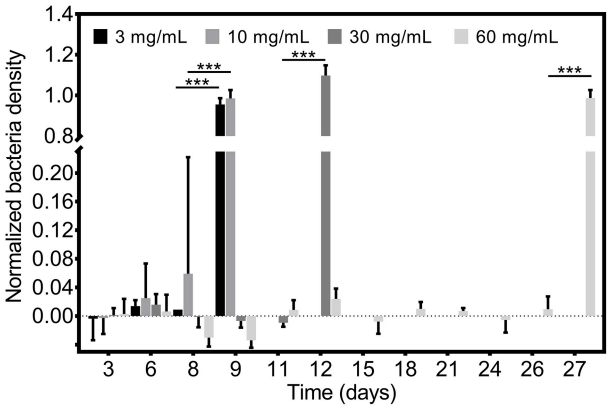

FIGURE 2 | Antibacterial efficacy of PU+auranofin coated catheters. PU+auranofin coatings formulated at 4 different auranofin coating concentrations (3, 10, 30, and 60 mg/mL) were incubated with 2×10^6 CFU/mL MRSA USA300 and normalized bacteria density was determined following 18 h. Data are shown as mean ± standard deviation where $^{***}p < 0.001$ indicates significance between days using two-way ANOVA with Tukey's *post-hoc* analysis ($n = 3$).

formulated using 3 and 10 mg/mL auranofin solutions. At 8 days, 95 ± 31 μg of auranofin had released from the 3 mg/mL auranofin coatings and 319 ± 62 μg of auranofin was released from the 10 mg/mL coatings. As with the media release studies quantified using bacterial microdilution methods, a greater cumulative release was observed from the PU+auranofin coatings formulated using 10 mg/mL auranofin compared to 3 mg/mL auranofin at 8 days. However, the values quantified for water release were significantly greater than those observed in media. These differences may arise from the differences in the release environment for the two methods used. Media components may adsorb onto or absorb into the catheter coating over time and potentially form interactions with auranofin or PU, slowing drug release. The water environment lacks these interactions and may therefore enable a greater release. The differences in pH (pH 7.4 for the media vs. 6 for the water) may also factor in, as has previously been observed for polyurethane materials (Chen et al., 2014).

The *in vitro* auranofin release profile studies confirmed planktonic bacterial inhibition by individual catheter release samples at PU+auranofin coating compositions formulated using 3, 10, 30, and 60 mg/mL auranofin. Given the potent activity of auranofin at low concentrations, we examined whether auranofin release from these coatings was also able to inhibit the growth of MRSA at a 20 times greater bacterial concentration than the standard microdilution assay. **Figure 2** shows the efficacy of MRSA growth inhibition for this greater bacterial challenge (2×10^6 CFU/mL) upon bacterial incubation with PU+auranofin coating release solutions collected over time. We found that the coating release samples were able to completely inhibit bacterial growth for samples collected at time points identical to the microdilution assays conducted at lower bacteria concentrations. Namely, PU+auranofin coatings formulated with the 3 and 10 mg/mL auranofin were effective over 8 days, while those formulated with 30 and 60 mg/mL auranofin were effective for 11 and 26 days, respectively.

Having confirmed multi-day *in vitro* efficacy of all coating formulations examined, we investigated whether changing the coating formulation process could affect efficacy. Specifically, we determined whether the catheter coating time in the PU+auranofin solution changed its efficacy. Holding the auranofin concentration in the coating solution constant at 3 mg/mL, we examined coating times of 5 s, 1 h, and 7 days in addition to the 1 day coating time utilized for all other experiments. Release samples taken over time from each of these coatings were examined for their bacterial growth inhibition efficacy using a 2×10^6 CFU/mL MRSA concentration as shown in **Figure 3**. We observed that catheters coated for 1 and 7 days behaved similarly, inhibiting MRSA growth over 8 days. Interestingly, catheters coated for 5 s and 1 h exhibited antibacterial activity against MRSA for 7 days. These findings suggested that even short coating periods lead to significant drug incorporation on the catheter capable of releasing and inhibiting bacterial growth over a period of 1 week. Effective above MIC release can be extended by 1 day if the coating duration is increased. For future translation of these materials, rapid production is possible without significantly compromising efficacy.

Next we examined whether PU+auranofin coated catheters were able to inhibit bacterial growth using both the inner and outer surface of the coated catheters. The results of a Kirby Bauer assay using PU+auranofin coated catheters formulated using 3, 10, 30, and 60 mg/mL auranofin are shown in **Figure 4**. For these experiments coated catheters were cut in half lengthwise and plated with either the inner surface of the catheter (i.e., the catheter lumen) or the outer surface face down on MRSA coated agar; controls of uncoated catheters were also included. A clear zone of inhibition surrounded all PU+auranofin coated catheter samples regardless of whether the inner or outer surface

was exposed to the bacteria. In contrast, the uncoated samples did not exhibit any bacterial growth inhibition. Positive controls of 30 μg vancomycin discs were included and performed as expected with an average zone of inhibition diameter of 1.48 ± 0.2 cm. Quantitative comparison between inner and outer surface catheter coatings in terms of drug loading and efficacy are difficult to make as small differences in sample size and shape can alter the shape and size of the zone of inhibition that is observed surrounding these samples. Further, a degree of dose dependent release was suggested by the smaller clearing generated in the presence of the catheter material coated with 3 mg/mL auranofin compared to the other coating formulations examined.

Overall, our investigations demonstrated that catheter coatings generated with 3 and 10 mg/mL auranofin were highly effective in inhibiting bacterial growth albeit over shorter timescales compared to the 30 and 60 mg/mL auranofin coating conditions. For the purposes of *in vitro* characterization, we proceeded with using the 3 and 10 mg/mL auranofin coating concentrations for further analysis of coating morphology, mechanical properties, antibiofilm efficacy, and cytocompatibility. For conditions that may require lengthier application, the greater auranofin coating concentrations of 30 and 60 mg/mL are possible options that can be explored.

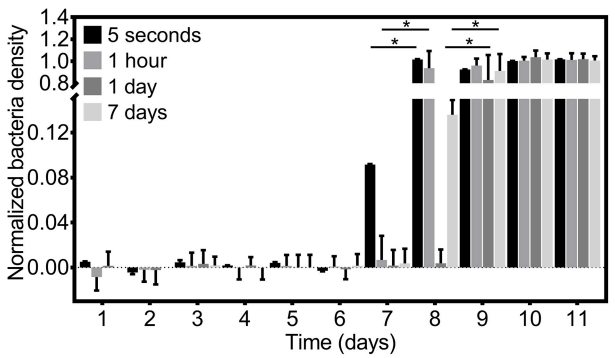

FIGURE 3 | Antibacterial efficacy of PU+auranofin coated catheters formulated by varying coating times. PU+auranofin coatings formulated at 4 different coating times (5 s, 1 h, 1 day, and 7 days) at an auranofin coating concentration of 3 mg/mL were incubated with 2×10^6 CFU/mL MRSA USA300 and normalized bacteria density was determined following 18 h. Data are shown as mean ± standard deviation where $^*p < 0.05$ indicates significance between days using two-way ANOVA with Tukey's *post-hoc* analysis ($n = 3$).

Catheter Coating Morphology and Mechanical Properties

Having determined that PU+auranofin coatings lead to effective auranofin release and MRSA inhibition, we sought to determine if coating the catheter altered the implant material. Light microscope images of the coatings formulated with PU+auranofin solutions containing 3 and 10 mg/mL auranofin demonstrate a slightly rough exterior, with discernible differences from the PU only coated Teflon catheter (**Figure 5**). SEM imaging of the catheters confirmed surface texturization in the PU+auranofin coated catheters compared to the PU only coated catheters (**Figure 5**). Compared with PU only coatings, the added surface texture may result from the interaction of auranofin with the PU during the drying process, preventing a completely smooth surface from forming.

The thickness of these coatings on flat PTFE sheets was examined via profilometry for PU+auranofin coatings formulated with auranofin coating concentrations of 3 and 10 mg/mL. **Figure 6A** shows the average thickness of PU only and PU+auranofin coatings. The average thickness of PU only coatings was 307.7 ± 16.6 μm; auranofin loaded PU coatings had average thicknesses of 292.5 ± 17.7 and 313.1 ± 20.5 μm for 3 and 10 mg/mL auranofin, respectively. The presence of auranofin did not lead to statistically significant changes in coating thicknesses between these three groups, despite the effect on coating morphology.

To further evaluate the mechanical properties of the PU+auranofin coatings, tensile tests were performed on standalone coatings. As seen in **Figure 6B**, PU coating stiffness decreased when 10 mg/mL but not 3 mg/mL auranofin was included in the coating process compared to PU only. PU only coatings exhibited an elastic modulus of 10.3 ± 0.8 MPa vs. 10.1 ± 0.8 MPa and 7.7 ± 0.4 MPa for PU+auranofin coatings formulated from 3 to 10 mg/mL auranofin, respectively. The

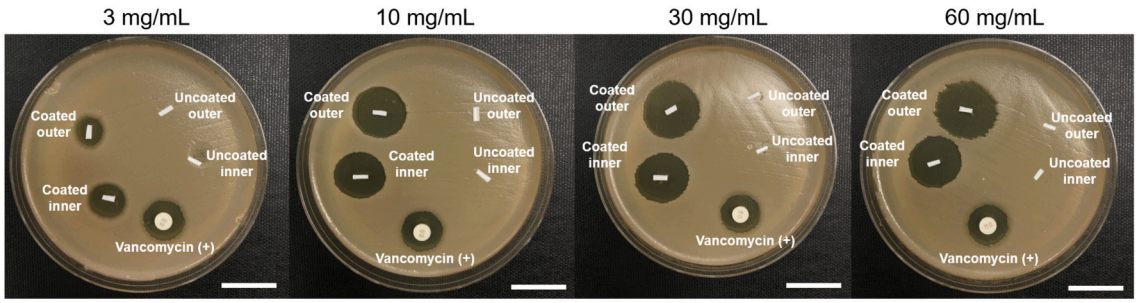

FIGURE 4 | Examining the effect of PU+auranofin catheter inner and outer surfaces on MRSA USA300. Tryptic soy broth agar coated with USA300 was exposed to the inner and outer surfaces of coated bisected catheters for PU only and PU+auranofin coated materials formulated at 4 different auranofin concentrations (3, 10, 30, and 60 mg/mL). Vancomycin discs containing 30 μg of vancomycin were used as a positive control (Scale bar = 10 mm).

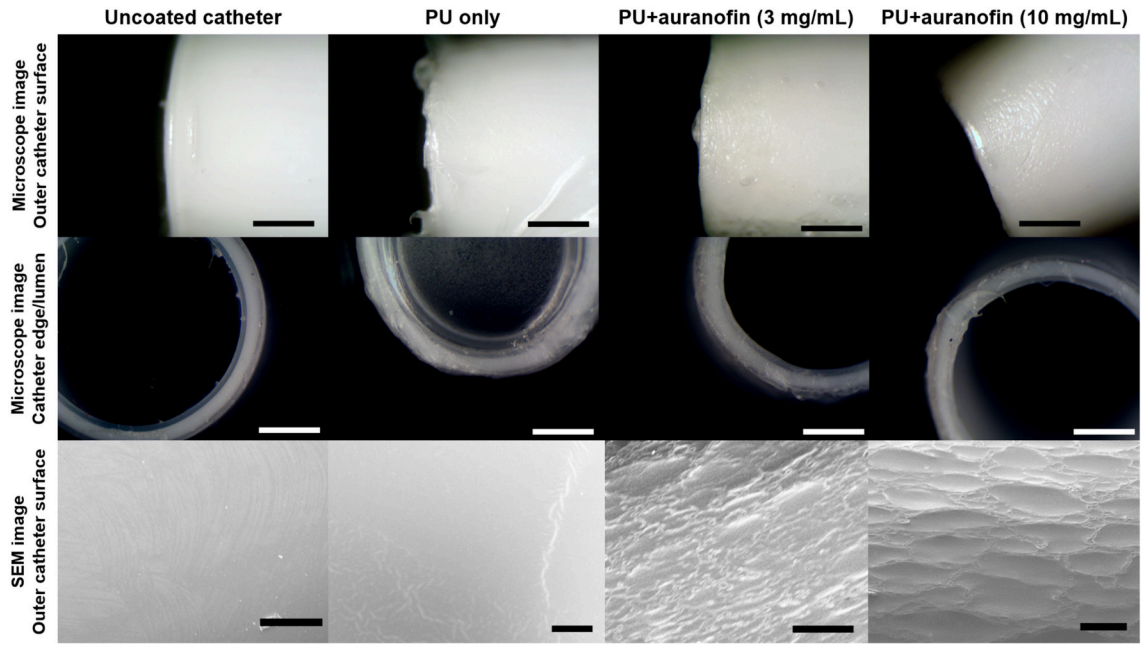

FIGURE 5 | Catheter coating morphology examined via light microscopy and scanning electron microscopy. Coatings formulated with PU only and PU+auranofin at auranofin concentrations of 3 and 10 mg/mL coated for 1 day are shown [Scale bars = 500 μm (light microscope) and 50 μm (SEM)].

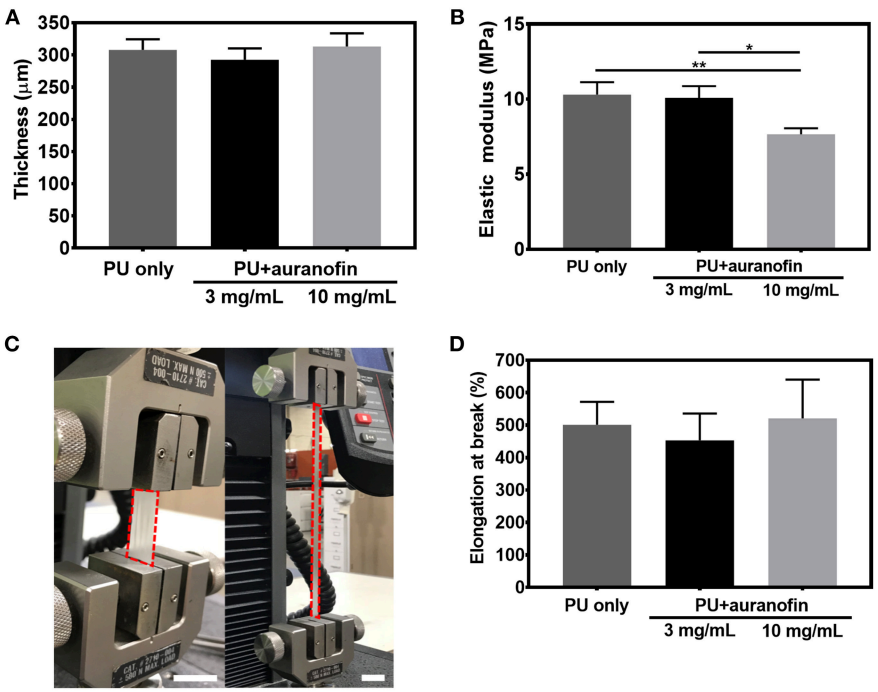

FIGURE 6 | Thickness and mechanical properties of coated catheters. **(A)** Thickness of PU only and PU+auranofin (3 and 10 mg/mL auranofin coating concentration) on PTFE. **(B)** Tensile elastic moduli of PU and PU+auranofin (3 and 10 mg/mL auranofin coating concentration) standalone coatings. **(C)** Representative digital image displaying elongation of standalone PU+auranofin coating formulated with 3 mg/mL auranofin during tensile testing nearing failure (scale bars = 25 mm). **(D)** Percent elongation at break of PU and PU+auranofin (3 and 10 mg/mL auranofin coating concentration) standalone coatings. Data are shown as mean ± standard deviation with $*p < 0.05$ and $**p < 0.001$ for moduli values between samples analyzed using one-way ANOVA with Tukey's *post-hoc* analysis ($n = 3$).

decreased stiffness may result from disruption of the hydrogen bonding in the PU hard segments, which is known to reinforce the material (Shoeib et al., 2010). This effect has been observed with poly(ethylene glycol), where the oxygen atoms in the backbone act as hydrogen bond acceptors that weaken the PU hard segments (Park et al., 2001). The auranofin molecule has nine hydrogen bond acceptors and may have a similar effect. The coatings are highly stretchable as seen in **Figure 6C**. There was no statistical difference between the percent elongation at break (∼500%) between PU coatings formulated with and without auranofin (**Figure 6D**), in agreement with what has previously been reported for PU coatings (La Francesca et al., 2018). Overall, the incorporation of auranofin does not appreciably impact the tensile properties of these coatings compared to PU only, maintaining the high degree of stretchability which will be important for future clinical use on catheters.

In vitro Antibiofilm Efficacy of Coated Catheters

Having examined the morphological and mechanical properties of the PU+auranofin coatings, we next determined how biofilm formation was affected by the drug coatings. Auranofin was previously suggested to inhibit preformed *S. aureus* biofilms within 2 h of exposure, although with limited bactericidal activity likely due to the lack of metabolic activity required for target effectiveness within biofilm bacteria (Torres et al., 2016). Our work expands upon these previous findings, now examining the effect that auranofin has on biofilm prevention, as would be the case for a newly introduced medical implant.

To further examine the potential for using PU+auranofin coated catheters clinically, coated catheter segments formulated using 3 and 10 mg/mL auranofin were exposed to MRSA and then examined for biofilm formation over 48 h. PU+vancomycin, auranofin only (lacking PU, formulated with 3 mg/mL auranofin), and PU only coatings were also examined along with uncoated catheters. Vancomycin, a potent glycopeptide antibiotic highly effective against MRSA (Abebe et al., 2014), was loaded onto the catheters as a control to test its antibiofilm efficacy in comparison to auranofin coatings. Biofilm accumulation on catheter segments was visualized using an IVIS imaging system as seen in **Figure 7A** with luminescence indicating the presence of bacteria. Subsequently, the number of colony forming units (CFUs) attached on catheters was quantified by detaching the colonies and counting, as shown in **Figure 7B**.

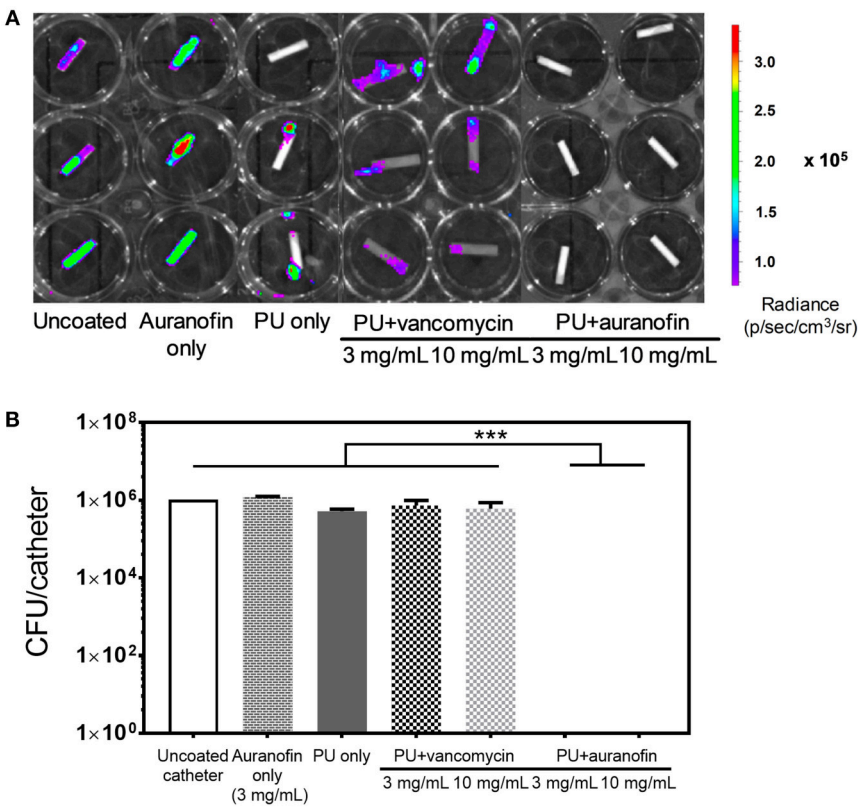

FIGURE 7 | Antibiofilm efficacy of coated catheters. **(A)** Bioluminescence (radiance) of MRSA USA300 Lac::Lux examined using IVIS. Catheters were either uncoated or coated with auranofin only (at a 3 mg/mL coating concentration), PU only, PU+vancomycin, or PU+auranofin at 2 different drug coating concentrations (3 and 10 mg/mL). Samples were exposed to USA300, rinsed, and potentially attached biofilms were allowed to mature over 2 days prior to measurement. **(B)** The colony forming units of USA300 recovered from the different catheter groups imaged in **(A)**. Data are shown as mean ± standard deviation where $^{***}p < 0.001$ indicates significance between CFU for the samples evaluated using one-way ANOVA ($n = 3$).

With the exception of the PU+auranofin coatings, all catheters tested exhibited bacterial luminescence. Both PU+auranofin formulations completely inhibited bacterial attachment.

We saw that PU+vancomycin and auranofin only coatings did not exhibit any statistical difference in bacterial CFU attachment as compared to uncoated catheters. Due to vancomycin hydrophilicity, we hypothesize that vancomycin is released rapidly from these coatings, leading to a lack in efficacy in preventing biofilm formation. Auranofin only coatings are also likely highly unstable due to the lack of a polymer carrier and are similarly unable to prevent bacterial attachment.

Interestingly, PU only coatings showed a 1-log reduction in bacterial attachment as compared to uncoated catheters. This antibiofilm activity of PU has previously been observed (Martìnez-Martìnez et al., 1990; Lopez-Lopez et al., 1991; Zdrahala and Zdrahala, 1999) and is likely due to the smooth PU surface as we observed with SEM. Overall, formulating auranofin in a PU catheter coating enabled both bacterial growth inhibition in planktonic cultures over time and complete prevention of bacterial surface attachment, which was not possible for either PU or auranofin alone.

In vitro Cytotoxicity Evaluation of Coated Catheters

The PU+auranofin coatings developed in this work are highly promising as antibacterial materials. Future translation of these materials requires that the materials are biocompatible. The drug coated catheters will eventually be employed as functioning devices; in this scenario, they will be exposed to circulating blood. For this reason, we tested the auranofin coated devices in the presence of human erythrocytes to see if the various drug coating concentrations could incite lysis. The hemolysis of PU+auranofin coatings at all formulations developed (i.e., 3, 10, 30, and 60 mg/mL of auranofin coating concentrations), PU only coatings, auranofin only coatings (formulated using a 3 mg/mL auranofin solution), and uncoated catheters was compared with hRBC negative and positive controls (i.e., untreated and Triton X-100 treated hRBCs, respectively), as shown in **Figure 8A**. We did not observe any significant difference in normalized hemolysis between any of the tested coating groups and the untreated controls, indicating excellent hemocompatibility of the PU+auranofin coated catheters.

We also evaluated the cytotoxicity of PU+auranofin coatings formulated using 3 mg/mL auranofin, PU only, and uncoated catheters incubated in cell culture media for 24 h on hepatocellular carcinoma cells. HepG2 cells were selected due to their widespread use as *in vitro* models for liver metabolism of toxins (Guillouzo et al., 2007). Initially we examined the viability of HepG2 cells with non-coating incorporated auranofin (**Figure S2**). We observed that the half maximal inhibitory concentration (IC_{50}) for viability for non-coating incorporated auranofin fell between 16 and 32 μg/mL, which corresponds with IC_{50} values of auranofin previously reported for HepG2 cells (Liu et al., 2015). **Figure 8B** shows the percentage of viable cells upon exposure to catheter release media. None of the formulations tested affected the viability of HepG2 cells compared to a no catheter control. From the *in vitro* media release studies, a concentration of 3 μg/mL auranofin for the 24 h release sample could be estimated, falling well below the IC_{50} concentration. The catheter alone and PU alone coating was not expected to have any effect on the cells, as previously FDA approved materials. Similarly, auranofin is typically administrated orally to patients at an auranofin concentration of 6 mg/mL per day for antirheumatic therapy and has demonstrated no cumulative toxicity during long-term treatments (Egsmose et al., 1995).

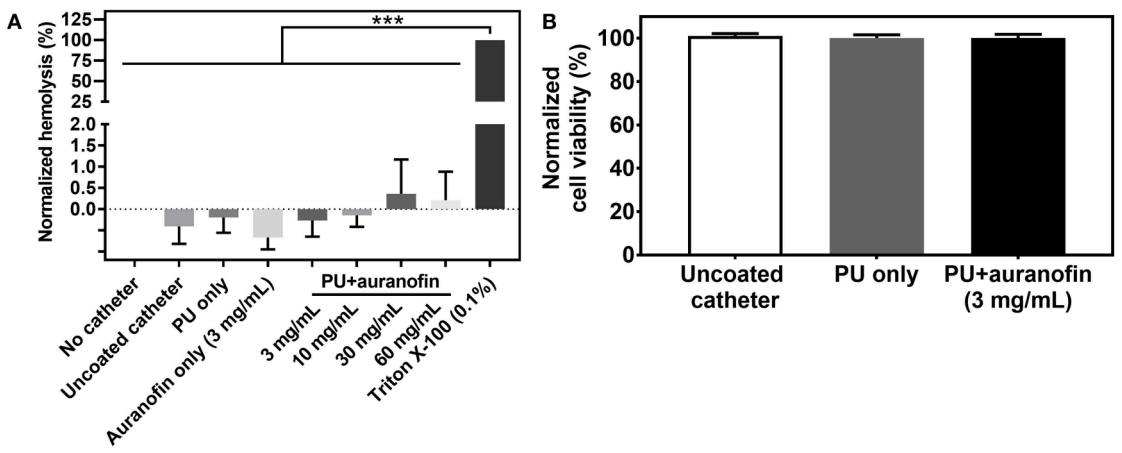

FIGURE 8 | Cytotoxicity of PU+auranofin coatings. **(A)** Percent normalized hemolysis of hRBCs exposed to uncoated catheters, PU only, auranofin only (formulated at a 3 mg/mL auranofin coating concentration), PU+auranofin (formulated at 3, 10, 30, and 60 mg/mL auranofin coating concentrations) compared to negative controls of untreated hRBCs and a Triton X-100 incubated positive control. **(B)** Normalized HepG2 liver cell viability upon exposure to media incubated with uncoated catheters, PU only, and PU+auranofin (formulated at a 3 mg/mL auranofin coating concentration) catheters for 24 h. Data are shown as mean ± standard deviation. Statistical significance was evaluated using one-way ANOVA ($n = 3$) and is shown as $^{***}p < 0.001$ indicating statistical significance between the positive control (Triton X-100 with hRBCs) and other conditions tested. No statistical significance was noted between the other hemolysis conditions tested or between the different HepG2 viability conditions examined ($p > 0.5$).

Therefore, auranofin has terrific potential to be utilized as an antibacterial and antibiofilm therapy without significant concern for human toxicity.

CONCLUSIONS

Solvent casting PU+auranofin catheter coatings yielded materials that prevented the attachment of MRSA and the accumulation of bacteria that enables biofilm formation. Auranofin release profiles estimated in bacteria media demonstrated the potential to achieve 26 days of above MIC release for specific formulations of this coating. A large initial release in the first day was followed by a slow sustained release. MRSA growth inhibition was observed between 8 and 26 days depending on the auranofin concentration utilized during coating formation. These coatings exceed the maximal 2 week period of efficacy observed for previously reported antimicrobial catheters. Most importantly, the coatings were capable of completely preventing MRSA biofilm formation, a property unique to the combined PU+auranofin coating and not observed with auranofin or PU alone. The PU+auranofin coating did not adversely affect catheter structure. Finally, we observed that these coatings are non-toxic to healthy hRBCs and HepG2 cells, important for future preclinical and clinical translation of these products. Intravascular catheters can be used over a 72 to 96 h time period (Brown and Rowland, 2013); adding an inhibitory drug such as auranofin in the form of a sustained release coating can prevent infection by planktonic and biofilm bacteria, potentially limiting CRBSIs.

AUTHOR CONTRIBUTIONS

HL, SS, and NV-G contributed equally to this work. HL, SS, NV-G, and NT designed and carried out experiments. AS, EM, and BF designed experiments and directed research. HL, NV-G, SS, and AS wrote the manuscript. All authors analyzed results, revised the manuscript, and approved of the final version.

FUNDING

This work was supported by grants from the National Institutes of Health (1P20GM121344 to BF and P01 grant AI083214 to EM) and the Office of Naval Research (N000141712120 to AS) and funds from Brown University to AS.

ACKNOWLEDGMENTS

The authors thank Brown University for the use of their facilities and funding. Specifically, the authors would like to acknowledge Joseph Orchardo and the Environmental Chemistry facilities at Brown University for assisting with ICP-OES and Anthony McCormick and the Institute for Molecular and Nanoscale Innovation's Electron Microscopy Facility at Brown for assisting with SEM.

SUPPLEMENTARY MATERIAL

The Supplementary Material for this article can be found online at: https://www.frontiersin.org/articles/10.3389/fcimb.2019.00037/full#supplementary-material

REFERENCES

AbdelKhalek, A., Abutaleb, N. S., Elmagarmid, K. A., and Seleem, M. N. (2018). Repurposing auranofin as an intestinal decolonizing agent for vancomycin-resistant enterococci. *Sci. Rep.* 8:8353. doi: 10.1038/s41598-018-26674-0

Abebe, A., Tener, M., Waller, S., and el Atrouni, W. (2014). Catheter-related bloodstream infections review. *Hosp. Med. Clin.* 3, e32–e49. doi: 10.1016/j.ehmc.2013.08.002

Alberti, K. G., Zimmet, P. Z., Grady, N. P. O., Raad, I. I., Rijnders, B. J. A., Sherertz, R. J., et al. (2014). NIH Public Access. *Diabet. Med.* 15, 6–12. doi: 10.1002/(SICI)1096-9136(199807)15:7<539::AID-DIA668>3.0.CO;2-S

Bonilla, M., Denicola, A., Novoselov, S. V., Turanov, A. A., Protasio, A., Izmendi, D., et al. (2008). Platyhelminth mitochondrial and cytosolic redox homeostasis is controlled by a single thioredoxin glutathione reductase and dependent on selenium and glutathione. *J. Biol. Chem.* 283, 17898–17907. doi: 10.1074/jbc.M710609200

Brooks, B. D., and Brooks, A. E. (2014). Therapeutic strategies to combat antibiotic resistance. *Adv. Drug Deliv. Rev.* 78, 14–27. doi: 10.1016/j.addr.2014.10.027

Brown, D., and Rowland, K. (2013). Optimal timing for peripheral IV replacement? *J. Fam. Pract.* 62, 200–202.

Brown, M. R., Allison, D. G., and Gilbert, P. (1988). Resistance of bacterial biofilms to antibiotics: a growth-rate related effect? *J. Antimicrob. Chemother.* 22, 777–780. doi: 10.1093/jac/22.6.777

Cassetta, M. I., Marzo, T., Fallani, S., Novelli, A., and Messori, L. (2014). Drug repositioning: Auranofin as a prospective antimicrobial agent for the treatment of severe staphylococcal infections. *Biometals* 27, 787–791. doi: 10.1007/s10534-014-9743-6

Chen, H., Li, Y., Liu, Y., Gong, T., Wang, L., and Zhou, S. (2014). Highly pH-sensitive polyurethane exhibiting shape memory and drug release. *Polym. Chem.* 5, 5168–5174. doi: 10.1039/C4PY00474D

Costerton, J. W. (1999). Bacterial biofilms: a common cause of persistent infections. *Science* 284, 1318–1322. doi: 10.1126/science.284.5418.1318

Curtin, J. J., and Donlan, R. M. (2006). Using bacteriophages to reduce formation of catheter-associated biofilms by *Staphylococcus epidermidis*. *Antimicrob. Agents Chemother.* 50, 1268–1275. doi: 10.1128/AAC.50.4.1268-1275.2006

Dai, T., Gupta, A., Huang, Y.-Y., Sherwood, M. E., Murray, C. K., Vrahas, M. S., et al. (2013). Blue light eliminates community-acquired methicillin-resistant *Staphylococcus aureus* in infected mouse skin abrasions. *Photomed. Laser Surg.* 31, 531–538. doi: 10.1089/pho.2012.3365

Danese, P. N. (2002). Antibiofilm approaches: prevention of catheter colonization. *Chem. Biol.* 9, 873–880. doi: 10.1016/S1074-5521(02)00192-8

Darouiche, R. O., Raad, I. I., Heard, S. O., Thornby, J. I., Wenker, O. C., Gabrielli, A., et al. (1999). A comparison of two antimicrobial-impregnated central venous catheters. *N. Engl. J. Med.* 340, 1–8. doi: 10.1056/NEJM199901073400101

de la Fuente-Núñez, C., Reffuveille, F., Fernández, L., and Hancock, R. E. (2013). Bacterial biofilm development as a multicellular adaptation: antibiotic resistance and new therapeutic strategies. *Curr. Opin. Microbiol.* 16, 580–589. doi: 10.1016/j.mib.2013.06.013

Debnath, A., Parsonage, D., Andrade, R. M., He, C., Cobo, E. R., Hirata, K., et al. (2012). A high-throughput drug screen for *Entamoeba histolytica* identifies a new lead and target. *Nat. Med.* 18, 956–960. doi: 10.1038/nm.2758

Díez-Martínez, R., García-Fernández, E., Manzano, M., Martínez, Á., Domenech, M., Vallet-Reg,í, M., et al. (2016). Auranofin-loaded nanoparticles as a new therapeutic tool to fight streptococcal infections. *Sci. Rep.* 6:19525. doi: 10.1038/srep19525

Ding, M., Li, J., Tan, H., and Fu, Q. (2012). Self-assembly of biodegradable polyurethanes for controlled delivery applications. *Soft Matter* 8, 5414–5428. doi: 10.1039/c2sm07402h

Donlan, R. M. (2002). Biofilms: Microbial life on surfaces. *Emerg. Infect. Dis.* 8, 881–890. doi: 10.3201/eid0809.020063

Egsmose, C., Lund, B., Borg, G., Pettersson, H., Berg, E., Brodin, U., et al. (1995). Patients with rheumatoid arthritis benefit from early 2nd line therapy: 5 year followup of a prospective double blind placebo controlled study. *J. Rheumatol.* 22, 2208–2213.

Fischer, M., Vahdatzadeh, M., Konradi, R., Friedrichs, J., Maitz, M. F., Freudenberg, U., et al. (2015). Multilayer hydrogel coatings to combine hemocompatibility and antimicrobial activity. *Biomaterials* 56, 198–205. doi: 10.1016/j.biomaterials.2015.03.056

Flemming, H.-C., Wingender, J., Szewzyk, U., Steinberg, P., Rice, S. A., and Kjelleberg, S. (2016). Biofilms: an emergent form of bacterial life. *Nat. Rev. Microbiol.* 14, 563–575. doi: 10.1038/nrmicro.2016.94

Fu, W., Forster, T., Mayer, O., Curtin, J. J., Lehman, S. M., and Donlan, R. M. (2010). Bacteriophage cocktail for the prevention of biofilm formation by *Pseudomonas aeruginosa* on catheters in an *in vitro* model system. *Antimicrob. Agents Chemother.* 54, 397–404. doi: 10.1128/AAC.00669-09

Fuchs, B. B., Rajamuthiah, R., Souza, A. C. R., Eatemadpour, S., Rossoni, R. D., Santos, D. A., et al. (2016). Inhibition of bacterial and fungal pathogens by the orphaned drug auranofin. *Future Med. Chem.* 8, 117–132. doi: 10.4155/fmc.15.182

Guillouzo, A., Corlu, A., Aninat, C., Glaise, D., Morel, F., and Guguen-Guillouzo, C. (2007). The human hepatoma HepaRG cells: a highly differentiated model for studies of liver metabolism and toxicity of xenobiotics. *Chem. Biol. Interact.* 168, 66–73. doi: 10.1016/j.cbi.2006.12.003

Gwisai, T., Hollingsworth, N. R., Cowles, S., Tharmalingam, N., Mylonakis, E., Fuchs, B. B., et al. (2017). Repurposing niclosamide as a versatile antimicrobial surface coating against device-associated, hospital-acquired bacterial infections. *Biomed. Mater.* 12, 045010. doi: 10.1088/1748-605X/aa7105

Harbut, M. B., Vilchèze, C., Luo, X., Hensler, M. E., Guo, H., Yang, B., et al. (2015). Auranofin exerts broad-spectrum bactericidal activities by targeting thiol-redox homeostasis. *Proc. Natl. Acad. Sci. U.S.A.* 112, 4453–4458. doi: 10.1073/pnas.1504022112

Hassanein, H. H., Georgey, H. H., Fouad, M. A., El Kerdawy, A. M., and Said, M. F. (2017). Synthesis and molecular docking of new imidazoquinazolinones as analgesic agents and selective COX-2 inhibitors. *Future Med. Chem.* 9, 553–578. doi: 10.4155/fmc-2016-0240

He, X., Zhai, Z., Wang, Y., Wu, G., Zheng, Z., Wang, Q., et al. (2012). New method for coupling collagen on biodegradable polyurethane for biomedical application. *J. Appl. Polym. Sci.* 126, E354–E361. doi: 10.1002/app.36742

Heilmann, C., Gerke, C., Perdreau-Remington, F., and Götz, F. (1996). Characterization of Tn917 insertion mutants of *Staphylococcus epidermidis* affected in biofilm formation. *Infect. Immun.* 64, 277–82.

Hook, A. L., Chang, C. Y., Yang, J., Luckett, J., Cockayne, A., Atkinson, S., et al. (2012). Combinatorial discovery of polymers resistant to bacterial attachment. *Nat. Biotechnol.* 30, 868–875. doi: 10.1038/nbt.2316

Kamal, G. D., Pfaller, M. A., Rempe, L. E., and Jebson, P. J. R. (1991). Reduced intravascular catheter infection by antibiotic bonding: a prospective, randomized, controlled trial. *JAMA J. Am. Med. Assoc.* 265, 2364–2368. doi: 10.1001/jama.1991.03460180070035

Koo, H., Allan, R. N., Howlin, R. P., Stoodley, P., and Hall-Stoodley, L. (2017). Targeting microbial biofilms: current and prospective therapeutic strategies. *Nat. Rev. Microbiol.* 15, 740–755. doi: 10.1038/nrmicro.2017.99

La Francesca, S., Aho, J. M., Barron, M. R., Blanco, E. W., Soliman, S., Kalenjian, L., et al. (2018). Long-term regeneration and remodeling of the pig esophagus after circumferential resection using a retrievable synthetic scaffold carrying autologous cells. *Sci. Rep.* 8, 4123. doi: 10.1038/s41598-018-22401-x

Lewis, K., Spoering, A., Kaldalu, N., Keren, I., and Shah, D. (2005). "Persisters: specialized cells responsible for biofilm tolerance to antimicrobial agents," in *Biofilms, Infection, and Antimicrobial Therapy* (Boca Raton, FL; London; New York, NY; Singapore: Taylor & Francis), 241–256.

Li, Y. H., and Tian, X. L. (2016). Quorum sensing and bacterial social interactions in biofilms: bacterial cooperation and competition. *Stress Environ. Regul. Gene Expr. Adapt. Bact.* 2, 1197–1205. doi: 10.1002/9781119004813.ch116

Lim, Y., Jana, M., Luong, T. T., and Lee, C. Y. (2004). Control of glucose- and NaCl-induced biofilm formation by rbf in *Staphylococcus aureus*. *J. Bacteriol.* 186, 722–729. doi: 10.1128/JB.186.3.722-729.2004

Lin, K., O'Brien, K. M., Trujillo, C., Wang, R., Wallach, J. B., Schnappinger, D., et al. (2016). Mycobacterium tuberculosis thioredoxin reductase is essential for thiol redox homeostasis but plays a minor role in antioxidant defense. *PLoS Pathog.* 12:e1005675. doi: 10.1371/journal.ppat.1005675

Liu, N., Huang, H., Dou, Q. P., and Liu, J. (2015). Inhibition of 19S proteasome-associated deubiquitinases by metal-containing compounds. *Oncoscience* 2, 457–466. doi: 10.18632/oncoscience.167

Lopez-Lopez, G., Pascual, A., and Perea, E. J. (1991). Effect of plastic catheter material on bacterial adherence and viability. *J. Med. Microbiol.* 34, 349–353. doi: 10.1099/00222615-34-6-349

Lu, J., and Holmgren, A. (2014). The thioredoxin antioxidant system. *Free Radic. Biol. Med.* 66, 75–87. doi: 10.1016/j.freeradbiomed.2013.07.036

Lundstrom, J., and Holmgren, A. (1990). Protein disulfide-isomerase is a substrate for thioredoxin reductase and has thioredoxin-like activity. *J. Biol. Chem.* 265, 9114–9120.

Maki, D. G., Kluger, D. M., and Crnich, C. J. (2006). The risk of bloodstream infection in adults with different intravascular devices: a systematic review of 200 published prospective studies. *Mayo Clin. Proc.* 81, 1159–1171. doi: 10.4065/81.9.1159

Maki, D. G., Stolz, S. M., Wheeler, S., and Mermel, L. A. (1997). Prevention of central venous catheter-related bloodstream infection by use of an antiseptic-impregnated catheter: a randomized, controlled trial. *Ann. Intern. Med.* 127, 257–266. doi: 10.7326/0003-4819-127-4-199708150-00001

Martìnez-Martìnez, L., Pascual, A., and Perea, E. J. (1990). Effect of three plastic catheters on survival and growth of *Pseudomonas aeruginosa*. *J. Hosp. Infect.* 16, 311–318. doi: 10.1016/0195-6701(90)90003-7

Park, J. H., Lee, K. B., Kwon, I. C., and Bae, Y. H. (2001). PDMS-based polyurethanes with MPEG grafts: mechanical properties, bacterial repellency, and release behavior of rifampicin. *J. Biomater. Sci. Polym. Ed.* 12, 629–645. doi: 10.1163/156856201316883458

Pearson, S., Lu, H., and Stenzel, M. H. (2015). Glycopolymer self-assemblies with gold(I) complexed to the core as a delivery system for auranofin. *Macromolecules* 48, 1065–1076. doi: 10.1021/ma502263x

Pugach, J. L., DiTizio, V., Mittelman, M. W., Bruce, A. W., DiCosmo, F., and Khoury, A. E. (1999). Antibiotic hydrogel coated foley catheters for prevention of urinary tract infection in a rabbit model. *J. Urol.* 162, 883–887. doi: 10.1097/00005392-199909010-00084

Raad, I., Darouiche, R., Hachem, R., Mansouri, M., and Bodey, G. P. (1996). The broad-spectrum activity and efficacy of catheters coated with minocycline and rifampin. *J. Infect. Dis.* 173, 418–424. doi: 10.1093/infdis/173.2.418

Raad, I., Hanna, H., Jiang, Y., Dvorak, T., Reitzel, R., Chaiban, G., et al. (2007). Comparative activities of daptomycin, linezolid, and tigecycline against catheter-related methicillin-resistant *Staphylococcus* bacteremic isolates embedded in biofilm. *Antimicrob. Agents Chemother.* 51, 1656–1660. doi: 10.1128/AAC.00350-06

Ritz, D., and Beckwith, J. (2001). Roles of thiol-redox pathways in bacteria. *Annu. Rev. Microbiol.* 55, 21–48. doi: 10.1146/annurev.micro.55.1.21

Saha, K., Butola, B. S., and Joshi, M. (2014). Drug release behavior of polyurethane/clay nanocomposite: film vs. nanofibrous web. *J. Appl. Polym. Sci.* 131, 1–9. doi: 10.1002/app.40824

Shah, H., Bosch, W., Hellinger, W. C., and Thompson, K. M. (2013). Intravascular catheter-related bloodstream infection. *Neurohospitalist* 3, 144–151. doi: 10.1177/1941874413476043

Shoeib, T., Atkinson, D. W., and Sharp, B. L. (2010). Structural analysis of the anti-arthritic drug Auranofin: its complexes with cysteine, selenocysteine and their fragmentation products. *Inorganica Chim. Acta* 363, 184–192. doi: 10.1016/j.ica.2009.08.034

Shukla, S., and Shukla, A. (2018). Tunable antibiotic delivery from gellan hydrogels. *J. Mater. Chem. B.*6, 6444–6458. doi: 10.1039/C8TB00980E

Stewart, P. S. (2002). Mechanisms of antibiotic resistance in bacterial biofilms. *Int. J. Med. Microbiol.* 292, 107–113. doi: 10.1078/1438-4221-00196

Sweeney, N., Lipker, L., Hanson, A., Bohl, C., Engel, K., Kalous, K., et al. (2017). Docking into *Mycobacterium tuberculosis* thioredoxin reductase protein yields pyrazolone lead molecules for methicillin-resistant *Staphylococcus aureus*. *Antibiotics* 6:E4. doi: 10.3390/antibiotics6010004

Tejman-Yarden, N., Miyamoto, Y., Leitsch, D., Santini, J., Debnath, A., Gut, J., et al. (2013). A reprofiled drug, auranofin, is effective against metronidazole-resistant *Giardia lamblia*. *Antimicrob. Agents Chemother.* 57, 2029–2035. doi: 10.1128/AAC.01675-12

Thangamani, S., Mohammad, H., Abushahba, M. F. N., Sobreira, T. J. P., and Seleem, M. N. (2016). Repurposing auranofin for the treatment of cutaneous staphylococcal infections. *Int. J. Antimicrob. Agents* 47, 195–201. doi: 10.1016/j.ijantimicag.2015.12.016

Torres, N. S., Abercrombie, J. J., Srinivasan, A., Lopez-Ribot, J. L., Ramasubramanian, A. K., and Leung, K. P. (2016). Screening a commercial library of pharmacologically active small molecules against *Staphylococcus aureus* biofilms. *Antimicrob. Agents Chemother.* 60, 5663–5672. doi: 10.1128/AAC.00377-16

Trautner, B. W., and Darouiche, R. O. (2004). Role of biofilm in catheter-associated urinary tract infection. *Am. J. Infect. Control* 32, 177–183. doi: 10.1016/j.ajic.2003.08.005

Wilson, S. E. (2004). *Vascular Access: Principles and Practice,4th Edn*. Philadelphia, PA: Mosby.

Xue, L., and Greisler, H. P. (2003). Biomaterials in the development and future of vascular grafts. *J. Vasc. Surg.* 37, 472–480. doi: 10.1067/mva.2003.88

Zdrahala, R. J., and Zdrahala, I. J. (1999). Biomedical applications of polyurethanes: a review of past promises, present realities, and a vibrant future. *J. Biomater. Appl.* 14, 67–90. doi: 10.1177/088532829901400104

Zhou, C., Wu, Y., Thappeta, K. R. V., Subramanian, J. T. L., Pranantyo, D., Kang, E.-T., et al. (2017). *In vivo* anti-biofilm and anti-bacterial non-leachable coating thermally polymerized on cylindrical catheter. *ACS Appl. Mater. Interfaces* 9, 36269–36280. doi: 10.1021/acsami.7b07053

Conflict of Interest Statement: The authors declare that the research was conducted in the absence of any commercial or financial relationships that could be construed as a potential conflict of interest.

frontiers in Cellular and Infection Microbiology

ORIGINAL RESEARCH
published: 26 March 2019
doi: 10.3389/fcimb.2019.00067

Virtual Screen for Repurposing of Drugs for Candidate Influenza a M2 Ion-Channel Inhibitors

Draginja Radosevic[1], Milan Sencanski[1], Vladimir Perovic[1], Nevena Veljkovic[1], Jelena Prljic[1], Veljko Veljkovic[2], Emily Mantlo[3], Natalya Bukreyeva[3], Slobodan Paessler[3,4] and Sanja Glisic[1]*

[1] Center for Multidisciplinary Research, Institute of Nuclear Sciences VINCA, University of Belgrade, Belgrade, Serbia, [2] Biomed Protection, Galveston, TX, United States, [3] Department of Pathology, University of Texas Medical Branch, Galveston, TX, United States, [4] Institute for Human Infections and Immunity, University of Texas Medical Branch, Galveston, TX, United States

Influenza A virus (IAV) matrix protein 2 (M2), an ion channel, is crucial for virus infection, and therefore, an important anti-influenza drug target. Adamantanes, also known as M2 channel blockers, are one of the two classes of Food and Drug Administration-approved anti-influenza drugs, although their use was discontinued due to prevalent drug resistance. Fast emergence of resistance to current anti-influenza drugs have raised an urgent need for developing new anti-influenza drugs against resistant forms of circulating viruses. Here we propose a simple theoretical criterion for fast virtual screening of molecular libraries for candidate anti-influenza ion channel inhibitors both for wild type and adamantane-resistant influenza A viruses. After *in silico* screening of drug space using the EIIP/AQVN filter and further filtering of drugs by ligand based virtual screening and molecular docking we propose the best candidate drugs as potential dual inhibitors of wild type and adamantane-resistant influenza A viruses. Finally, guanethidine, the best ranked drug selected from ligand-based virtual screening, was experimentally tested. The experimental results show measurable anti-influenza activity of guanethidine in cell culture.

Keywords: influenza A, IAV matrix protein 2, drug repurposing, virtual screening, drug resistance

OPEN ACCESS

Edited by:
Rodolfo García-Contreras, National Autonomous University of Mexico, Mexico

Reviewed by:
Alan G. Goodman, Washington State University, United States
Richard Yuqi Zhao, University of Maryland, School of Medicine, United States

***Correspondence:**
Slobodan Paessler
slpaessl@utmb.edu

Specialty section:
This article was submitted to Clinical Microbiology, a section of the journal Frontiers in Cellular and Infection Microbiology

Received: *24 October 2018*
Accepted: *04 March 2019*
Published: *26 March 2019*

Citation:
Radosevic D, Sencanski M, Perovic V, Veljkovic N, Prljic J, Veljkovic V, Mantlo E, Bukreyeva N, Paessler S and Glisic S (2019) Virtual Screen for Repurposing of Drugs for Candidate Influenza a M2 Ion-Channel Inhibitors. Front. Cell. Infect. Microbiol. 9:67. doi: 10.3389/fcimb.2019.00067

INTRODUCTION

Influenza is a serious global public health concern. Regardless of the availability of antiviral drugs and vaccines, according to the World Health Organization's estimates, influenza is the cause of 3 to 5 million cases of severe illness and about 290,000–650,000 deaths in seasonal outbreaks worldwide (WHO Influenza, 2018). Annual "flu" vaccination has a primary role in preventing influenza A and B virus infections and increasing population immunity even though the efficacy of the seasonal flu vaccines may vary from year to year (Bridges et al., 2013). Since the current flu vaccination approach is imperfect, a substantial portion of the population is susceptible to infection even after vaccination every year. Therefore, alternative strategies should be considered to improve our therapeutic abilities for those patients that develop clinical flu. This would be especially important in the pandemic setting with rapid virus transmission due to the currently limited ability for fast, new vaccine production (Bridges et al., 2013). Current treatment and prophylaxis against seasonal influenza is limited to the only licensed class of antivirals, namely neuraminidase inhibitors (NAIs).

Oseltamivir and zanamivir are currently licensed worldwide while peramivir and laninamivir are approved in some countries (Ison, 2017). The frequency of NAI resistance in currently circulating strains is low, <1% (Hurt et al., 2016), but resistance to oseltamivir, the most widely used NAI, was extensive amongst former seasonal H1N1 viruses in 2008. (Hurt et al., 2009), and was detected in localized clusters of oseltamivir-resistant H1N1pdm09 (Hurt et al., 2011). Nevertheless, the therapeutic window for treatment with these drugs is very short and patients benefit the most when treated 24–48 h after the onset of "flu" symptoms (Ison, 2017).

The first of the two classes of FDA-approved anti-influenza drugs are adamantanes, amantadine and rimantadine, that inhibit viral replication by blocking the wild-type (WT) M2 proton channel.

IAV matrix protein 2 (M2), an ion channel protein, is one of the most conserved viral proteins and essential for efficient virus replication, and is thus an important anti-influenza drug target (Takeda et al., 2002). Matrix protein 2 (M2) is a 97-residue-long viral protein that encompasses a 19-residue-long hydrophobic transmembrane domain (TM) that forms a homotetrameric proton-selective channel involved in proton conductance and drug binding (Lamb et al., 1985; Sakaguchi et al., 1997). Adamantanes have been used successfully against influenza A virus infection for more than 30 years because of their wide accessibility and low price (Dolin et al., 1982). However, as a consequence of the lack of activity against influenza B (Mould et al., 2003), adverse effects, and the rapid emergence of resistance during treatment or even in the absence of selective drug pressure, the Centers for Disease Control and Prevention (CDC) have strongly recommended against the use of this class of drugs (CDC, 2006). The molecular basis for resistance to adamantanes is connected with several amino acid substitutions and the M2-S31N variant is found in more than 95% of the currently circulating influenza A viruses (Dong et al., 2015). The expansion of M2 viruses with S31N mutation in the early 2000s is not a consequence of drug selection pressure but is connected to advantageous substitutions elsewhere in the virus, in a process denoted as genetic "hitch-hiking" (Simonsen et al., 2007). On the other hand, the latest report of M2 S31 and D31 viruses in Australia suggests that the role of the M2 N31 residue in viral fitness is no longer as important as it used to be (Hurt et al., 2017). Considering all these facts, new effective anti-influenza M2 inhibitors that target both WT and S31N mutant are greatly needed. Several high-resolution M2 structures that provide important insights into the favorable structural features can be employed for designing new M2 inhibitors (Hong and DeGrado, 2012).

A recent, and very popular drug discovery approach—drug repurposing (DR), wherein old drugs are given new indication by exploring new molecular pathways and targets for intervention (Strittmatter, 2014)- offers potential economic advantage and shorter regulatory process for the clinical approval. The continuous increase of drug-resistant pathogens is a great challenge for treatment of infectious diseases and DR serves as an alternative approach for rapid identification of effective therapeutics (Zheng et al., 2018). Drug repurposing (DR) applied to viral infectious diseases integrates both screening of bioactive small-molecule collections and computational methods to find a molecule, a pathway, or a biological activity that could be used against the virus of interest (Mercorelli et al., 2018). Two clinical trials against influenza viruses with repositioned drugs are currently underway: (1) The first trial (phase 2b/3clinical trial) combines clarithromycin and naproxen along with oseltamivir in a triple-drug combination and; (2) the second trial is focused on testing efficacy of an antiparasitic drug, nitazoxanide, against influenza viruses (Phase III) (Mercorelli et al., 2018).

In this study we propose a simple theoretical criterion for fast virtual screening of molecular libraries for candidate anti-influenza M2 ion channel inhibitors both for wild type and adamantane-resistant influenza A viruses. After *in silico* screening of drug space using the EIIP/AQVN filter, and further filtering of drugs by ligand based virtual screening and molecular docking, we proposed the five best candidate drugs as potential dual inhibitors of wild type and adamantane-resistant influenza A viruses.

MATERIALS AND METHODS

For screening of drugs for repurposing to select candidates for influenza M2 inhibitors, 2,627 approved small molecule drugs from DrugBank (http://www.drugbank.ca) were screened. To define the predictive criterion for the selection of Influenza M2 candidates, the learning set (**Supplementary Tables 1**, **2**) was composed of all active compounds from ChEMBL Target Report Card (https://www.ebi.ac.uk/chembl/target/inspect/CHEMBL613740) (EMBL-EBI. ChEMBL). (EMBL-EBI. ChEMBL. Available online: https://www.ebi.ac.uk/chembl/ (accessed on June 30, 2018) against influenza A virus M2 (Target ID CHEMBL613740) both for wild type (WT) and S31N, with corresponding IC50 values. The total number of reported compounds for WT and S39N of M2 channel were 50 and 49, respectively. After removal of duplicates and inactive compounds, the final number of compounds was 15 for WT and 12 for the S31N mutant (**Supplementary Tables 1**, **2**). The control data sets were compounds from PubChem compounds database (http://www.ncbi.nlm.nih.gov/pccompound).

Virtual Screening

The virtual screening (VS) protocol included the application of subsequent filters to select candidate dual inhibitors of M2 ion channel. The first EIIP/AQVN filter approach was employed for *in silico* screening of the ChEMBL Target Report Card (https://www.ebi.ac.uk/chembl/target/inspect/CHEMBL613740) and DrugBank (http://www.drugbank.ca) (Wishart et al., 2006) and then proceeded by ligand-based screening.

EIIP/AQVN

The EIIP for organic molecules can be determined by the following simple equation derived from the "general model pseudopotential (Veljkovic et al., 2011).

$$\mathrm{EIIP} = 0.25Z^{*}\sin(1.04\pi Z^{*})/2\pi \quad (1)$$

where Z* is the average quasi valence number (AQVN) determined by

$$Z^* = \sum m(niZi/N) \quad (2)$$

Where *Zi* is the valence number of the *i*th atomic component, *ni* is the number of atoms of the *i*th component, *m* is the number of atomic components in the molecule, and *N* is the total number of atoms. EIIP values calculated according to Equations (1, 2) are expressed in Rydberg units (Ry).

Ligand-Based Virtual Screening

To screen selected compounds from Drugbank, both learning set compounds and candidates from the previous step were converted to 3D sdf format from smiles. GRIND descriptors of molecules were calculated, based on molecular interaction field (MIF) probes (Duran et al., 2009). Computation method for descriptor generation was GRID with step 0.5. Applied probes (mapped regions of molecule surface) were DRY (hydrophobic interactions) O (hydrogen bond acceptor) N1 (hydrogen bond donor) and TIP (molecular shape descriptor). Discretization Method was AMANDA (Duran et al., 2008), with scale factor 0.55. Cut off was set to: DRY −0.5 O −2.6 N1 −4.2 TIP −0.75. Encoding Method was MACC2 and weights were the following: DRY: −0.5, O: −2.6, N1: −4.2, TIP: −0.75. Number of PCA components was set to five. Explained variance of such obtained model was 58.84%. Then, learning set compounds were imported and served for screening the candidate compound database. All calculations were carried in Pentacle software version 1.06 for Linux (Pastor et al., 2000).

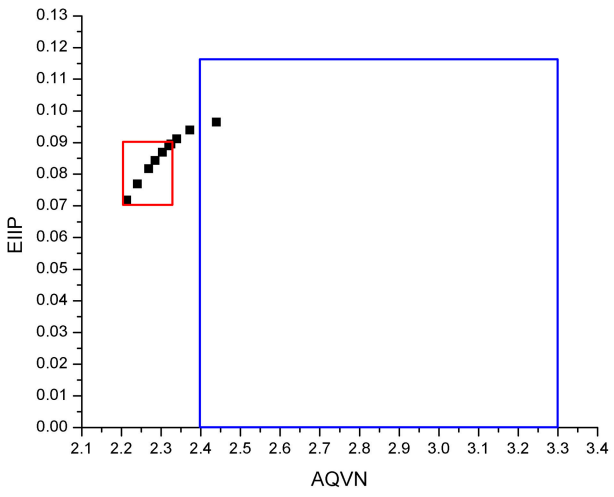

FIGURE 1 | Schematic presentation of the EIIP/AQVN criterion for selection of candidate M2 inhibitors. Common domain of active compounds for both WT and S31N M2 (red) with AQVN (2.21–2.32), EIIP (0.071–0.089). Chemical space (blue) with AQVN (2.40–3.30) EIIP (0.000–0.116)—EIIP/AQVN domain of homologous distribution of >90% compounds from PubChem Compound Database.

Molecular Docking

Receptor Preparation

Crystal structures of the wild type M2 channel and the S31N mutant channel were downloaded from RCSB PDB database (https://www.rcsb.org/) with PDBIDs 2KQT (Cady et al., 2010) and 2LY0 (Wang et al., 2013) respectively. All ligands, ions and water molecules were removed from structures. All hydrogen atoms were added on protein structures and then truncated to only polar hydrogen atoms during the preparation process. The receptor was prepared in ADT Tools 1.5.6 (Sanner, 1999; Morris et al., 2009).

Ligand Preparation

Ligands were converted from 3Dsdf to mol2 format and imported to Avogadro software in order to protonate them at physiological pH. Molecules were prepared for MOPAC 2016 (Stewart, 2016) and geometrically optimized on PM7 (Stewart, 2013) level of theory. They were further prepared for molecular docking in ADT Tools.

Molecular Docking

A grid box with dimensions 24 × 24 × 24 A was placed in the center of the binding site of the protein receptor. Exhaustiveness was set to 50. Molecular docking was carried in Autodock Vina (Trott and Olson, 2010).

In vitro Efficacy Testing of Guanethidine Against Influenza a (h1n1) Virus

Influenza A/CA/07/2009 (H1N1) virus was premixed with 1, 10, and 100 μM of guanethidine and incubated at 37C for 1 hr. Positive control wells were prepared by mixing influenza A/CA/07/2009 (H1N1) virus with 10 μM of merimepodib. MDCK cells were then infected in triplicates with influenza A/CA/07/2009 (H1N1) virus / drug mixture. After ∼1 h of incubation at 37°C and 5% CO2, cells were washed with serum free media and 1× of each compound dose was added to the cells. Virus control wells as well as untreated control wells were included in triplicates. Cells were incubated at 37C and 5% CO2 and samples were collected at 0, 1, 2, and 3 days post-infection. Samples were stored at −80°C until the day of analysis. The influenza virus titer in MDCK cells via TCID50 was performed for each sample collected at days 0, 1, and 2 post-infection.

RESULTS

The virtual screening (VS) protocol in this study was based on the application of sequential filters to select candidate dual inhibitors of the M2 ion channel. Previously it was shown for molecular targets in diverse pathological states that small molecules with similar AQVN and EIIP values interact with the common therapeutic targets (Veljkovic et al., 2011, 2013). This resulted in determining criteria for virtual screening of molecular libraries for compounds with similar therapeutic properties (Veljkovic et al., 2013). The learning set consists of M2 WT (**Supplementary Table 1**), and M2 S31N mutant (**Supplementary Table 2**) ion channel inhibitors from the ChEMBL Target Report Card (https://www.ebi.ac.uk/chembl/

TABLE 1 | Approved drugs screened for candidate anti-M2 inhibitors.

Drugbank accession number	Name	Chemical formula	AQVN	EIIP
DB00915	Amantadine	C10H17N	2.214286	0.071739
DB06689	Ethanolamine Oleate	C18H34O2.C2H7NO	2.215385	0.071958
DB00153	Ergocalciferol	C28H44O	2.219178	0.072708
DB00898	Ethanol	C2H6O	2.222222	0.073303
DB01105	Sibutramine	C17H26ClN	2.222222	0.073303
DB01158	Bretylium	C11H17BrN	2.233333	0.075425
DB00804	Dicyclomine	C19H35NO2	2.245614	0.077673
DB00146	Calcidiol	C27H44O2	2.246575	0.077845
DB01436	Alfacalcidol	C27H44O2	2.246575	0.077845
DB00154	Dihomo-$\hat{I}^3$-linolenic acid	C20H34O2	2.25	0.078451
DB00592	Piperazine	C4H10N2	2.25	0.078451
DB01191	Dexfenfluramine	C12H16F3N	2.25	0.078451
DB01431	Allylestrenol	C21H32O	2.259259	0.080048
DB00375	Colestipol	C8H23N5.C3H5ClO	2.26087	0.080319
DB00330	Ethambutol	C10H24N2O2	2.263158	0.080701
DB00162	Vitamin A	C20H30O	2.27451	0.082539
DB01365	Mephentermine	C11H17N	2.275862	0.082751
DB01170	Guanethidine	C10H22N4	2.277778	0.08305
DB00132	Alpha-Linolenic Acid	C18H30O2	2.28	0.083392
DB06809	Plerixafor	C28H54N8	2.288889	0.084723
DB08868	Fingolimod	C19H33NO2	2.290909	0.085017
DB00858	Drostanolone	C20H32O2	2.296296	0.085784
DB00136	Calcitriol	C27H44O3	2.297297	0.085924
DB00910	Paricalcitol	C27H44O3	2.297297	0.085924
DB00376	Trihexyphenidyl	C20H31NO	2.301887	0.086554
DB01022	Phylloquinone	C31H46O2	2.303797	0.086811
DB00191	Phentermine	C10H15N	2.307692	0.087326
DB00313	Valproic Acid	C8H16O2	2.307692	0.087326
DB01577	Methamphetamine	C10H15N	2.307692	0.087326
DB06204	Tapentadol	C14H23NO	2.307692	0.087326
DB06709	Methacholine	C8H18NO2	2.310345	0.087669
DB08887	Icosapent ethyl	C22H34O2	2.310345	0.087669
DB01187	Iophendylate	C19H29IO2	2.313725	0.088098
DB01337	Pancuronium	C35H60N2O4	2.316832	0.088483
DB00947	Fulvestrant	C32H47F5O3S	2.318182	0.088648
DB01083	Orlistat	C29H53NO5	2.318182	0.088648
DB00387	Procyclidine	C19H29NO	2.32	0.088868
DB00942	Cycrimine	C19H29NO	2.32	0.088868
DB08804	Nandrolone decanoate	C28H44O3	2.32	0.088868

target/inspect/CHEMBL613740) (EMBL-EBI. ChEMBL). The AQVN/EIIP descriptor values were calculated for the learning set (**Figure 1**) and range for selection was based on their distribution. AQVN descriptor values were in range 2.21–2.32 for WT and 2.21–2.44 for S31N mutant. More than 80% of the compounds of WT inhibitors and 83% M2 S31N mutant ion channel inhibitors from the learning set were inside the common active domain for both while having AQVN and EIIP values within the intervals of (2.21–2.32) and (0.071–0.089). Inside this common active domain is also amantadine with AQVN/EIIP 2.214/0.0717. The reported domain was selected as a criterion for the selection of compounds representing candidate dual M2 WT and S31 mutant ion channel inhibitors (**Figure 1**). By applying the EIIP/AQVN-based virtual screening criterion, 39 drugs were chosen (**Table 1**) out of 2,627 approved drugs from the DrugBank (http://www.drugbank.ca) (Wishart et al., 2006).

All 39 selected drugs were imported in Pentacle software, protonated at pH 7.4, and aligned toward principal moment of inertia. In ligand based virtual screening, we used centroid distance method as criteria for similarity between learning set and candidate compounds. Top 5 candidates from DrugBank selection are presented in **Table 2**.

TABLE 2 | Five best candidates from virtual screening, with Drugbank ID, Similarity distance, structure, and EIIP descriptor values.

Drugbank ID	Name	Similarity distance from centroid	Structure	AQVN	EIIP
DB01170	Guanethidine	1.3446	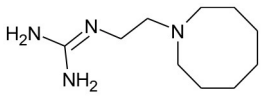	2.277778	0.08305
DB00191	Phentermine	1.4234	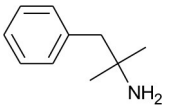	2.307692	0.087326
DB01577	Methamphetamine	1.4334	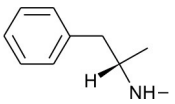	2.307692	0.087326
DB01191	Dexfenfluramine	1.5377	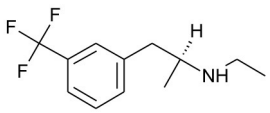	2.25	0.078451
DB00942	Cycrimine	1.6057	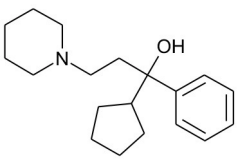	2.32	0.088868

TABLE 3 | Docking energies of five best candidates from virtual screening, with Drugbank ID, Docking energies, and affinity ratio.

Drugbank ID	Name	Docking energy on WT M2 channel (kcal/mol)	Docking energy on S31N mutant M2 channel (kcal/mol)	Affinity ratio WT:S31N*
DB00942	Cycrimine	−8.3	−8.3	1
DB01191	Dexfenfluramine	−6.3	−6.0	0.6
DB01170	Guanethidine	−5.9	−5.7	0.71
DB00191	Phentermine	−5.3	−4.8	0.43
DB01577	Methamphetamine	−4.8	−4.5	0.6

*$Ratio = \frac{K_1}{K_2} = exp\left(\frac{(\Delta G_1 - \Delta G_2)}{RT}\right)$.

We further carried out molecular docking of five candidates to both the wild type M2 channel and S31N mutant channel. The docking energies obtained are presented in **Table 3**. The candidate with the lowest binding energy and equal affinity to both WT channel and S31N mutant channel was cycrimine, with docking energy −8.3 kcal/mol. Docked conformations of cycrimine are presented on **Figures 1**, **2**. In both WT and S31N mutant of M2 channel, cycrimine conserves corresponding intermolecular receptor-ligand interactions, Ala 30 and Ser 31 in case of WT and Asn 31 in the case of the S31N mutant. As presented on **Figures 2**, **3**, the orientation of cycrimine, compared to crystal coordinates of amandatine and M2WJ332 show cycrimine's ability to form hydrogen bond interactions with Ser 31 i.e., Asn 31, while keeping hydrophobic interactions with Ala 30. This could be a possible explanation as to why cycrimine shows relatively high and equal affinity to both WT and S31N mutant M2 channels (−8.3 kcal/mol, or 800 nM). Other compounds show similar binding patterns as cycrimine; however, in most other cases the affinity ratio is in favor of the WT M2 channel protein.

In order to validate our *in silico* screening approach, we examined the antiviral activity of guanethidine, the top candidate from the DrugBank selection (**Table 2**), *in vitro*. As a positive control, influenza virus was premixed with 10 uM of merimepodib, an IMPDH inhibitor with known antiviral activity against a variety of viruses including influenza (Markland et al., 2000; Tong et al., 2018). Addition of guanethidine to cells infected with 2009 H1N1 pandemic influenza virus resulted in significantly lower viral titers in a dose-dependent

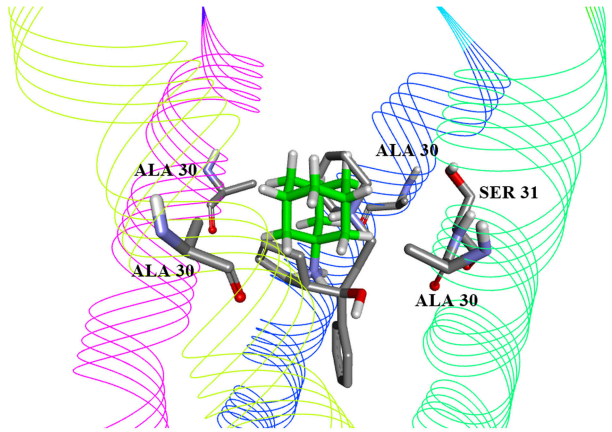

FIGURE 2 | Best-ranking docked conformation of Cycrimine (gray carbon atoms) in solid state NMR structure of WT M2 channel (PDB 2KQT), compared to amantadine coordinates in complex (green carbon atoms).

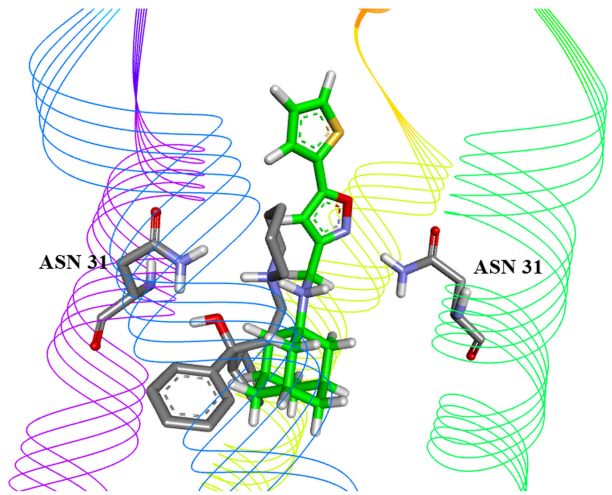

FIGURE 3 | Best-ranking docked conformation of Cycrimine (gray carbon atoms) in solid state NMR structure of S31N mutant M2 channel (PDB 2LY0), compared to drug M2WJ332 coordinates in complex (green carbon atoms).

manner. Both 100 and 10 μM guanethidine treatment resulted in significant reductions in viral titers at day 1 post-infection, with 100 μM of guanethidine producing a 1–2 log reduction in viral titers.

DISCUSSION

Current prevention and treatment options for influenza A and B infections are insufficient due to increased clinical use of licensed antivirals leading to the emergence of resistant viral strains (Hayden and de Jong, 2011). In a quest for new preventive and therapeutic options to minimize drug resistance and threats of outbreaks of pandemic viruses, the main obstacle is the fact that drug development is an expensive, time-consuming, and risky enterprise. Therefore, drug repurposing represents a promising therapeutic strategy for many viral diseases including anti-influenza A and B treatment. Various predictive computational approaches have been developed to identify drug repositioning opportunities against influenza viruses (Sencanski et al., 2015). Previously, the EIIP/AQVN criterion has been proven to be an efficient filter in virtual screening of molecular libraries for candidate inhibitors of HIV and Ebola virus infection (Tintori et al., 2007; Veljkovic et al., 2015a,b). Using this approach, ibuprofen was selected as an inhibitor of the Ebola virus infection, and this prediction was later experimentally confirmed (Zhao et al., 2016; Paessler et al., 2018.)

To select drug candidates for M2 inhibitors, the virtual screening protocol in our study was based on the application of successive filters. The previous study of EIIP/AQVN distribution of compounds from the PubChem database (http://www.ncbi.nlm.nih.gov/pccompound) showed that 92.5% compounds from PubChem are homogenously distributed inside EIIP and AQVN intervals (0.00–0.11 Ry) and (2.4–3.3), respectively (Veljkovic et al., 2011). The domain that encompasses the majority of known chemical compounds was designated as a "basic EIIP/AQVN chemical space" (BCS). Results of the application of VS based on the EIIP/AQVN filter in this study showed that the active group of candidate M2 inhibitors is very specific, belonging to the sparse cluster of compounds that are out of BCS. This finding indicates that testing only a minor fraction of the compounds from the active EIIP/AQVN domain has a greater chance to inhibit M2 function than compounds with any other EIIP/AQVN values. The proposed AQVN/EIIP interval for the selection of dual M2 inhibitor candidates encompasses only 3% of all chemical molecules. It is therefore not surprising that the previous results from the high-throughput screening had a 10- to 100-fold lower hit rate compared to screens for other targets (Balgi et al., 2013). These results confirm that the M2 is a challenging target for selective inhibition and drug development. In the course of further analysis in our study, the next following two filters were applied in selection of candidates with dual inhibition against M2 WT and M2 S31N mutant protein. First, by applying ligand based virtual screening, the candidates were selected using lowest distance from centroid in the PCA model. This model was based on variables constructed from MIF descriptors of compounds from the learning set. Therefore, their pharmacophore similarity was criteria for the selection. Structure-based approach, as the next step, allows the docking of selected compounds from the first step into both crystal structures of M2 WT and S31N mutant proteins. In this step, the output docking energies (binding free energies) were used as criteria to rank the candidates. In order to address candidate compounds in more detail, the affinity ratio was also calculated. Two of the best candidates are presented in **Figures 2**, **3**, and in **Tables 2**, **3**. The biological significance of docking energy is to select the best candidate that targets both the WT and S31N mutant form of M2. i.e., a dual target candidate. We carried out docking energy comparisons for all candidates, and calculated their ratio with prior conversion to Ki values (docking energy has logarithmic dependency of Ki).

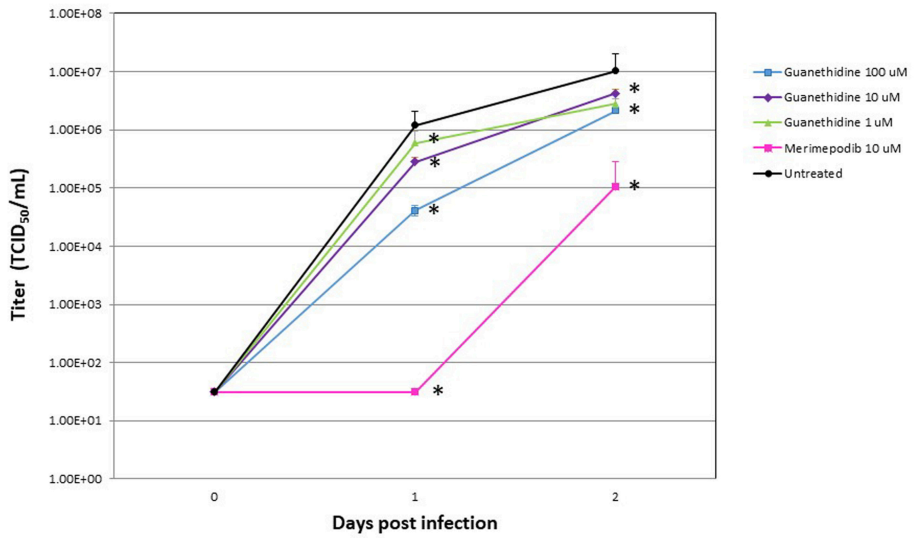

FIGURE 4 | Influenza A/CA/07/2009 (H1N1) viral titers at 0, 1, and 2 days post-infection (dpi) after treatment with the indicated drug concentrations. Ten micromolar (10 μM) merimepodib was used as a positive control. Results are plotted as the means of triplicate observations, with standard deviations shown. Significant decrease in viral load is marked by asterisk.

Ratio of equilibrium constants between two equilibrium systems (in our case, WT and S31N mutant M2 receptors) that share same ligand in the same environment gives information about that ligand's preference to a certain receptor type. The closer the value of Ki ratio is to 1, the more the ligand is prone to target both receptor types equally and therefore, the ligand is a better dual target candidate. It should also be emphasized that it was assumed that the selected dual inhibitors targeting both M2 proteins might have advantages over mono inhibitors. This is reflected in a higher genetic barrier that enables dual inhibitors to preserve activity if the mutant reverts back to WT sequence (Ma et al., 2016; Wang, 2016).

We selected guanethidine as the best ranked compound from ligand-based virtual screening for further experimental validation. In the experiments with influenza A/CA/07/2009 (H1N1) it was shown that guanethidine inhibits influenza virus production (**Figure 4**) in a dose-dependent manner.

Another of the best ranked inhibitors from our computational study, methamphetamine, has actually documented good inhibitory activity against influenza A (Chen et al., 2012). It was previously demonstrated that methamphetamine inhibits influenza A virus replication *in vitro* primarily *via* acting at the viral replication stage in which M2 plays a major role. Another drug among the best ranked candidates for repurposing against M2 is cycrimine, a drug used to reduce levels of acetylcholine to balance levels of dopamine in the treatment of Parkinson's disease (Kafer and Poch, 1957; Fahn, 2015). Interestingly, the anti-influenza drug amantadine, previously repurposed for treatment of Parkinson's disease, also causes anticholinergic-like side effects (Horstink et al., 2006). In addition, as amantadine and cycrimine are in the same EIIP/AQVN domain, it can be expected from previous studies that they share same therapeutic targets. Other drugs selected as potential M2 inhibitors are ergocalciferol, calcidiol, alfacalcidol. This result is very interesting as vitamin D metabolites were previously connected to potential anti-influenza activity (Gruber-Bzura, 2018). Another FDA approved drug with documented anti-influenza properties, Alpha-Linolenic Acid, was also selected as a potential M2 inhibitor in our study, indicating the usefulness of the proposed screen (Bai et al., 2012).

In conclusion, the results presented here suggest that guanethidine represents a promising molecular template for further development of drugs against influenza virus. Other selected drugs from our computational study present valuable starting points for further experimental investigations in a quest for safe, new treatments for human and animal influenza infections.

DATA AVAILABILITY

All datasets generated for this study are included in the manuscript and/or the **Supplementary Files**.

AUTHOR CONTRIBUTIONS

SP, SG, DR, and VV conceived and designed the study. VP developed the analysis tools. DR, SG, MS, VV, NV, JP, EM, and NB analyzed the data. EM and NB performed the experiments. DR, MS, VP, NV, JP, VV, EM, NB, SP, and SG drafted the work. SG, DR, VV, and SP wrote the paper. DR, MS, VP, NV, JP, VV, EM, NB, SP, and SG agreed on the final approval of the manuscript

to be published and agreed to be accountable for all aspects of the work.

ACKNOWLEDGMENTS

This work was supported by the Ministry of Education, Science and Technological Development of the Republic of Serbia (Grant no. 173001).

SUPPLEMENTARY MATERIAL

The Supplementary Material for this article can be found online at: https://www.frontiersin.org/articles/10.3389/fcimb.2019.00067/full#supplementary-material

Supplementary Table 1 | The learning set (M2 WT).

Supplementary Table 2 | The learning set (M2 S31N).

REFERENCES

Bai, S. W., Chen, C. Y., Ji, J., Xie, Q. M., Ma, Y., Sun, B. L., et al. (2012). Inhibition effect of alpha-lipoic acid on the propagation of influenza a virus in MDCK cells. *Pak. Vet. J*. 32, 101–106.

Balgi, A. D., Wang, J., Cheng, D. Y., Ma, C., Pfeifer, T. A., Shimizu, Y., et al. (2013). Inhibitors of the influenza A virus M2 proton channel discovered using a high-throughput yeast growth restoration assay. *PLoS ONE* 8:e55271. doi: 10.1371/journal.pone.0055271

Bridges, C., Peasah, S., and Meltzer, M. (2013). "The control of influenza and cost effectiveness of interventions," in *Influenza Textbook*, eds R. G. Webster, A. S. Monto, T. J. Braciale, and R. A. Lamb (Hoboken, NY: Wiley-Blackwell), 419–433.

Cady, S. D., Schmidt-Rohr, K., Wang, J., Soto, C. S., Degrado, W. F., and Hong, M. (2010). Structure of the amantadine binding site of influenza M2 proton channels in lipid bilayers. *Nature* 463, 689–692. doi: 10.1038/nature08722

CDC (2006). High levels of adamantane resistance among influenza A (H3N2) viruses and interim guidelines for use of antiviral agents-United States, 2005-06 influenza season. MMWR Morb. *Mortal. Wkly*. 55, 44–46.

Chen, Y. H., Wu, K. L., and Chen, C. H. (2012). Methamphetamine reduces human influenza A virus replication. *PLoS ONE* 7:e48335. doi: 10.1371/journal.pone.0048335

Dolin, R., Reichman, R. C., Madore, H. P., Maynard, R., Linton, P. N., and Webber-Jones, J. (1982). A controlled trial of amantadine and rimantadine in the prophylaxis of influenza A infection. *N. Engl. J. Med*. 307, 580–584. doi: 10.1056/NEJM198209023071002

Dong, G., Peng, C., Luo, J., Wang, C., Han, L., Wu, B., et al. (2015). Adamantane-resistant influenza A viruses in the World (1902–2013): frequency and distribution of M2 gene mutations. *PLoS ONE* 10:e0119115. doi: 10.1371/journal.pone.0119115

Duran, A., Comesaña, G., and Pastor, M. (2008). Development and validation of AMANDA, a new algorithm for selecting highly relevant regions in molecular interaction fields. *J. Chem. Inf. Model*. 48, 1813–1823. doi: 10.1021/ci800037t

Duran, A., Zamora, I., and Pastor, M. (2009). Suitability of GRIND-based principal properties for the description of molecular similarity and ligand-based virtual screening. *J. Chem. Inf. Model*. 49, 2129–2138. doi: 10.1021/ci900228x

Fahn, S.The medical treatment of Parkinson disease from James Parkinson to George Cotzias (2015). *Mov. Disord*. 30, 4–18. doi: 10.1002/mds.26102

Gruber-Bzura, B. M. (2018). Vitamin D and influenza-prevention or therapy? *Int. J. Mol. Sci*. 16:19. doi: 10.3390/ijms19082419

Hayden, F. G., and de Jong, M. D. (2011). Emerging influenza antiviral resistance threats. *J. Infect. Dis*. 203, 6–10. doi: 10.1093/infdis/jiq012

Hong, M., and DeGrado, W. F. (2012). Structural basis for proton conduction and inhibition by the influenza M2 protein. *Protein Sci.* 21, 1620–1633. doi: 10.1002/pro.2158

Horstink, M., Tolosa, E., Bonuccelli, U., Deuschl, G., Friedman, A., Kanovsky, P., et al. (2006). European Federation of Neurological Societies; Movement Disorder Society-European Section. Review of the therapeutic management of Parkinson's disease. Report of a joint task force of the European Federation of Neurological Societies and the Movement Disorder Society-European Section. Part I: early (uncomplicated) Parkinson's disease. *Eur. J. Neurol*. 13, 1170–1185. doi: 10.1111/j.1468-1331.2006.01547.x

Hurt, A., Komadina, N., Deng, Y. M., Kaye, M., Sullivan, S., Subbarao, K., et al. (2017). Detection of adamantane-sensitive influenza A(H3N2) viruses in Australia, 2017: a cause for hope? *Euro Surveill*. 22:17-00731. doi: 10.2807/1560-7917.ES.2017.22.47.17-00731

Hurt, A. C., Besselaar, T. G., Daniels, R. S., Ermetal, B., Fry, A., Gubareva, L., et al. (2016). Global update on the susceptibility of human influenza viruses to neuraminidase inhibitors, 2014–2015. *Antiviral Res.* 132, 178–185. doi: 10.1016/j.antiviral.2016.06.001

Hurt, A. C., Ernest, J., Deng, Y. M., Iannello, P., Besselaar, T. G., Birch, C., et al. (2009). Emergence and spread of oseltamivir-resistant A (H1N1) influenza viruses in Oceania, South East Asia and South Africa. *Antiviral Res.* 83, 90–93. doi: 10.1016/j.antiviral.2009.03.003

Hurt, A. C., Hardie, K., Wilson, N. J., Deng, Y. M., Osbourn, M., Gehrig, N., et al. (2011). Community transmission of oseltamivir-resistant A (H1N1) pdm09 influenza. *N. Engl. J. Med*. 365, 2541–2542. doi: 10.1056/NEJMc1111078

Ison, M. G. (2017). Antiviral treatments. *Clin. Chest Med*. 38, 139–153. doi: 10.1016/j.ccm.2016.11.008

Kafer, J. P., and Poch, G. F. (1957). Cycrimine, a new drug in the treatment of Parkinson's disease and Parkinsonism. *Prensa Med. Argent* 44, 1071–1075.

Lamb, R. A., Zebedee, S. L., and Richardson, C. D. (1985). Influenza virus M2 protein is an integral membrane protein expressed on the infected-cell surface. *Cell* 40, 627–633. doi: 10.1016/0092-8674(85)90211-9

Ma, C., Zhang, J., and Wang, J. (2016). Pharmacological characterization of the spectrum of antiviral activity and genetic barrier to drug resistance of M2-S31N channel blockers. *Mol. Pharmacol*. 90, 188–198. doi: 10.1124/mol.116.105346

Markland, W., McQuaid, T. J., Jain, J., and Kwong, A. D. (2000). Broad-spectrum antiviral activity of the IMP dehydrogenase inhibitor VX-497: a comparison with ribavirin and demonstration of antiviral additivity with alpha interferon. *Antimicrob. Agents Chemother*. 44, 859–866. doi: 10.1128/AAC.44.4.859-866.2000

Mercorelli, B., Palù, G., and Loregian, A. (2018). Drug repurposing for viral infectious diseases: how far are we? *Trends Microbiol*. 26, 865–876. doi: 10.1016/j.tim.2018.04.004

Morris, G. M., Huey, R., Lindstrom, W., Sanner, M. F., Belew, R. K., Goodsell, D. S., et al. (2009). Autodock4 and AutoDockTools4: automated docking with selective receptor flexiblity. *J. Comput. Chem*. 16, 2785–2791. doi: 10.1002/jcc.21256

Mould, J. A., Paterson, R. G., Takeda, M., Ohigashi, Y., Venkataraman, P., Lamb, R. A., et al. (2003). Influenza B virus BM2 protein has ion channel activity that conducts protons across membranes. *Dev. Cell* 5, 175–184. doi: 10.1016/S1534-5807(03)00190-4

Paessler, S., Huang, C., Sencanski, M., Veljkovic, N., Perovic, V., Glisic, S., et al. (2018). Ibuprofen as a template molecule for drug design against Ebola virus. *Front. Biosci.* 23, 947–953. doi: 10.2741/4627

Pastor, M., McLay, I., Pickett, S., and Clementi, S. (2000). Grid-Independent descriptors (GRIND): a novel class of alignment-independent three-dimensional molecular descriptors. *Med. Chem*. 43, 3233–3243. doi: 10.1021/jm000941m

Sakaguchi, T., Tu, Q., Pinto, L. H., and Lamb, R. A. (1997). The active oligomeric state of the minimalistic influenza virus M2 ion channel is a tetramer. *Proc. Natl. Acad. Sci. U.S.A.* 94, 5000–5005. doi: 10.1073/pnas.94.10.5000

Sanner, M. F. (1999). Python: a programming language for software integration and development. *J. Mol. Graphics Mod*. 1, 57–61.

Sencanski, M., Radosevic, D., Perovic, V., Gemovic, B., Stanojevic, M., Veljkovic, N., et al. (2015). Natural products as promising therapeutics for treatment of influenza disease. *Curr. Pharm. Des*. 21, 5573–5588. doi: 10.2174/1381612821666151002113426

Simonsen, L., Viboud, C., Grenfell, B. T., Dushoff, J., Jennings, L., Smit, M., et al. (2007). The genesis and spread of reassortment human influenza A/H3N2 viruses conferring adamantane resistance. *Mol. Biol. Evol.* 24, 1811–1820. doi: 10.1093/molbev/msm103

Stewart, J. J. P. (2013). Optimization of parameters for semiempirical methods VI: more modifications to the NDDO approximations and re-optimization of parameters. *J. Mol. Mod.* 19, 1–32. doi: 10.1007/s00894-012-1667-x

Stewart, J. J. P. (2016). *MOPAC2016. Stewart Computational Chemistry*. Colorado Springs, CO. Availaible online at: http://OpenMOPAC.net.

Strittmatter, S. M. (2014). Overcoming drug development bottlenecks with repurposing: old drugs learn new tricks. *Nat. Med.* 20,590–591. doi: 10.1038/nm.3595

Takeda, M., Pekosz, A., Shuck, K., Pinto, L. H., and Lamb, R. A. (2002). Influenza a virus M2 ion channel activity is essential for efficient replication in tissue culture. *J. Virol.* 76, 1391–1399. doi: 10.1128/JVI.76.3.1391-1399.2002

Tintori, C., Manetti, F., Veljkovic, N., Perovic, V., Vercammen, J., Hayes, S., et al. (2007). Novel virtual screening protocol based on the combined use of molecular modeling and electron-ion interaction potential techniques to design HIV-1 integrase inhibitors. *J. Chem. Inf. Model.* 47,1536–1544. doi: 10.1021/ci700078n

Tong, X., Smith, J., Bukreyeva, N., Koma, T., Manning, J. T., Kalkeri, R., et al. (2018). Merimepodib, an IMPDH inhibitor, suppresses replication of Zika virus and other emerging viral pathogens. *Antiviral Res.* 149, 34–40. doi: 10.1016/j.antiviral.2017.11.004

Trott, O., and Olson, A. J. (2010). AutoDock Vina: improving the speed and accuracy of docking with a new scoring function, efficient optimization and multithreading. *J. Comput. Chem.* 31, 455–461. doi: 10.1002/jcc.21334

Veljkovic, N., Glisic, S., Perovic, V., and Veljkovic, V. (2011). The role of long-range intermolecular interactions in discovery of new drugs. *Exp. Opin. Drug Disc.* 6, 1263–1270. doi: 10.1517/17460441.2012.638280

Veljkovic, N., Glisic, S., Prljic, J., Perovic, V., and Veljkovic, V. (2013). Simple and general criterion for "*in silico*" screening of candidate HIV drugs. *Curr. Pharm. Biotechnol.* 14, 561–569. doi: 10.2174/1389201014051311111105301

Veljkovic, V., Goeijenbier, M., Glisic, S., Veljkovic, N., Perovic, V., Sencanski, M., et al. (2015a). *In silico* analysis suggests repurposing of ibuprofen for prevention and treatment of EBOLA virus disease. *F1000Res.* 4:104. doi: 10.12688/f1000research.6436.1

Veljkovic, V., Loiseau, P. M., Figadere, B., Glisic, S., Veljkovic, N., Perovic, V., et al. (2015b). Virtual screen for repurposing approved and experimental drugs for candidate inhibitors of EBOLA virus infection. *F1000Res.* 4:34. doi: 10.12688/f1000research.6110.1

Wang, J. (2016). M2 as a target to combat influenza drug resistance: what does the evidence say? *Future Virol.* 11, 1–4. doi: 10.2217/fvl.15.95

Wang, J., Wu, Y., Ma, C., Fiorin, G., Wang, J., Pinto, L. H., et al. (2013). Structure and inhibition of the drug-resistant S31N mutant of the M2 ion channel of influenza A virus. *Proc. Natl. Acad. Sci. U.S.A.* 110, 1315–1320. doi: 10.1073/pnas.1216526110.

WHO Influenza (2018). *Factsheet; March*. Available online at: http://www.who.int/en/news-room/fact-sheets/detail/influenza-(seasonal) (Accessed *August* 25, 2018).

Wishart, D. S., Knox, C., Guo, A. C, Shrivastava, S., Hassanali, M., Stothard, P., et al. (2006). DrugBank: a comprehensive resource for in silico drug discovery and exploration. *Nucleic Acids Res.* 34(Database issue):D668–D672. doi: 10.1093/nar/gkj067

Zhao, Y., Ren, J., Harlos, K., Jones, D. M., Zeltina, A., Bowden, T. A., et al. (2016). Toremifene interacts with and destabilizes the Ebola virus glycoprotein. *Nature* 535, 169–172. doi: 10.1038/nature18615

Zheng, W., Sun, W., and Simeonov, A. (2018). Drug repurposing screens and synergistic drug-combinations for infectious diseases. *Br. J. Pharmacol.* 175,181–191. doi: 10.1111/bph.13895

Conflict of Interest Statement: The authors declare that the research was conducted in the absence of any commercial or financial relationships that could be construed as a potential conflict of interest.

frontiers in Cellular and Infection Microbiology

REVIEW
published: 11 June 2019
doi: 10.3389/fcimb.2019.00193

Drug Repurposing to Fight Colistin and Carbapenem-Resistant Bacteria

Lucie Peyclit[1,2], *Sophie Alexandra Baron*[1,2] *and Jean-Marc Rolain*[1,2]*

[1] *Faculté de Médecine et de Pharmacie, IRD, APHM, MEPHI, Aix Marseille Univ, Marseille, France,* [2] *IHU Méditerranée Infection, Marseille, France*

The emergence of new resistance mechanisms, the failure of classical antibiotics in clinic, the decrease in the development of antibiotics in the industry are all challenges that lead us to consider new strategies for the treatment of infectious diseases. Indeed, in recent years controversy has intensified over strains resistant to carbapenem and/or colistin. Various therapeutic solutions are used to overcome administration of last line antibiotics. In this context, drug repurposing, which consists of using a non-antibiotic compound to treat multi-drug resistant bacteria (MDR), is encouraged. In this review, we first report what may have led to drug repurposing. Main definitions, advantages and drawbacks are summarized. Three major methods are described: phenotypic, computational and serendipity. In a second time we will focus on the current knowledge in drug repurposing for carbapenem and colistin-resistant bacteria with different studies describing repurposed compounds tested on Gram-negative bacteria. Furthermore, we show that drug combination therapies can increase successful by drug repurposing strategy. In conclusion, we discuss the pharmaceutical industries that have little interest in reprofiling drugs due to lack of profits. We also consider what a clinician might think of the indications of these uncommon biologists to treat MDR bacterial infections and avoid therapeutic impasses.

Keywords: repurposing, multi-drug resistance (MDR), bacteria, colistin resistance, carbapenam resistant enterobacteriaceae

OPEN ACCESS

Edited by:
Maria Tomas,
Complexo Hospitalario Universitario A Coruña, Spain

Reviewed by:
Rafael Ayerbe Algaba,
Institute of Biomedicine of Seville (IBIS), Spain
Anastasia Antoniadou,
National and Kapodistrian University of Athens, Greece

***Correspondence:**
Jean-Marc Rolain
jean-marc.rolain@univ-amu.fr

Specialty section:
This article was submitted to Clinical Microbiology, a section of the journal Frontiers in Cellular and Infection Microbiology

Received: *28 February 2019*
Accepted: *20 May 2019*
Published: *11 June 2019*

Citation:
Peyclit L, Baron SA and Rolain J-M (2019) Drug Repurposing to Fight Colistin and Carbapenem-Resistant Bacteria. Front. Cell. Infect. Microbiol. 9:193. doi: 10.3389/fcimb.2019.00193

INTRODUCTION

Nowadays, despite recent scientific progress, infectious diseases must always be taken into consideration. The World Health Organization (WHO) closely examines such concerns in order to have an effective health system (World Health Organization, 2018). For 50 years, we have been confronted with the end of the golden age of antibiotic discovery, while some antimicrobial substances have existed for years (Gould, 2016). Due to significant progress that has largely contributed to reducing the number of deaths from infectious diseases, pharmaceutical companies have developed a decreasing interest in these drugs (Conly and Johnston, 2005).

In addition, the use of an antibiotic and the emergence of its resistance are inevitable and intrinsically linked (Mohr, 2016). Although this is not a new phenomenon but a natural one, WHO analysis warns against this serious situation which is the impact, nature and spread of global antimicrobial resistance (Global Antimicrobial Resistance Surveillance System, 2019 Report Early implementation). These resistant bacteria are found in every kind of environment: water, animals, humans, plants and food (Rolain, 2013; Zenati et al., 2016; Bachiri et al., 2017; Tafoukt et al., 2017). The inappropriate use of antimicrobial agents and the spread of antibacterial resistance are among factors that lead to a high rate of resistance in clinical, animals, and even in environmental isolates

(Roca et al., 2015; Bassetti et al., 2017). Partly because of drug pressure, resistance can occur more easily and affect all types of antibiotics as for the last-line antibiotics used in human medicine drug for resistant bacterial infections (Biswas et al., 2012). In recent years, we have seen an increase in the use of carbapenems as a result of an increase in the carbapenem resistance of Gram-negative bacteria (GNB) (Diene and Rolain, 2013). For example, Monaco et al. showed in Italy that among 191 clinical strains isolated from November 2013 to April 2014, 178 (93%) *Klebsiella pneumoniae* had KPC enzymes (carbapenemases), with 76 (43%) resistant to colistin (Monaco et al., 2014). Although the same situation has been reported with colistin (Olaitan et al., 2014), it has received more attention: last-line treatments may no longer be effective, increasing the risk of spreading infections (Biswas et al., 2012). To combat frequent epidemics and the challenge of rapid spread, new alternatives to last resort treatments must be considered to avoid treatment failure.

As a result, alternatives to antibiotics to treat resistant germs should be a priority (Bassetti et al., 2017). The use of old drugs can be a solution like "forgotten" antibiotics polymyxins, fosfomycin, minocycline or mecillinam, which are still used in clinical settings (Cassir et al., 2014). There is also a renewed interest in antibiotic combinations to circumvent resistance (Lenhard et al., 2016). For example, the synergistic activity of sulfonamide-associated colistin was evaluated against colistin-resistant clinical bacteria (Okdah et al., 2018). But "non antibiotic" solutions can also been considered as alternatives for the therapeutic management of infections (Aslam et al., 2018). Various studies showed that *Clostridium difficile* can be inhibited using bacteriophages or several ongoing trials use antimicrobial peptides as alternatives or preventive treatments in the future (Aslam et al., 2018).

The fight to treat multi-drug resistant (MDR) infections must also include a change in mentality. Rolain and Baquero denounced the fact that society does not accept the use of toxic but effective antibiotics in treatment of life-threatening infections, but on the other hand society can tolerate potential toxicities of other drugs, such as anti-cancer. With the progress of medicine in the management of adverse reactions and the improved monitoring of antibiotic concentrations, old drugs or dosages rejected due to their adverse effects have to be reconsidered (Rolain and Baquero, 2016). In this way, one other promising alternative on which this review focuses is drug repurposing, also called repositioning (Mercorelli et al., 2018). This therapeutic shift is the subject of several studies in different pathologies including cancer (Sleire et al., 2017), heart diseases (Sun et al., 2018), Alzheimer's disease (Kim, 2015) or depression (Ebada, 2017).

In infectiology, repurposing studies are now being carried out (Torres et al., 2016; Soo et al., 2017; D'Angelo et al., 2018; Zheng et al., 2018; Miró-Canturri et al., 2019). In general, the most common bacteria are first tested or those most at risk or in a therapeutic deadlock. If this review focuses on drug repurposing that have been tested on MDR bacteria, it seems important to precise that resistance is rarely crossed and if a molecule is active on a specific species, this compound will potentially be active regardless of its resistance mechanisms. This is because this molecule affects a new target, generally independent of the antibiotic target, as we will see below with ciclopirox (Carlson-Banning et al., 2013), gallium (Goss et al., 2018), and zidovudine (Elwell et al., 1987). Therefore, it can expand the scope to combinations tested on sensitive GNB as for minocycline and polymyxin B tested with non-antibiotics drugs (Schneider et al., 2017). It offers a diversified and still exploitable field of possibilities (Schneider et al., 2017). For carbapenem and colistin-resistant isolates, a few articles are published on this specificity for which we are striving to synthesize them. The aim is thus to identify an innovative therapeutic strategy against these bacteria in a cost-effective and efficient way.

In this review, we will define drug repurposing and its characteristics. We will then make an inventory of what has already been published as a drug for reuse in general and in particular to address the problem of carbapenem and colistin-resistant bacteria. Finally, we will see what prospects exist for this therapeutic strategy.

DISCOVERY OF AN ANTIBACTERIAL POTENTIAL IN NON-ANTIBIOTIC DRUGS

What Does Drug Repurposing Mean?

A drug class is assigned to a molecule to describe and group similary together drugs because of their therapeutic use, their biochemical mechanism, by their way of action or their chemical structure. As defined by Waksman in 1947, "*an antibiotic is a chemical substance, produced by micro-organisms, which has the capacity to inhibit the growth of and even to destroy bacteria and other micro-organisms*" (Mohr, 2016). The current trend therefore seems to be moving away from this definition. Indeed, in recent years, drug repositioning seems to have been "a promising field in drug discovery that identifies new therapeutic opportunities for existing drugs" (Doan et al., 2011). The common idea is that to accelerate discovery of new treatment, using old drugs that could potentially treat disease for which the treatments used no longer work or when we no longer have therapeutic solutions must be used (Langedijk et al., 2015). Sir James Black, pharmacologist and Nobel laureate said in 1888: "*The most fruitful basis for the discovery of a new drug is to start with an old drug*" (Chen et al., 2016). It could help to overcome an initial bottleneck in drug development process. It may therefore be a better compromise between risk and reward than other approaches to drug development (Ashburn and Thor, 2004).

What Are Advantages and Drawbacks?

Drug repurposing present real economic advantages. All studies about structure, pharmacological properties as bioavailability or safety profiles for example have already been conducted. With these drugs, it is possible to skip preclinical trials because toxicity and pharmacokinetic are already known and a certain hindsight has been taken for several years. Drugs can move directly to Phase 2 to test their effectiveness (Mercorelli et al., 2018).

Repurposing drugs can offer new pathways or targets to study new perspectives for curing diseases. As many antibiotics already affect DNA, membrane or protein translation, other pathways essential for bacterial growth, remain available for activity of molecules, such as assimilation pathways of essential compounds

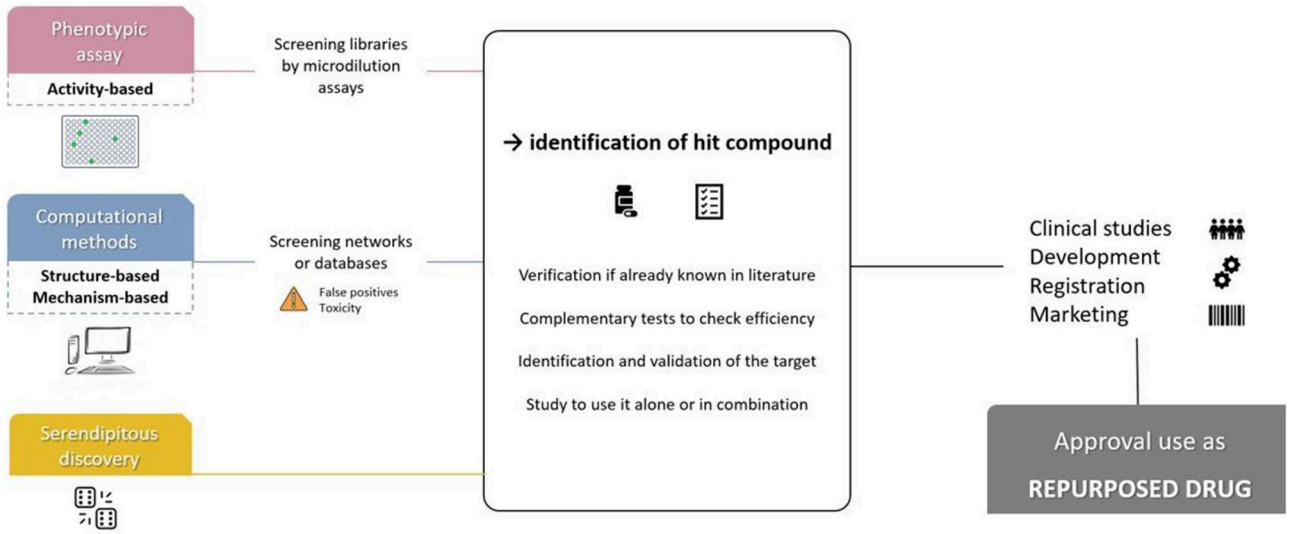

FIGURE 1 | Main steps used for drug repurposing strategy.

like sugars or amino acids. Combined strategies that reduce resistance can be used to achieve several targets that could affect bacterial metabolism (Mercorelli et al., 2018; Zheng et al., 2018).

Moreover, this method is favorable to academic or small laboratories because of disinterest of pharmaceutical industries. Without patents, these industries do not see any fruitful interest in it because of rapid emerging resistance (Fernandes and Martens, 2017) and a narrower spectrum of activity (Zheng et al., 2018).

On the other hand, this solution cannot be totally miraculous. Drug repurposing does not work all the time due to the high minimal inhibitory concentration (MIC) (Mercorelli et al., 2018) or inconsistent plasma concentrations tolerated in humans. Dose tested for this new indication is important and can lead to human toxicity (Zheng et al., 2018), what society fears (Rolain and Baquero, 2016). Concerning galenic, an optimization of formulation can also be foreseen if a physico-chemical incompatibility is observed.

How to Process to Repurpose Drugs?

Considered an innovative strategy (Doan et al., 2011), three major methods can lead a drug to be repurposed, as shown in **Figure 1**.

First, phenotypic assay can be performed by high throughput and screening of commercial, public, pharmaceutical compound libraries (Jung et al., 1997; Kim, 2015). These assays consist in classical broth microdilution to identify a hit (Torres et al., 2016). Once antibacterial activity is found, MIC assay is performed to confirm results according to CLSI guidelines (Sun et al., 2016b). Compared to other methods, phenotypic tests have the advantage of being highly physiologically relevant because the effect is observed directly on bacteria (Zheng et al., 2018).

Advances in genomics and bioinformatics modified drug repositioning approach. It consists of *in silico* structure or mechanism-based assays that work with virtual databases. This has been made possible through the prospective development of drug databases and activities, the exchange of information on compounds in collaborative networks and the abundance of resources on the Internet (Hodos et al., 2016). These new calculation tools make it possible to analyse all the different data accumulated in the field that man alone cannot study because they are too complex. This can ensure the understanding and prediction of molecules by generating hypotheses about biological mechanisms (Hodos et al., 2016). Limit to these approaches is that pathways, targets or other data must be already known. Moreover, false positive and toxicity are problematic issues found after identification of a hit (Mercorelli et al., 2018). However, for emerging diseases, this could be a quick way to find an effective molecule as was done for the coronavirus in 2013 (Law et al., 2013).

The last approach is random discovery and can include all types of configurations. Indeed, the side effects of one drug in one disease may be effective for another, such as for the antidepressant bupropion reoriented as an anti-tobacco drug (Hodos et al., 2016). It can be mere coincidence as sulfamides were known for antibacterial properties and finally also employed for antidiabetic ones (Deuil, 1956). However, these unexpected observations could also potentially be identified by informatics methods, in view of knowledge of compound side effects (Hodos et al., 2016).

Despite all these techniques, if a molecule is identified, it must then go through the steps of its clinical evaluation.

CURRENT KNOWLEDGE IN DRUG REPURPOSING FOR CARBAPENEM AND COLISTIN RESISTANCE?

Studies generally screen MDR bacteria to ensure a broader spectrum of action (Hijazi et al., 2018) and sometimes bacteria

TABLE 1 | Relevant repurposing reports for carbapenem and colistin resistant bacteria.

	Compound	Approved use or known as	Activity -alone or in combination with-	Tested bacteria	Resistance phenotypes (and/or)	References
Infectiology	Zidovudine	Antiretroviral	Alone	*Escherichia coli* *Klebsiella pneumoniae*	Carbapenems Colistin	Peyclit et al., 2018
			Colistin	*E. coli* *K. pneumoniae* *Enterobacter cloacae* *Pseudomonas aeruginosa* *Acinetobacter baumannii*	Carbapenems Colistin	Hu et al., 2018; Loose et al., 2018
			Tigecycline	*E. coli* *K. pneumoniae*	Carbapenems	Ng et al., 2018
	Niclosamide	Anthelminthic	Colistin	*A. baumannii* *K. pneumoniae*	Colistin	Ayerbe-Algaba et al., 2018
	Pentamidine	Antiprotozoal	Alone			Cebrero-Cangueiro et al., 2018
			Rifampicin	*K. pneumoniae* *E. coli* *E. cloacae*	Carbapenems Colistin	Cebrero-Cangueiro et al., 2018
			Aminoglycosides			Cebrero-Cangueiro et al., 2018
	Ciclopirox	Antifungal	Alone	*E. coli* *K. pneumoniae* *A. baumannii*	Carbapenems	Carlson-Banning et al., 2013
Oncology	5-fluorouracil	Antineoplastic	Zidovudine	*A. baumannii*	Carbapenems	Cheng et al., 2019
	Mitotane	Antineoplastic	Polymyxin B	*A. baumannii* *P. aeruginosa* *K. pneumoniae*	Carbapenems Polymyxin	Tran et al., 2018
	Gallium	Antineoplastic	Alone	ESKAPE species	MDR	Hijazi et al., 2018
	Tamoxifen Raloxifen Toremifen	SERM	Polymyxin B	*P. aeruginosa* *K. pneumoniae* *A. baumannii*	Colistin	Hussein et al., 2017
Central Nervous System	Sertraline	Antidepressant	Polymyxin B	*P. aeruginosa* *K. pneumoniae*	Colistin Carbapenems	Otto et al., 2019
	Citalopram	Antidepressant	Polymyxin B	*A. baumannii* *E. coli* *K. pneumoniae*	Colistin Carbapenems	Otto et al., 2019
	Fluspirilene	Antipsychotic	Colistin	*A. baumannii*	Carbapenems	Cheng et al., 2019
Metabolism	Bay 11-7082	Anti-inflammatory	Colistin	*A. baumannii*	Carbapenems	Cheng et al., 2019
	Spironolactone	Diuretic	Polymyxin B	*E. coli*	Carbapenems	Otto et al., 2019
Natural compound	Resveratrol	Stilbene	Alone	*E. coli* *Enterobacter aerogenes*		Seukep et al., 2016
			Streptomycin	*K. pneumoniae*	MDR	Seukep et al., 2016
			Ciprofloxacin	*P. aeruginosa* *Providencia stuartii* *E. cloacae*		Seukep et al., 2016
			Colistin	*E. coli* *K. pneumoniae* *A. baumannii* *Serratia marcescens* *Proteus mirabilis*	Colistin Carbapenems	Cannatelli et al., 2018
	Pterostilbene	Anticancer Antioxidant	Polymyxin B	*K. pneumoniae*	Colistin	Zhou et al., 2018
	Eugenol	Essential oil	Colistin	*E. coli*	Colistin	Wang et al., 2018

SERM, Selective estrogen receptor modulator.

only with colistin or carbapenem resistance to treat the ongoing issue (Ayerbe-Algaba et al., 2018). Several major studies have performed drug repurposing on MDR bacteria belonging to the ESKAPE (*Enteroccocus faecium, S. aureus, K. pneumoniae, A. baumannii, Pseudomonas aeruginosa, Enterobacter* species) group (**Table 1**). Seven non-antibacterial compounds inhibited the growth of an *Acinetobacter baumannii* strain resistant to most antibiotics including carbapenems: 3 antineoplastics (5-fluorouracil, 6-thioguanine and pifithrin-μ), 1 anti-rheumatic (auranofin), 1 antipsychotic (fluspirilene), 1 anti-inflammatory (Bay 11-7082), and 1 alcohol deterrent (disulfiram). Five-fluorouracil and 6-thioguanine seemed to be the best candidates for repurposing to treat MDR clinical *A. baumannii*. Their IC90 values or MIC were lower than standard plasma drug concentration levels in human, suggesting a possible use without major adverse events (Cheng et al., 2019).

All mechanisms of action and targets are considered because the objective is to escape therapeutic drug classes. Each repurposed molecule can be used to study a new pathway (**Figure 2**). An antifungal agent developed nearly forty years ago, ciclopirox, also has good repurposing criteria, as shown by an American study conducted in 2013 (Carlson-Banning et al., 2013). Due to its excellent safety profile, it has already been repurposed in various pathologies such as myeloma, or as an anti-human immunodeficiency virus drug. It prevents enzyme actions, essential for cellular metabolism or functions, by inhibiting the availability of co-factors. Its activity was proved against MDR *E. coli*, *K. pneumoniae*, and *A. baumannii* strains. They demonstrated a novel mechanism of action: ciclopirox affects the galactose and LPS salvage pathways (Carlson-Banning et al., 2013). In addition, the bacterial activity of gallium has been known for more than 80 years but is first used as an anti-cancer agent. Due to its chemical similarity to iron, gallium inhibits ferric redox reactions or pathways, and then bacterial growth. In this matter, it has a broad spectrum of activity, in particular MDR ESKAPE pathogens (Rangel-Vega et al., 2015; Hijazi et al., 2018). In fact, a phase 2 trial in cystic fibrosis patients assess the activity of gallium and suggests its safety and

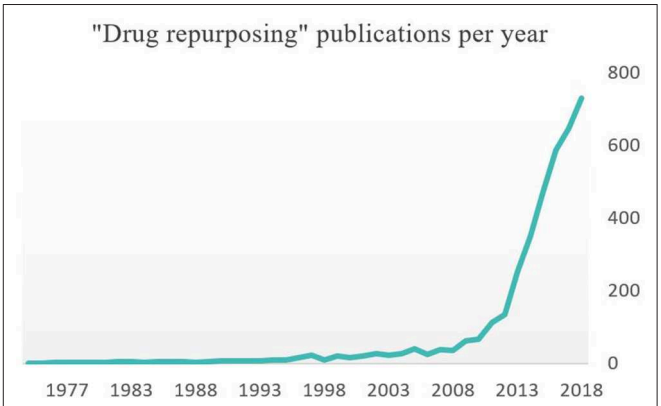

FIGURE 3 | Annual number of publications on PubMed search engine with "drug repurposing" keyword.

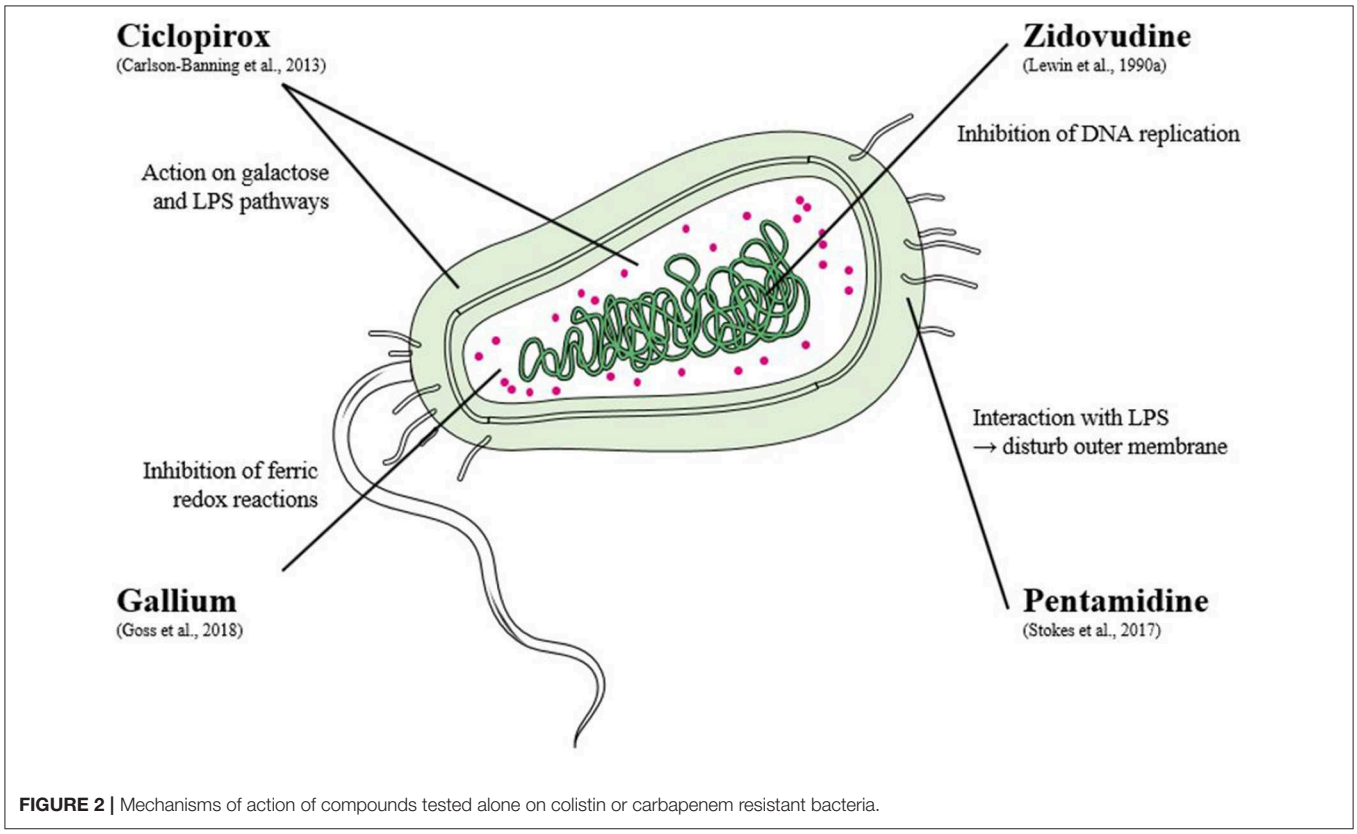

FIGURE 2 | Mechanisms of action of compounds tested alone on colistin or carbapenem resistant bacteria.

efficacy for human infections (Goss et al., 2018). This once again represents potential and promising targets for the control of infectious germs.

It can be noticed that all pharmaceutical classes can be involved, from anticancer to anti-inflammatory and also antiparasitic drugs. Pachón-Ibáñez et al. and the study of Stokes (Stokes et al., 2017) of the previous year showed that pentamidine was effective against polymyxin resistant strains. This antiprotozoal agent usually effective in trypanosomiasis, leishmaniasis and some fungal infections was here tested against 8 *Enterobacteriaceae* (5 *K. pneumoniae*, 1 *E. coli* and 2 *Enterobacter cloacae*). Pentamidine was bactericidal for 7 strains which carried out carbapenemases or showed colistin resistance. Moreover, these effects potentiated activity of other antibiotics due to a synergistic activity with rifampicin, or aminoglycosides for *E. cloacae*. With rifampicin, combination was effective against most of the strains tested (Cebrero-Cangueiro et al., 2018).

In this context of drug reprofiling, various studies identified the antiretroviral zidovudine, also called azidothymidine (AZT), as an active molecule against resistant *Enterobacteriaceae* (Doléans-Jordheim et al., 2011; Peyclit et al., 2018). The interest in drug repurposing in MDR enterobacterial infections has revived the forgotten antibacterial properties of this drug mentioned for the first time in 1986 (Elwell et al., 1987). On a series of *Enterobacteriaceae* with different colistin resistance profiles (*mcr-1* gene, *mgrB* or *pmrB* mutations), its antibacterial action was confirmed with MICs ranging from 0.2 and 6.25 μM. Pharmacokinetic data showed that AZT concentrations found would be compatible with plasma concentrations obtained for doses used in human medicine (Peyclit et al., 2018). Due to a relatively rapid mutation frequency (Doléans-Jordheim et al., 2011) and resistant strains already reported (Lewin et al., 1990a), it would appear that zidovudine is more suitable for use in combination. Indeed, zidovudine was tested in various associations with antibiotics from different class (Lewin et al., 1990b; Mascellino et al., 1993). In a recent article (Hu et al., 2018), checkerboard analysis with colistin showed synergistic activity against 60.87% of the Extended spectrum ß-lactamases (ESBL) *E. coli*, 87.1% of the ESBL *K. pneumoniae,* 100% of NDM-1 producing strains and 92.31% of colistin resistant (*mcr*-1) *E. coli*. With this bactericidal combination, the activity of colistin has been improved, which could reduce the dose of colistin for a better effect (Hu et al., 2018). Patented in 2014 (Hu and Coates, 2014), it has been enrolled in a Phase 1 clinical trial. Results showed that the association had a bactericidal activity on plasma concentration on *mcr-1* positive strains and that it was well tolerated by the healthy volunteers involved in the study (Loose et al., 2018). Further human studies can be undertaken to confirm these results, but they confirm that AZT can be a recovery therapy against MDR bacteria and thus help clinicians avoid therapeutic impasses.

Finally, in order to anticipate the emergence of resistance in bacteria, some molecules have the significant advantage of not being used alone, of focusing on multiple targets and thus eradicating the infection as quickly as possible.

Drug Combination Therapy Increases Successful Drug Repurposing

After finding a positive response to a new use, if it does not sufficiently meet the criteria of efficacy, safety, pharmacodynamics, non-toxicity, combination studies with another drug may be considered in order to use it effectively. Drug combinations consist on an association of two or more drugs in order to enhance efficacy of therapeutic strategy and increase chances of clinical applications. It broadens the spectrum of activity of useful antibiotics, for example for serious infections requiring urgent and effective treatment (Zheng et al., 2018). The use of two or more drugs has an impact on different targets, increasing the impairment of microbial function and reducing the risk of resistance emergence (Zheng et al., 2018). The main goal of drug association is to produce a synergistic effect: effect produced by combination is greater than that achieved with any of the drugs used alone. Moreover, if one compound has low activity, another can potentiate and increase it. This reduces the concentration of each individual molecule and can therefore be used at lower doses. This is a real advantage when one knows toxicity of certain drugs (Sun et al., 2016a; Zheng et al., 2018). Sun et al. showed the use of drug combinations reduced toxicity. It increased activity compared to a single therapy when cytotoxicity was proven allowing the use of some drugs in human medicine that were not conceivable on their own (Sun et al., 2016a).

Drug Repurposing for Combination With Known Antibiotics

Research in drug repurposing for combination with known antibiotics on carbapenem and/or colistin-resistant bacteria has mainly been conducted in association with polymyxins drugs (**Table 1**). Niclosamide, an anthelmintic drug, known to be active against most tapeworms, seems to interact with the negatively charged outer membrane of colistin-resistant strains leading to a synergistic effect with colistin. This effect was observed on 18 strains with 13 colistin-resistant *A. baumannii* (*pmrB* altered), and 2 colistin-resistant *K. pneumoniae* (*mgrB* and *pmrB* altered) (Ayerbe-Algaba et al., 2018). Colistin combination therapy with selective estrogen receptor modulators (SERM) as tamoxifen, raloxifen and toremifen also exhibited good activity against polymyxin-resistant *P. aeruginosa*, *K. pneumoniae*, and *A. baumannii.* Tested *in-vitro* concentrations could be achievable for human concentration (Hussein et al., 2017; Schneider et al., 2017). In 2019, fluspirilene and Bay 11-7082 have shown promising results by resensitizing a resistant *A. baumannii* to overcome colistin resistance (Cheng et al., 2019). Regarding polymyxin B, synergistic activity with mitotane, an antineoplastic approved for carcinoma treatment, was studied *in-vitro* on 10 strains including carbapenem or polymyxin-resistant GNB. Tests were also carried out on infections of mouse burn wounds, which led to a promising result for the treatment of this type of infection (Tran et al., 2018). Using knowledge of the mechanisms of action, an approach was also tested with some channel-blocking molecules. Indeed, these efflux pump

inhibitors did not have an effect on bacteria alone but combined with an antibiotic, they demonstrated restoration of its activity. The effect is more or less strong but as for neuroleptics (prochlorperazine, chlorpromazine, promazine) associated with meropenem appear to be effective against MDR *A. baumannii* (Yang and Chua, 2013).

Otto et al., showed a potential efficacy of 7 drugs, including 3 antidepressants (amitriptyline, imipramine and sertraline) and 4 antipsychotics (chlorpromazine, clonazepam, haloperidol, and levopromazine) with polymyxin B against 20 tested GNB displaying various resistance mechanisms including carbapenemases (Otto et al., 2019). Only sertraline, chlorpromazine and levopromazine had a synergism effect with polymyxin B against *A. baumannii*, *E. coli* and *K. pneumoniae* isolates. Among all non-antibiotics, only spironolactone, which had only a good efficacy against *E. coli* isolates, showed non-toxic levels of minimum concentration for synergy with polymyxin B (Otto et al., 2019). These findings show that non-antibiotics molecules can be effective in combination but studies need to be pursued to develop association with effective concentrations that are clinically tolerated (Otto et al., 2019).

Natural Compounds for New Combinations Should Not Be Excluded

Although some natural compounds are not FDA-approved, some may also be part of this process for which a compound is used in another known property. The stilbene and polyphenol resveratrol is produced by various plants (as grapes and blueberries) and is known to have various antioxidant properties and chemopreventive activities. In the bark from *Nauclea pobeguinii,* Cameroonian researchers found this compound and tested it on GNB with MDR phenotypes. It was active alone and in a synergy with streptomycin and ciprofloxacin (Seukep et al., 2016). Rossolini et al. demonstrated in 2018 activity of resveratrol as an antimicrobial agent in combination with colistin on a panel of colistin-resistant (chromosomic or plasmid resistance) GNB (Cannatelli et al., 2018). Resveratrol seems to potentiate colistin activity and thus makes it possible to restore its action among different species and resistance pathways. Thus, another natural compound, pterostilbene, derived from blueberries and grapes and known for its anticancer, anti-inflammatory and antioxidant effects, appears to enhance polymyxin activity *in vitro* and *in vivo* (Zhou et al., 2018). They demonstrated synergistic

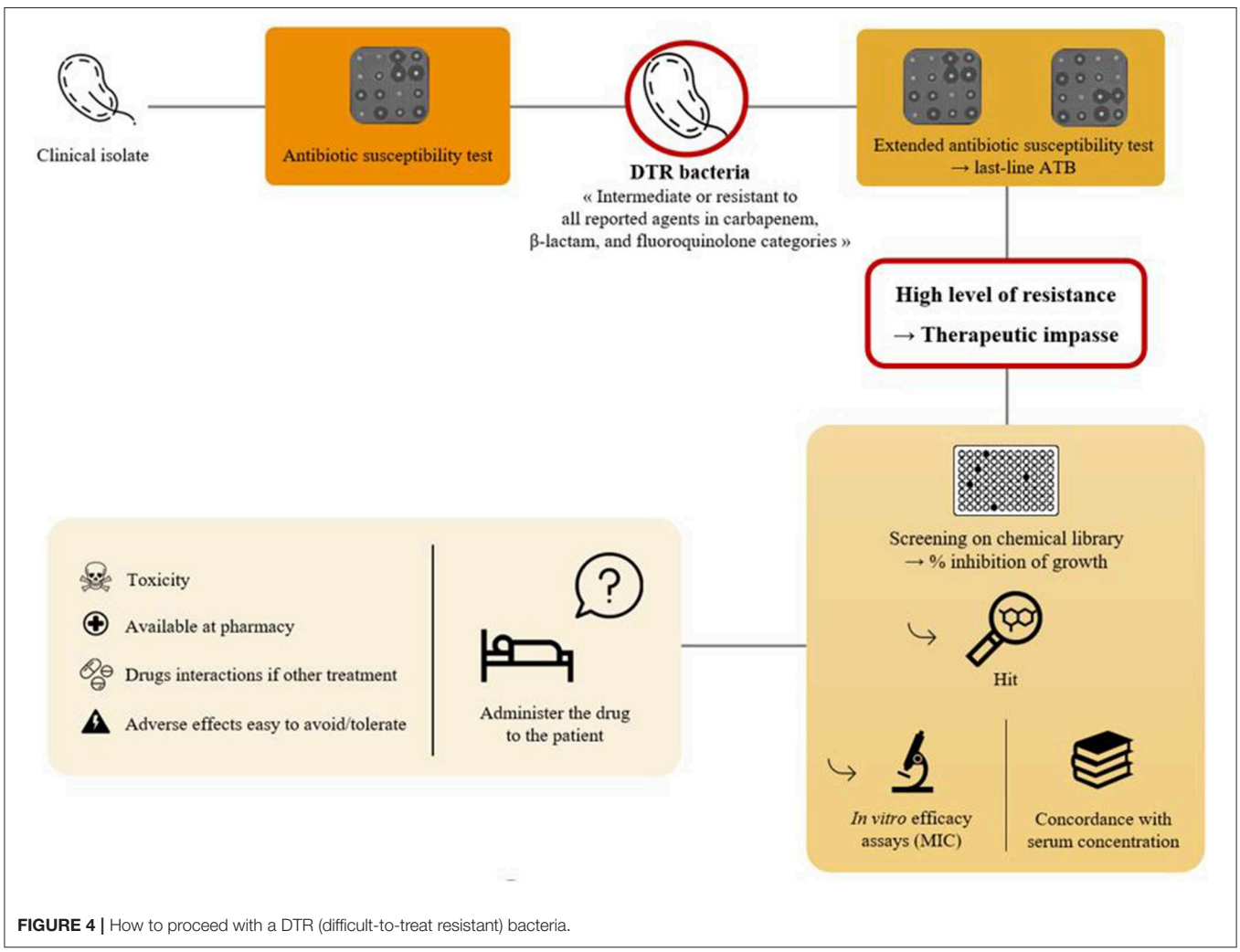

FIGURE 4 | How to proceed with a DTR (difficult-to-treat resistant) bacteria.

effects with colistin and with polymyxin B in *mcr-1* positive strains by 8-fold reducing MIC of polymyxin B with 32μg/ml (Zhou et al., 2018). Pterostilbene could therefore affect *mcr-1* function and restore antibacterial activity of polymyxin B in resistant isolates. Probably safe for human clinical practice and possibly not exerting selective pressure associated with the current ATB, it is therefore considered a good candidate for drug repurposing (Zhou et al., 2018). Lastly, eugenol is a phenylpropanoid present in essential oil of many plants. Thirteen animal *E. coli* strains with colistin resistance were subjected to MIC, time kill and checkerboard assays to evaluate combination between colistin and eugenol (Wang et al., 2018). They observed that *mcr-1* gene expression was down regulated by eugenol and suggested a possible binding between eugenol and MCR-1 protein. (Wang et al., 2018).

All these molecules are still being tested *in vitro* or in clinical trials and none have yet received new indication for MDR infection treatment. However, research on drug repurposing is gaining new dynamism if we can refer to the number of annual publications in recent years (**Figure 3**).

PERSPECTIVES

In conclusion, this review therefore addresses two main aspects, both the emerging drug repurposing strategy and resistance to last-line antibiotics, carbapenems, and colistin. A new economic model is to be considered for antibiotic development because industries do not seem interested in this new strategy (Zheng et al., 2018). Indeed, as antibiotics are not part of chronic treatment strategies, this could not be as economically attractive (Conly and Johnston, 2005). This disinterest in antibiotics research is reflected in their absence in programs of future developments of major pharmaceutical companies (Spellberg et al., 2004). Start-ups or small companies, on the other hand, can see an interest in taking back antibiotics that have failed in clinical phases, for example. They believe they have different drug development strategies and do not require as many benefits to cover their costs compared to multinational pharmaceutical companies (Fernandes and Martens, 2017). However, Phase 3 clinical trials for new and repurposed drugs remain very expensive: it is estimated between $40 million and $300 million of USD (Azvolinsky, 2017). With such a budget, this does not work in favor of small firms.

As for the question of how to treat bacterial resistance, only one answer has not been found and the future offers us new possibilities. Various strategies are being considered as treatment using fecal microbiota (Davido et al., 2017), antimicrobial peptides (Hashemi et al., 2017) or bacteriophages (Parmar et al., 2017). A *Streptomyces sp.* present in alkaline soil in Ireland has been in the spotlight recently to inhibit growth of MDR bacteria (Terra et al., 2018) which reminds of Flemming discovery. Additionally, the discovery and studies on the CRISPR/Case9 system may suggest that it may be the ultimate weapon to fight infectious diseases and thus control antibiotic resistance (Doerflinger et al., 2017).

Question of drug repurposing remains rather wide. Although this seems to be a better solution, drug combinations can also lead to adverse interactions. First, toxic side effects can be increased. Then, concerning compound galenic, physico-chemical interactions and differences in stability, solubility and conservation can result from the combination of two molecules making it incompatible. Formulation then becomes more complicated (Sun et al., 2016a). On the other hand, we must change this vision where each drug belongs to only one box. Clinicians may have difficulty understanding why a biologist recommends the use of an anti-cancer or anti-inflammatory drug to treat their cystic fibrosis patient's bacteremia rather than a last resort antibiotic they have always used. Communication in this sense remains essential between health professionals and clinical studies to prove these activities are critical. However, with current knowledge on drug repurposing as antibacterial agents and the problematic to find an alternative therapeutic in some situations, screening of non-antibiotics in a "à la carte" way can be an issue (**Figure 4**). In the area of personalized medicine, we could imagine a personalized antibiotic susceptibility testing in case of infection caused by a highly resistant bacterium. If all last-line antibiotics have been tested and appear insufficient to successfully treat the patient, testing non-antibiotic drugs that are potentially active on the pathogen, alone or in combination with antibiotics, could help clinicians use these drugs. As previously reported by Kadri et al., these difficult-to-threat bacteria refer to bacteria that are resistant to all first-line antibiotics. It represents less than 1% of isolates and those that are resistant to second-line antibiotics are even rare (Kadri et al., 2018). This solution, combined with monitoring of serum levels and adverse events such as dialysis of a nephrotoxic drug (Rolain and Baquero, 2016), could offer great potential for treating a patient with this MDR bacterium. The problem remains to be able to routinely test a large panel of molecules, in an automated, reproducible, and not too expensive way.

AUTHOR CONTRIBUTIONS

LP, SB, and J-MR drafted and revised the manuscript. All authors read and approved the final manuscript.

FUNDING

This work was supported by the French Government under the ≪Investissements d'avenir≫ (Investments for the Future) program managed by the Agence Nationale de la Recherche (ANR, fr: National Agency for Research), (reference: Méditerranée Infection 10-IAHU-03). This work was supported by Région Provence-Alpes-Côte d'Azur and European funding FEDER PRIMI.

ACKNOWLEDGMENTS

We thank CookieTrad for English correction.

REFERENCES

Ashburn, T. T., and Thor, K. B. (2004). Drug repositioning: identifying and developing new uses for existing drugs. *Nat. Rev. Drug Discov.* 3, 673–683. doi: 10.1038/nrd1468

Aslam, B., Wang, W., Arshad, M. I., Khurshid, M., Muzammil, S., Rasool, M. H., et al. (2018). Antibiotic resistance: a rundown of a global crisis. *Infect. Drug Resist.* 11, 1645–1658. doi: 10.2147/IDR.S173867

Ayerbe-Algaba, R., Gil-Marqués, M. L., Jiménez-Mejías, M. E., Sánchez-Encinales, V., Parra-Millán, R., Pachón-Ibáñez, M. E., et al. (2018). synergistic activity of niclosamide in combination with colistin against colistin-susceptible and colistin-resistant *Acinetobacter baumannii* and *Klebsiella pneumoniae*. *Front. Cell. Infect. Microbiol.* 8:348. doi: 10.3389/fcimb.2018.00348

Azvolinsky, A. (2017). *Repurposing existing drugs for new indications*. The Scientist. Available online at: https://www.the-scientist.com/features/repurposing-existing-drugs-for-new-indications-32285 (accessed May 19, 2019).

Bachiri, T., Bakour, S., Lalaoui, R., Belkebla, N., Allouache, M., Rolain, J. M., et al. (2017). Occurrence of Carbapenemase-producing *Enterobacteriaceae* isolates in the wildlife: first report of OXA-48 in wild boars in Algeria. *Microb. Drug Resist.* 24, 337–345. doi: 10.1089/mdr.2016.0323

Bassetti, M., Poulakou, G., Ruppe, E., Bouza, E., Van Hal, S. J., and Brink, A. (2017). Antimicrobial resistance in the next 30 years, humankind, bugs and drugs: a visionary approach. *Intensive Care Med.* 43, 1464–1475. doi: 10.1007/s00134-017-4878-x

Biswas, S., Brunel, J. M., Dubus, J. C., Reynaud-Gaubert, M., and Rolain, J. M. (2012). Colistin: an update on the antibiotic of the 21st century. *Expert Rev. Anti. Infect. Ther.* 10, 917–934. doi: 10.1586/eri.12.78

Cannatelli, A., Principato, S., Colavecchio, O. L., Pallecchi, L., and Rossolini, G. M. (2018). Synergistic activity of colistin in combination with resveratrol against colistin-resistant gram-negative pathogens. *Front. Microbiol.* 9:1808. doi: 10.3389/fmicb.2018.01808

Carlson-Banning, K. M., Chou, A., Liu, Z., Hamill, R. J., Song, Y., and Zechiedrich, L. (2013). Toward repurposing ciclopirox as an antibiotic against drug-resistant *Acinetobacter baumannii*, *Escherichia coli*, and *Klebsiella pneumoniae*. *PLoS ONE* 8:e69646. doi: 10.1371/journal.pone.0069646

Cassir, N., Rolain, J. M., and Brouqui, P. (2014). A new strategy to fight antimicrobial resistance: the revival of old antibiotics. *Front. Microbiol.* 5:551. doi: 10.3389/fmicb.2014.00551

Cebrero-Cangueiro, T., Álvarez-Marín, R., Labrador-Herrera, G., Smani, Y., Cordero-Matía, E., Pachón, J., et al. (2018). *In vitro* Activity of pentamidine alone and in combination with aminoglycosides, tigecycline, rifampicin, and doripenem against clinical strains of carbapenemase-producing and/or colistin-resistant *Enterobacteriaceae*. *Front. Cell. Infect. Microbiol.* 8:363. doi: 10.3389/fcimb.2018.00363

Chen, H., Wu, J., Gao, Y., Chen, H., and Zhou, J. (2016). Scaffold repurposing of old drugs towards new cancer drug discovery. *Curr. Top. Med. Chem.* 16, 2107–2114. doi: 10.2174/1568026616666160216155556

Cheng, Y. S., Sun, W., Xu, M., Shen, M., Khraiwesh, M., Sciotti, R. J., et al. (2019). Repurposing screen identifies unconventional drugs with activity against multidrug resistant *Acinetobacter baumannii*. *Front. Cell. Infect. Microbiol.* 8:438. doi: 10.3389/fcimb.2018.00438

Conly, J., and Johnston, B. (2005). Where are all the new antibiotics? The new antibiotic paradox. *Can. J. Infect. Dis. Med. Microbiol.* 16, 159–160. doi: 10.1155/2005/892058

D'Angelo, F., Baldelli, V., Halliday, N., Pantalone, P., Polticelli, F., Fiscarelli, E., et al. (2018). Identification of FDA-approved drugs as antivirulence agents targeting the *pqs* quorum-sensing system of *Pseudomonas aeruginosa*. *Antimicrob. Agents Chemother.* 24:62. doi: 10.1128/AAC.01296-18

Davido, B., Batista, R., Michelon, H., Lepainteur, M., Bouchand, F., Lepeule, R., et al. (2017). Is faecal microbiota transplantation an option to eradicate highly drug-resistant enteric bacteria carriage? *J. Hosp. Infect.* 95, 433–437. doi: 10.1016/j.jhin,.2017.02.001

Deuil, R. (1956). Treatment for diabetes with sulfamide hypoglycemic agents. *Rev. Prat.* 6, 3687–3694.

Diene, S. M., and Rolain, J. M. (2013). Investigation of antibiotic resistance in the genomic era of multidrug-resistant gram-negative bacilli, especially *Enterobacteriaceae Pseudomonas Acinetobacter*. *Expert Rev. Anti. Infect. Ther.* 11, 277–296. doi: 10.1586/eri.13.1

Doan, T. L., Pollastri, M., Walters, M. A., and Georg, G. I. (2011). The future of drug repositioning: old drugs, new opportunities. *Annu. Rep. Med. Chem.* 46, 385–401. doi: 10.1016/B978-0-12-386009-5.00004-7

Doerflinger, M., Forsyth, W., Ebert, G., Pellegrini, M., and Herold, M. J. (2017). CRISPR/Cas9-The ultimate weapon to battle infectious diseases? *Cell. Microbiol.* 19:e12693. doi: 10.1111/cmi.12693

Doléans-Jordheim, A., Bergeron, E., Bereyziat, F., Ben-Larbi, S., Dumitrescu, O., Mazoyer, M.-A., et al. (2011). Zidovudine (AZT) has a bactericidal effect on enterobacteria and induces genetic modifications in resistant strains. *Eur. J. Clin. Microbiol. Infect. Dis.* 30, 1249–1256. doi: 10.1007/s10096-011-1220-3

Ebada, M. E. (2017). Drug repurposing may generate novel approaches to treating depression. *J. Pharm. Pharmacol.* 69, 1428–1436. doi: 10.1111/jphp.12815

Elwell, L. P., Ferone, R., Freeman, G. A., Fyfe, J. A., Hill, J. A., Ray, P. H., et al. (1987). Antibacterial activity and mechanism of action of 3'-azido-3'-deoxythymidine (BW A509U). *Antimicrob. Agents Chemother.* 31, 274–280. doi: 10.1128/aac.31.2.274

Fernandes, P., and Martens, E. (2017). Antibiotics in late clinical development. *Biochem. Pharmacol.* 133, 152–163. doi: 10.1016/J.BCP.2016.09.025

Global Antimicrobial Resistance Surveillance System, GLASS, Report early implementation (2019). Available online at: http://apps.who.int/iris/bitstream/handle/10665/259744/9789241513449-eng.pdf;jsessionid$=$35205369C15F36F8D21041F11B82FE9F?sequence$=$1 (accessed January 11, 2019).

Goss, C. H., Kaneko, Y., Khuu, L., Anderson, G. D., Ravishankar, S., Aitken, M. L., et al. (2018). Gallium disrupts bacterial iron metabolism and has therapeutic effects in mice and humans with lung infections. *Sci. Transl. Med.* 10:eaat7520. doi: 10.1126/scitranslmed.aat7520

Gould, K. (2016). Antibiotics: from prehistory to the present day. *J. Antimicrob. Chemother.* 71, 572–575. doi: 10.1093/jac/dkv484

Hashemi, M. M., Rovig, J., Weber, S., Hilton, B., Forouzan, M. M., and Savage, P. B. (2017). Susceptibility of colistin-resistant, gram-negative bacteria to antimicrobial peptides and ceragenins. *Antimicrob. Agents Chemother.* 25:61. doi: 10.1128/AAC.00292-17

Hijazi, S., Visaggio, D., Pirolo, M., Frangipani, E., Bernstein, L., and Visca, P. (2018). Antimicrobial activity of gallium compounds on ESKAPE pathogens. *Front. Cell. Infect. Microbiol.* 8:316. doi: 10.3389/fcimb.2018.00316

Hodos, R. A., Kidd, B. A., Shameer, K., Readhead, B. P., and Dudley, J. T. (2016). *In silico* methods for drug repurposing and pharmacology. *Wiley Interdiscip. Rev. Syst. Biol. Med.* 8, 186–210. doi: 10.1002/wsbm.1337

Hu, Y., and Coates, P. A. (2014). *Combination Comprising Zidovudine and Polymyxin*. Available online at: https://patentimages.storage.googleapis.com/cc/40/e6/680e19429422ab/WO2014147405A1.pdf (accessed May 19, 2019).

Hu, Y., Liu, Y., and Coates, A. (2018). Azidothymidine produces synergistic activity in combination with colistin against antibiotic-resistant *Enterobacteriaceae*. *Antimicrob. Agents Chemother.* 63:e01630-18. doi: 10.1128/AAC.01630-18

Hussein, M. H., Schneider, E. K., Elliott, A. G., Han, M., Reyes-Ortega, F., Morris, F., et al. (2017). From breast cancer to antimicrobial: combating extremely resistant gram-negative "superbugs" using novel combinations of polymyxin B with selective estrogen receptor modulators. *Microb. Drug Resist.* 23, 640–650. doi: 10.1089/mdr.2016.0196

Jung, M.-L., Contreras, J.-M., Morice, C., Simon, J.-M., Didier, B., and Langer, T. (1997). *The Prestwick Chemical Library : a valuable tool for screening. PNAS* Available online at: http://www.whocc.no/atc_ddd_index/.6.https://www.mims.com/.8.WIPO-WorldIntellectualPropertyOrganization.www.wipo.int/.9.Vidal.http://www.vidal.fr/.10 (accessed October 6, 2018).

Kadri, S. S., Adjemian, J., Lai, Y. L., Spaulding, A. B., Ricotta, E., Prevots, D. R., et al. (2018). Difficult-to-treat resistance in gram-negative bacteremia at 173 US hospitals: retrospective cohort analysis of prevalence, predictors, and outcome of resistance to all first-line agents. *Clin. Infect. Dis.* 67, 1803–1814. doi: 10.1093/cid/ciy378

Kim, T. W. (2015). Drug repositioning approaches for the discovery of new therapeutics for Alzheimer's disease. *Neurotherapeutics* 12, 132–142. doi: 10.1007/s13311-014-0325-7

Langedijk, J., Mantel-Teeuwisse, A. K., Slijkerman, D. S., and Schutjens, M. H. (2015). Drug repositioning and repurposing: terminology and definitions in literature. *Drug Discov. Today* 20, 1027–1034. doi: 10.1016/J.DRUDIS.2015.05.001

Law, G. L., Tisoncik-Go, J., Korth, M. J., and Katze, M. G. (2013). Drug repurposing: a better approach for infectious disease drug discovery? *Curr. Opin. Immunol.* 25, 588–592. doi: 10.1016/j.coi.2013.08.004

Lenhard, J. R., Nation, R. L., and Tsuji, B. T. (2016). Synergistic combinations of polymyxins. *Int. J. Antimicrob. Agents* 48, 607–613. doi: 10.1016/j.ijantimicag,.2016.09.014

Lewin, C. S., Allen, R., and Amyes, S. G. (1990a). Zidovudine-resistance in salmonella typhimurium and *Escherichia coli*. *J. Antimicrob. Chemother.* 25, 706–8.

Lewin, C. S., Allen, R. A., and Amyes, S. G. (1990b). Antibacterial activity of fluoroquinolones in combination with zidovudine. *J. Med. Microbiol.* 33, 127–131. doi: 10.1099/00222615-33-2-127

Loose, M., Naber, K. G., Hu, Y., Coates, A., and Wagenlehner, F. M. E. (2018). Serum bactericidal activity of colistin and azidothymidine combinations against mcr-1-positive colistin-resistant *Escherichia coli*. *Int. J. Antimicrob. Agents* 52, 783–789. doi: 10.1016/j.ijantimicag.2018.08.010

Mascellino, M. T., Iona, E., Iegri, F., Gregoris, P., and Farinelli, S. (1993). *In vitro* activity of zidovudine alone and in combination with ciprofloxacin against salmonella and *Escherichia coli*. *FEMS Immunol. Med. Microbiol.* 7, 23–28. doi: 10.1111/j.1574-695X.1993.tb00377.x

Mercorelli, B., Pal,ù, G., and Loregian, A. (2018). Drug repurposing for viral infectious diseases: how far are we? *Trends Microbiol.* doi: 10.1016/j.tim.2018.04.004

Miró-Canturri, A., Ayerbe-Algaba, R., and Smani, Y. (2019). Drug repurposing for the treatment of bacterial and fungal infections. *Front. Microbiol.* 10:41. doi: 10.3389/fmicb.2019.00041

Mohr, K. I. (2016). History of antibiotics research. *Curr. Top. Microbiol. Immunol.* 398, 237–272. doi: 10.1007/82_2016_499

Monaco, M., Giani, T., Raffone, M., Arena, F., Garcia-Fernandez, A., Pollini, S., et al. (2014). *Colistin resistance superimposed to endemic carbapenem-resistant Klebsiella pneumoniae*: a *rapidly evolving problem in Italy, November 2013 to April 2014. Euro Surveill.* 19. Available online at: http://www.ncbi.nlm.nih.gov/pubmed/25358041 (accessed January 9, 2019).

Ng, S. M. S., Sioson, J. S. P., Yap, J. M., Ng, F. M., Ching, H. S. V., Teo, J. W. P., et al. (2018). Repurposing zidovudine in combination with tigecycline for treating carbapenem-resistant *Enterobacteriaceae* infections. *Eur. J. Clin. Microbiol. Infect. Dis.* 37, 141–148. doi: 10.1007/s10096-017-3114-5

Okdah, L., Le Page, S., Olaitan, A. O., Dubourg, G., Hadjadj, L., and Rolain, J.-M. (2018). New therapy from old drugs: synergistic bactericidal activity of sulfadiazine with colistin against colistin-resistant bacteria, including plasmid-mediated colistin-resistant mcr-1 isolates. *Int. J. Antimicrob. Agents* 51, 775–783. doi: 10.1016/j.ijantimicag.2018.01.027

Olaitan, A. O., Diene, S. M., Kempf, M., Berrazeg, M., Bakour, S., Gupta, S. K., et al. (2014). Worldwide emergence of colistin resistance in *Klebsiella pneumoniae* from healthy humans and patients in Lao PDR, Thailand, Israel, Nigeria and France owing to inactivation of the PhoP/PhoQ regulator mgrB: an epidemiological and molecular study. *Int. J. Antimicrob. Agents* 44, 500–507. doi: 10.1016/j.ijantimicag.2014.07.020

Otto, R. G., van Gorp, E., Kloezen, W., Meletiadis, J., van den Berg, S., and Mouton, J. W. (2019). An alternative strategy for combination therapy: Interactions between polymyxin B and non-antibiotics. *Int. J. Antimicrob. Agents* 53, 34–39. doi: 10.1016/j.ijantimicag.2018.09.003

Parmar, K. M., Hathi, Z. J., and Dafale, N. A. (2017). Control of multidrug-resistant gene flow in the environment through bacteriophage intervention. *Appl. Biochem. Biotechnol.* 181, 1007–1029. doi: 10.1007/s12010-016-2265-7

Peyclit, L., Baron, S. A., Yousfi, H., and Rolain, J. M. (2018). Zidovudine: a salvage therapy for mcr-1 plasmid-mediated colistin-resistant bacterial infections? *Int. J. Antimicrob. Agents* 52. doi: 10.1016/j.ijantimicag.2018.03.012

Rangel-Vega, A., Bernstein, L. R., Mandujano-Tinoco, E. A., García-Contreras, S. J., and García-Contreras, R. (2015). Drug repurposing as an alternative for the treatment of recalcitrant bacterial infections. *Front. Microbiol.* 6:282. doi: 10.3389/fmicb.2015.00282

Roca, I., Akova, M., Baquero, F., Carlet, J., Cavaleri, M., Coenen, S., et al. (2015). The global threat of antimicrobial resistance: science for intervention. *New Microbes New Infect.* 6, 22–29. doi: 10.1016/j.nmni.2015.02.007

Rolain, J.-M. (2013). Food and human gut as reservoirs of transferable antibiotic resistance encoding genes. *Front. Microbiol.* 4:173. doi: 10.3389/fmicb.2013.00173

Rolain, J. M., and Baquero, F. (2016). The refusal of the society to accept antibiotic toxicity: missing opportunities for therapy of severe infections. *Clin. Microbiol. Infect.* 22, 423–427. doi: 10.1016/j.cmi.2016.03.026

Schneider, E. K., Reyes-Ortega, F., Velkov, T., and Li, J. (2017). Antibiotic–non-antibiotic combinations for combating extremely drug-resistant gram-negative 'superbugs.' *Essays Biochem.* 61, 115–125. doi: 10.1042/EBC20160058

Seukep, J. A., Sandjo, L. P., Ngadjui, B. T., and Kuete, V. (2016). Antibacterial and antibiotic-resistance modifying activity of the extracts and compounds from *Nauclea pobeguinii* against gram-negative multi-drug resistant phenotypes. *BMC Complement. Altern. Med.* 16:193. doi: 10.1186/s12906-016-1173-2

Sleire, L., Førde, H. E., Netland, I. A., Leiss, L., Skeie, B. S., and Enger, P. Ø. (2017). Drug repurposing in cancer. *Pharmacol. Res.* 124, 74–91. doi: 10.1016/j.phrs.2017.07.013

Soo, V., Kwan, B., Quezada, H., Castillo-Juárez, I., Pérez-Eretza, B., García-Contreras, S., et al. (2017). Repurposing of anticancer drugs for the treatment of bacterial infections. *Curr. Top. Med. Chem.* 17, 1157–1176. doi: 10.2174/1568026616666160930131737

Spellberg, B., Powers, J. H., Brass, E. P., Miller, L. G., and Edwards, J. E. (2004). Trends in Antimicrobial drug development: implications for the future. *Clin. Infect. Dis.* 38, 1279–1286. doi: 10.1086/420937

Stokes, J. M., MacNair, C. R., Ilyas, B., French, S., Côté, J. P., Bouwman, C., et al. (2017). Pentamidine sensitizes gram-negative pathogens to antibiotics and overcomes acquired colistin resistance. *Nat. Microbiol.* 2:17028. doi: 10.1038/nmicrobiol.2017.28

Sun, J., Yang, J., Chi, J., Ding, X., and Lv, N. (2018). Identification of drug repurposing candidates based on a miRNA-mediated drug and pathway network for cardiac hypertrophy and acute myocardial infarction. *Hum. Genomics* 12, 52. doi: 10.1186/s40246-018-0184-0

Sun, W., Sanderson, P. E., and Zheng, W. (2016a). Drug combination therapy increases successful drug repositioning. *Drug Discov. Today* 21, 1189–1195. doi: 10.1016/j.drudis.2016.05.015

Sun, W., Weingarten, R. A., Xu, M., Southall, N., Dai, S., Shinn, P., et al. (2016b). Rapid antimicrobial susceptibility test for identification of new therapeutics and drug combinations against multidrug-resistant bacteria. *Emerg. Microbes Infect.* 9:5. doi: 10.1038/emi.2016.123

Tafoukt, R., Leangapichart, T., Hadjadj, L., Bakour, S., Diene, S. M., Rolain, J.-M., et al. (2017). Characterization of bla OXA-538, a new variant of bla OXA-48 in shewanella xiamenensis isolated from river water in Algeria. *J. Glob. Antimicrob. Resist.* doi: 10.1016/j.jgar.2017.11.008

Terra, L., Dyson, P. J., Hitchings, M. D., Thomas, L., Abdelhameed, A., Banat, I. M., et al. (2018). A novel alkaliphilic streptomyces inhibits ESKAPE pathogens. *Front. Microbiol.* 9:2458. doi: 10.3389/fmicb.2018.02458

Torres, N. S., Abercrombie, J. J., Srinivasan, A., Lopez-Ribot, J. L., Ramasubramanian, A. K., and Leung, K. P. (2016). Screening a commercial library of pharmacologically active small molecules against *Staphylococcus aureus* biofilms. *Antimicrob. Agents Chemother.* 60, 5663–5672. doi: 10.1128/AAC.00377-16

Tran, T. B., Wang, J., Doi, Y., Velkov, T., Bergen, P. J., and Li, J. (2018). Novel Polymyxin Combination with antineoplastic mitotane improved the bacterial killing against polymyxin-resistant multidrug-resistant gram-negative pathogens. *Front. Microbiol.* 9:721. doi: 10.3389/fmicb.2018.00721

Wang, Y. M., Kong, L. C., Liu, J., and Ma, H. X. (2018). Synergistic effect of eugenol with Colistin against clinical isolated colistin-resistant *Escherichia coli* strains. *Antimicrob. Resist. Infect. Control* 7:17. doi: 10.1186/s13756-018-0303-7

World Health Organization, W. H. O. (2018). *Les 10 principales causes de mortalité (Top 10 causes of death)*. Available online at: https://www.who.int/fr/news-room/fact-sheets/detail/the-top-10-causes-of-death (accessed January 11, 2019).

Yang, Y., and Chua, K. L. (2013). Assessment of the effect of efflux pump inhibitors on in vitro antimicrobial susceptibility of multidrug-resistant *Acinetobacter baumannii*. *Int. J. Antimicrob. Agents* 42, 283–284. doi: 10.1016/J.IJANTIMICAG.2013.05.011

Zenati, K., Touati, A., Bakour, S., Sahli, F., and Rolain, J. M. (2016). Characterization of NDM-1- and OXA-23-producing *Acinetobacter baumannii* isolates from inanimate surfaces in a hospital environment in Algeria. *J. Hosp. Infect.* 92, 19–26. doi: 10.1016/j.jhin.2015.09.020

Zheng, W., Sun, W., and Simeonov, A. (2018). Drug repurposing screens and synergistic drug-combinations for infectious diseases. *Br. J. Pharmacol.* 175, 181–191. doi: 10.1111/bph.13895

Zhou, Y., Liu, S., Wang, T., Li, H., Tang, S., Wang, J., et al. (2018). Pterostilbene, a potential MCR-1 inhibitor that enhances the efficacy of polymyxin B. *Antimicrob. Agents Chemother.* 27:62. doi: 10.1128/AAC.02146-17

Conflict of Interest Statement: The authors declare that the research was conducted in the absence of any commercial or financial relationships that could be construed as a potential conflict of interest.

frontiers in Cellular and Infection Microbiology

ORIGINAL RESEARCH
published: 02 July 2019
doi: 10.3389/fcimb.2019.00236

Repurposing Azithromycin and Rifampicin Against Gram-Negative Pathogens by Combination With Peptidomimetics

Kristin R. Baker[1,2], Bimal Jana[1,2], Anna Mette Hansen[3], Hanne Mørck Nielsen[4], Henrik Franzyk[3]* and Luca Guardabassi[1,5]*

[1] Department of Veterinary and Animal Sciences, Faculty of Health and Medical Sciences, University of Copenhagen, Frederiksberg, Denmark, [2] Department of Biomedical Sciences, Ross University School of Veterinary Medicine, Basseterre, Saint Kitts and Nevis, [3] Department of Drug Design and Pharmacology, Faculty of Health and Medical Sciences, University of Copenhagen, Copenhagen, Denmark, [4] Department of Pharmacy, Faculty of Health and Medical Sciences, University of Copenhagen, Copenhagen, Denmark, [5] Department of Pathobiology and Population Sciences, Royal Veterinary College, Hatfield, United Kingdom

Synthetic peptidomimetics may be designed to mimic functions of antimicrobial peptides, including potentiation of antibiotics, yet possessing improved pharmacological properties. Pairwise screening of 42 synthetic peptidomimetics combined with the antibiotics azithromycin and rifampicin in multidrug-resistant (MDR) *Escherichia coli* ST131 and *Klebsiella pneumoniae* ST258 led to identification of two subclasses of α-peptide/β-peptoid hybrids that display synergy with azithromycin and rifampicin (fractional inhibitory concentration indexes of 0.03–0.38). Further screening of the best three peptidomimetics in combination with a panel of 21 additional antibiotics led to identification of peptidomimetics that potentiated ticarcillin/clavulanate and erythromycin against *E. coli*, and clindamycin against *K. pneumoniae*. The study of six peptidomimetics was extended to *Pseudomonas aeruginosa*, confirming synergy with antibiotics for five of them. The most promising compound, H-(Lys-βNPhe)$_8$-NH$_2$, exerted only a minor effect on the viability of mammalian cells ($EC_{50} \geq 124$–$210\,\mu M$), and thus exhibited the highest selectivity toward bacteria. This compound also synergized with rifampicin and azithromycin at sub-micromolar concentrations (0.25–0.5 μM), thereby inducing susceptibility to these antibiotics at clinically relevant concentrations in clinical MDR isolates. This peptidomimetic lead and its analogs constitute promising candidates for efficient repurposing of rifampicin and azithromycin against Gram-negative pathogens.

Keywords: peptidomimetic, antibiotic potentiation, multidrug resistance, synergy, Gram-negative, antibiotic adjuvant

OPEN ACCESS

Edited by:
Rodolfo García-Contreras, National Autonomous University of Mexico, Mexico

Reviewed by:
Frank Schweizer, University of Manitoba, Canada
César de la Fuente, Massachusetts Institute of Technology, United States

****Correspondence:***
Kristin R. Baker
kribake@sund.ku.dk
Henrik Franzyk
henrik.franzyk@sund.ku.dk

Specialty section:
This article was submitted to Clinical Microbiology, a section of the journal Frontiers in Cellular and Infection Microbiology

Received: *30 January 2019*
Accepted: *14 June 2019*
Published: *02 July 2019*

Citation:
Baker KR, Jana B, Hansen AM, Nielsen HM, Franzyk H and Guardabassi L (2019) Repurposing Azithromycin and Rifampicin Against Gram-Negative Pathogens by Combination With Peptidomimetics. Front. Cell. Infect. Microbiol. 9:236. doi: 10.3389/fcimb.2019.00236

INTRODUCTION

Traditional antimicrobial therapies have become ineffective in treating infections caused by multidrug-resistant (MDR) Gram-negative pathogens. Thus, new therapeutic strategies are required to manage these infections (Doi et al., 2017; World Health Organisation, 2017). Emergence of resistance to mono-drug therapies has drawn attention to combination therapies with new agents that limit resistance development or overcome resistance mechanisms (Kalan and Wright, 2011; Brown, 2015; Ribeiro et al., 2015; Brown and Wright, 2016; Melander and Melander, 2017; Singh et al., 2017; Moon and Huang, 2018). In this regard, co-application of certain peptides has been

found to constitute a promising means for overcoming intrinsic resistance to certain classes of antimicrobials (e.g., macrolides, lincosamides and rifamycins) in Gram-negative pathogens due to their ability to increase the permeability of the outer membrane (Gill et al., 2015; Baker et al., 2018).

Despite the potential utility of peptides as potentiators of antibiotics, their clinical use is hampered by unfavorable pharmacological properties. In particular, many peptides also affect the viability of mammalian cells and possess inherently low stability toward proteolytic degradation, which (particularly for linear peptides) represents a major obstacle for their development into drugs (Ghosh and Haldar, 2015; Mojsoska and Jenssen, 2015; Molchanova et al., 2017a). While most naturally occurring peptides consist exclusively of α-amino acid residues, peptidomimetics incorporate unnatural amino acids or mimics thereof, resulting in alternative backbones that resist enzymatic cleavage (Molchanova et al., 2017a). In addition, end modifications (Jahnsen et al., 2015) may broaden the chemical space covered. These features of peptidomimetics enable design of compounds with fine-tuned physicochemical properties that confer enhanced antibacterial activity as well as an improved pharmacological profile (Méndez-Samperio, 2014). Moreover, certain peptidomimetics have proved capable of potentiating traditional antibiotics (Renau et al., 2002; Goldberg et al., 2013; Jammal et al., 2015; Lainson et al., 2017), suggesting a possible role in combination therapy. Despite displaying several features that are superior to those of peptides, their therapeutic potential relies on technological advances to enable reduced production cost, improved bioavailability, and minimized toxicity toward host cells (Molchanova et al., 2017a). Nonetheless, recent advances in synthesis of peptidomimetics has enabled investigation of diverse compound arrays, thus facilitating identification of peptidomimetic antibiotic adjuvants with suitable pharmacological properties.

Benefiting from already available peptidomimetic arrays (Hein-Kristensen et al., 2011; Jahnsen et al., 2012, 2014, 2015; Liu et al., 2013), we performed a search for peptidomimetics capable of circumventing the intrinsically low susceptibility to certain antibiotics in Gram-negative pathogens. To address potential toxicity issues, which are considered the most critical factor currently limiting the therapeutic use of peptidomimetics, the screening process was designed so that only compounds that potentiate antibiotics at sub-micromolar nontoxic concentrations were pursued. Thus, screening of pairwise peptidomimetic-antibiotic combinations led to identification of α-peptide/β-peptoid hybrids capable of inducing susceptibility to azithromycin and rifampicin (below their putative clinical breakpoints) in clinical MDR isolates of *Escherichia coli*, *K. pneumoniae* and *P. aeruginosa*.

MATERIALS AND METHODS

Bacterial Strains, Antibiotics and Media

Bacterial strains used in this study comprise MDR clinical isolates of *E. coli* ST131 (Cerquetti et al., 2010) and *K. pneumoniae* ST258 (Jana et al., 2017), and American type culture collection (ATCC) strains: ATCC 25922 (*E. coli*), ATCC 13883 (*K. pneumoniae*), and ATCC 27853 (*P. aeruginosa*). Additional clinical isolates of *E. coli*, *K. pneumoniae*, and *P. aeruginosa* resistant to β-lactams (including carbapenems and cephalosporins) were provided by Laurent Poirel, Université de Fribourg, Switzerland. The following growth media was routinely used for bacterial culturing: Luria-Burtani (LB), cation-adjusted Mueller-Hinton agar (MHA) and broth (MHB II). All assays were performed in cation-adjusted MHA or MHB II. Antibiotics were purchased from Sigma-Aldrich and the peptidomimetic collection (**Table S1**) was curated and provided by Henrik Franzyk. This collection contained peptoids, α-peptide/β-peptoid hybrids, and a variety of end-group modifications, thereby representing a wide range of physicochemical and structural properties, including varied cationic character, length and hydrophobicity. Stock solutions were prepared by dissolving the compounds in deionized water, while test solutions were obtained by further dilution with MHB II medium.

Peptidomimetic Synthesis

α-Peptide/β-peptoid peptidomimetics were synthesized on a Rink amide resin (loading: 0.5–0.7 mmol/g; 0.05–0.1 mmol scale) in Teflon reactors (10 mL) by standard Fmoc-based solid-phase synthesis using the appropriate dimeric building blocks (Bonke et al., 2008; Jahnsen et al., 2014). Fmoc deprotection was performed with excess 20% piperidine in DMF (2 × 10 min, each time with 5 mL; shaking at room temperature). After Fmoc deprotection (and after coupling as well) the resin was washed with DMF, MeOH, and DCM (each 3 × 3 min with 5 mL). Coupling was performed with the appropriate building block (2.0 equiv. for loading, 2.5 equiv for the first two elongations, and 3.0 equiv. for subsequent elongations) and PyBOP/DIPEA (1:2 equiv. relative to the building block) in DMF (2–3 mL) for >2 h under shaking at room temperature. Capping was applied after the fourth coupling via treatment with Ac_2O–DIPEA–NMP 1:2:3 (5 mL, 10 min at room temperature). Final Fmoc deprotection was followed by attachment of any N-terminal end group: the carboxylic acid (5 equiv.) corresponding to the desired moiety was added under conditions identical to those applied for the above coupling procedure used for the dimeric building blocks. Cleavage and simultaneous side chain deprotection: Excess TFA-CH_2Cl_2 90:10 (2 × 30 min under shaking at room temperature). The filtrate was collected and the resin was eluted with CH_2Cl_2 (2 mL). The combined filtrates were concentrated in vacuo, and co-evaporated three times with toluene. The crude products were purified by using preparative HPLC, and the resulting pure fractions were freeze-dried as previously described (Jahnsen et al., 2012, 2015; Skovbakke et al., 2015; Molchanova et al., 2017b).

Antimicrobial Susceptibility Testing

Minimal inhibitory concentrations (MICs) of peptidomimetics, antibiotics and their combinations were determined by broth microdilution according to the Clinical Laboratory Standards Institute performance standards (Clinical and Laboratory Standards Institute, 2013). Based on previous studies indicating that among a range of tested antibiotics

TABLE 1 | Susceptibility of MDR *E. coli* ST131 and *K. pneumoniae* ST258 to rifampicin (RIF) or azithromycin (AZM) in combination with peptidomimetics[a].

Species	ABX	Peptidomimetic number (0.5 μM)																																				
		1	2	3	4	5	6	7	8	9	10	11	12	13	**14**	**15**	16	17	18	19	20	21	22	23	24	**25**	**26**	27	**28**	29	30	31	32	33	34	35	36	37	38	39	40	41	42
E. coli ST131	RIF[b]	–	+	–	+	–	–	+	+	+	–	+	+	+	–	–	+	+	+	+	–	–	–	+	+	–	–	+	–	+	+	+	+	+	+	+	–	+	+	+	+	–	+
K. pneumoniae ST258	(0.5 μg/mL)	–	+	+	+	+	+	+	+	+	+	+	+	+	+	–	+	+	+	+	+	+	+	+	+	+	–	+	+	+	+	+	+	+	+	+	+	+	+	+	+	+	+
E. coli ST131	AZM[c]	–	+	+	+	–	–	+	+	+	+	+	+	+	–	–	+	+	+	–	+	+	–	+	+	–	–	+	–	+	+	+	+	+	+	+	+	+	+	+	+	–	+
K. pneumoniae ST258	(1 μg/mL)	–	+	+	+	+	+	+	+	+	+	+	+	+	+	+	+	+	+	+	+	+	+	+	+	+	+	+	+	+	+	+	+	+	+	+	+	+	+	+	+	+	+

Peptidomimetics that were studied further are indicated in bold (see ***Table 2*** *for sequences of these).*

[a]*Growth (+) and growth inhibition (–).*

[b]*At 0.5 μg/mL.*

[c]*At 1 μg/mL.*

belonging to several classes azithromycin and rifampicin displayed a high propensity to synergize with peptides, and hence these antibiotics were chosen for the initial screening of peptidomimetics to identify possible antibiotic adjuvants (Jammal et al., 2015; Baker et al., 2016, 2018; Corbett et al., 2017; Lyu et al., 2017; Wu et al., 2017; Domalaon et al., 2018a,b; Yang et al., 2018). Here, a sub-MIC concentration of 0.5 μM peptidomimetic was tested in combination with 0.5 μg/mL rifampicin or 1 μg/mL azithromycin in 96-well plates, followed by inoculum addition according to CLSI guidelines. At these concentrations, control wells containing either peptidomimetic or antibiotic individually did not inhibit growth. Since rifampicin and azithromycin mainly are used to treat infections with Gram-positive pathogens only CLSI clinical breakpoints were available for such bacteria. Hence the clinically relevant test concentrations were selected based on the CLSI susceptibility breakpoints for *Staphylococcus* species (Clinical and Laboratory Standards Institute, 2017): rifampicin (1 μg/mL) and azithromycin (2 μg/mL). Potentiation of additional antibiotics by peptidomimetics was determined by using commercial 96-well plates containing varied concentrations of standard antibiotics (COMPAN1F; Trek Diagnostic Systems Inc.). The peptidomimetics were added immediately prior to inoculation with pathogen, and then MICs were determined as above. The MICs of peptidomimetic/antibiotic combinations were determined according to the method above, and the concentration ratios were selected based upon checkerboard results with 2:1 and 1:4 ratio of peptidomimetic with rifampicin or azithromycin, respectively. Minimal bactericidal concentrations (MBCs) were determined by using growth-curve assay plates. MIC plates were prepared as above, and then the plates were incubated at 37°C with continuous shaking. Growth was recorded at 10 min intervals as optical density (OD) at 600 nm during 24 h. At 24 h, for wells without growth, a sample was diluted 10-fold in sterile saline (0.9% sodium chloride) and plated onto MHA, following CLSI guidelines (Clinical and Laboratory Standards Institute, 1999).

Checkerboard Synergy Assay

The potential synergistic effects in peptidomimetic-antibiotic combinations were assessed by using a two-dimensional checkerboard assay (Garcia, 2010). Briefly, twofold dilutions of peptide and antibiotic were prepared in MBH II media along the X- and Y-axis, respectively, in 96-well plates. The inoculum was added to the plates, and subsequently these were incubated for 18–20 h. All steps for inoculum preparation and broth microdilution were in accordance with the CLSI guidelines (Clinical and Laboratory Standards Institute, 2013). The fractional inhibitory concentration index (FICI) was calculated as $[MIC_{A(A+B)}/MIC_{A(alone)}] + [MIC_{B(A+B)}/MIC_{B(alone)}]$, where $MIC_{A(A+B)}$ represents the MIC of antibiotic (A) in combination with peptidomimetic (B), while $MIC_{B(A+B)}$ represents the MIC of peptidomimetic (B) in combination with antibiotic (A). $MIC_{A(alone)}$ and $MIC_{B(alone)}$ represent the MIC of each compound individually. FICI values of ≤0.5 were interpreted as synergy.

TABLE 2 | Peptidomimetics studied: sequence, cytotoxicity, and MIC in clinical isolates of *E. coli, K. pneumoniae* and *P. aeruginosa*.

No.	Compound	MW (g/mol)	Charge	Length (residues)	Cytotoxicity (μM)		MIC (μM) and Selectivity Index (SI[d]; in brackets)					
					NIH 3T3 EC_{50} ± SD	HepG2 EC_{50} ± SD	*E. coli* ST131		*K. pneumoniae* ST258		*P. aeruginosa* ATCC 27853	
Subclass I												
1	H-(Lys-βNPhe)$_8$-NH_2	3470.44	+9	16	210.60 ± 26.78	123.97 ± 0.81	2	(84)	16	(10)	1	(167)
14	Ac-(Lys-βNPhe)$_6$-NH_2	2478.44	+6	12	323.50 ± 45.78	233.53 ± 7.95	4	(70)	64	(4)	16	(17)
15	Ac-(Lys-βNPhe)$_8$-NH_2	3286.24	+8	16	216.57 ± 23.12	121.37 ± 0.06	1	(169)	32	(5)	1	(169)
Subclass II												
25	NDab[a]-Lys-βNspe-hArg-βNspe)$_3$-NH_2	2975.85	+8	13	166.90 ± 5.53	85.01 ± 3.06	2	(63)	8	(16)	8	(63)
26	[Spermine-Ac][b]-(Lys-βNspe-hArg-βNspe)$_3$-NH_2	3346.14	+10	13	53.20 ± 2.94	59.62 ± 0.71	1	(56)	8	(7)	2	(28)
28	TODA[c]-(Lys-βNspe-hArg-βNspe)$_3$-NH_2	2807.85	+6	13	217.57 ± 18.05	118.23 ± 2.05	2	(84)	16	(10)	16	(10)

[a] *NDab, $H_2NCH_2CH_2NHCH_2(C=O)$.*
[b] *Spermine-Ac, $H_2N(CH_2)_3NH(CH_2)_4NH(CH_2)_3NHCH_2(C=O)$.*
[c] *TODA, $H_3CO(CH_2)_2O(CH_2)_2O(CH_2)(C=O)$.*
[d] *SI was calculated as the average of the EC_{50} values for HepG2 and NIH 3T3 cells divided by the MIC.*

Determination of Cell Viability and Selectivity Indexes for Peptidomimetics

NIH 3T3 and HepG2 cells (both from ATCC, Manassas, VA, USA) were cultured in flat-bottomed 96-well MicroWell™ plates (NUNC, Roskilde, Denmark) at seeding densities of ∼23,000 and ∼22,000 cells/well, respectively, and then cultured for 22–24 h under standard culturing conditions (37°C, 5% CO_2, humidified air) to reach 80–90% confluence. NIH 3T3 were cultured in Dulbecco's modified Eagle's medium (DMEM) supplemented with 10% (v/v) newborn-calf serum (NCS) (Gibco, Paisly, UK), while HepG2 were cultured in Eagle's minimum essential medium (EMEM) supplemented with 10% (v/v) fetal bovine serum (FBS, Gibco, Paisly, UK), sodium pyruvate (1 mM), and non-essential amino acids (1%, v/v). Both culturing media were further supplemented with penicillin (100 U/mL), streptomycin (100 μg/mL), and L-glutamine (2 mM).

Effect on cell viability was determined in NIH 3T3 fibroblasts and HepG2 hepatocytes by using the MTS/PMS assay measuring metabolic activity. Briefly, the adhered cells were washed with 37°C Hanks' balanced salt solution (HBSS from Sigma-Aldrich, St. Louis, MO, USA), containing 10 mM HEPES (AppliChem, Darmstadt, Germany), and adjusted to pH 7.4, and were then exposed for 1 h to 100 μL of test compound(s) dissolved in the appropriate culturing medium without serum for each cell line. After exposure the cells were washed with HBSS containing 10 mM HEPES (pH 7.4) and 100 μL of an MTS/PMS solution, consisting of 240 μg/mL MTS (Promega, Madison, WI, USA) and 2.4 μg/mL PMS (SigmaAldrich, Buchs, Switzerland) in HBSS, was added to the cells, which then were incubated for 1 h at 37°C with horizontal shaking under light protection. Absorbance was measured at 492 nm by using a POLARstar OPTIMA plate reader (BMG Labtech, Offenburg, Germany). The relative viability was calculated according to Equation (1) with absorbance values obtained after incubation of cells with test compound; incubation with SDS (0.2%, w/v in medium) defined 100% cell death (Abs_{pos}), while the absorbance of cells incubated with medium defined 0% cell death (Abs_{neg}).

$$Relative\ viability\ (\%) = \frac{(Abs_{sample} - Abs_{pos})}{(Abs_{neg} - Abs_{pos})} \times 100\% \quad (1)$$

EC_{50} values were calculated by using GraphPad Prism 7 (GraphPad Software, La Jolla, CA, USA) via fitting of the relative cell viability to the concentration of the test compound by using Equation (2):

$$Relative\ viability\ (\%) = \frac{Top - Bottom}{1 + 10^{(LogIC_{50} - Log[peptidomimetic]) \times Hill\ slope}} \quad (2)$$

With top and bottom representing the mean highest and lowest observed values, respectively. The Hill slope represents a factor for the steepness of the linear part of the curve. In order to prevent erroneous calculation, the top and bottom values were constrained to 100 and 0%, respectively. Data were collected from technical triplicates. The selectivity index was calculated as the average effect on cell viability (EC_{50} values for HepG2 and NIH 3T3 cells) divided by the MIC.

Time-Kill Assay

Time-kill kinetic assays were performed in MDR *E. coli* ST131, MDR *K. pneumoniae* ST258, and *P. aeruginosa* ATCC 27853. Overnight cultures were subcultured in MHB II and grown to the logarithmic phase, after which ∼10^6 CFU/mL cells were transferred to 15-mL round-bottom Falcon tubes. Bacterial cells were incubated at 37°C with aeration in the presence or absence of antibiotic, peptidomimetic or a combination of these at 2 × MIC (as observed in the growth curves; **Table 6**). At time points 0, 1, 2, 4, 8, and 24 h, 100 μl cells were serially diluted 10-fold in sterile 0.9% NaCl, and then 10 μl aliquots were plated on MHA in triplicate. The CFU/mL from each condition was calculated from counted colonies following 18–24 h incubation

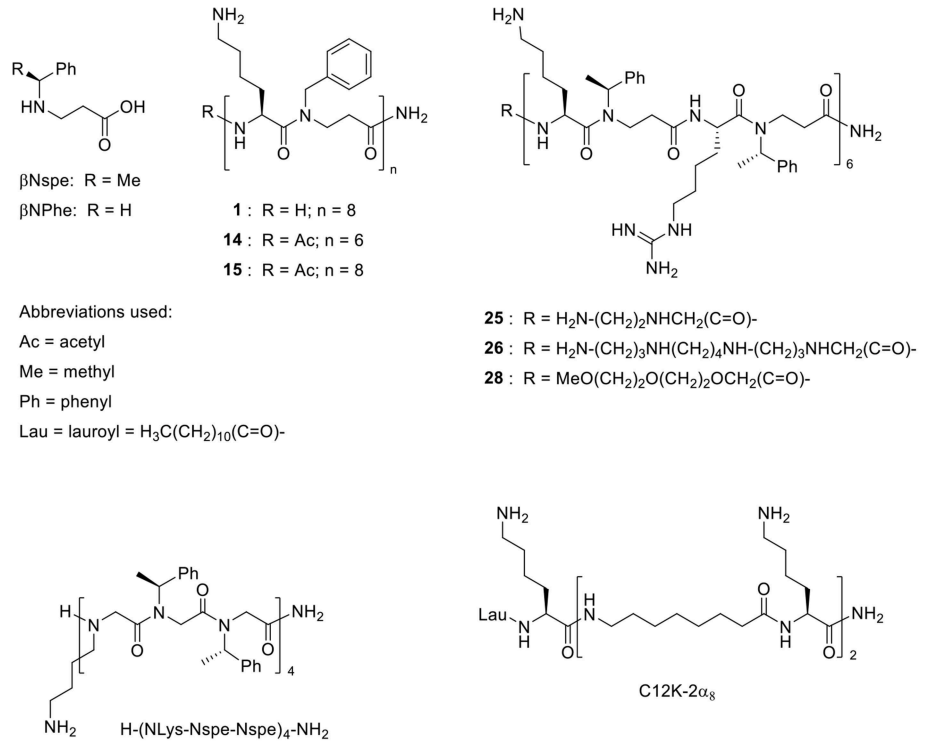

FIGURE 1 | Structures of the α-peptide/β-peptoid hybrids listed in **Table 2** and similar compounds that exhibit activity *in vivo* (Zaknoon et al., 2011; Czyzewski et al., 2016, respectively).

at 37°C. The detection limit was $\sim 10^2$ CFU/mL. The CFU/mL of each culture was graphed in GraphPad Prism 7 over time (h), and all graphs represent the average and standard error from two separate experiments (i.e., biological duplicates). Synergy was defined as a $\geq$2-log$_{10}$ CFU/mL decrease for the cultures exposed to the antibiotic-peptidomimetic combination vs. either compound individually. Bactericidal activity was defined as a $\geq$3-log$_{10}$ CFU/mL decrease after 24 h incubation.

RESULTS

Identification of Two Subclasses of Peptidomimetics That Induce Susceptibility to Rifampicin and Azithromycin in Gram-Negative Pathogens

Screening of peptidomimetic-antibiotic combinations was performed in order to identify potentiators of rifampicin and azithromycin in MDR *Escherichia coli* sequence type 131 (ST131) and *K. pneumoniae* ST258 epidemic clones. This involved 42 selected diverse peptidomimetics that were combined at 0.5 μM with each antibiotic at concentrations approximating the clinical breakpoints in Gram-positive species (i.e., 0.5 μg/mL and 1 μg/mL, for rifampicin and azithromycin, respectively) (Clinical and Laboratory Standards Institute, 2017). Three peptidomimetics (i.e., **1**, **15,** and **26**) were found to inhibit growth of both species in the presence of rifampicin, while one compound (i.e., **1**) prevented growth in combination with azithromycin (**Table 1**). These peptidomimetics represent two subclasses of α-peptide/β-peptoid hybrids: subclass I (e.g., **1** and **15**) comprising lysine-based compounds with achiral β-peptoid phenylalanine-like residues, and subclass II (e.g., **26**) displaying both Lys and homoarginine (hArg) as cationic residues together with α-chiral β-peptoid hydrophobic Phe-like residues (**Table 2**; **Figure 1**). The effect on cell viability of these three peptidomimetics was tested toward the mammalian cells lines mouse fibroblasts (NIH 3T3) and human hepatocytes (HepG2), which revealed that **1** and **15** exhibited promising cell selectivity (i.e., EC_{50} >100 μM) while peptidomimetic **26** proved to affect cell viability the most with EC_{50} values in the range 50–60 μM (**Table 2**). These peptidomimetics were further screened for potentiation of additional 21 antibiotics (**Table 3**) at sub-MIC concentrations of $\leq$1 μM (**Table 2**). In presence of peptidomimetics **1**, **15,** or **26**, the MIC of rifampicin (>2 μg/mL) was reduced to below 1 μg/mL in both MDR *E. coli* and *K. pneumoniae*, while the MIC of erythromycin was reduced from >4 μg/mL to $\leq$2 μg/mL in MDR *E. coli*, confirming the results from the primary screening. In addition, the MIC of clindamycin in MDR *K. pneumoniae* was reduced from >4 μg/mL to 2 μg/mL in presence of 1 μM of **26**, while the MIC of ticarcilllin/clavulanic acid in *E. coli* was reduced from 64 μg/mL to 16 μg/mL in presence of 0.5 μM of **1**. Since this *E. coli* strain was already susceptible to ticarcillin/clavulanic acid, this combination was not studied further. Growth

TABLE 3 | Potentiation of antibiotics by peptidomimetics in MDR *E. coli* ST131 and *K. pneumoniae* ST258; MICs (μg/mL) of antibiotics in presence and absence of peptidomimetics; MICs reduced ≥4-fold in presence of a peptidomimetic are indicated in bold.

Strain	***K. pneumoniae* ST258**				***E. coli* ST131**			
Peptidomimetic	**1**	**15**	**26**	**antibiotic alone**	**1**	**15**	**26**	**antibiotic alone**
	1 μM	**1 μM**	**1 μM**	**-**	**0.5 μM**	**0.5 μM**	**0.25 μM**	**-**
β-lactams								
Ampicillin	>16	>16	>16	>16	>16	>16	>16	>16
Penicillin	>8	>8	>8	>8	>8	>8	>8	>8
Oxacillin (2% NaCl)	>4	>4	>4	>4	>4	>4	>4	>4
Amoxicillin/clavulanic acid (2:1)	>32	>32	>32	>32	8	8	8/4	16
Ticarcillin	>64	>64	>64	>64	>64	>64	ND	>64
Ticarcillin/clavulanic acid (2:1)	>64	>64	>64	>64	**16**	32	ND	64
Cephalosporins and Carbapenems								
Cefazolin	>16	>16	>16	>16	>16	>16	>16	>16
Cefovecin	>8	>8	>8	>8	>8	>8	>8	>8
Cefoxitin	>16	>16	>16	>16	>16	4	ND	8
Cefpodoxime	>16	>16	>16	>16	>16	>16	>16	>16
Ceftiofur	>4	>4	>4	>4	>4	>4	ND	>4
Imipenem	>8	>8	>8	>8	≤1	≤1	≤1	≤1
Aminoglycosides								
Amikacin	32	32	16	32	>32	8	8	16
Gentamicin	≤1	2	≤1	2	>8	>8	>8	>8
fluoroquinolone								
Enrofloxacin	>2	>2	>2	>2	>2	>2	>2	>2
Marbofloxacin	>2	>2	>2	>2	>2	>2	>2	>2
Miscellaneous								
Chloramphenicol	>16	>16	>16	>16	≤4	≤4	≤4	≤4
Clindamycin	>4	>4	**2**	>4	4	>4	>4	>4
Doxycycline	≤2	≤2	≤2	4	≤2	≤2	≤2	≤2
Erythromycin	>4	>4	>4	>4	**1**	**2**	**2**	>4
Rifampicin	**≤1**	**≤1**	**≤1**	>2	**≤1**	**≤1**	**≤1**	>2
Trimethoprim/sulfamethoxazole	>38	>38	>38	>38	>38	>38	>38	>38

*Peptidomimetic MICs are reported in **Table 2** and as follows: 16, 32, 8, 2, 1 and 1 μM, respective to the order listed in **Table 3**.*

inhibition occurred at concentrations ≥4-fold below the MICs of the peptidomimetic (except for **15** in *E. coli*) and antibiotic alone, indicating that the combinations exerted synergistic effects. Synergy was confirmed by the checkerboard assay, and fractional inhibitory concentration indexes (FICIs) ranged from 0.05 to 0.38 (**Table 4**). With FICIs ranging from 0.05 to 0.07, the synergistic peptidomimetic-rifampicin interactions in *K. pneumoniae* were especially potent. The peptidomimetic **26**-clindamycin synergistic interaction in *K. pneumoniae* was also potent, however, due to the relatively high effect of **26** on the viability of eukaryotic cells, this combination was not studied further.

To explore additional compounds within the two identified subclasses of peptidomimetics, found to enhance the antibacterial effect of rifampicin and azithromycin, the study was extended to include three additional peptidomimetics, **14** and **25**, **28** (also belonging to subclasses I or II; **Table 2**). These three peptidomimetics also exhibited an ability to potentiate rifampicin and azithromycin in MDR *E. coli* and *K. pneumoniae* (**Table 4**). Overall, the degree of synergy was similar to that seen for combinations containing **1**, **15,** and **26**, resulting in potentiation of rifampicin and azithromycin (to reach MICs of ≤1 and ≤8 μg/mL, respectively) in both species. Similar to the subclass I compounds (i.e., **1** and **15**), peptidomimetic **14** displayed the lowest effect on cell viability with EC_{50} values of 323 μM and 234 μM in NIH 3T3 and HepG2, respectively (**Table 2**). In contrast, peptidomimetic **25** had a noticeably higher effect on cell viability with EC_{50} values in the range 80–170 μM, although somewhat less toxic than the highly cationic peptidomimetic **26**. Among, the subclass II compounds, peptidomimetic **28** had the least effect on cell viability (EC_{50} >100 μM). Overall, the HepG2 liver cell line was more sensitive to the peptidomimetics than the fibroblast cells (i.e., NIH 3T3).

We extended our study to species outside Enterobacteriaceae by including a reference strain of *P. aeruginosa*, which displayed a susceptibility pattern similar to that found for *E. coli* (**Table 2**). Similarly, synergy was observed with FICIs ranging from

TABLE 4 | Interaction of azithromycin (AZM) and rifampicin (RIF) with peptidomimetics in *E. coli* ST131, *K. pneumoniae* ST258, and *P. aeruginosa* as determined in the checkerboard assay.

Species	Antibiotic (μg/mL)			Peptidomimetic (μM)			FICI
	Agent	MIC alone	MIC in combination	Compound no.	MIC alone	MIC in combination (Selectivity index)	
***E. coli* ST131**							
	AZM	8	1	**1**	2	0.25 (669)	0.25
			1	**14**	4	0.25 (1114)	0.19
			1	**15**	1	0.13 (1352)	0.25
			0.5	**25**	2	0.25 (504)	0.19
			1	**26**	1	0.25 (226)	0.38
			0.5	**28**	2	0.5 (336)	0.31
	RIF	4	0.06	**1**	2	0.5 (335)	0.27
			0.25	**14**	4	0.25 (1114)	0.13
			0.5	**15**	1	0.13 (1352)	0.25
			0.5	**25**	2	0.25 (504)	0.25
			0.5	**26**	1	0.25 (226)	0.38
			0.13	**28**	2	0.5 (336)	0.28
***K. pneumoniae* ST258**							
	AZM	32	4	**1**	16	0.5 (335)	0.16
			4	**14**	64	2 (139)	0.16
			8	**15**	32	0.5 (338)	0.27
			8	**25**	8	0.5 (252)	0.31
			8	**26**	8	0.5 (113)	0.31
			4	**28**	16	2 (84)	0.25
	RIF	16	0.25	**1**	16	0.5 (335)	0.05
			1	**14**	64	1 (279)	0.08
			0.5	**15**	32	0.5 (338)	0.05
			0.06	**25**	8	1 (126)	0.13
			0.06	**26**	8	0.5 (113)	0.07
			0.5	**28**	16	1 (168)	0.09
	CLI	125	4	**26**	8	0.5 (113)	0.09
***P. aeruginosa* ATCC 27853**							
	AZM	>128	8	**1**	1	0.25 (669)	0.28
			1	**14**	16	4 (70)	0.25
			2	**15**	1	0.5 (338)	0.51
			4	**25**	8	1 (126)	0.14
			0.5	**26**	2	1 (56)	0.50
			0.5	**28**	16	2 (84)	0.13
	RIF	32	1	**1**	1	0.25 (669)	0.28
			1	**14**	16	4 (70)	0.28
			0.5	**15**	1	0.5 (338)	0.52
			0.06	**25**	8	1 (126)	0.13
			0.06	**26**	2	0.5 (113)	0.25
			0.06	**28**	16	4 (42)	0.25

Compound numbers are stated in bold.

0.13 to 0.5, except for combinations with peptidomimetic **15**, which only displayed a slight potentiation of antibiotic activity (i.e., FICIs >0.5; **Table 4**). In the presence of sub-MIC concentrations of peptidomimetics **1**, **14**, **15**, **25**, **26**, or **28**, the MICs of azithromycin were reduced 32- to 512-fold, corresponding to MIC values within the range 0.5-8 μg/mL in the synergistic combinations (**Table 4**). However, the most pronounced enhancement of antibiotic potency was observed when the peptidomimetics were used in combination treatment of *K. pneumoniae*, since the peptidomimetics in this case could be applied in 8- to 64-fold lower concentrations than their MICs as compared to only 2- to 16-fold lower than their MICs in *E. coli* and *P. aeruginosa*.

As a preliminary investigation of the therapeutic potential of the present subclasses of peptidomimetic antibiotic adjuvants, their cell selectivity was estimated as a measure that reflects both antibacterial activity and effect on viability of mammalian cells. Typically, a cell selectivity index (SI) is calculated as the ratio between the averaged EC_{50} values and the MIC of the peptidomimetic in each bacterial species. Peptidomimetics **1** and **15**, belonging to subclass I, proved to be the most selective against *E. coli* and *P. aeruginosa* over mammalian cells with SIs within the range 84–169 (**Table 2**). When targeting MDR *K. pneumoniae* all compounds displayed poor selectivity, with **25** having a modest SI of 16. As the MICs of the peptidomimetics in combination with antibiotics were lower, the SIs of the combinations with azithromycin or rifampicin were improved, assuming a negligible contribution from the antibiotics to the negative effects on mammalian cell viability, since these were employed in clinically relevant concentrations (Baker et al., 2018). Toward *E. coli*, the most favorable combinations, containing peptidomimetics **14** and **15**, would have approximated SIs >1,000 (**Table 4**). However, these two peptidomimetics were less selective against *K. pneumoniae* and *P. aeruginosa* with SIs within the range 70–338. While **14** had the highest EC_{50} (**Table 2**), the concentration of **14** required in synergistic combinations were $\geq$1 μM and 4 μM, in *K. pneumoniae* and *P. aeruginosa*, respectively, (**Table 4**). Likewise, compound **15** did not display synergy with any of the antibiotics in *P. aeruginosa* (**Table 4**). In contrast, peptidomimetic **1** exhibited synergy with both rifampicin and azithromycin at submicromolar concentrations with estimated SIs $\geq$335 against all three species (**Table 4**). With an average EC_{50} >150 μM, peptidomimetic **1** was also considered relatively non-toxic in itself. In addition, peptidomimetic **1** was the only compound that exhibited synergy at submicromolar concentrations in combination with antibiotics at clinically relevant concentrations in all three species, and thus this compound was selected for further studies.

Bacterial Growth and Killing in Presence of Peptidomimetic 1-Antibiotic Combinations

To ascertain that susceptibility of clinical isolates of Enterobacteriaceae and *P. aeruginosa* to combinations of peptidomimetic **1** with rifampicin or azithromycin could be induced, the combinations were tested with respect to MIC against several MDR isolates of each species. Overall, peptidomimetic **1** (at $\leq$1 μM) induced susceptibility to rifampicin and azithromycin in 83% of the isolates (i.e., in 30 of 36 isolates; **Table 5**). Notably, most *E. coli* isolates proved susceptible to 0.25–0.5 μg/mL rifampicin and 2–4 μg/mL azithromycin in combination with 0.5–1 μM peptidomimetic **1**. While submicromolar concentrations of **1** in the majority of *K. pneumoniae* isolates were sufficient to induce susceptibility to rifampicin and azithromycin, three isolates required considerably higher concentrations of **1** (i.e., 2–8 μM). By contrast *P. aeruginosa* isolates typically required 1–8 μM of **1** to reduce the MIC of rifampicin and azithromycin to 0.5 μg/mL and 4–8 μg/mL, respectively.

TABLE 5 | MICs of Peptidomimetic (PM) **1**-rifampicin and PM **1**-azithromycin combinations in *E. coli*, *K. pneumoniae*, and *P. aeruginosa* clinical isolates and reference strains.

	PM 1 / Rifampicin	PM 1/ Azithromycin
Species	**MIC (μM/μg mL^{-1})**	**MIC (μM/μg mL^{-1})**
***E. coli* Isolates**		
1	0.5/0.25	0.5/2
2	1/0.5	0.5/2
3	0.5/0.25	0.5/2
4	0.5/0.25	1/4
5	0.5/0.25	1/4
6	1/0.5	1/4
7	0.5/0.25	1/4
8	0.5/0.25	1/4
9	0.5/0.25	0.5/2
10	0.5/0.25	0.5/2
ST131	0.5/0.25	1/4
ATCC 25922	0.5/0.25	0.5/2
***K. pneumoniae* Isolates**		
1	0.5/0.25	>4/16
2	8/4	0.5/2
3	0.5/0.25	0.5/2
4	1/0.5	0.5/2
5	0.5/0.25	1/4
6	2/1	0.5/2
7	1/0.5	0.5/2
8	0.5/0.25	0.5/2
9	0.5/0.25	0.5/2
10	4/2	>4/16
ST258	0.5/0.25	4/16
ATCC 13883	0.5/0.25	0.5/2
***P. aeruginosa* Isolates**		
1	1/0.5	1/4
2	1/0.5	2/8
3	1/0.5	1/4
4	1/0.5	2/8
5	0.5/0.25	1/4
6	1/0.5	1/4
7	1/0.5	1/4
8	1/0.5	0.5/2
9	1/0.5	1/4
10	4/2	1/4
11	8/4	>4/16
ATCC 27853	0.5/0.25	1/4

To understand the dynamics of the interaction of peptidomimetic **1** with antibiotics, the kinetics of bacterial growth and killing were investigated by growth-curve and time-kill assays. All combinations exhibited synergistic growth inhibition or bactericidal activity in growth-curve and time-kill assays. The growth curves of the combinations corresponded well to the MICs (**Table 6**) found in static growth assays (**Tables 4**, **5**). In the time-kill assays, the concentrations of tested compounds were 2-fold above the MIC observed in the growth-curve assays,

TABLE 6 | MIC and MBC of peptidomimetic (PM) **1** (μM), azithromycin (AZM) and rifampicin (RIF) (μg/mL) and combinations (peptidomimetic + antibiotic) as determined in the growth-curve assay.

	E. coli ST131		*K. pneumoniae* ST258		*P. aeruginosa* ATTC 27853	
Agent	**MIC**	**MBC**	**MIC**	**MBC**	**MIC**	**MBC**
AZM	8	>16	>32	>32	>128	>128
PM1 + AZM	0.25 + 1	0.5 + 2	0.5 + 4	4 + 32	0.25 + 8	0.5 + 16
RIF	>4	>4	>16	>16	>64	>64
PM1 + RIF	0.25 + 0.31	0.25 + 0.31	0.25 + 0.125	0.25 + 0.125	0.5 + 1	1 + 2
PM1	1	1	8	16–32	1	2

since a 2-fold higher bacterial concentration was used. The tested peptidomimetic **1**-rifampicin combinations were bactericidal in all three species, as at least a 3-log reduction in CFU/mL was reached within the initial 4 h of exposure (**Figures 3A–C**). Similarly, peptidomimetic **1**-azithromycin combinations (**Figures 3D,F**) were bactericidal in *E. coli* and *P. aeruginosa*. However, in *K. pneumoniae* (**Figure 3E**), the combination was bacteriostatic as it only reduced the initial inoculum CFU by ∼1.5 log, also reflecting the high MBC, measured at the end of the growth-curve assay (**Table 6**). Although the MBCs of combinations in *P. aeruginosa* were only 2-fold higher than the MIC (**Table 6**), in the time-kill assay this species started to recover after 4 h of exposure to the rifampin- and azithromycin-peptidomimetic **1** combinations (**Figures 3C,F**). A similar, but less pronounced, trend was observed for the **1**-rifampicin combination in *E. coli*, for which the CFU concentration had increased at the 24 h time point (**Figure 3A**). In addition, reduced growth was seen for *E. coli* and *P. aeruginosa* in the presence of **1** alone (at concentrations 2-fold below the MIC) within the first 4 h of exposure (**Figures 3A,C,D**).

DISCUSSION

In the present study an array of peptidomimetics was screened in order to identify possible potentiators of antibiotics against MDR Gram-negative pathogens. In particular, the aim was to repurpose antibiotics typically used against Gram-positive pathogens. This enabled identification of a lead compound, peptidomimetic **1**, which exhibited high cell selectivity and displayed synergy with rifampicin and azithromycin at submicromolar, sub-MIC concentrations. Moreover, this compound was found capable of inducing susceptibility to antibiotics in MDR strains and clinical isolates of *E. coli*, *K. pneumoniae* and *P. aeruginosa*. Initial characterization of five additional peptidomimetics with similar structural composition also revealed potent antibacterial synergy with rifampicin and azithromycin, suggesting that the α-peptide/β-peptoid backbone constitutes a promising template for design of potentiators of antibiotics that Gram-negative pathogens are intrinsically resistant to.

The structural features of the peptidomimetics, identified as antibiotic adjuvants, have been examined in previous studies, focusing on the structure-activity relationships as potential directly antimicrobial agents (Jahnsen et al., 2014; Molchanova et al., 2017b); yet the present work constitutes the first report on their potential for synergy with traditional antibiotics. While the effect of human serum albumin and plasma on the antibiotic adjuvant activity was not addressed in this study, we have in previous work found that the antibacterial activity of similar peptidomimetics (belonging to the same peptidomimetic class) is independent of the presence of physiological concentration human serum albumin, while test in 25% plasma in fact increased their antimicrobial potency (Hein-Kristensen et al., 2013; Citterio et al., 2016). Likewise, the mechanism of synergy has not been investigated in the present study, but this type of peptidomimetics was previously found to exhibit bactericidal activity via membrane permeabilization (Hein-Kristensen et al., 2011), suggesting that at low concentrations these compounds may cause non-lethal membrane alterations that facilitate enhanced influx of antibiotics. The transient growth inhibition induced by these compounds at sub-MIC concentrations in growth-curve and time-kill assays (**Figures 2**, **3**) supports this hypothesis. The six studied peptidomimetics range in length from 12 to 16 residues and display N-terminal end groups (**Table 2**; **Figure 1**). Subclass I peptidomimetics display a 1:1 ratio of alternating Lys residues and βNPhe peptoid units as well as either no end group or an acetyl group at the N-terminus (**Table 1**). Compound **1** had previously been found to be active against the Gram-negative *E. coli*, *P. aeruginosa*, *Acinetobacter baumannii* and *Salmonella Typhimurium* as well as the Gram-positive *Staphylococcus pseudintermedius* (Molchanova et al., 2017b), while **15** had proved antibacterial against *E. coli* (Jahnsen et al., 2012). Interestingly, compound **14** at 1 μM has been shown to block the pro-inflammatory effect of LPS (Skovbakke et al., 2015), thereby implying that LPS released from lysed bacteria might constitute a less critical issue when applying this compound as an antibiotic adjuvant.

In accordance with the high structural similarity between **1** and **15**, these analogs exhibited almost equipotent antibacterial, cytotoxic activity and potentiation of antibiotics (**Tables 2**, **4**). Nonetheless, **1** appeared to exert slightly more efficient potentiation of antibiotics in *P. aeruginosa*. In contrast, **14** is four residues shorter than **15**, and hence exhibited a less pronounced effect on the viability of mammalian cells, since this effect is strongly dependent on oligomer length (Jahnsen et al., 2014). Nonetheless, shortening of oligomer length gives rise to a concomitantly lower antibacterial activity, as also seen in the MDR strains of *K. pneumoniae* and *P. aeruginosa* (**Table 2**), yet **14** retained a similar degree of synergy with antibiotics (**Table 4**). Consequently, the selectivity indexes for

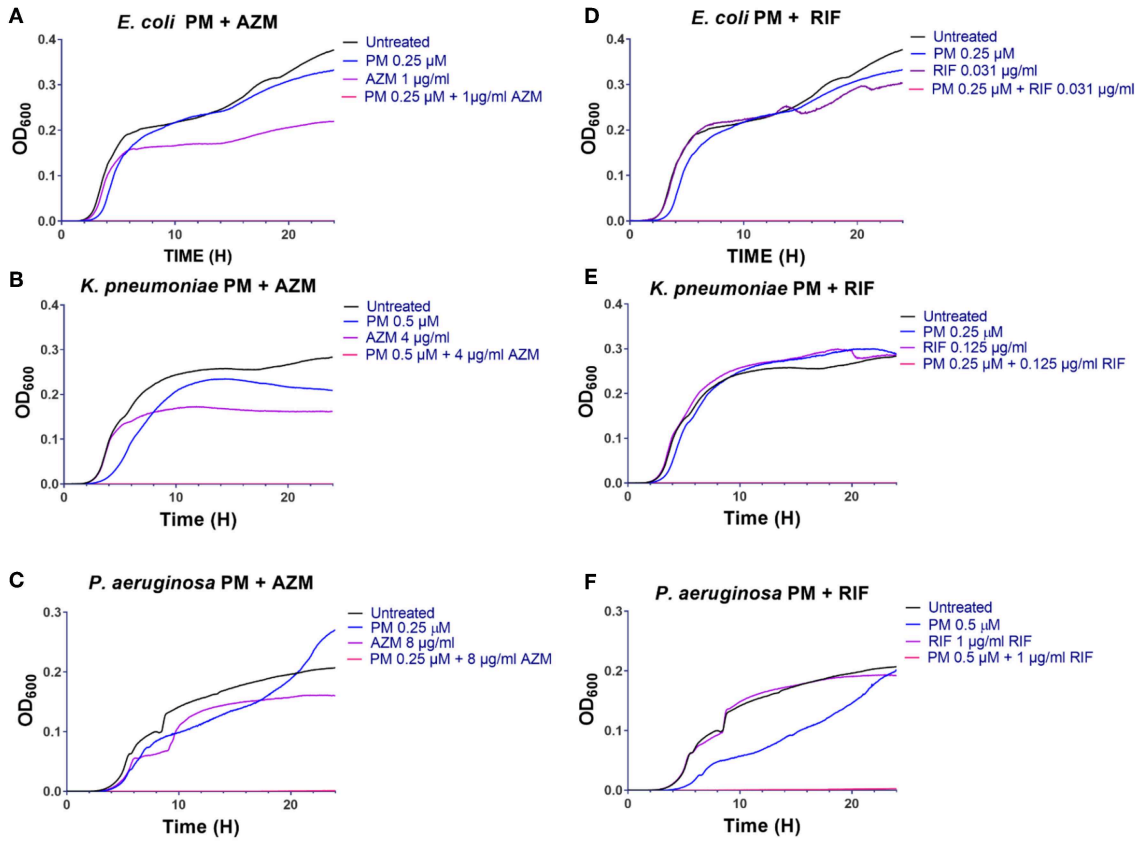

FIGURE 2 | Peptidomimetic **1** potentiates activity of azithromycin and rifampicin in growth-curve assays **(A–F)**. Growth of *E. coli* ST131 **(A,D)**, *K. pneumoniae* ST258 **(B,E)** and *P. aeruginosa* ATCC 27853 **(C,F)** in absence or presence of antibiotic, peptidomimetic (PM) **1** or their combinations were recorded at regular intervals by measuring the optical density (OD) of each culture at 600 nm, and then these data were graphed over time (h). Initial bacterial concentration was ~5 × 10^5 CFU/mL. The MIC values of each compound are listed in **Table 6**.

14 in combination with rifampicin or azithromycin in *E. coli* proved to be the most favorable among all of the peptidomimetic-antibiotic combinations tested. However, due to the typically 2- to 8-fold higher concentrations of **14** in synergistic combinations, these gave rise to less pronounced selectivity for *K. pneumoniae* and *P. aeruginosa* over mammalian cells (as reflected in its SIs; **Table 2**). While subclass I and II peptidomimetics share the same α-peptide/β-peptoid hybrid backbone structure, subclass II is characterized by a mixed Lys and hArg content (in a 1:1 ratio) of cationic residues (**Table 2**). The increased effect of subclass II peptidomimetics **25** and **26** on the viability of mammalian cell lines may be correlated to the presence of hArg residues displaying guanidinium functionalities, which confer an increased propensity to interact with, and thereby disrupt, mammalian membranes (Chan et al., 2006; Hein-Kristensen et al., 2011; Findlay et al., 2012; Jahnsen et al., 2014). However, even though **28** belongs to subclass II it had a similarly low effect on mammalian cell viability as that of compounds **1** and **15**, which may be explained by its modification with a polar PEG-like moiety (i.e., 3,6,9-trioxadecanoyl; TODA) instead of a cationic moiety containing amine functionalities (i.e., NDab or spermine-acetyl moiety present in **25** and **26**, respectively). Thus, the increased effect of **25** and **26** on mammalian cell viability may be due to their increased net cationic charge (Jahnsen et al., 2015). Moreover, while **28** retained antibacterial potency similar to its parent unmodified compound, it had a lower effect on mammalian cell viability than the parent compound (for NIH 3T3: EC_{50} ~218 μM vs. 117 μM) (Jahnsen et al., 2015), suggesting that introduction of the TODA moiety is beneficial with respect to therapeutic utility.

Interestingly, nine compounds in the peptidomimetic array contained the subclass II core structure, yet only four compounds were detected as potentiators of antibiotics. Another shorter peptidomimetic (i.e., **10**) also potentiated rifampicin activity (but not that of azithromycin) in MDR *E. coli*. In contrast, the other five compounds (i.e., **9**, **12**, **13**, **27**, and **29**) did not exhibit any potentiation activity, detectable at the low concentrations tested in the screening (**Table 1**). This suggests that addition of a palmitoyl moiety (in **9**, **12**, **13**), a cinnamoyl moiety (in **27**), a fluorinated phenylalanine (in **29**), or shorter oligomers (i.e., **9** and **13**) may result in lowered potency or abolish potentiation, while similar modifications (e.g., in **29**) did not alter the antibacterial activity (Jahnsen et al., 2015). Based on these observations, there appears to be distinct physicochemical and/or overall structural requirements for achieving efficient potentiation of antibiotics and high direct antibacterial activity, respectively.

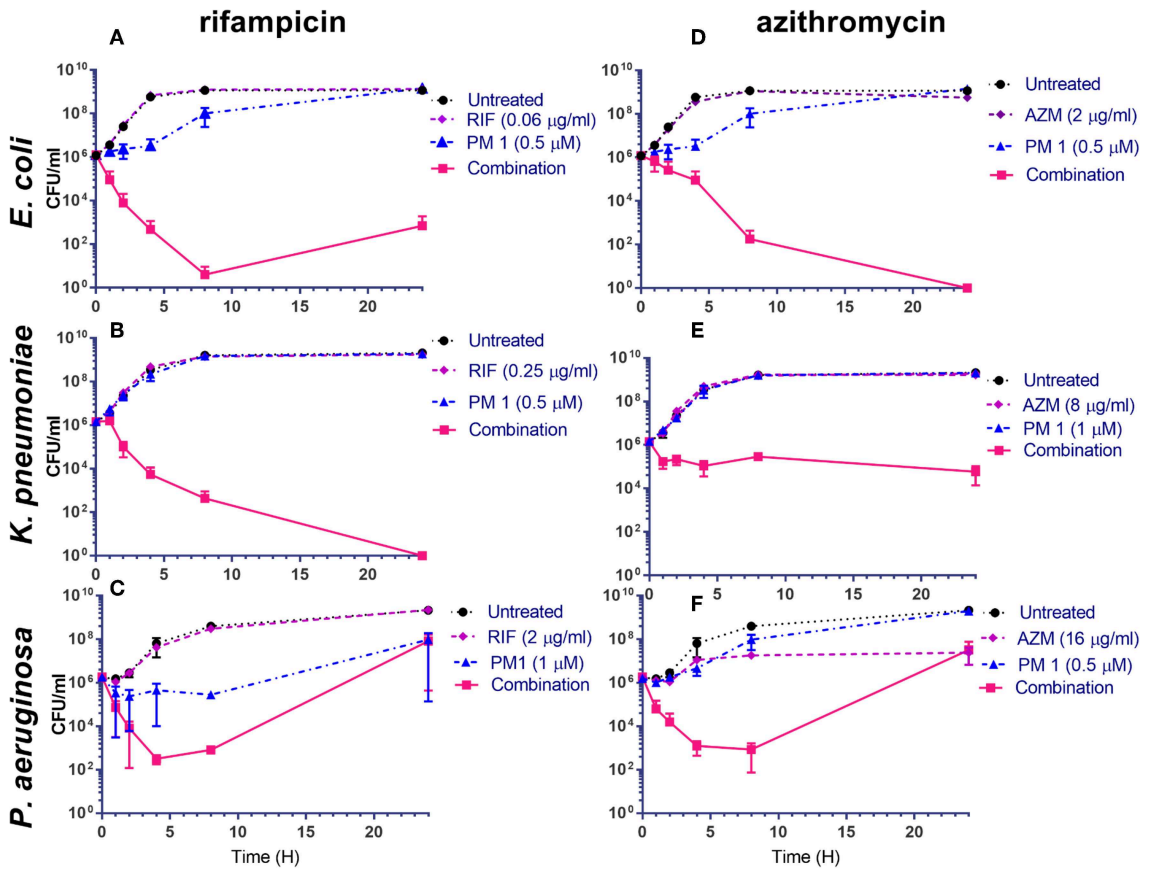

FIGURE 3 | Peptidomimetic **1**-combinations enhance bactericidal activity **(A–F)**. Time-kill kinetics for *E. coli* ST131 **(A,D)**, *K. pneumoniae* ST258 **(B,E)** and *P. aeruginosa* ATTC 27853 **(C,F)** exposed to peptidomimetic (PM) **1**, azithromycin (AZM), rifampicin (RIF), peptidomimetic-antibiotic combinations or without treatment (controls); CFU/mL data are graphed at time points 0, 1, 2, 4, 8, and 24 h of exposure. Initial bacterial concentration was ~10^6 CFU/mL. The MBC values of each compound are listed in **Table 6**.

The present results infer that peptidomimetic **1** has a potential for repurposing rifampicin and azithromycin for treatment of MDR Gram-negative infections. While this peptidomimetic was considered to be the most promising due to its low toxicity (with ensuing favorable cell selectivity) and ability to exert synergy with antibiotics at submicromolar levels in all three species, the additional peptidomimetics with low effect on mammalian cell viability, characterized in this study, may also merit further investigation. Since a prerequisite for successful combination therapy is that the effective concentrations of both peptidomimetic and antibiotic can be achieved at the infection site, it is critical that future studies address *in vivo* pharmacokinetic/pharmacodynamics and acute toxicity to assess the clinical potential of such peptidomimetic-antibiotic combinations. In particular, co-formulation of antibiotic and peptidomimetics as nanoparticles would be preferable to ensure *in vivo* co-localization of the compounds in the appropriate ratios (Carmona-Ribeiro and de Melo Carrasco, 2014; Liu et al., 2016; Nordström and Malmsten, 2017). While *in vivo* data currently are lacking for the α-peptide/β-peptoid hybrids described in the present study, peptidomimetics (including the 12-mer, H-(NLys-Nspe-Nspe)$_4$-NH_2 and the pentamer C12K-2α_8) displaying similar structural features such as a high content of both cationic and hydrophobic residues (aromatic or aliphatic) have previously been found to exhibit *in vivo* activity (antibacterial and antiparasitic, respectively) (Zaknoon et al., 2011; Czyzewski et al., 2016). Based on overall structural similarity, the peptidomimetics identified in the present study appear likely to possess physicochemical properties compatible with *in vivo* activity. Moreover, clinical breakpoints for rifampicin and azithromycin may be used to estimate the therapeutic potential of the antibiotics in these drug combinations. Although no clinical breakpoint points are available for these antibiotics in Enterobacteriaceae or *P. aeruginosa*, bactericidal efficacy of the **1**-rifampicin combination occurred at concentrations ranging from 0.06 to 2 μg/mL in time-kill assays, which is below the resistance breakpoint for rifampicin alone in *Staphylococcus* species (R ≥4 μg/mL) (Clinical and Laboratory Standards Institute, 2017). Similarly, at concentrations below the azithromycin resistance breakpoint for *Salmonella typhi* (R ≥32 μg/mL), the **1**-azithromycin combination exerted growth-inhibitory and bactericidal activity.

Recent studies also indicate that antibacterial efficacy of azithromycin therapy against Gram-negative pathogens *in vivo* is considerably higher than implied by *in vitro* susceptibility testing in standard MHB media (Lin et al., 2015; Ersoy et al., 2017). Importantly, low concentrations ($\leq 1\,\mu M$) of peptidomimetic **1** were able to induce susceptibility to azithromycin and rifampicin in most of the clinical isolates tested. Thus the low effect of **1** on viability of mammalian cells and its high potency in combination with antibiotics may facilitate circumvention of pharmacological obstacles frequently associated with antimicrobial peptides and peptidomimetics (Molchanova et al., 2017a).

AUTHOR CONTRIBUTIONS

KB, HF, and LG conceived and designed the study. KB, BJ, HF, and LG contributed to experimental design. KB, BJ, and AH performed experiments. HN provided cytotoxicity experiments and data. KB wrote the first draft of the manuscript. HF, LG, AH, HN, and KB wrote sections of the manuscript. All authors edited, revised, and approved the manuscript for submission.

ACKNOWLEDGMENTS

We thank Laurent Poirel for providing the clinical isolates used in this study. The study was supported by the University of Copenhagen research centre for Control of Antibiotic Resistance (UC-CARE).

SUPPLEMENTARY MATERIAL

The Supplementary Material for this article can be found online at: https://www.frontiersin.org/articles/10.3389/fcimb.2019.00236/full#supplementary-material

REFERENCES

Baker, K. R., Jana, B., Franzyk, H., and Guardabassi, L. (2016). A high-throughput approach to identify compounds that impair envelope integrity in *Escherichia coli*. *Antimicrob. Agents Chemother.* 60, 5995–6002. doi: 10.1128/AAC.00537-16

Baker, K. R., Jana, B., Hansen, A. M., Vissing, K. J., Nielsen, H. M., Franzyk, H., et al. (2018). Repurposing azithromycin and rifampicin against Gram-negative pathogens by combination with peptide potentiators. *Int. J. Antimicrob. Agents.* 53, 868–872. doi: 10.1016/j.ijantimicag.2018.10.025

Bonke, G., Vedel, L., Witt, M., Jaroszewski, J. W., Olsen, C. A., and Franzyk, H. (2008). Dimeric building blocks for solid-phase synthesis of α-peptide-β-peptoid chimeras. *Synthesis.* 2008, 2381–2390. doi: 10.1055/s-2008-1067171

Brown, D. (2015). Antibiotic resistance breakers: can repurposed drugs fill the antibiotic discovery void? *Nat. Rev. Drug Discov.* 14, 821–832. doi: 10.1038/nrd4675

Brown, E. D., and Wright, G. D. (2016). Antibacterial drug discovery in the resistance era. *Nature* 529, 336–343. doi: 10.1038/nature17042

Carmona-Ribeiro, A., and de Melo Carrasco, L. (2014). Novel formulations for antimicrobial peptides. *Int. J. Mol. Sci.* 15, 18040–18083. doi: 10.3390/ijms151018040

Cerquetti, M., Giufrè, M., García-Fernández, A., Accogli, M., Fortini, D., Luzzi, I., et al. (2010). Ciprofloxacin-resistant, CTX-M-15-producing *Escherichia coli* ST131 clone in extraintestinal infections in Italy. *Clin. Microbiol. Infect.* 16, 1555–1558. doi: 10.1111/j.1469-0691.2010.03162.x

Chan, D. I., Prenner, E. J., and Vogel, H. J. (2006). Tryptophan- and arginine-rich antimicrobial peptides: structures and mechanisms of action. *Biochim. Biophys. Acta Biomembr.* 1758, 1184–1202. doi: 10.1016/j.bbamem.2006.04.006

Citterio, L., Franzyk, H., Palarasah, Y., Emil, T., Valentina, R., and Gram, L. (2016). Improved *in vitro* evaluation of novel antimicrobials: potential synergy between human plasma and antibacterial peptidomimetics, AMPs and antibiotics against human pathogenic bacteria. *Res. Microbiol.* 167, 72–82. doi: 10.1016/j.resmic.2015.10.002

Clinical and Laboratory Standards Institute (1999). *Methods for Determining Bactericidal Activity of Antimicrobial Agents; Approved Guidline,* Wayne, PA: Vol 19. CLSI document M26-A, Clinical and Laboratory Standards Institute.

Clinical and Laboratory Standards Institute (2013). *Performance Standards for Antimicrobial Disk and Dilution Susceptibility Tests for Bacteria Isolated From Animals; Approved Standard, 4th ed,* Wayne, PA: vol 8. CLSI document VET01-A4, Clinical and Laboratory Standards Institute.

Clinical and Laboratory Standards Institute (2017). *Performance Standards for Antimicrobial Susceptibility Testing, 27th ed,* Wayne, PA: CLSI M100. Clinical and Laboratory Standards Institute.

Corbett, D., Wise, A., Langley, T., Skinner, K., Trimby, E., Birchall, S., et al. (2017). Potentiation of antibiotic activity by a novel cationic peptide: potency and spectrum of activity of SPR741. *Antimicrob. Agents Chemother* 22, 1–10. doi: 10.1128/AAC.00200-17

Czyzewski, A. M., Jenssen, H., Fjell, C. D., Waldbrook, M., Chongsiriwatana, N. P., Yuen, E., et al. (2016). *In vivo*, *in vitro*, and *in silico* characterization of peptoids as antimicrobial agents. *PLoS ONE* 11:e0135961. doi: 10.1371/journal.pone.0135961

Doi, Y., Bonomo, R. A., Hooper, D. C., Kaye, K. S., Johnson, J. R., Clancy, C. J., et al. (2017). Gram-negative bacterial infections: Research priorities, accomplishments, and future directions of the antibacterial resistance leadership group. *Clin. Infect. Dis.* 64, S30–S35. doi: 10.1093/cid/ciw829

Domalaon, R., Brizuela, M., Eisner, B., Findlay, B., Zhanel, G. G., and Schweizer, F. (2018a). Dilipid ultrashort cationic lipopeptides as adjuvants for chloramphenicol and other conventional antibiotics against Gram-negative bacteria. *Amino Acids*. 51, 383–393. doi: 10.1007/s00726-018-2673-9

Domalaon, R., Sanchak, Y., Koskei, L. C., Lyu, Y., Zhanel, G. G., Arthur, G., et al. (2018b). Short proline-rich lipopeptide potentiates minocycline and rifampin against multidrug- and extensively drug-resistant *Pseudomonas aeruginosa*. *Antimicrob. Agents Chemother.* 62, e02374–e02317. doi: 10.1128/AAC.02374-17

Ersoy, S. C., Heithoff, D. M., Barnes, L., Tripp, G. K., House, J. K., Marth, J. D., et al. (2017). Correcting a fundamental flaw in the paradigm for antimicrobial susceptibility testing. *EBioMedicine* 20, 173–181. doi: 10.1016/j.ebiom.2017.05.026

Findlay, B., Szelemej, P., Zhanel, G. G., and Schweizer, F. (2012). Guanidylation and tail effects in cationic antimicrobial lipopeptoids. *PLoS ONE* 7:e41141. doi: 10.1371/journal.pone.0041141

Garcia, L. S. (ed.). (2010). "Synergism testing: broth microdilution checkerboard and broth macrodilution methods," in *Clinical Microbiology Procedures Handbook, 3rd Edition* (Washington, DC: American Society of Microbiology Press), 140–162.

Ghosh, C., and Haldar, J. (2015). Membrane-Active Small Molecules: Designs Inspired by Antimicrobial Peptides. *ChemMedChem* 10, 1606–1624. doi: 10.1002/cmdc.201500299

Gill, E. E., Franco, O. L., and Hancock, R. E. (2015). Antibiotic adjuvants: diverse strategies for controlling drug-resistant pathogens. *Chem. Biol. Drug Des.* 85, 56–78. doi: 10.1111/cbdd.12478

Goldberg, K., Sarig, H., Zaknoon, F., Epand, R. F., Epand, R. M., and Mor, A. (2013). Sensitization of gram-negative bacteria by targeting the membrane potential. *FASEB J.* 27, 3818–3826. doi: 10.1096/fj.13-227942

Hein-Kristensen, L., Franzyk, H., Holch, A., and Gram, L. (2013). Adaptive evolution of *Escherichia coli* to an α-peptide/β-peptoid peptidomimetic induces stable resistance. *PLoS ONE* 8:e73620. doi: 10.1371/journal.pone.0073620

Hein-Kristensen, L., Knapp, K. M., Franzyk, H., and Gram, L. (2011). Bacterial membrane activity of α-peptide/β-peptoid chimeras: influence of amino acid composition and chain length on the activity against different bacterial strains. *BMC Microbiol.* 11:144. doi: 10.1186/1471-2180-11-144

Jahnsen, R. D., Frimodt-Møller, N., and Franzyk, H. (2012). Antimicrobial activity of peptidomimetics against multidrug-resistant *Escherichia coli*: a comparative study of different backbones. *J. Med. Chem.* 55, 7253–7261. doi: 10.1021/jm300820a

Jahnsen, R. D., Sandberg-Schaal, A., Vissing, K. J., Nielsen, H. M., Frimodt-Møller, N., and Franzyk, H. (2014). Tailoring cytotoxicity of antimicrobial peptidomimetics with high activity against multidrug-resistant *Escherichia coli*. *J. Med. Chem.* 57, 2864–2873. doi: 10.1021/jm401335p

Jahnsen, R. O., Sandberg-Schaal, A., Frimodt-Møller, N., Nielsen, H. M., and Franzyk, H. (2015). End group modification: efficient tool for improving activity of antimicrobial peptide analogues towards Gram-positive bacteria. *Eur. J. Pharm. Biopharm.* 95, 40–46. doi: 10.1016/j.ejpb.2015.01.013

Jammal, J., Zaknoon, F., Kaneti, G., Goldberg, K., and Mor, A. (2015). Sensitization of gram-negative bacteria to rifampin and OAK combinations. *Sci. Rep.* 5:9216. doi: 10.1038/srep09216

Jana, B., Cain, A. K., Doerrler, W. T., Boinett, C. J., Fookes, M. C., Parkhill, J., et al. (2017). The secondary resistome of pneumoniae. *Sci. Rep.* 7:42483. doi: 10.1038/srep42483

Kalan, L., and Wright, G. D. (2011). Antibiotic adjuvants: multicomponent anti-infective strategies. *Expert Rev. Mol. Med.* 13:e5. doi: 10.1017/S1462399410001766

Lainson, J. C., Daly, S. M., Triplett, K., Johnston, S. A., Hall, P. R., and Diehnelt, C. W. (2017). Synthetic antibacterial peptide exhibits synergy with oxacillin against MRSA. *Med. Chem. Lett.* 8, 853–857. doi: 10.1021/acsmedchemlett.7b00200

Lin, L., Nonejuie, P., Munguia, J., Hollands, A., Olson, J., Dam, Q., et al. (2015). Azithromycin synergizes with cationic antimicrobial peptides to exert bactericidal and therapeutic activity against highly multidrug-resistant gram-negative bacterial pathogens. *EBioMedicine* 2, 690–698. doi: 10.1016/j.ebiom.2015.05.021

Liu, X., Li, Z., Wang, X., Chen, Y., Wu, F., Men, K., et al. (2016). Novel antimicrobial peptide–modified azithromycin-loaded liposomes against methicillin-resistant *Staphylococcus aureus*. *Int. J. Nanomed.* 11, 6781–6794. doi: 10.2147/IJN.S107107

Liu, Y., Knapp, K. M., Yang, L., Molin, S., Franzyk, H., and Folkesson, A. (2013). High *in vitro* antimicrobial activity of β-peptoid-peptide hybrid oligomers against planktonic and biofilm cultures of *Staphylococcus epidermidis*. *Int. J. Antimicrob. Agents* 41, 20–27. doi: 10.1016/j.ijantimicag.2012.09.014

Lyu, Y., Yang, X., Goswami, S., Gorityala, B. K., Idowu, T., Domalaon, R., et al. (2017). Amphiphilic tobramycin–lysine conjugates sensitize multidrug resistant gram-negative bacteria to rifampicin and minocycline. *J. Med. Chem.* 60, 3684–3702. doi: 10.1021/acs.jmedchem.6b01742

Melander, R. J., and Melander, C. (2017). The challenge of overcoming antibiotic resistance: an adjuvant approach? *ACS Infect. Dis.* 3, 559–563 doi: 10.1021/acsinfecdis.7b00071

Méndez-Samperio, P. (2014). Peptidomimetics as a new generation of antimicrobial agents: current progress. *Infect. Drug Resist.* 7, 229–237. doi: 10.2147/IDR.S49229

Mojsoska, B., and Jenssen, H. (2015). Peptides and peptidomimetics for antimicrobial drug design. *Pharmaceuticals* 8, 366–415 doi: 10.3390/ph8030366

Molchanova, N., Hansen, P. R., Damborg, P., Nielsen, H. M., and Franzyk, H. (2017b). Lysine-based α-peptide/β-peptoid peptidomimetics: influence of hydrophobicity, fluorination, and distribution of cationic charge on antimicrobial activity and cytotoxicity. *ChemMedChem* 12, 312–318. doi: 10.1002/cmdc.201600553

Molchanova, N., Hansen, P. R., and Franzyk, H. (2017a). Advances in development of antimicrobial peptidomimetics as potential drugs. *Molecules* 22:1430. doi: 10.3390/molecules22091430

Moon, S. H., and Huang, E. (2018). Lipopeptide paenipeptin analogues potentiate clarithromycin and rifampin against carbapenem-resistant pathogens. *Antimicrob. Agents Chemother.* 62, e00329–e00318. doi: 10.1128/AAC.00329-18

Nordström, R., and Malmsten, M. (2017). Delivery systems for antimicrobial peptides. *Adv. Colloid Interface Sci.* 242, 17–34. doi: 10.1016/j.cis.2017.01.005

Renau, T. E., Léger, R., Yen, R., She, M. W., Flamme, E. M., Sangalang, J., et al. (2002). Peptidomimetics of efflux pump inhibitors potentiate the activity of levofloxacin in *Pseudomonas aeruginosa*. *Bioorganic Med. Chem. Lett.* 12, 763–766. doi: 10.1016/S0960-894X(02)00006-9

Ribeiro, S. M., Fuente-Núñez, C., Baquir, B., Faria-Junior, C., Franco, O. L., and Hancock, R. E. W. (2015). Antibiofilm peptides increase the susceptibility of carbapenemase-producing *Klebsiella pneumoniae* clinical isolates to β-lactam antibiotics. *Antimicrob. Agents Chemother.* 59, 3906–3912. doi: 10.1128/AAC.00092-15

Singh, S. B., Young, K., and Silver, L. L. (2017). What is an "ideal" antibiotic? discovery challenges and path forward. *Biochem. Pharmacol.* 133, 63–73. doi: 10.1016/j.bcp.2017.01.003

Skovbakke, S. L., Larsen, C. J., Heegaard, P. M. H., Moesby, L., and Franzyk, H. (2015). Lipidated α-peptide/β-peptoid hybrids with potent anti-inflammatory activity. *J. Med. Chem.* 58, 801–813. doi: 10.1021/jm501341h

World Health Organisation (2017). *Global Priority List Of Antibiotic-Resistant Bacteria To Guide Research, Discovery, And Development Of New Antibiotics*. World Health Organisation. Available online at: http://www.who.int/medicines/publications/global-priority-list-antibiotic-resistant-bacteria/en/ (accessed Jan 29, 2019)

Wu, X., Li, Z., Li, X., Tian, Y., Fan, Y., Yu, C., et al. (2017). Synergistic effects of antimicrobial peptide DP7 combined with antibiotics against multidrug-resistant bacteria. *Drug Des. Devel. Ther.* 11, 939–946. doi: 10.2147/DDDT.S107195

Yang, X., Domalaon, R., Lyu, Y., Zhanel, G., and Schweizer, F. (2018). Tobramycin-linked efflux pump inhibitor conjugates synergize fluoroquinolones, rifampicin and fosfomycin against multidrug-resistant *Pseudomonas aeruginosa*. *J. Clin. Med.* 7:158. doi: 10.3390/jcm7070158

Zaknoon, F., Wein, S., Krugliak, M., Meir, O., Rotem, S., Ginsburg, H., et al. (2011). Antiplasmodial properties of acyl-lysyl oligomers in culture and animal models of malaria. *Antimicrob. Agents Chemother.* 55, 3803–3811. doi: 10.1128/AAC.00129-11

Conflict of Interest Statement: The authors declare that the research was conducted in the absence of any commercial or financial relationships that could be construed as a potential conflict of interest.

Advantages of publishing in Frontiers

OPEN ACCESS
Articles are free to read for greatest visibility and readership

FAST PUBLICATION
Around 90 days from submission to decision

HIGH QUALITY PEER-REVIEW
Rigorous, collaborative, and constructive peer-review

TRANSPARENT PEER-REVIEW
Editors and reviewers acknowledged by name on published articles

Frontiers
Avenue du Tribunal-Fédéral 34
1005 Lausanne | Switzerland

Visit us: www.frontiersin.org
Contact us: info@frontiersin.org | +41 21 510 17 00

REPRODUCIBILITY OF RESEARCH
Support open data and methods to enhance research reproducibility

DIGITAL PUBLISHING
Articles designed for optimal readership across devices

FOLLOW US
@frontiersin

IMPACT METRICS
Advanced article metrics track visibility across digital media

EXTENSIVE PROMOTION
Marketing and promotion of impactful research

LOOP RESEARCH NETWORK
Our network increases your article's readership